



THE HONG KONG
POLYTECHNIC UNIVERSITY

香港理工大學

Pao Yue-kong Library

包玉剛圖書館

Copyright Undertaking

This thesis is protected by copyright, with all rights reserved.

By reading and using the thesis, the reader understands and agrees to the following terms:

1. The reader will abide by the rules and legal ordinances governing copyright regarding the use of the thesis.
2. The reader will use the thesis for the purpose of research or private study only and not for distribution or further reproduction or any other purpose.
3. The reader agrees to indemnify and hold the University harmless from and against any loss, damage, cost, liability or expenses arising from copyright infringement or unauthorized usage.

IMPORTANT

If you have reasons to believe that any materials in this thesis are deemed not suitable to be distributed in this form, or a copyright owner having difficulty with the material being included in our database, please contact lbsys@polyu.edu.hk providing details. The Library will look into your claim and consider taking remedial action upon receipt of the written requests.

**CHOLESTEROL BIOSYNTHESIS: A
CRITICAL DETERMINANT OF CANCER
STEMNESS AND DRUG RESISTANCE IN
HEPATOCELLULAR CARCINOMA?**

MOK HO KIT

PhD

THE HONG KONG POLYTECHNIC UNIVERSITY

2022

The Hong Kong Polytechnic University
Department of Applied Biology and Chemical Technology

**Cholesterol biosynthesis: A critical determinant of cancer
stemness and drug resistance in hepatocellular carcinoma?**

Mok Ho Kit

A thesis submitted in partial fulfilment of the requirements for the
degree of Doctor of Philosophy

August 2021

CERTIFICATE OF ORIGINALITY

I hereby declare that this thesis is my own work and that, to the best of my knowledge and belief, it reproduces no material previously published or written, nor material that has been accepted for the award of any other degree or diploma, except where due acknowledgement has been made in the text.

(Signed)

Mok Ho Kit

(Name of Student)

Abstract

Hepatocellular carcinoma (HCC), the major malignancy of liver cancers, accounts for the third leading cause of cancer related mortality worldwide in 2020. In spite of the vaccination and recent advances in screening and diagnosis, most HCC patients are diagnosed at their advanced stages. Unfortunately, the treatment options for the advanced HCC patients are limited. Sorafenib and lenvatinib, the molecular-targeted drugs against multiple kinases, are approved by FDA, yet with slight survival benefit due to the acquired drug resistance. The unsatisfactory clinical results have therefore prompted us to elucidate the drug resistance mechanism so as to develop a novel therapeutic strategy against HCC.

To mimic the clinical situation, we have established sorafenib- and lenvatinib-resistant HCC patient-derived tumor xenografts (PDTXs) through several rounds of drug administration. RNA sequencing coupled with pathway analysis was performed to compare gene expression profiles between drug-resistant PDTXs and their mock counterparts. Strikingly, cholesterol biosynthesis was mostly and commonly upregulated in both drug-resistant PDTXs. Drug-resistant cells showed enriched liver CSC populations. Therefore, we examined whether cholesterol biosynthesis was augmented in enhanced liver CSC populations. Firstly, we found that this pathway was upregulated in enhanced liver CSC populations via *in vitro* passages of hepatospheres with administration of chemotherapeutic drugs. Furthermore, we found that this pathway was preferentially activated in liver CSCs compared to normal liver stem cells by comparing the genetic profiles between CD133⁺ and CD133⁻ cells from liver regeneration and HCC mouse models. Using Upstream Regulatory Analysis, sterol regulatory element-binding protein 2 (SREBP2) was found to be the upstream regulator of the activated cholesterol biosynthesis in both drug-resistant PDTXs and CSCs-enriched hepatospheres.

Using lentiviral-based CRISPR activation and knockdown approaches, SREBP2-mediated cholesterol biosynthesis was found to be crucial in the regulation of acquired drug resistance in HCC via augmentation of liver CSCs with clinical significance. Similarly, exogenous cholesterol-treated and high cholesterol-utilizing HCC cells showed enhanced cancer stemness and drug resistance. Specifically, molecularly targeted drugs, including sorafenib and lenvatinib, induced the activation of caspase 3 (CASP3), which subsequently induced the nuclear translocation of SREBP2 from the endoplasmic reticulum, resulting in activation of the

cholesterol biosynthesis-driven sonic hedgehog (SHH) signalling pathway, mediated via 25-hydroxycholesterol (25-OHC). The correlation among CASP3 activity, SREBP2 and SHH signalling was further reinforced by the positive correlation among cleaved CASP3, SREBP2 and GLI-1 in HCC clinical samples.

Finally, the therapeutic efficacy of targeting cholesterol biosynthesis by using simvastatin, an FDA-approved drug in lowering cholesterol, was tested to override the drug resistance in HCC. The combined treatment of simvastatin and sorafenib/lenvatinib not only suppressed growth of patient-derived HCC organoids, but also exerted maximal growth suppression in two PDTX models by inhibiting liver CSC populations.

In summary, our findings reveal that HCC cells expand CSC populations via CASP3-dependent, SREBP2-mediated cholesterol biosynthesis in combatting the tyrosine kinase inhibitor therapy and that targeting cholesterol biosynthesis can overcome the drug resistance in HCC cells.

(472 words)

Acknowledgements

I would like to thank all those who helped me walk through the PhD journey. It would not be the most pleasant one, but definitely the most unforgettable one.

To Dr. Terence Lee Kin Wah, my PhD supervisor, who first came up with the idea for this project, and who guided me through the long process of academic research. He is an extraordinary scientist who has numerous ideas that cannot wait to execute. He is also keen on learning new methodologies and would not hesitate to invest into new technologies as long as they can serve the purpose. Though overwhelmed by day-to-day administrative and departmental works, he always prioritizes students and his teammates' requests, like meetings and discussions, in topics not just research, but also personal matters. I sincerely thank for his patient guidance, and wholeheartedly I wish he and his team keep excelling in the research.

To Dr. Carmen Leung Oi Ning, my senior at the TLEE Lab, who first introduced me to the academic research, and who always did a terrific job in accomplishing the manuscript. Sometimes I just needed to think what she cannot do so to work extra hard on the experiments. I thank to her forgiveness and great toleration when I repeatedly made silly mistakes during my stay at the TLEE Lab, both in the experiments and interpersonal relationships. Sincerely I am grateful for her presence and supports when I utterly need assistance.

To Dr. Eunice Lau Yuen Ting, Dr. Doris Leung Hoi Wing and Dr. Nicole Ho Pui Yu, who offered generous advice and experimental assistance in my project.

To Dr. Sara Ying Fan, Dr. Azam Zulfikar, Mr. Victor Ma, Ms. Katherine Chung Po Sin, Ms. Martina Lei Mang Leng, and Ms. Rainbow Leung Wing Hei, my teammates at the TLEE Lab, who shared many ups and downs and celebrating meals in these years.

To Dr-to-be Shilpa Gurung, who always believes in me and continuously encourage me to achieve my dreams.

To Ms. Peggy Kwok Fung Yee, the administrative staff in the Department of Applied Biology and Chemical Technology, who provided tremendous assistance in processing all the tedious documents required for my graduation requirements and thesis submission.

To Dr. Stephanie Ma Kwai Yee, Dr. Carol Tong Man, Dr. Eric Wong Tin Lok, Dr. Johnson Ng Kai Yu, Dr. Lena Zhou Lei, our collaborators at the SMA Lab in the University of Hong Kong, who have generously provided data, explanations, and scientific discussions. I thank to their kind accommodation as well when we moved our works to HKU during the shutdown of PolyU.

To all my friends and family members, for their patience and love.

To Ms. Hila Tai Yin Ting, for her accompany, sacrifice, and endless waiting so that I can concentrate at my research. I also thank to her mom for the delicious food, and to her four lovely dogs for their warm cuddles.

To Ms. Joyce Lam Chung Yan, for her cheers, supports, and cups of coffee so that I can continue to strive through the days and nights.

Finally, to my mother, Mrs. Elaine Mok Yuk Ling, for her unconditional love and support. I wish her good health, happiness, and speedy recovery.

Publications

1. **Mok EH**#, Leung CO#, Zhou L, Lei MM, Leung HW, Tong M, Wong TL, Lau EY, Ng IO, Ding J, Yun JP, Yu J, Zhu HL, Lin CH, Ma S, Lee TK. Caspase-3-induced SREBP2 activation drives drug resistance through the promotion of cholesterol biosynthesis in hepatocellular carcinoma; submitted. (#co-first author, manuscript under review)
2. Leung HW#, Leung CO#, Lau EY, Chung KPS, **Mok EH**, Lei MM, Leung RW, Tong M, Keng VW, Ma C, Zhao Q, Ng IO, Ma S, Lee TK. EPHB2 activates β -catenin to enhance cancer stem cell properties and drive sorafenib resistance in hepatocellular carcinoma. *Cancer Res* 2021; 81:3229-40. (#co-first authors) (Impact Factor: 12.701)
3. Ho NP#, Leung CO#, Wong TL, Lau EY, Lei MM, **Mok EH**, Leung HW, Tong M, Ng IO, Yun JP, Ma S, Lee TK. The interplay of UBE2T and Mule in regulating Wnt/ β -catenin activation to promote hepatocellular carcinoma progression. *Cell Death Dis* 2021;12(2):148. (#co-first authors) (Impact Factor: 8.469)
4. **Mok EH**, Lee TK. The Pivotal Role of the Dysregulation of Cholesterol Homeostasis in Cancer: Implications for Therapeutic Targets. *Cancers* 2020;12(6):1410. (Impact Factor: 6.63)
5. **Mok EH**, Leung CON, Lee TK. MAP9/ERCC3 signalling cascade: A new insight on understanding the chromosomal instability in hepatocellular carcinoma. *EBioMed* 2020; 54:102709. (Impact Factor: 8.143)
6. Leung HW#, Lau EY#, Leung CO, Lei MM, **Mok EH**, Ma V, Cho WC, Ng IO, Yun JP, Cai SH, Yu HJ, Ma S, Lee TK. NRF2/SHH signalling cascade promotes tumor-initiating cell lineage and drug resistance in hepatocellular carcinoma. *Cancer Lett* 2020; 476:48-56. (#co-first authors) (Impact Factor: 8.679)

Conference Presentations and Awards

1. **Mok EH**#, Leung CO#, Lei MM, Lee TK. Caspase-3-induced SREBP2 activation drives drug resistance through the promotion of cholesterol biosynthesis in hepatocellular carcinoma. 2nd ABCT Research Postgraduate Symposium in the Biology Discipline 2021, 2021.
This presentation was awarded *The Best Oral Presentation Award (1/25)*.
2. **Mok EH**#, Leung CO#, Lei MM, Lee TK. Caspase-3-induced SREBP2 activation drives drug resistance through the promotion of cholesterol biosynthesis in hepatocellular carcinoma. State Key Laboratory of Liver Research (HKU) & Theme-Based Research Scheme Project on Liver Cancer Stemness, 2020.
3. **Mok EH**#, Leung CO#, Lei MM, Lee TK. SREBP2 Activation Drives Drug Resistance through Promotion of Cholesterol Biosynthesis-driven Sonic Hedgehog Signalling (SHH) Pathway in Hepatocellular Carcinoma. The Liver Week 2020 Virtual Conference, 2020.
This presentation was awarded *Free Paper Best Presentation Award*.
4. **Mok EH**, Leung HW, Lee TK. Nuclear Factor (Erythroid-derived 2)-like 2 promotes Tumor-initiating Cell Lineage and Drug Resistance in Hepatocellular Carcinoma. Cold Spring Harbor Asia – Liver Biology, Diseases & Cancer 2019 – Awaji Japan, 2019.

Grant Support

This study was generously financed by,

1. **RGC General Research Fund** (15104119 to T.K. Lee),
2. **Collaborative Research Fund** (C7026-18G),
3. **Research Impact Fund** (R5050-18F), and
4. **The Theme-Based Research Scheme Project** (T12-704/16-R to T.K. Lee, S. Ma, and I.O.L. Ng).

We sincerely thank for the munificent support from the above-mentioned grants.

Table of Contents

CERTIFICATE OF ORIGINALITY	i
Abstract.....	ii
Acknowledgements.....	iv
Publications.....	vi
Conference Presentations and Awards	vii
Grant Support	viii
Table of Contents	ix
List of Figures.....	xiii
List of Tables	xv
List of Abbreviations	xvi
1 Introduction.....	2
1.1 Hepatocellular carcinoma (HCC)	2
1.1.1 Epidemiology and etiology of HCC	2
1.1.2 Treatment regimens for HCC.....	3
1.2 Introduction to Cancer Stem Cells (CSCs).....	10
1.2.1 Functional properties of CSCs	12
1.2.2 Identification of liver CSC markers	13
1.2.3 Signalling pathways of liver CSCs	14
1.2.4 CSCs and drug resistance.....	15
1.3 The Role of Cholesterol Biosynthesis in Cancers	17
1.3.1 Dysregulated cholesterol production in cancer cells.....	17
1.3.2 The relationship between cholesterol and HCC pathogenesis	19
1.3.3 The role of cholesterol metabolism in regulation of CSCs.....	20
1.3.4 Cholesterol and resistance to cancer therapy	21
1.4 Hypothesis and aims of study	23
2 Materials and methods	26

2.1	Materials	26
2.2	Methods	31
2.2.1	<i>In vivo</i> models	31
2.2.2	<i>In vitro</i> models	34
2.2.3	<i>Ex vivo</i> models	35
2.2.4	Functional experiments	35
3	Cholesterol biosynthesis is activated in drug-resistant HCC patient-derived tumor xenografts	43
3.1	Introduction.....	43
3.2	Experimental outline.....	45
3.3	Results.....	46
3.3.1	Successful establishment of sorafenib- and lenvatinib-resistant PDTXs.....	46
3.3.2	Cholesterol biosynthesis is the most upregulated pathway in both drug-resistant PDTXs.....	48
3.3.3	SREBP2 is the upstream regulator of drug-resistant-mediated cholesterol biosynthesis.....	51
3.4	Discussion.....	52
4	Cholesterol biosynthesis is preferentially activated in liver CSCs	56
4.1	Introduction.....	56
4.2	Experimental Outline	58
4.3	Results.....	59
4.3.1	SREBP2-mediated cholesterol biosynthesis is the most upregulated pathway in CSC-enriched hepatospheres	59
4.3.2	Cholesterol homeostasis is increased in CD133 ⁺ liver CSCs, but not in regenerating liver cells	62
4.4	Discussion.....	63
5	SREBP2-mediated cholesterol biosynthesis regulates liver CSCs and has clinical significance.....	66
5.1	Introduction.....	66

5.2	Experimental outline.....	67
5.3	Results.....	70
5.3.1	SREBP2 expression and cholesterol levels in a panel of HCC cells	70
5.3.2	SREBP2 regulates cholesterol biosynthesis genes and cholesterol levels in HCC cells	71
5.3.3	SREBP2 regulates the self-renewal and tumorigenic ability of HCC cells	73
5.3.4	SREBP2 regulates the expression of liver CSC markers in HCC cells	76
5.3.5	SREBP2 regulates the migration and invasion abilities of HCC cells.....	78
5.3.6	Cholesterol biosynthesis is the major effector of SREBP2-mediated CSC signalling.....	80
5.3.7	High cholesterol-utilizing HCC cells exhibit enhanced liver CSC properties.....	83
5.3.8	SREBP2-mediated cholesterol biosynthesis promotes poor prognosis in HCC patients	85
5.4	Discussion.....	87
6	SREBP2-mediated cholesterol biosynthesis is a critical determinant of drug resistance in HCC cells.....	91
6.1	Introduction.....	91
6.2	Experimental outline.....	92
6.3	Results.....	94
6.3.1	SREBP2-mediated cholesterol biosynthesis is activated in drug-resistant HCC cells	94
6.3.2	SREBP2-mediated cholesterol biosynthesis regulates the sensitivity of HCC cells to sorafenib/lenvatinib treatments.....	95
6.3.3	Cleavage of SREBP2 occurs in response to drug treatment	97
6.3.4	CASP3-mediated SREBP2 activation occurs in response to drug treatment.....	99
6.3.5	The clinical relevance of SREBP2 overexpression in drug resistance and its correlation with CASP3 expression	102
6.4	Discussion.....	104
7	SHH signalling cascade is the downstream effector of SREBP2-mediated CSC functions and drug resistance	108

7.1	Introduction.....	108
7.2	Experimental outline.....	110
7.3	Results.....	111
7.3.1	The sonic hedgehog signalling pathway is regulated by SREBP2-mediated cholesterol biosynthesis	111
7.3.2	Abolishment of SHH signalling offsets the SREBP2-mediated CSC properties	112
7.3.3	Oxysterol 25-OHC is critical for SREBP2-mediated SHH signalling activation	114
7.3.4	Correlation among cleaved CASP3, SREBP2 and GLI-1 in HCC clinical samples	116
7.4	Discussion.....	118
8	Simvastatin enhances the effect of drug treatment in <i>organotypic ex vivo</i> human HCC clinical samples and HCC PDTX models.....	121
8.1	Introduction.....	121
8.2	Experimental outline.....	123
8.3	Results.....	124
8.3.1	Simvastatin regulates CSC properties and drug resistance.....	124
8.3.2	Simvastatin enhances the effect of drug treatment in <i>organotypic ex vivo</i> human HCC clinical samples.....	126
8.3.3	Simvastatin enhances the effect of drug treatment in HCC PDTX models	127
8.4	Discussion.....	130
9	Conclusion and future perspective	135
9.1	Conclusion	135
9.2	Future perspective.....	138
	References	141
	Appendices.....	159

List of Figures

Figure 1.1 Treatment options for HCC based on BCLC staging system.....	4
Figure 1.2 Molecular targets of sorafenib.....	7
Figure 1.3 Molecular targets of lenvatinib.....	8
Figure 1.4. Proposed models for CSCs.....	11
Figure 1.5. Key signalling pathways in liver CSCs.....	15
Figure 1.6. Cholesterol biosynthesis in cancer cells.....	19
Figure 3.1. Survival curves adopted from the SHARP and REFLECT clinical trials.....	44
Figure 3.2. Experimental outline in Chapter 3.....	45
Figure 3.3. Tumor growth curves of both drug-resistant and drug-responsive PDTXs.....	47
Figure 3.4. Cholesterol biosynthesis is commonly enriched in both drug-resistant PDTXs...	49
Figure 3.5. Filipin staining of cholesterol deposition in drug-resistant PDTXs.....	50
Figure 3.6. Upstream regulatory analysis of drug-resistant PDTXs.....	51
Figure 4.1. Experimental outline in Chapter 4.....	58
Figure 4.2. SREBP2-mediated cholesterol biosynthesis was upregulated in CSC-enriched HCC populations.....	60
Figure 4.3. SREBP2-mediated cholesterol biosynthesis was enhanced in CSC-enriched hepatosphere population.....	61
Figure 4.4. GSEA enrichment plot of CD133 ⁺ HCC models and regenerating liver cells.....	62
Figure 5.1. Experimental outline in Chapter 5.....	69
Figure 5.2. Expression of SREBP2 and level of cholesterol in a panel of HCC cells.....	70
Figure 5.3. SREBP2 regulates cholesterol gene expression levels and total cholesterol levels.....	72
Figure 5.4. SREBP2 regulates self-renewal and tumorigenicity in HCC cells.....	74
Figure 5.5. SREBP2 regulates expression of CSC markers in HCC cells.....	78
Figure 5.6. SREBP2 regulates the migration and invasion abilities of HCC cells.....	80
Figure 5.7. Cholesterol biosynthesis is the major effector of SREBP2-mediated CSC functions in HCC cells.....	81
Figure 5.8. Cholesterol increases the size and proliferation rate of HCC cells <i>ex vivo</i>	82
Figure 5.9. HCC cells with high cholesterol utilization exhibit enhanced liver CSC properties.....	84
Figure 5.10. SREBP2 overexpression is correlated with poor prognosis.....	86
Figure 6.1. Experimental outline in Chapter 6.....	93

Figure 6.2. Cholesterol and SREBP2 are activated in drug-resistant HCC cells.....	94
Figure 6.3. SREBP2 regulates the sensitivity of HCC cells to sorafenib and lenvatinib.	96
Figure 6.4. Cholesterol attenuates the efficacy of sorafenib and lenvatinib in shSREBP2 HCC cells.	96
Figure 6.5. Short stress induced by drugs activates SREBP2 translocation.	98
Figure 6.6. The activity of CASP3 is upregulated in response to drug challenges in HCC. .	100
Figure 6.7. CASP3 induces SREBP2 activation in response to drug treatment in HCC cells.	102
Figure 6.8. Expression of CASP3 and SREBP2 exhibit clinical significance and are correlated.....	103
Figure 7.1. Experimental outline in Chapter 7.....	110
Figure 7.2. SREBBP-mediated cholesterol biosynthesis drives activation of the SHH signalling pathway.	111
Figure 7.3. Inhibition of the SHH signalling pathway offsets elevated CSC properties via SREBP2-mediated cholesterol biosynthesis.	113
Figure 7.4. Oxysterol 25-OHC drives SREBP2-mediated SHH signalling activation.....	115
Figure 7.5. Cleaved CASP3, SREBP2 and GLI-1 are clinically related to each other.....	117
Figure 8.1. Experimental outline in Chapter 8.....	123
Figure 8.2. Simvastatin regulates liver CSC properties and drug resistance.	125
Figure 8.3. Simvastatin enhances drug efficacy in HCC organoids.	126
Figure 8.4. Simvastatin enhances the drug effect in two HCC PDTX models.....	128
Figure 8.5. Simvastatin suppresses cholesterol deposition in two HCC PDTX models.....	129
Figure 8.6. Combo treatment of simvastatin and sorafenib shows no viable side-effect in PDTX mice.	129
Figure 9.1 Summary of the study.....	138

List of Tables

Table 1.1. Summary of liver CSC markers.....	13
Table 2.1. Cell lines.	26
Table 2.2. Primers for qPCR.....	26
Table 2.3. shRNA and sgRNA sequences.	27
Table 2.4. Antibodies.....	27
Table 2.5. List of other chemicals.....	29
Table 5.1. Primary engraftment of PLC/PRF/5 cells.....	75
Table 5.2. Primary engraftment of MHCC-97L cells.....	75
Table 5.3. Primary engraftment of Hep3B cells.	75
Table 5.4. Primary engraftment of PLC/PRF/5 cells.....	84
Table 8.1. Summary of the main clinical trials using statins in cancer therapy.	133

List of Abbreviations

25-Hydroxycholesterol	25-OHC
27-Hydroxycholesterol	27-OHC
3-Hydroxy-3-methylglutaryl-CoA	HMG-CoA
3-Hydroxy-3-methylglutaryl-CoA reductase	HMGCR
3-Hydroxy-3-methylglutaryl-CoA synthase 1	HMGCS1
3-Hydroxy-3-methylglutaryl-CoA synthase 2	HMGCS2
3,5-Diethoxycarbonyl-1,4-dihydrocollidine	DDC
4',6-diamidino-2-phenylindole	DAPI
7-Dehydrocholesterol reductase	DHCR7
Acetyl-CoA acetyltransferase 1	ACAT1
Acetyl-CoA acyltransferase 2	ACAA2
Adenosine triphosphate	ATP
American Association for the Study of Liver Diseases	AASLD
Barcelona Clinic Liver Cancer	BCLC
Basic-helix-loop-helix leucine zipper	bHLH-Zip
BODIPY-cholesterol	BCHOL
Body mass index	BMI
Bovine serum albumin	BSA
Cancer stem cells	CSCs
Carbon tetrachloride	CCl ₄
Caspase-2	CASP2
Caspase-3	CASP3
Caspase-7	CASP7
Caspase-8	CASP8
Caspase-9	CASP9
Cholesterol-25-hydroxylase	CH25H
Clustered regularly interspaced short palindromic repeats	CRISPR
Complementary DNA	cDNA
Control	CTL
Cyclooxygenase-2	COX-2
Dimethyl sulfoxide	DMSO

Diphosphomevalonate decarboxylase	MVD
Dulbecco's modified eagle medium	DMEM
Endoplasmic reticulum	ER
Epithelial cell adhesion molecule	EpCAM
Epithelial mesenchymal transition	EMT
European Association for the Study of the Liver	EASL
Extreme Limiting Dilution Analysis	ELDA
Farnesyl diphosphate synthase	FDPS
Farnesyl pyrophosphate	FPP
Farnesyl-diphosphate farnesyltransferase 1	FDFT1
Fetal bovine serum	FBS
Fibroblast growth factor receptor	FGFR
Fluorescein isothiocyanate	FITC
Fluorescence activated cell sorting	FACS
Fluorouracil	5-FU
Food and Drug Administration	FDA
Gene set enrichment analysis	GSEA
Geranylgeranyl pyrophosphate	GGPP
GLI family zinc finger 1	GLI-1
GLI family zinc finger 2	GLI-2
GLI family zinc finger 3	GLI-3
Glutathione	GSH
Half-maximal inhibitory concentration	IC50
Hematopoietic stem and progenitor cells	HSPCs
Hepatitis B virus	HBV
Hepatitis C virus	HCV
Hepatocellular carcinoma	HCC
Hepatocyte growth factor	HGF
High-density lipoprotein	HDL
Horseradish peroxidase	HRP
Immunofluorescence	IF
Immunoglobulin G	IgG
Immunohistochemistry	IHC

Ingenuity pathway analysis	IPA
Insulin-induced gene protein 1	INSIG1
Liver X receptors	LXR _s
Low-density lipoprotein	LDL
Low-density lipoprotein receptor	LDLR
Mechanistic target of rapamycin complex 1	mTORC1
Messenger RNA	mRNA
Mitogen-activated protein kinase	MAPK
N-nitrosodiethylamine	DEN
NaCl, EDTA, Tris-Cl, & NP-40	NETN
Non target control	NTC
Non-alcoholic steatohepatitis	NASH
Nonalcoholic fatty liver	NAFL
Nonalcoholic fatty liver disease	NAFLD
Nonobese diabetic/severe combined immunodeficiency	NOD/SCID
Oxidosqualene cyclase	OSC
Patched-1 protein	PTCH1
Patched-2 protein	PTCH2
Patient-derived tumor xenografts	PDX _s
Percutaneous ethanol injection	PEI
Percutaneous radiofrequency ablation	PRA
Phosphate-buffered saline	PBS
Phycoerythrin	PE
Platelet-derived growth factor receptor	PDGFR
Poly (2-hydroxyethyl methacrylate)	PolyHEMA
Programmed death protein 1	PD-1
Programmed death-ligand 1	PD-L1
Propidium iodide	PI
Proprotein convertase subtilisin kexin type 9	PCSK9
Prostate specific antigen	PSA
Quantitative reverse transcription polymerase chain reaction	qPCR
Rapidly accelerated fibrosarcoma	Raf
Reactive oxygen species	ROS

Ribonucleic acid	RNA
Short hairpin RNA	shRNA
Single guide RNA	sgRNA
Site 1 protease	S1P
Site 2 protease	S2P
Smoothened protein	SMO
Sodium dodecyl sulphate	SDS
Sonic hedgehog	SHH
Squalene epoxidase	SQLE
Sterol regulatory element	SRE
Sterol regulatory element-binding protein 2	SREBP2
Sterol-C5-desaturase	SC5D
Suppressor of fused homolog	SUFU
Transarterial chemoembolization	TACE
Transcriptional coactivator with PDZ-binding motif	TAZ
Tyrosine kinase inhibitors	TKIs
Vascular endothelial growth factor receptor	VEGFR
Yes-associated protein	YAP

CHAPTER 1
INTRODUCTION

1 Introduction

1.1 Hepatocellular carcinoma (HCC)

The liver is the central organ that helps to balance most chemical reactions in the body. The liver not only restores homeostasis but also disposes of metabolic wastes through the production of bile. However, similar to other organs, the liver is vulnerable to malignant tumors. Liver cancer is a stepwise consequence arising from chronic inflammation (1). Liver cancer begins with damages either from viral infections, alcohol abuse or unhealthy dietary habits (2). Hepatocellular carcinoma, or HCC, is the major primary liver cancer arising from hepatocytes and accounts for 75%-85% of all liver cancers (3). When HCC develops, liver regeneration fails and mutated and damaged liver tissues are not replenished (4).

1.1.1 Epidemiology and etiology of HCC

HCC was the sixth most frequently diagnosed cancer and third leading cause of cancer related mortality worldwide in 2020 (3). The mortality to incidence ratio is 0.92, indicating that HCC patients have a high risk for mortality (3). Another signature of HCC is that both the incidence and mortality rate are 2 to 3 times higher in men than in women across different countries (3), probably related to the higher chance of exposure to various forms of risk factors in men. Over the past three decades, a threefold increase in the incidence rate was observed in the United States partly owing to the outbreak of hepatitis C virus (HCV) infection from 1945 to 1965, as well as the progressive development of obesity-related fatty liver diseases in developed countries (5). Nevertheless, developing countries are the main contributor of newly diagnosed cases, and China accounts for over 50% of new cases and deaths yearly (6). In Hong Kong, with the most current available data is from 2018, and the trend was consistent with the global setting. Liver cancer was the fifth most common cancer type in Hong Kong, and it was the third leading cause of cancer-related death (7).

Major risk factors contributing to HCC are chronic inflammation with hepatitis B virus (HBV) or HCV, aflatoxin-polluted food, heavy alcoholic intake, obesity, type 2 diabetes and nonalcoholic fatty liver disease (NAFLD) (3). However, the prevalence of viral- and alcohol-induced HCC has been declining recently, while fat-related liver diseases have become the major pathogenic promoters of HCC (8).

The decreased prevalence of HBV and HCV has greatly contributed to the decline in incidence and mortality rates of HCC since the 1990s in many high-risk countries in Eastern and South-Eastern Asia, such as Japan, China and the Republic of Korea (9, 10). Vaccination against HBV and the reduction of exposure to aflatoxin have resulted in great successes for public health. Although the current situation is encouraging, elimination of viral hepatitis remains the central strategy for preventing liver cancers worldwide, as HBV and HCV infections account for over 50% and 20% of liver cancers, respectively (11). The situation is particularly severe in countries without proper medical interventions available. For example, in the African region where HBV predominates as the cause of liver cancer, only 6% of the population has access to HBV vaccines (12).

In contrast, regions with previously low incidence rates have recently experienced a major increase in cases or have maintained case numbers at a high level in recent years. These countries are mainly in developed regions such as Europe and Northern America (10, 13). This observation is consistent with the influence of a high-fat and high-sugar diet that contributes to diabetes and NAFLD in these countries. In particular, the prevalence of NAFLD has increased dramatically to 25% worldwide (14). NAFLD includes a series of diseases, including nonalcoholic fatty liver (NAFL) and nonalcoholic steatohepatitis (NASH), which can develop into cirrhotic liver disease and eventually HCC (15, 16). The prevalence of NASH is estimated to increase by nearly 60% by 2030 in Japan, China, Spain, the UK, Germany, and the USA (17). This has therefore prompted a close investigation of disrupted fat metabolism in liver cancers.

1.1.2 Treatment regimens for HCC

The best curative option for HCC can only be offered when the disease is diagnosed in the early stages (18). Unfortunately, liver cancer is often ‘silent’ and lacks obvious symptoms; thus, HCC is often diagnosed at late stages (19). At that point, few or limited treatment options can be offered. However, as for all cancers, it is still critical to design a treatment regimen for HCC. At present, the American Association for the Study of Liver Diseases (AASLD) and European Association for the Study of the Liver (EASL) have both adopted the Barcelona Clinic Liver Cancer (BCLC) staging system, which is regarded as a standard clinical staging system (20). Treatment options are hence suggested and offered according to different stages in the BCLC staging system (Figure 1.1) (18). Broadly, according to the staging system, patients with Stage

A HCC (very early and early stage) are subject to curative treatment, including hepatic resection, orthotopic liver transplantation, or percutaneous local ablative treatment; patients in Stage B (intermediate stage with asymptomatic but multinodular HCC) are suggested to be treated with transarterial chemoembolization (TACE); and for Stage C patients (progressive, invasive and extrahepatic HCC), targeted therapy with sorafenib and lenvatinib is the only endorsed first-line treatment; however, the effect only lasts for approximately 3 months (21, 22). Unfortunately, for terminal HCC patients, supportive care from family and friends is the only option available.

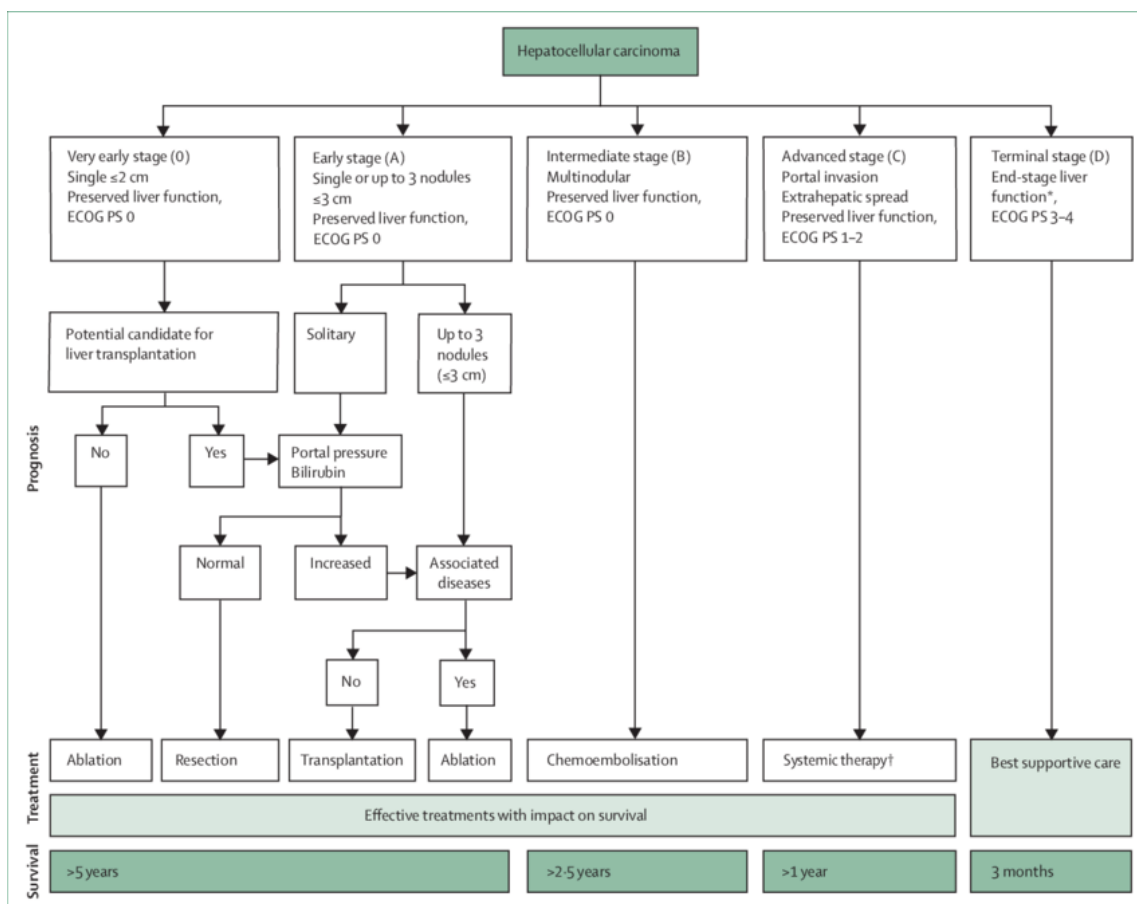


Figure 1.1 Treatment options for HCC based on BCLC staging system.

HCC is classified into five stages of prognosis that are each linked to first-line treatment suggestion. The expected treatment outcome is expressed as median survival corresponding to HCC staging and treatment received. Reused with permission from Forner, Reig, and Bruix’s work (18). Permission conveyed through Copyright Clearance Centre, please see Appendi for the copyright approval letter.

1.1.2.1 Surgical therapy

1.1.2.1.1 Hepatic resection

Upon a thorough evaluation of remaining liver function and tumor extent, this potentially curative method removes the disease-infected part of the liver. However, the disease is still at a high risk for recurrence (over 70%) within a 5-year window because the remaining part of liver tissue can develop HCC (23). Therefore, a precise hepatic reserve assessment is carried out. In Asian countries, the indocyanine green retention test is assessed, whereas clinical traces of portal hypertension and increased levels of bilirubin are monitored in Western countries (24). In addition, a model for end-stage liver disease scoring ≤ 8 indicates that the preserved part of the liver functions well and predicts long-term survival (25). However, such one-off treatment is not recommended for angiogenic and metastatic HCC (26).

1.1.2.1.2 Liver transplantation

Orthotopic liver transplantation removes malignant liver cancer cells and the whole diseased liver; therefore, it is regarded as the best treatment for HCC. However, given its requirement for resources, the ability to obtain a suitable liver for transplantation varies across the globe and by time. Patients who receive liver transplantation have been reported to have a disease-free survival rate as high as 70% (27). Such definitive treatment requires certain criteria for screening eligible patients. The standard has been defined, referred to as the Milan criteria, in which eligible patients have a single tumor that is below 5 cm in diameter or 3 cm in diameter at most, or up to three lesions (28). Alternatives are offered if the patient does not meet the requirements. Local or locoregional therapy can be used to decrease the tumor size until it fits the criteria for organ transplantation (29).

There are two sources of liver donation, living donors and deceased donors. Despite the fact that living donor transplantation is performed worldwide with Asian countries as the pioneer, higher risks of morbidity (5-20%) and mortality (0.3%) are recorded with this manner of transplantation compared to those associated with deceased donor transplantation (30). Moreover, HCC recurrence is also higher with living donor transplantation (20-30%) than with deceased donor transplantation (5-15%) (31). This phenomenon can be explained by the fact that those who receive living donor transplantation have acute liver diseases and can no longer wait for a suitable deceased donor transplant. Even though these patients may receive new and healthy liver tissue, intrinsic oncogenesis contributes to recurrence.

1.1.2.1.3 Local ablation treatment

There are two forms of percutaneous ablation, namely, percutaneous radiofrequency ablation (PRA) and percutaneous ethanol injection (PEI). Ablation is a localized destruction of small tumors, and therefore, it is used for tumors smaller than 3 cm in size. Patients who do not meet the criteria for liver transplantation or resection because of either limited medical resources or liver malfunction are advised to take such alternatives. In terms of completeness of tumor destruction and 3-year recurrence-free survival rate, PRA has a better performance than PEI, 96% versus 90% and 50% versus 40%, respectively (32). However, PEI is better for tumors smaller than 2 cm in diameter and can completely eradicate these tumors (33).

1.1.2.2 Chemotherapy

1.1.2.2.1 Transarterial chemoembolization (TACE)

Cancer requires substantial oxygen levels and nutrients to meet its fast proliferation and growth rate. To achieve this, cancer, particularly HCC, which is a highly vascular cancer, usually develops its own blood vessels that branch out to the main arteries. TACE targets such newly formed tumor blood vessels and is performed by infusion of both chemotherapeutic agents and gel-form particles to block the artery branches and eradicate the cancer. TACE is applied to patients who have HCC showing no angiogenesis or metastasis that cannot be removed by resection. The main advantage of TACE is that it causes minimal disturbance to the blood supply to liver tissues. Additionally, the 2-year overall survival rate in patients receiving TACE has been shown to be twofold higher than that of patients in the control group (34). TACE has also recently been used to reduce tumor size before liver transplantation (35).

1.1.2.3 Molecular targeted therapy

1.1.2.3.1 Sorafenib

If locoregional therapy such as TACE fails to eradicate HCC tumors effectively, chemotherapeutics targeting various molecular signalling pathways can be applied. However, most HCCs cannot be treated with conventional chemotherapies due to dose-dependent toxicities, multidrug resistance and unwanted side effects. Among several multikinase inhibitors, sorafenib was the first FDA-approved drug for treating advanced-stage HCC (21). Sorafenib, an orally active form of a multikinase inhibitor, targets Raf kinase, receptor for

vascular endothelial growth factor (VEGFR) and receptor for platelet-derived growth factor (PDGFR), thus reducing cancer proliferation and the development of blood vessels (Figure 1.2). However, despite its significant effect on inhibiting the growth of cancer cells, sorafenib can only delay the onset of advanced HCC and lengthen the overall survival time by 3 months compared to the placebo-treated control group (10.7 months versus 7.9 months) (21). In addition, sorafenib is associated with multiple side effects, including diarrhoea, hypertension, weight loss and abdominal pain (21).

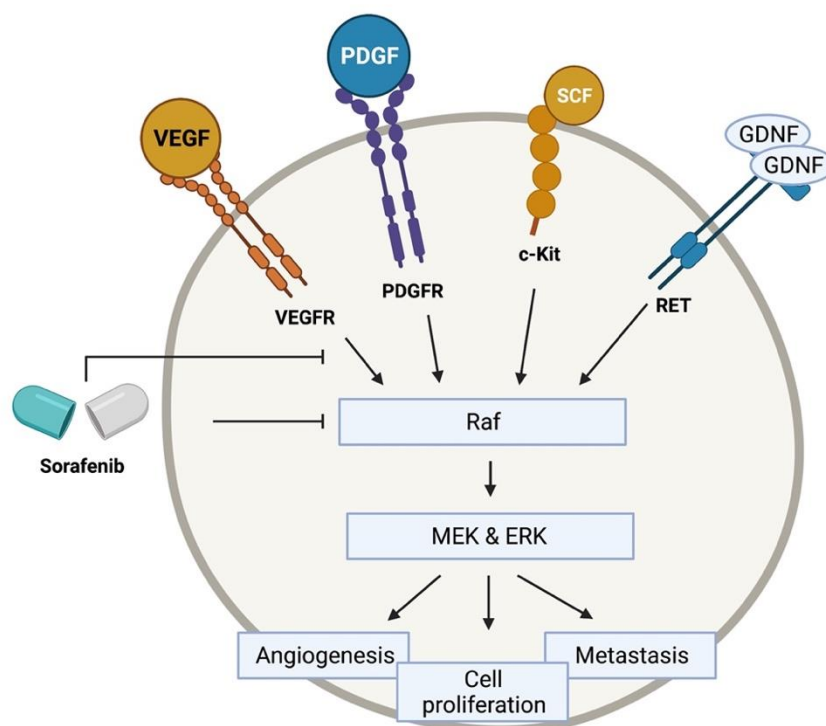


Figure 1.2 Molecular targets of sorafenib.

Sorafenib is a multi-kinase inhibitor that can suppress the activity of VEGFR, PDFGR, c-Kit, & RET so as to decrease angiogenesis, cell proliferation, and metastasis in cancer cells. Referenced with permission from Wilhelm, Carter & Lynch et al.'s work (36). Permission conveyed through Copyright Clearance Centre, please see Appendi for the copyright approval letter.

1.1.2.3.2 Lenvatinib

Lenvatinib, similar to sorafenib, is a multikinase inhibitor targeting VEGFR1-3, fibroblast growth factor receptors FGFR1-4, PDGFR- α , RET and KIT that was shown to be noninferior

to sorafenib in the phase III REFLECT trial (Figure 1.3). In this trial, nearly 960 patients were included from approximately 20 countries in the Asia Pacific, European and North American regions. Patients were divided equally into groups that received either sorafenib or lenvatinib. The median overall survival time with lenvatinib was 13.6 months, and with sorafenib it was 12.3 months (22). The progression-free survival rate, time to progression and objective response rate were also improved with lenvatinib (22). Therefore, lenvatinib was approved for use in the USA, EU and most Asian countries as a first-line targeted therapy in 2018.

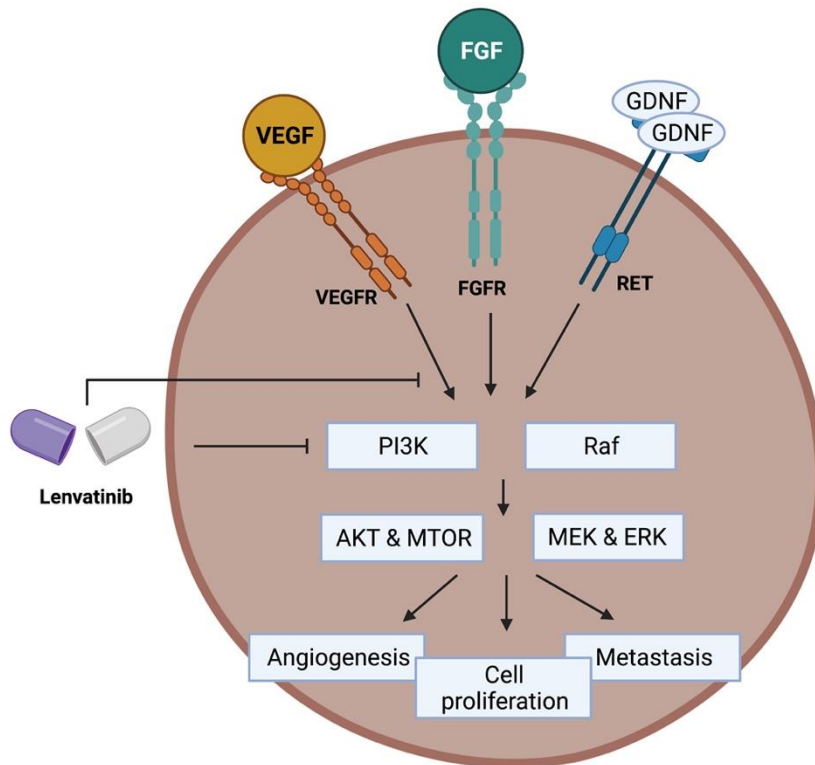


Figure 1.3 Molecular targets of lenvatinib.

Lenvatinib is a multi-kinase inhibitor that can suppress the activity of VEGFR, FGFR, RET & PI3K pathway so as to decrease angiogenesis, cell proliferation, and metastasis in cancer cells. Referenced with permission from Mossenta, Busato, & Baboci et al.'s work (37). Permission conveyed through Copyright Clearance Centre, please see Appendi for the copyright approval letter.

1.1.2.4 Immunotherapy

Immune checkpoint inhibitors have emerged as an unprecedented treatment option for advanced-stage HCC (38). The major principle of this approach is to reboot the patient's own immune system, which is suppressed by cancer cells via PD-1/PD-L1 or CTLA immune checkpoints (39, 40). Once these checkpoints are activated, inhibitory signals are transcribed

in immune cells, thus prohibiting them from killing cancer cells. Nivolumab, a human anti-PD-1 monoclonal antibody, demonstrated a promising result in patients with advanced HCC, where the objective response rate was 15% in the dose-escalation phase and 20% in the dose-expansion phase (41). Although side effects are notably present, the overall profile is still regarded as acceptable when compared to the underlying HCC clinical situation. A recent phase III clinical trial (NCT03434379) evaluating bevacizumab with the PD-L1 inhibitor atezolizumab showed a superior outcome in terms of overall and progression-free survival rates compared to the use of sorafenib alone in advanced HCC patients (42). Because of this exciting result, the FDA has approved the use of bevacizumab in combination with atezolizumab as the first-line treatment for unresectable HCC patients (43).

1.2 Introduction to Cancer Stem Cells (CSCs)

An early diagnosis provides HCC patients with the best chance for survival. Recent developments in stem cell biology have revealed that a small but important component of tumorigenic cell populations, cancer stem cells (CSCs), play a vital role in tumorigenesis (44). This subset of cancer cells has been found to generate new tumors in xenograft transplantation studies (45). Furthermore, since CSCs play a central role in cancer development, drug resistance, metastasis and recurrence, CSCs are a therapeutic target for cancer treatment (46). By recognizing cell surface markers specifically expressed on CSCs, hepatic CSCs have been well characterized and identified. To explain the heterogeneity of cancer cells, two models are suggested (Figure 1.4) (47). One is a stochastic model in which every cell within the tumor population can initiate new tumor tissue due to intrinsic stochastic factors. On the other hand, the hierarchical model states that cancer cells are organized in a hierarchical manner resembling a normal stem cell structure where CSCs sit at the top of the hierarchical structure. Heterogeneity increases each time CSCs replicate, and genetic changes are involved.

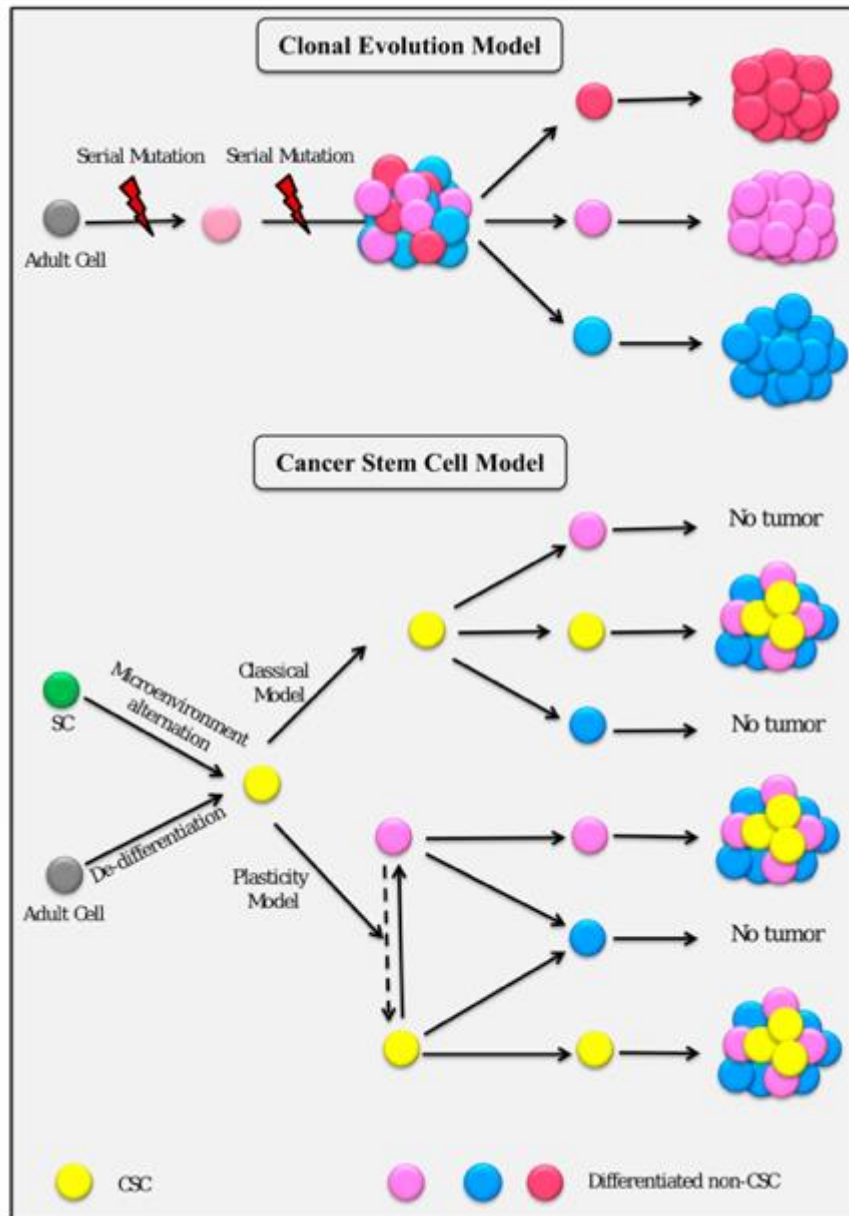


Figure 1.4. Proposed models for CSCs.

In the stochastic model, each individual cell has the ability to develop into new tumor tissues. The heterogeneity of tumors hence comes from the random gene mutation arisen from individual cell. In the hierarchical model, CSC sits at the top of the hierarchy, undergoing asymmetric cell division and differentiating into a new but different offspring cell. But at the same time, the hierarchical model remains vivid when one cancer cell stays undifferentiated so to keep the stemness (47). The figure is adopted from Afify & Seno's work under the permission of Creative Commons Attribution 4.0 International License (47). Please see Appendi for the concerned license.

1.2.1 Functional properties of CSCs

1.2.1.1 Tumorigenicity

Cancer cells have continuously expressed many genes that are promoting stemness properties. Therefore, these stemness-related genes are regarded as oncogenic and granting the cancer cells a nonstop proliferation. For example, SOX2, a stemness transcription factor, is overexpressed and initiating tumor formation in osteosarcoma (48). Meanwhile, the suppression of NANOG, another stemness transcription factor, reduces the cancer stemness and tumor formation in HCC (49). For epithelial cell adhesion molecule (EpCAM)⁺ CSCs, Wnt signalling, which is well known is to maintains tumorigenicity in cancers (50, 51), is highly activated to drive tumorigenesis (51, 52). In addition, CD133⁺ CSCs has activated the Notch signalling pathway to support tumor growth in HCC (53).

1.2.1.2 Self-renewal

In the cancer stem cell model (Figure 1.4), self-renewal ability maintains stemness via driving asymmetric division that allows other daughter cells differentiate but at least one cell stays as cancer stem cell. The current cell lineage tracing techniques provide a solid technical support to identify the origin of CSCs (54). In intestinal cancer, the LGR5⁺ cancer cells not only generate extra LGR5⁺ cells but also produce other intestinal adenoma cell types (55). Interestingly, KRT20⁺ cancer cells are found to be differentiated from LGR5⁺ CSCs and continues to maintain stem cell plasticity in the colorectal cancer (56). Moreover, NOTCH1⁺ CSCs in colon cancer are capable of producing heterogenous progenies but conserved undifferentiated NOTCH1⁺ cells via indefinite self-renewal ability (57).

1.2.1.3 Metastasis

Epithelial-mesenchymal transition (EMT) is a process where epithelial cells acquire mesenchymal features and linked to malignancy, aggressiveness and metastasis (58, 59). Recently, EMT has been correlated to CSCs in tumorigenesis (60, 61). The induction of EMT increases the expression of cancer stemness markers such as SOX2 and NANOG (62). This has further verified in oesophageal squamous cell carcinoma where the SOX expression promotes EMT progression (63). In addition, the progression of EMT has given rise to CD44⁺CD24⁻ mesenchymal cells in oesophageal squamous cell carcinoma with stemness properties for example the self-renewal ability, drug resistance, and migration and invasion (64). Similar phenomenon is also observed in CD44⁺CD24⁻ breast cancer cells where EMT

status enhances invasiveness of CSCs than bulk breast cancer cells (65). Further, hypoxia and inflammation collectively arising in the tumor microenvironment induce EMT in cancer, and hence promoting matrix remodelling and tumor metastasis (66).

1.2.2 Identification of liver CSC markers

By using both functional and cell surface markers, CSCs, a small subset of cancer cells, can be detected and characterized. Functionally, CSCs are a side population with a phenotype that can actively pump the Hoechst 33342 dye (67). In addition, the elevation in aldehyde dehydrogenase activity is regarded as a differentiation tool between normal stem cells and CSCs and can be measured by the ALDEFLUOR assay (68). This special property has been used in HCC in the detection of both normal hepatic progenitor cells and CSCs (69). Recently, HCC cells with reduced reactive oxygen species (ROS) levels and suppressed 26S proteasome activity were characterized as CSCs (70). On the other hand, HCC cells expressing the CD133⁺, CD90⁺, EpCAM, CD13⁺, CD24⁺, CD44⁺ and CD47⁺ markers were regarded as CSCs (Table 1.1).

Table 1.1. Summary of liver CSC markers.

CSC markers	Functions in liver CSCs	References
CD13	Induce sphere formation and tumorigenicity; resistant to fluorouracil (5-FU) and doxorubicin treatment; protect cells from ROS-induced DNA damage	(71, 72)
CD24	Induce sphere formation and tumorigenicity; enhance stemness gene expression, migration and invasion ability; resistant to cisplatin; promote STAT3 signalling and NANOG expression; co-express with CD133 to produce inducible nitric oxide synthase and Notch signalling to enhance secondary tumor formation	(73, 74)
CD44	Induce sphere formation and tumorigenicity; stabilize the c-Met-induced stemness characteristics; resistant to sorafenib	(75)
CD47	Resistant to sorafenib; promote NF-κB signalling to drive expression of cathepsin S	(76, 77)
CD133	Induce sphere formation, tumorigenicity, colony formation, and stemness gene expression	(77)

EpCAM	Induce sphere formation and tumorigenicity; enhance invasive ability, resistant to 5-FU, activate Wnt/ β -catenin signalling, and SALL4 expression (78, 79)
ICAM-1	Induce sphere formation, tumorigenicity and metastases; Form an expression loop with NANOG (80)
LGR5	Induce sphere formation and tumorigenicity; resistant to sorafenib and cisplatin; enhance stemness gene expression; activate Wnt/ β -catenin signalling (81-84)

1.2.3 Signalling pathways of liver CSCs

There are several oncogenic pathways particularly being activated continuously in liver CSCs. Apart from the well known Wnt/ β -catenin and IL-6/STAT3 signalling which support the liver cancer stemness (85, 86), other signalling pathways have also reported to promote liver CSCs (Figure 1.5).

In NF- κ B signalling cascade, CD47, the marker for liver CSC, has played an important role (77). In chemo-resistant hepatospheres, CD47 was found to be preferentially expressed in which the protease cathepsin S was supporting such development. Cathepsin S secreted by CD47⁺ hepatospheres activates PAR2 which in term promotes the nuclear translocation of NF- κ B to further increase the transcription and expression level of cathepsin S itself (76).

Stem cell renewal and differentiation is tightly regulated by hippo signalling (87). Transcription coactivator with PDZ-binding motif (TAZ), the downstream effector of hippo signalling, was predominantly expressed in HCC (88). However, the knockdown of TAZ could alternatively promote the expression of another effector of this pathway, Yes-associated protein (YAP), together with the expression of CD90, the cells were resistant to 5-FU drug challenges (89).

The mitogen-activated protein kinase (MAPK) signalling was activated by extracellular stimuli either by tumor-suppressor proteins such as apoptosis-stimulating protein of p53 or by growth factors such as hepatocyte growth factor (HGF) (90, 91). HGF secreted by cancer-associated fibroblasts transactivates the c-Met receptor and induces downstream MAPK signalling to activate FRA1-mediated transcription of HEY1 to support the cancer initiation properties in liver CSCs (90, 91).

Sonic hedgehog (SHH) pathway has also served an important role in regulating tumorigenesis, invasiveness, and recurrence via maintaining CSCs in HCC (92). In HCC tissues, the mRNA level of SHH signalling molecule, *GLI-1*, was overexpressed and linked to poorer disease-free and overall survival (93). Also, the activation of SHH pathway promoted the expression of CD133 to support HCC development through CSC expansion (94). Our team has previously reported the linkage between NRF2 and SHH signalling cascade in promoting CSC and drug resistance in HCC (95).

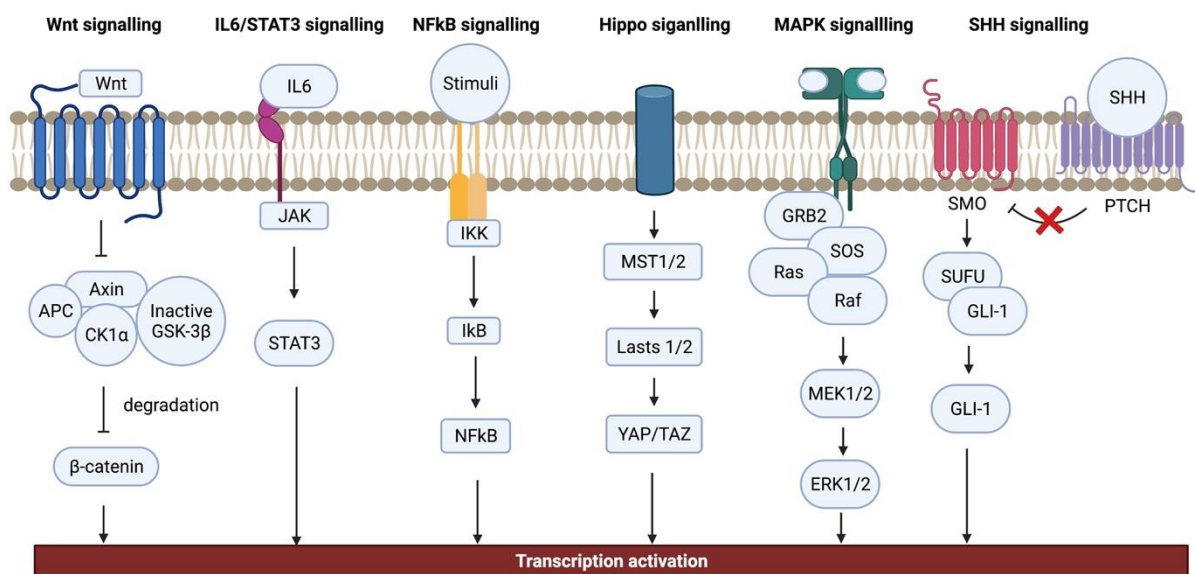


Figure 1.5. Key signalling pathways in liver CSCs.

Wnt/β-catenin and IL-6/STAT3 are the main signalling pathways that promote liver cancer stemness properties. Recent studies have indicated that NF-κB, Hippo, MAPK and SHH signalling pathways are also playing crucial roles in regulating liver cancer stemness. The figure is remade with reference to Tsui, Chan & Ng’s work under the permission of Creative Commons Attribution 4.0 International License (96). Please see Appendi for the concerned license.

1.2.4 CSCs and drug resistance

Having the ability to self-renew and differentiate into heterogeneous populations of cancer cells, CSCs are currently suggested to be responsible for drug resistance in response to therapeutic agents. Although cancer therapy could successfully abolish a bulk of proliferating tumor cells, a subset of persistent CSCs survives as they can induce cell cycle arrest and hence

enter quiescent state (97, 98). In glioblastoma multiforme, a small subset of endogenous tumor cells demonstrating stem-cell properties are in quiescent status and responsible for long-term tumor development. Therefore, this group of cells leads to cancer relapse through inducing transient populations of highly proliferative cells (99). Similarly, in bladder cancer, the label-retaining quiescent CSCs are recruited during the gap periods between chemotherapy cycles and repopulate residual tumors via an unexpected cell expansion, which is similar to the mobilization of tissue-resident stem cells in wound repair (99, 100).

CSCs are responsible to DNA damage induced by radiotherapy and chemotherapy (101, 102). There are several protections against oxidative DNA damage being executed by CSCs. For example, CSCs expressing a high level of CD44, which controls the intracellular level of glutathione (GSH), show an enhanced production for GSH, resulting in a strong protective effect against sorafenib-induced ROS (103). Concomitantly, lower ROS levels have been reported in CSCs and are associated with enhanced free radical scavenging systems that give rise to an increased production of GSH, eventually leading to resistant against radiotherapy-induced ROS (104). In addition, when compared to CD133⁻ tumor cells, CD133⁺ human glioblastoma cells isolated from glioma patient xenografts and primary glioblastoma patient specimens preferentially activate the DNA damage repair checkpoint in response to radiotherapy and hence leading to a more rapid DNA repair (105). Interestingly, the inhibition of Notch pathway with gamma-secretase inhibitors enhances the sensitivity of glioma stem cells to radiation via the suppression of PI3K/AKT activation and also upregulation of truncated apoptotic isoforms Mcl-1, but without affecting the response to DNA damage (106).

In response to oxidative stress and DNA damage, CSCs mediate toxic efflux quickly in HCC (107). Another effect that CSCs contribute to drug resistance is coming from their plasticity (107). Furthermore, some stemness markers and RNAs affiliated with CSCs can be therapeutic targets to address the chemotherapy resistance. For instance, NANOG⁺ CSCs are associated with sorafenib resistance (108), whereas the THOR, a conserved long non-coding RNA, inhibits CSCs and increases HCC sensitivity to sorafenib (109). Moreover, CSCs plasticity promotes HCC molecular and biological diversity, thus leading to a poor prognosis (110). Molecularly, CSC-associated marker DDK1 is suggested to be a prognostic indicator for HCC via CSC analysis (110, 111).

1.3 The Role of Cholesterol Biosynthesis in Cancers

Accumulating evidence has suggested that cholesterol biosynthesis is important in cancer development and hence the its targetable therapeutic implications have been gaining attention in both the prevention and treatment of cancers (112). However, the role of cholesterol remains controversial in tumorigenicity (113). Contradictory, studies have reported that cholesterol in cancer development can be tissue- and cancer-specific (114). Hypercholesteremia could lead to higher risks in breast and prostate cancers (115, 116), but some other prospective cohort analyses show no association (117, 118).

1.3.1 Dysregulated cholesterol production in cancer cells

Cholesterol is mainly synthesized in the liver and intestine, but cancer cells have hijacked the process so to produce more cholesterol either for cell expansion or activation of oncogenic pathways. The *de novo* cholesterol biosynthesis involves more than 20 enzymes that are located in different subcellular compartments in the cell, for example the cytosol, endoplasmic reticulum (ER), or peroxisomes (119) (Figure 1.6). The first step starts from the condensation of two acetyl-CoA molecules to produce one 3-hydroxy-3-methylglutaryl coenzyme A (HMG-CoA). Hence, HMG-CoA reductase (HMGCR), the first limiting enzyme involved in this pathway, converts HMG-CoA to mevalonate (119). Mevalonate is then subsequently converted to farnesyl pyrophosphate (FPP), squalene, and finally cholesterol under a series of enzymatic activities (120). FPP, apart from contributing to cholesterol production, is also the precursor of geranylgeranyl pyrophosphate (GGPP). Both FPP and GGPP drive protein prenylation that is involved in oncogenic proteins activation, such as Ras GTPases (121-123). In addition to HMGCR, recently squalene epoxidase (SQLE) has also been considered to be another rate-limiting enzyme in synthesizing cholesterol (124). The product cholesterol is then secreted into the bloodstream in the form of apolipoprotein complex, and is either embedded as part of the plasma membrane, or used for metabolite production to synthesize bile acids or steroid compounds (125). The synthesis of cholesterol in liver is dominantly regulated by the SREBP2 (126).

SREBP2 has two forms, premature and mature. The former one is synthesized and rest on the ER membrane (127). The activation of SREBP2 requires two proteolytic activities that happen in the Golgi apparatus, where site 1 protease (S1P) and S2P cleave consecutively to free the N-terminal of SREBP2 (127, 128). The N-terminal of SREBP2, or mature SREBP2, now is able

to enter the nuclear and bind to the promoter region of the genes that contain conserved DNA region, called sterol regulatory elements (SRE), hence increasing the transcription level of those genes (129). These genes are particularly involved in the cholesterol biosynthesis, for examples, HMGCR, SQLE, and low-density lipoprotein receptor (LDLR) (129). The activity of mature SREBP2 can also be enhanced by mammalian target of rapamycin complex 1 (mTORC1) via suppressing the nuclear entry of lipin1 which attenuates mature SREBP2 (130). In normal cells, the cholesterol biosynthesis via SREBP2 regulation is a negative-feedback loop: a low intracellular cholesterol level initiates SREBP2 activity while a high intracellular cholesterol level inhibits SREBP2 activity. However, this feedback mechanism is dysregulated in cancer cells: SREBP2 is activated disregard to cholesterol availability (131, 132). In order to process the excessive amount of intracellular cholesterol, cancer cells enhance the expression of acyl-CoA: cholesterol acyltransferase 1 (ACAT1), which converts cholesterol to cholesterol ester that is a storage form of cholesterol in cancer cells. Hence, the stored cholesterol esters are used as a reservoir for rapid cell expansion (133-135). The inhibition of ACAT1 using CP-113818 is shown to decrease migration and progression in breast and prostate cancers (133, 136).

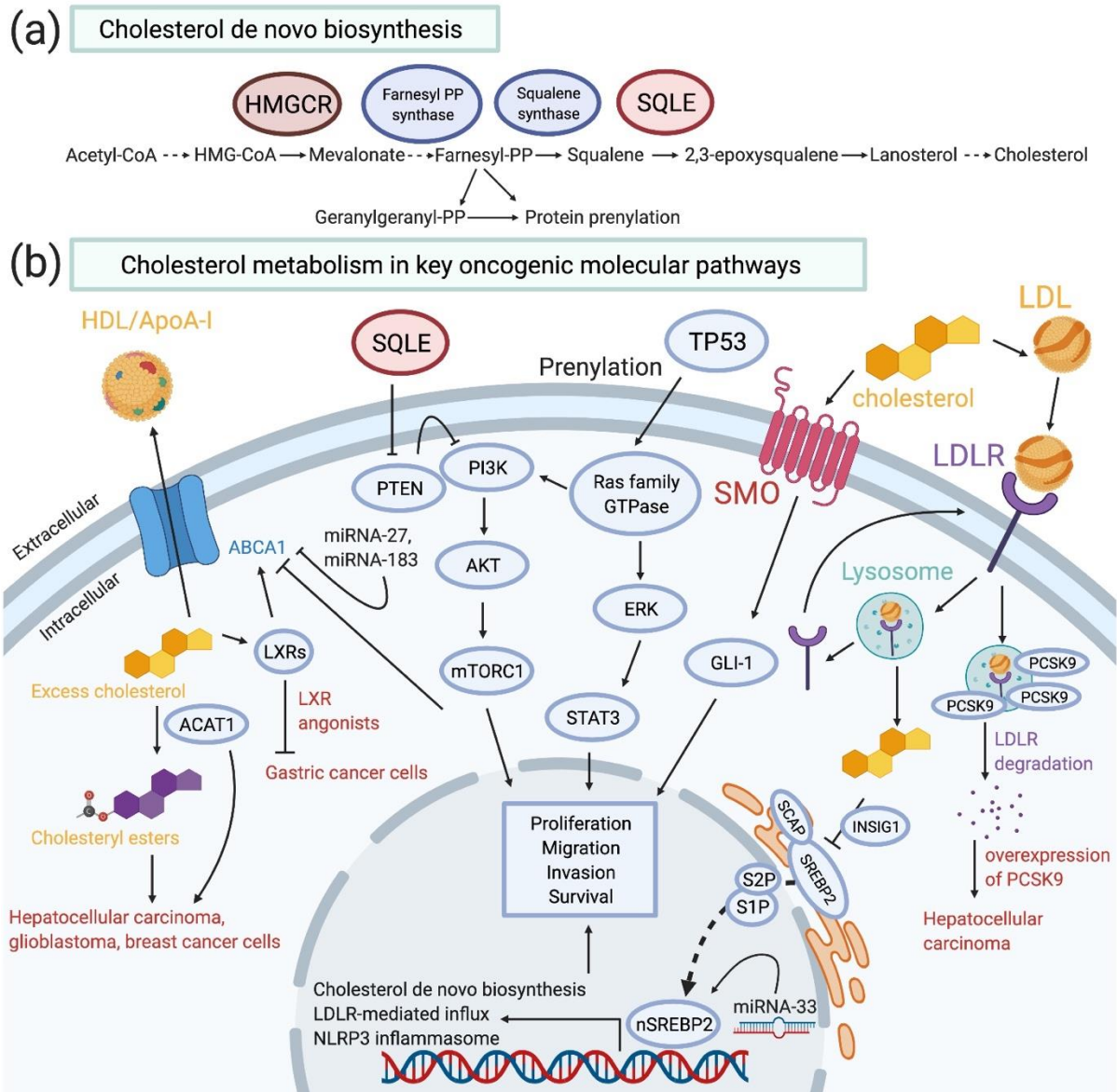


Figure 1.6. Cholesterol biosynthesis in cancer cells.

(A) The simplified *de novo* cholesterol biosynthesis. (B) cholesterol metabolism involved in key oncogenic molecular pathways. The figure is adopted from Mok & Lee's work under the permission of Creative Commons Attribution 4.0 International License (120). Please see Appendi for the concerned license.

1.3.2 The relationship between cholesterol and HCC pathogenesis

HCC is the major malignancy of the liver, which is also the primary site in synthesizing cholesterol and lipoproteins (137). Some studies have revealed that a positive association is linked between hypercholesteremia and HCC, which can be used as a prognostic marker for HCC (138, 139). In children with hepatoblastoma and patients with cirrhosis HCC, total

cholesterol in blood are enhanced dramatically. This situation cannot be seen in patients without HCC (140-142). As discussed before, the elevated cholesterol is most likely due to the overriding of cholesterol biosynthesis in HCC cells (138, 143). However, in an all-inclusive prospective study in Korea including nearly 1.2 million participants, an inverse correlation between cholesterol levels and liver cancer incidence has been observed (144). Also, the HBV- and HCV-induced HCC patients show decreased cholesterol, high-density lipoprotein (HDL)-cholesterol and LDL-cholesterol when compared to those in the normal counterparts (145, 146). Meanwhile, low serum LDL-cholesterol levels are related to increased risk of HCC mortality (147). In addition, a low serum cholesterol levels (< 100 mg/dL) in the patients before operative or liver transplant shows a lower disease-free survival when compared to those patients with high serum cholesterol levels (> 100 mg/dL) (148). Similarly, in Taiwan, poor prognosis is observed in patients with low BMI and serum cholesterol in comparison to those patients with relatively high BMI and serum cholesterol after operative surgery (149).

Hence, current clinical and preclinical studies show a strong connection between alterations in serum cholesterol levels and HCC. Despite of some studies have suggested that an inverse correlation between blood cholesterol and HCC incidence and development, it is rarely that high cholesterol levels would inhibit HCC onset since one of the results of HCC is to produce high amount of cholesterol. It is therefore crucial to study the role of elevated cholesterol level because of the contributing factors prior to HCC initiation, such as an unhealthy diet or diabetes, at different research levels.

1.3.3 The role of cholesterol metabolism in regulation of CSCs

As mentioned in Section 1.2, CSCs have been suggested to play an important role in tumor initiation, recurrence and chemoresistance, in which dysregulated cholesterol metabolism has been shown to be involved (150). Although CSCs are a small subset of cancer cells, a growing body of evidence indicates that the utility of CSCs can explain the failure of current conventional chemotherapy due to the development of resistance to the drugs over time that eventually leads to tumor relapse (151). Therefore, by understanding the correlation between CSC and cholesterol biosynthesis may provide new therapeutic regimen in treating cancers.

By comparing the expression profiles between anchorage-independent tumorspheres and their differentiated counterparts using global genome expression microarray, cholesterol biosynthesis has scored the top five out of 15 homeostatic pathways, demonstrating the

abnormal regulation of cholesterol to support tumor formation via CSCs propagation (152). Likewise, LDL-cholesterol is shown to regulate stemness properties in colorectal cancer cells, including spheroid formation ability, stemness gene expression and migration ability, via MAPK pathway activation (153). Furthermore, genes involved in the superpathway of cholesterol biosynthesis are found to be overexpressed in patient-derived glioblastoma CSC-enriched sphere cells by comparing the RNA sequencing data to the differentiated counterparts, for example farnesyl diphosphate synthase (FDPS) and hydroxymethylglutaryl-CoA synthase (HMGCS). Therefore, the administration of FDPS inhibitors, alendronate and zoledronate, abolished the glioblastoma progression (154). Moreover, metformin, an antidiabetic drug, is demonstrated to lower cellular cholesterol level and hence attenuating the stemness properties in breast cancer cells (155). Similarly, metformin suppresses EpCAM⁺ HCC cells and hence the tumor proliferation (156). Interestingly, excessive amount of cholesterol can inactivate Lpcat3, which is responsible for producing polyunsaturated phospholipid and therefore driving stem cell proliferation in intestinal cancer (157). The inhibition of Lpcat3 or overexpression of SREBP2 hence promotes intestinal tumor formation in *Apc^{min}*-induced tumor mice (157).

1.3.4 Cholesterol and resistance to cancer therapy

One of the major difficulties in cancer therapy is that patients would develop resistance to radiotherapy or chemotherapy. Since cholesterol and its metabolites serve as an energy reservoir for cancer cell proliferation and differentiation, cholesterol has therefore been linked to treatment failure. In HCC, the increase of mitochondrial cholesterol levels confers chemoresistance (158). The mechanism is further explained in another study: a toxic oxysterol which is the oxygenated form of cholesterol, 7-ketocholesterol, renders the efficacy of doxorubicin through upregulation of P-glycoprotein via the PI3K/mTOR signalling pathway (159). Another oxysterol, 25 hydroxycholesterol (25-OHC), decreases the chemotherapeutic drug efficacy in both *in vitro* and *in vivo* in gastric cancer model (160). Even when the endogenous cholesterol biosynthesis is diminished through the downregulation of FDPS and OSC, which are two enzymes involved in synthesizing cholesterol, chemo-resistant ovarian cancer cells increase the cholesterol uptake by enhancing the LDLR expression (161). In addition, the cholesterol has enhanced the expression of ABCG2 and MDR1, which are both drug efflux pump, along with the expression of liver X receptors (LXRs), which is the cholesterol receptor, and hence reducing the cisplatin and paclitaxel efficacy in ovarian cancer

(162). Moreover, the overexpression of genes involved in cholesterol biosynthesis conveys resistance to oestrogen deprivation in oestrogen receptor⁺ breast cancer (163). The enhanced cholesterol biosynthesis is also linked to poorer survival rate in breast cancer patients (164). In chronic myeloid leukaemia cells, the overexpression of ACAT1 has rendered the imatinib efficiency due to the accumulation of cholesterol esters (165). In lung adenocarcinoma, treatment of cholesterol inhibits the cytotoxic potential induced by oxaliplatin or carboplatin (166). Meanwhile, the treatment of LDL-cholesterol also decreases sorafenib-induced HCC cell death (167). Taking all together, it is unarguably that cholesterol has played a crucial role in developing resistance to cancer therapeutic options. However, the underlying mechanism need further research so as to better understand if cholesterol of its metabolites directly or indirectly hampers the drug efficacy.

1.4 Hypothesis and aims of study

HCC is often diagnosed at an advanced stage, and surgical removal is not feasible. Unresectable HCC is hence treated with TACE and systemic tyrosine kinase inhibitor (TKI) therapy. However, the intrinsic plasticity of HCC limits its response rate to TACE. Despite the significant primary effects of sorafenib and lenvatinib, patients eventually develop acquired drug resistance. It is therefore important to investigate the mechanisms driving acquired drug resistance in HCC. Combination treatment may serve as a better therapeutic strategy to prolong the survival of HCC patients.

Recently, accumulating evidence has suggested the existence of CSCs, which are crucial factors involved in therapeutic resistance. CSCs contribute to cancer progression via the promotion of tumorigenicity, metastasis and angiogenesis. Disrupted metabolic pathways allow for an enormous influx of energy and materials that help cancer cells divide and proliferate. The surviving repopulated cancer cells are hence resistant to drug interventions. Despite the successful identification of CSCs via phenotypic and functional methods, eradicating CSCs remains an unprecedented challenge.

To mimic the clinical situation of acquired drug resistance, sorafenib- and lenvatinib-resistant HCC PDTXs have been developed *in vivo* via a series of administrations of corresponding drugs. RNA sequencing analysis revealed that cholesterol biosynthesis is highly activated in the resistant clones. This finding is consistent with CSC-enriched HCC hepatospheres and HCC drug-resistant cells. Through different verification methods, such as immunofluorescence staining and western blotting analysis, SREBP2, which is the master regulator of cholesterol biosynthesis, is found to be highly upregulated in these cells. Therefore, we hypothesize that SREBP2-mediated cholesterol biosynthesis plays an important role in acquired drug resistance in HCC.

On the other hand, SREBP2 is known to be cleaved by CASP3 during apoptosis, which is a constant occurrence in HCC tumors during drug treatment. This finding prompted us to determine whether CASP3 indeed plays an unidentified apoptotic role by regulating SREBP2-mediated cholesterol biosynthesis and whether drug resistance is acquired during prolonged challenges.

Cholesterol has different metabolic functions inside the body. One of these important physiological roles is to act as a precursor for other sterol compounds that activate stemness-related pathways, such as SHH signalling. This prompts the investigation of the downstream effector of the CASP3-SREBP2-cholesterol signalling cascade.

Finally, the therapeutic implications of targeting cholesterol were examined. The FDA has approved statins as cholesterol-lowering drugs for patients with cardiovascular diseases. Thus, we investigate whether the combination of statins and TKIs could create synergistic effects in treating cancers.

In summary, the specific aims are as follows:

1. To understand the molecular mechanism of how cancer cells acquire drug resistance
2. To investigate the potential role of SREBP2-mediated cholesterol biosynthesis in the regulation of drug resistance in HCC by augmenting liver CSCs
3. To reveal the nonapoptotic role of CASP3 in regulating SREBP2-mediated cholesterol biosynthesis
4. To elucidate the downstream effector of any sterol compounds that activate survival signalling pathways in this CASP3-SREBP2-cholesterol cascade
5. To evaluate the therapeutic implications of targeting cholesterol biosynthesis in combination with TKI treatment to cure HCC

CHAPTER 2
MATERIALS AND METHODS

2 Materials and methods

2.1 Materials

Table 2.1. Cell lines.

Cell line	Pathological condition	Source/Vendor
HEK293T	Human embryonic kidney cells	Invitrogen, Thermo Fisher Scientific (Waltham, Massachusetts, USA)
HEK293FT	Human embryonic kidney cells	American Type Culture Collection (Manassas, Virginia, USA)
MIHA	Immortalized liver cells	A gift from Dr. J.R. Chowdhury, Albert Einstein College of Medicine, USA
PLC/PRF/5	HCC	Japan Cancer Research Bank (JCRB0406)
MHCC-97L	HCC	Liver Cancer Institute, Fudan University, China
Hep3B	HCC	American Type Culture Collection (Manassas, Virginia, USA)

Table 2.2. Primers for qPCR.

Gene	Forward primer (5'-3')	Reverse primer (3'-5')
SREBP2	CCCTGGGAGACATCGACGA	CGTTGCACTGAAGGGTCCA
HMGCR	TGATTGACCTTTCCAGAGCAAG	CTAAAATTGCCATTCCACGAGC
LDLR	TCTGCAACATGGCTAGAGACT	TCCAAGCATTCGTTGGTCCC
INSIG1	CCTGGCATCATCGCCTGTT	AGAGTGACATTCTCTGGATCTG
MVD	TGAAGGACAGCAACCAGTTC	CAGGAGATGGCATTGAGGTAAG
FDPS	AGGAATTGATGGCGAGAAGG	CCCAAAGAGGTCAAGGTAATCA

Table 2.3. shRNA and sgRNA sequences.

Gene	Forward primer (5'-3')
NTC	CCGGTTGTGCTCTTCATCTTGTGCGGCAACAAGATGAAGAGC ACCAATTTTTG
shSREBP2#66	CCGGGCAACAACAGACGGTAATGATCTCGAGATCATTACCGTCT GTTGTTGCTTTTT
shSREBP2#68	CCGGGACCTGAAGATCGAGGACTTTCTCGAGAAAGTCCTCGATC TTCAGGTCTTTTT
CTL	GATACGTCGGTACCGGACCG
sgSREBP2#03	GGGCGAGCGAAGCGGTGCGT
sgSREBP2#04	GCACCGCTTCGCTCGCCCAT

Table 2.4. Antibodies.

Target	Experiment	Condition	Vendor
	Western blot	1:500	BD Biosciences (San Jose, California, USA)
SREBP2	Immunofluorescence	1:50	Abcam (Cambridge, UK)
	Immunohistochemical staining	1:100	Abcam (Cambridge, UK)
CASP3	Western blot	1:1000	Abcam (Cambridge, UK)
	Immunohistochemical staining	1:100	Cell Signalling Technology (Danvers, Massachusetts, USA)
GLI-1	Western blot	1:1000	Cell Signalling Technology (Danvers, Massachusetts, USA)
	Immunohistochemical staining	1:100	Oncogene Pharma (Shah Alam, Selangor, Malaysia)

SHH	Western blot	1:1000	Cell Signalling Technology (Danvers, Massachusetts, USA)
SUFU	Western blot	1:1000	Cell Signalling Technology (Danvers, Massachusetts, USA)
PTCH1	Western blot	1:1000	Cell Signalling Technology (Danvers, Massachusetts, USA)
PTCH2	Western blot	1:1000	Cell Signalling Technology (Danvers, Massachusetts, USA)
β-ACTIN	Western blot	1:5000	MilliporeSigma (Burlington, Massachusetts, USA)
HRP-conjugated mouse IgG	Western blot	1:1000 or 1:6000	GE Healthcare (Chicago, Illinois, USA)
PE mouse anti- human CD47	Flow cytometry	6 µl/test	BD Biosciences (San Jose, California, USA)
PE mouse anti- human CD24	Flow cytometry	6 µl/test	BD Biosciences (San Jose, California, USA)
PE mouse anti- human CD133	Flow cytometry	6 µl/test	BD Biosciences (San Jose, California, USA)
PE mouse IgG1, κ isotype control	Flow cytometry	6 µl/test	BD Biosciences (San Jose, California, USA)
PE mouse IgG2a isotype control	Flow cytometry	6 µl/test	BD Biosciences (San Jose, California, USA)

Table 2.5. List of other chemicals.

Chemicals	Vendor
Lenvatinib	Selleckchem (Houston, Texas, USA)
Sorafenib	LC Laboratories (Woburn, Massachusetts, USA)
Simvastatin	Calbiochem (San Diego, California, USA)
Dimethyl sulfoxide (DMSO)	MilliporeSigma (Burlington, Massachusetts, USA)
Puromycin	MilliporeSigma (Burlington, Massachusetts, USA)
Lipofectamine™ 2000 transfection reagent	Invitrogen™, Thermo Fisher Scientific (Waltham, Massachusetts, USA)
Annexin V-FITC reagent	BioVision (Milpitas, California, USA)
10X Annexin V binding buffer	BD Biosciences (San Jose, California, USA)
Methyl cellulose	MilliporeSigma (Burlington, Massachusetts, USA)
Matrigel™ Matrix	Corning (Corning, New York, USA)
Polybrene	MilliporeSigma (Burlington, Massachusetts, USA)
Insulin	MilliporeSigma (Burlington, Massachusetts, USA)
B27™	Gibco™, Thermo Fisher Scientific (Amarillo, Texas, USA)
Poly (2-hydroxyethyl methacrylate) (polyHEMA)	MilliporeSigma (Burlington, Massachusetts, USA)
TRIzol® Reagent	Invitrogen™, Thermo Fisher Scientific (Waltham, Massachusetts, USA)
PhosSTOP™	Roche (Basel, Switzerland)

cOmplete™ EDTA-free protease inhibitor cocktail	Roche (Basel, Switzerland)
Bovine serum albumin (BSA)	MilliporeSigma (Burlington, Massachusetts, USA)
Crystal violet	MilliporeSigma (Burlington, Massachusetts, USA)
BrightGreen 2X qPCR MasterMix-ROX	Applied Biological Materials (Vancouver, Canada)
WesternBright ECL HRP substrate	Advansta (San Jose, California, USA)
Z-DEVD-FMK (HY-12466)	MedChemExpress (Monmouth Junction, New Jersey, USA)
GANT61 (Synonyms: NSC 136476) (HY-13901)	MedChemExpress (Monmouth Junction, New Jersey, USA)

2.2 Methods

2.2.1 *In vivo* models

2.2.1.1 Patient samples

Paraffin-embedded specimens from 50 anonymous HCC patients who were diagnosed of primary HCC were achieved from the Sun Yat Sen University Cancer Centre. Complete clinical and pathological data were acquired as well. Patients received no chemotherapy nor radiotherapy before the surgery. The use of data was granted by the Institute Research Medical Ethics Committee.

91 randomly retrieved HCC samples from patients who received curative resection then sorafenib treatment from December 2008 to May 2010 were achieved from the Eastern Hepatobiliary Surgery Hospital. Characteristics of these patients could be found in the previous literature (168). Sorafenib was given at a dose of 400 mg twice a day. The use of data was approved by the Ethical Committee of the Second Military Medical University.

2.2.1.2 Patient derived tumor xenografts (PDXs)

PDX#1 and PY003 HCC patient tissues were obtained from patients underwent hepatectomy respectively at Queen Mary Hospital, Hong Kong and Pamela Youde Nethersole Easter Hospital, Hong Kong. These samples were from patients who received no previous local or systemic treatment prior to surgery. Consent was adopted and the study was approved by the ethics committee of the University of Hong Kong. The use of human clinical samples was granted by the Institutional Review Board of the University of Hong Kong/ Hospital Authority Hong Kong West Cluster.

2.2.1.3 Establishment of drug-resistant PDXs

Both drug-resistant PDXs were established in NOD/SCID mouse upon continuous feeding of either sorafenib or lenvatinib. For sorafenib-resistant PDX#1, it was successfully established after three rounds of 100 mg/kg/day sorafenib administration orally. Each round contained 31 days and the tumour was transferred to the secondary and tertiary mouse recipient.

For lenvatinib-resistant PY003, it was established upon four rounds of 30 mg/kg/day lenvatinib administration orally. Identical treatment protocol was applied to the secondary and tertiary

mouse recipient., yet for the quaternary mouse recipient was fed for 16 days due to the large tumour size.

Successful establishment of drug resistance was evidenced by an observation that there was no tumour suppression effect upon drug treatment when compared to the mock control arm. The protocol was approved and performed in accordance with the guidelines for the use of live animals in teaching and research at the Hong Kong Polytechnic University.

2.2.1.4 Human and mouse tissue processing for isolation of single cells

In order to obtain single cells, human and mouse tissue samples harvested from *in vivo* experiments were first cut into smaller pieces which were transferred to gentleMACS C tube (Miltenyi Biotec, Bergisch Gladbach, Germany) supplemented with 4 µg/ml Liberase and 20 µg/ml DNaseI. The mixtures were then dissociated in the gentleMACS dissociator (Miltenyi Biotec, Bergisch Gladbach, Germany) according to manufacturer' instructions.

2.2.1.5 Immunocompetent mouse models

In hydrodynamic tail vein injection mouse model, a mixture of plasmids were injected into six-to-eight-week-old male wild-type C57BL/6N mice according to the procedure previously described (169). In short, 7.5 µg of plasmids compassing human AKT1 (myristoylated AKT1) and human neuroblastoma Ras viral oncogene homolog (N-RasV12) together with sleeping beauty transposase in a ratio of 25:1 were aliquoted in a 2 ml saline (0.9% sodium chloride), filtered through 0.22 µm filter, and injected into the lateral tail vein of the mice in five to seven seconds.

For chemical carcinogenesis mouse model, N-nitrosodiethylamine (DEN) was intraperitoneally injected into male wild-type C57BL/6N in a concentration of 1 mg/kg at the age of two weeks. From age of eight weeks, carbon tetrachloride (CCl₄) was as well injected intraperitoneally of 0.2 ml/kg twice a week for a further 16 weeks. Mice were sacrificed and livers were harvested for histological analysis at the end of the experiment.

In liver regeneration model, 0.1% 3,5-diethoxycarbonyl-1,4-dihydrocollidine (DDC) was fed to six-to-eight-week-old male wild type C57BL/6J for three weeks. The protocol was adopted

by and performed in accordance to the guidelines for the use of live animals in teaching and research at the University of Hong Kong.

2.2.1.6 *In vivo* drug treatment assay

Flanks of BALB/C nude mice were injected with either 1×10^6 PY003 and 0.5×10^6 sorafenib-resistant PDTX#1 cells according to the cell dissociation protocol. Once the tumour reached approximately to a size of 7 mm (length) x 7 mm (width), the mice were randomly separated into four groups: DMSO, sorafenib (30 mg/kg), DMSO and simvastatin (4 mg/kg), and the combined treatment group (sorafenib and simvastatin). Simvastatin was dissolved in water while sorafenib was first dissolved in DMSO then diluted in water. Mice were treated in a daily basis according to their treatment orally. Tumour volume and body weight were measured every three days. Using the formular: $\text{volume (cm}^3\text{)} = \text{length} \times \text{width}^2 \times 0.5$, tumour volume was calculated. Upon 21 days, mice were harvested to obtain tumours for further analysis. This study protocol was approved by and performed in accordance to the guidelines for the use of live animals in teaching and research in the Hong Kong Polytechnic University. No specific randomization method was used and the sample size was chosen based on the significant *p*-values.

2.2.1.7 Tumorigenicity assay

In order to evaluate *in vivo* tumorigenicity, human HCC cells were suspended in a 1:1 ratio of culture medium and Matrigel™ Matrix, and subcutaneously injected into the flanks of the NOD/SCID mice in order to induce tumour xenografts. In brief, each mouse received two injections on each side, in total four injections per mouse, from each experimental group (NTC vs shSREBP2, CTL vs sgSREBP2, and BCHOL^{High} vs BCHOL^{Low}). Tumours were harvested at the end of the experiment. Tumour-initiating cell frequency was calculated using Extreme Limiting Dilution Analysis (ELDA) (170). This study protocol was approved by and performed in accordance to the guidelines for the use of live animals in teaching and research in the Hong Kong Polytechnic University. No specific randomization method was used and the sample size was chosen based on the significant *p*-values.

2.2.2 *In vitro* models

2.2.2.1 Cell culture

Human cell lines were cultured in Dulbecco's Modified Eagle Medium (DMEM) with high glucose supplemented with 10% heat-inactivated fetal bovine serum (FBS), 100 mg/mL penicillin G, and 50 µg/mL streptomycin at 37°C in a humidified chamber containing 5% CO₂. Lentiviral infected cells were cultured in complete DMEM medium supplemented with 2 µg/mL puromycin while CRISPR infected cells were maintained in medium supplemented with 0.2 µg/mL puromycin and 5 µg/mL blasticidin. Cells were used within 20 passages after thawing. Culturing medium was refreshed every two to three days and cells were passaged every three to four days. All cell lines used in this study were obtained between 2013 to 2016, regularly authenticated by morphologic observation and tested for absence of mycoplasma contamination (MycoAlert™, Lonza, Basel Switzerland).

2.2.2.2 Lentiviral-based transfection knockdown

Plasmids expressing shSREBP2 RNA were cloned into the pLKO.1 vector (Addgene, Watertown, Massachusetts, USA). Clone ID of the two shRNAs directed against SREBP2 are: TRCN0000020666 and TRCN0000020668. Scrambled shRNA non target control (NTC) was purchased from Sigma-Aldrich (St. Louis, Missouri, USA).

2.2.2.3 Overexpression of SREBP2 by CRISPR activation system

Upregulation of SREBP2 was achieved using Edit-R transcriptional activation system (Dharmacon™, Lafayette, Colorado, USA). In brief, Hep3B cells were first transfected to stably express dCas9-VP64-p65-Rta (dCas9-VPR) protein. The stable cells were then subsequently transduced of lentiviral sgRNAs directed against the promoter region of SREBP2. Product identification of the two sgRNAs directed against SREBP2 are as follow: SVC18111602 1-B-03 and SVC18111602 1-B-04.

2.2.2.4 Establishment of drug-resistant HCC cells

Sorafenib- and lenvatinib-resistant PLC/PRF/5 and MHCC-97L cells were established by continuous administration drug of gradually increasing concentration. For sorafenib-resistant clones, cells were trained up to 10 µM, while for lenvatinib-resistant clones, cells were trained

up to 30 μ M. Mock controls were produced by giving same volume of DMSO to the cells during the development of resistant cells.

2.2.3 *Ex vivo* models

2.2.3.1 Organoid culture

Patients' specimens from which received no previous local or systemic interventions were obtained at Queen Mary Hospital, Hong Kong. Consents were granted from all patients before the collection of liver tissues and the study was adopted by the ethics committee of the University of Hong Kong. Particularly for organoid culturing condition, cells were isolated and cultured according to published protocol (171).

2.2.3.2 CellTiter-Glo® cell viability assay

CellTiter-Glo® luminescent cell viability assay (Promega, Madison, Wisconsin, USA) was used to evaluate the cell viability in organoids after the treatment of sorafenib or lenvatinib and/or in combination of simvastatin for six days, according to the manufacturer's instruction. The experiments were repeated at least three times independently.

2.2.4 Functional experiments

2.2.4.1 Sphere formation assay

HCC cells were seeded on a pre-coated polyHEMA 24-well plate. Culturing medium was based at 0.25% methyl cellulose in DMEM/F12 medium, supplemented with 4 μ g/mL insulin, B27TM. One hundred microliters of fresh medium was applied every two days for total eight to ten days. The spheroids were harvested for subsequent analysis of SREBP2 expression level.

2.2.4.2 Limiting dilution assay

HCC cells were seeded in a serial dilution manner onto a 96-well plate pre-coated with polyHEMA. Sphere formation was scored after eight to twelve days under a phase contrast microscope. The frequency of spheroid-forming stem cell was calculated using the ELDA (170). The experiments were performed at least three times independently.

2.2.4.3 Migration and invasion assays

HCC cells were seeded on a transwell chamber (Merck Millipore, Burlington, Massachusetts, USA) of 8 µm pore size. Particularly for invasion, transwells were precoated with Matrigel™ Matrix. Inside the chamber, the culturing condition was serum free while outside the chamber, the condition was a complete medium which acted as a chemoattractant for the HCC cells. Cells that had invaded through the membrane and/or Matrigel™ Matrix to the outer chamber were fixed with 2% PFA in PBS and stained with crystal violet. Photographs of five randomly selected fields were captured and counted using ImageJ.

2.2.4.4 RNA extraction and quantitative PCR (qPCR) analysis

Total RNA was extracted using TRIzol reagent while complementary DNA (cDNA) was synthesized using PrimeScript RT Reagent Kit (Takara Bio, Kusatsu, Shiga, Japan), both following manufacturers' instruction. Detection was performed on QuantStudio™ 7 Flex Real-Time PCR System (Applied Biosystems™, Thermo Fisher Scientific, Waltham, Massachusetts, USA) under BrightGreen 2X qPCR Master Mix with primers specific to the genes of interest. The sequences of the primers were provided in Table 2.2. Relative expression differences were calculated using $2^{-\Delta\Delta CT}$ method against β -ACTIN.

2.2.4.5 Western blot analysis

Total proteins were extracted using NETN lysis buffer supplemented with protease inhibitor and phosphatase inhibitor or direct lysis using 2X SDS. The lysates were loaded onto an SDS-polyacrylamide gel and separated by gel electrophoresis. After the completion in gel running, the proteins were transferred to a polyvinylidene difluoride membrane. Primary antibodies being used were: SREBP2 (1:500, #557037, BD Pharmingen, San Jose, California, USA), GLI-1 (1:1000, #3538, Cell Signalling Technology, Danvers, Massachusetts, USA), SUFU (1:1000, #2520, Cell Signalling Technology, Danvers, Massachusetts, USA), SHH (1:1000, #2207, Cell Signalling Technology, Danvers, Massachusetts, USA), PTCH1 (1:1000, #2468, Cell Signalling Technology, Danvers, Massachusetts, USA), PTCH2 (1:1000, #2470, Cell Signalling Technology, Danvers, Massachusetts, USA) and β -ACTIN (1:5000, #A5316, Sigma-Aldrich, St. Louis, Missouri, USA). After overnight incubation at 4°C, secondary antibodies conjugated with horseradish peroxidase either anti-mouse or anti-rabbit were applied to the membrane. Signals were visualized using enhanced chemiluminescence method.

2.2.4.6 Flow cytometry

2.2.4.6.1 CSC surface markers analysis

PE-conjugated CD47 (BD Biosciences, San Jose, California, USA) and CD133 (BD Biosciences, San Jose, California, USA) antibodies were used to detect the surface marker expressed on HCC cells. In brief, the staining lasted for 30-60 minutes at 4°C with 2% FBS. Isotype-matched immunoglobulins served as controls. Samples were subjected to BD Accuri C6 flow cytometer (BD Biosciences, San Jose, California, USA) and analysed in Flowjo™ (BD Biosciences, San Jose, California, USA).

2.2.4.6.2 Annexin-V apoptosis assay

FITC-conjugated Annexin-V (BioVision, Milpitas, California, USA) and propidium iodide (PI) mixed in Annexin-V binding buffer (BD Biosciences, San Jose, California, USA) were applied to cells and stained for 30 minutes at room temperature. Samples were subjected to BD Accuri C6 flow cytometer (BD Biosciences, San Jose, California, USA) and analysed in Flowjo™ (BD Biosciences, San Jose, California, USA).

2.2.4.6.3 Isolation of BCHOL^{High} and BCHOL^{Low} populations

Cells were stained with BODIPY-cholesterol (BCHOL) (Avanti Polar Lipids, Alabaster, Alabama, USA) for 30 minutes on ice. Samples were subjected to BD FACS Aria III (BD Biosciences, San Jose, California, USA) for cell sorting. A margin was set at 2% to select both positive/BCHOL^{High} and negative/BCHOL^{Low} populations. Aliquots of BCHOL^{High} and BCHOL^{Low} sorted cells were examined for purity with a BD FACS Aria III (BD Biosciences, San Jose, California, USA) and Flowjo™ (BD Biosciences, San Jose, California, USA).

2.2.4.6.4 Isolation of CD133⁺ and CD133⁻ populations

Liver cells were purified by revised two-step collagenase perfusion method (171). Samples were then sorted on a BD Influx Cell Sorter (BD Biosciences, San Jose, California, USA) based on the CD133 (#11133182, Thermo Fisher Scientific, Waltham, Massachusetts, USA) marker staining expression. LIVE/DEAD Fixable Near-IR Dead Cell Stain Kit (#L34976, Thermo Fisher Scientific, Waltham, Massachusetts, USA) was used to exclude dead cells. In addition, CD45 (#559864, BD Biosciences, San Jose, California, USA) and TER119 (#557909, BD Biosciences, San Jose, California, USA) markers were used to exclude blood cells.

2.2.4.7 Staining

2.2.4.7.1 Filipin staining

Filipin (#F9765, Sigma-Aldrich, St. Louis, Missouri, USA) was used to stain free cholesterol in HCC cells. In brief, cells grown on glass coverslips were fixed in 4% PFA in PBS, quenched the paraformaldehyde group by 10 mM of glycine for 10 minutes. Cells were stained with filipin at 50 µg/ml for 1 hour. The cells were then washed with PBS, and counterstained the nucleus with propidium iodide. For frozen tissues, the steps were the same but filipin concentration was increased to 200 µg/ml. Slides were mounted using VECTASHIELD Antifade Mounting Medium (#H-1000, Vector Laboratories, Burlingame, California, USA). Fluorescence signal was visualized using Leica TCS SPE confocal microscope. Intensity of the staining were quantified using Nikon NIS-Elements Software (Melville, New York, USA).

2.2.4.7.2 Immunofluorescence staining

HCC cells were seeded on glass coverslips and further fixed in 4% PFA in PBS for 15 minutes in room temperature. 0.1% Triton-X100 was used to permeabilize the cells for 15 minutes after several washes of PBS and blocked with 5% BSA in TBST for one hour. Primary antibody was applied and stained at 4°C overnight. Secondary antibody conjugated with FITC together with DAPI for nucleus staining was added on the next day for 1 hour incubation under room temperature. Slides were mounted and subjected to Leica TCS SPE confocal microscope examination. Intensity of the staining were quantified using Nikon NIS-Elements Software (Melville, New York, USA).

2.2.4.7.3 Immunohistochemistry staining

Xylene was first used to deparaffinize the sections followed by rehydration in graded alcohols and distilled water. A standard microwave heating technique in Tris-EDTA buffer was performed to retrieve antigens on the slides. 3% hydrogen peroxide was then used to quench endogenous peroxidase activities. After that, the slides were immersed in serum free-protein block solution (DAKO, Santa Clara, California, USA) and subsequently incubated against anti-SREBP2 (#ab28482, Abcam, Cambridge, UK), cleaved CASP3 (Asp175) (#9664S, Cell Signalling Technology, Danvers, Massachusetts, USA), GLI-1 (#UM800063, Oncogene Pharma, Shah Alam, Selangor, Malaysia). Stained slides were washed thoroughly and incubated with anti-rabbit secondary Envision™ HRP-conjugated antibody (DAKO, Santa Clara, California, USA). Signals were visualized using Liquid DAB+ Substrate-Chromogen

System (DAKO, Santa Clara, California, USA). Mayer's hematoxylin was used to counterstain the slides which were examined under light microscope.

With no prior knowledge to the clinicopathological profile of the patients, the protein expression was quantified individually on two scoring parameters: 1 to 4 in terms of percentage (P) of expression: $\leq 10\%$ stained positive, $\leq 25\%$ stained positive, $< 50\%$ stained positive and ≥ 50 stained positive, respectively; 1 to 3 in terms of intensity (I): weak, moderate, and strong, respectively. Quick (Q) score was calculated on the formular: $Q = P \times I$. With a maximum score of 12, specimens scored below 6 were termed as 'low expression' while those scored above 6 were classified as 'high expression'.

2.2.4.8 Assay kits

2.2.4.8.1 CH25H ELISA kit

Level of cholesterol-25-hydroxylase (CH25H) was determined by CH25H ELISA Kit (Human) (#OKCD01912, Aviva Systems Biology, San Diego, California, USA). In brief, cells were lysed with NETN buffer, and 20 ng of total proteins were assayed following the protocol. Result was detected using a spectrophotometer at OD450 nm.

2.2.4.8.2 Cholesterol assay kit

Total cholesterol level was measured by Cholesterol/Cholesteryl Ester Quantitation Assay Kit (#ab65359, Abcam, Cambridge, UK). Briefly, a total of 1×10^6 cells were harvested to extract cholesterol in a solution of chloroform: isopropanol: NP40 in a ratio of 7:11:0.1 in a micro-homogenizer. Organic phase which contained cholesterol was transferred to a new clean tube after centrifuging at 15,000g for 10 minutes. The solution was vacuum dried overnight and resuspended by the assay buffer. Result was detected using a spectrophotometer at OD570 nm.

2.2.4.8.3 CASP3 activity assay kit

The enzymatic CASP3 activity was assayed using CASP3 Activity Assay Kit (ab252897, Abcam, Cambridge, UK). In brief, a total of 1×10^6 cells were harvested and lysis against Caspase Cell Lysis Buffer provided in the kit. Cell lysates were centrifugated at 10,000g for 10 minutes. Supernatant was then transferred to a clean tube and assayed immediately. Result was detected by measuring fluorescence at Ex/Em= 400/505 nm.

2.2.4.9 Bioinformatics and statistical analysis

2.2.4.9.1 RNA sequencing

Total RNA of MHCC-97L (NTC and shSREBP2#66) and drug-resistant PDTXs (PDTX#1 and PY003) and their mock controls were extracted using TRIzol Reagent (Invitrogen™, ThermoFisher Scientific, Waltham, Massachusetts, USA) according to manufacturer's protocol. The quality was confirmed by Agilent 2100 bioanalyzer (Agilent Technologies, Santa Clara, California, USA) to have OD260/280 of between 1.8-2.0 whereas the RNA integrity number value was higher than 8.0. The qualified RNA samples were hence sequenced at the platform of Illumina Solexa sequencing using HiSeq 1500 sequencer (Illumina, San Diego, California, USA) for performing HiSeq sequencing run (pair-end sequencing of 101bp). Each sample had an average throughput of 10.8Gb and a total throughput of 21.5Gb. An average of 94% of the bases achieved a quality score of Q30 where Q30 denotes the accuracy of a base call to be 99.9%. Alignment, expression estimation and tests for differential expression were processed by RSEM 1.2.21 and EBSeq 1.6.0 Resulting values were indicated by Transcript Per Million.

2.2.4.9.2 Ingenuity pathway analysis for expression data

We compared the gene expression levels from different phenotypes (i.e., Mock control versus sorafenib/lenvatinib resistant PDTXs and differentiated progenies versus chemo-resistant hepatospheres). The Ingenuity Pathway Analysis (IPA) (QIAGEN, Germantown, Maryland, USA) was used to examine the functional associations among genes and generate a gene network with a high significance based on more interconnected genes being present than would be expected by chance. The significance of each network was estimated by the scoring system provided by IPA. The scores were determined by the number of differentially expressed genes within each of the networks and the strength of the associations between network members.

2.2.4.9.3 Gene set enrichment analysis for gene expression data

We compared the gene expression levels from different phenotypes (i.e., HCC mouse model (CD133⁺ over CD133⁻) versus liver regeneration model (CD133⁺ over CD133⁻) and NTC versus shSREBP2) and picked up the genes which had significant different expression for Gene set enrichment analysis (GSEA) by using Molecular Signatures Database (V3.0). GSEA was carried out by computing overlaps with hallmark gene sets (H), canonical pathways (CP) and gene ontology (GO) gene sets (C5), obtained from the Broad Institute (172). Genes in Gene

Set (K), Genes in Overlap (k), k/K and p -value were used to rank the pathways enriched in each phenotype.

2.2.4.9.4 Statistical analysis

Data obtained from qPCR, ELISA assay kits, limiting dilution assay, flow cytometry analysis for both stemness marker staining and Annexin-V apoptosis assay, migration and invasion assays, and the quantification of IF staining, were subjected to Student's t -test for calculating the statistical significance. The error bars indicate the means and standard deviations. Statistical difference of p -value lower than 0.05 was considered significant in the two-sided test (* p <0.05, ** p <0.01, *** p <0.001, and **** p <0.0001). Individual data point is excluded if it departs from the mean with more than 3 standard deviations. During data collection the investigators were not blinded to the group allocation. There is no assumption of any variations within each experimental group and the similar variance is statistically compared. For overall and disease-free survival, Kaplan-Meier survival analysis coupled with a log-rank test was used to determine the statistical significance.

CHAPTER 3

**CHOLESTEROL BIOSYNTHESIS IS
ACTIVATED IN DRUG-RESISTANT HCC
PATIENT-DERIVED TUMOR XENOGRAPHS**

3 Cholesterol biosynthesis is activated in drug-resistant HCC patient-derived tumor xenografts

3.1 Introduction

The advancement of TKIs has inarguably improved HCC patients' overall survival. However, the development of acquired drug resistance has limited the efficacy of TKIs and hence limits patients' long-term survival. TKIs are clinically prescribed to HCC patients in multiple cycles over a long period of time, but eventually, the residual surviving cancer cells repopulate and form tumors that are resistant to TKI treatment.

Sorafenib is an oral multikinase inhibitor against VEGFR, PDGFR, and Raf serine/threonine kinases. This TKI acts as an antiangiogenic agent and was superior for treating patients with unresectable HCC in the Sorafenib Hepatocellular Carcinoma Assessment Randomized Protocol (SHARP) investigation (21). However, patients' median overall survival was only prolonged by approximately 3 months (Figure 3.1A), and the disease eventually progressed.

Lenvatinib is also an oral multikinase inhibitor that targets VEGFR1-3, FGFR1-4, PDGFR, RET, and KIT. This novel antiangiogenic TKI is approved as another option for first-line treatment in unresectable HCC patients. According to an open-label, phase 3, multicentre, noninferiority trial (REFLECT), lenvatinib was demonstrated to be noninferior to sorafenib with respect to overall survival in advanced HCC patients: 13.6 months in the lenvatinib arm compared to 12.3 months in the sorafenib arm (22) (Figure 3.1B). Likewise, lenvatinib treatment eventually faces the challenge of tumor relapse due to acquired drug resistance. Therefore, it is crucial to identify the molecular regulator(s) of acquired sorafenib/lenvatinib resistance to benefit patient overall survival.

To understand the mechanism of sorafenib/lenvatinib resistance in HCC patients, it would be ideal to obtain fresh clinical samples from patients with HCC before and after sorafenib treatment. Unfortunately, these samples are not available due to ethical issues. To mimic this clinical situation, many researchers have employed *in vitro* establishment of sorafenib-resistant cells. However, the translational potential of this model is limited because it is not representative of the true clinical situation. For this purpose, we employed *in vivo* PDTXs derived directly from two samples from HCC patients and developed sorafenib- and lenvatinib-resistant PDTXs *in vivo* by administration with several collected rounds of sorafenib/lenvatinib

treatment. Upon successful establishment of these two drug-resistant PDTXs, RNA sequencing analysis was employed to compare the expression profiles of sorafenib- and lenvatinib-resistant PDTXs and their corresponding mock controls. Identification of the crucial pathways involved in acquired drug-resistant HCCs was further achieved using IPA. Next, we confirmed the potential pathway using protein expression analysis.

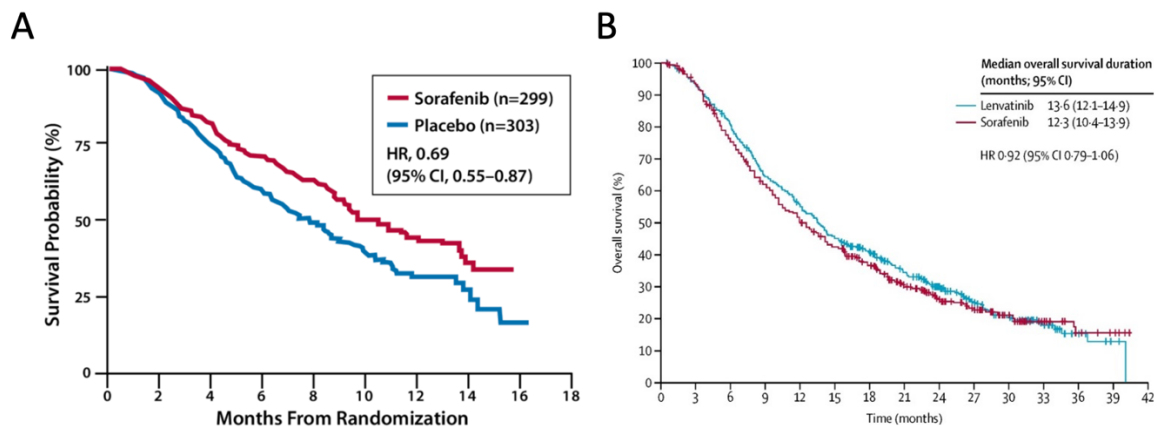


Figure 3.1. Survival curves adopted from the SHARP and REFLECT clinical trials.

(A) Sorafenib improves patients' overall survival by 3 months (21). Reproduced with permission from Llovert, Ricci, & Mazzaferro et al., Copyright Massachusetts Medical Society, see Appendi for the concerned license. (B) Lenvatinib was shown to be noninferior to sorafenib in advanced stage HCC (22). Reused with permission from Kudo, Finn, & Qin et al.'s work (22). Permission conveyed through Copyright Clearance Centre, please see Appendi for the copyright approval letter.

3.2 Experimental outline

(1) Sorafenib- and lenvatinib-resistant PDTXs were established. (2) Resistant tumors and their mock counterparts were collected for RNA sequencing; the data were then analyzed using IPA and GSEA. A summary of the experimental design is shown below (Figure 3.2).

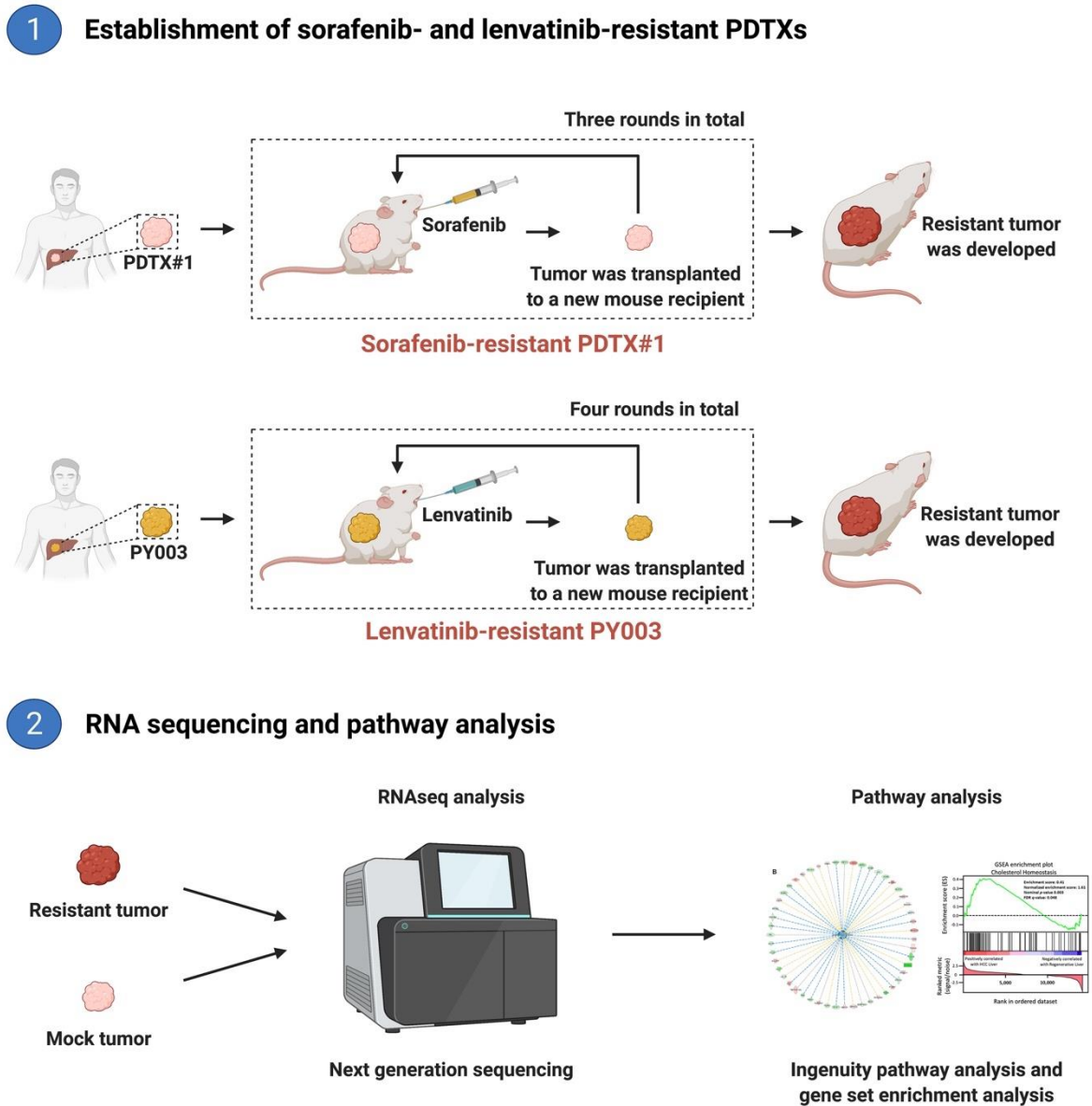


Figure 3.2. Experimental outline in Chapter 3.

The diagram summarizes the methods used to identify the altered pathways in sorafenib- and lenvatinib-resistant PDTXs.

3.3 Results

3.3.1 Successful establishment of sorafenib- and lenvatinib-resistant PDTXs

To mimic the clinical situation in which acquired drug resistance develops in HCC patients in response to sorafenib or lenvatinib treatments, two drug-resistant HCC PDTXs were developed (Figure 3.2). Primary tumors were harvested from HCC patients who did not receive any cancer treatments in prior to the operation and subsequently dissociated and inoculated into NOD/SCID mice as described in the Methods. PDTX mice were administered sorafenib or lenvatinib orally per day. After completion of one round of feeding, tumors were harvested, dissociated, and reinoculated into secondary mouse recipients. This cycle was repeated until successful establishment of a resistant tumor was achieved. Three rounds in total were needed to develop sorafenib resistance, whereas four rounds were needed for lenvatinib resistance, and both were verified to induce no tumor suppression treatment when compared to their control counterparts (Figure 3.3).

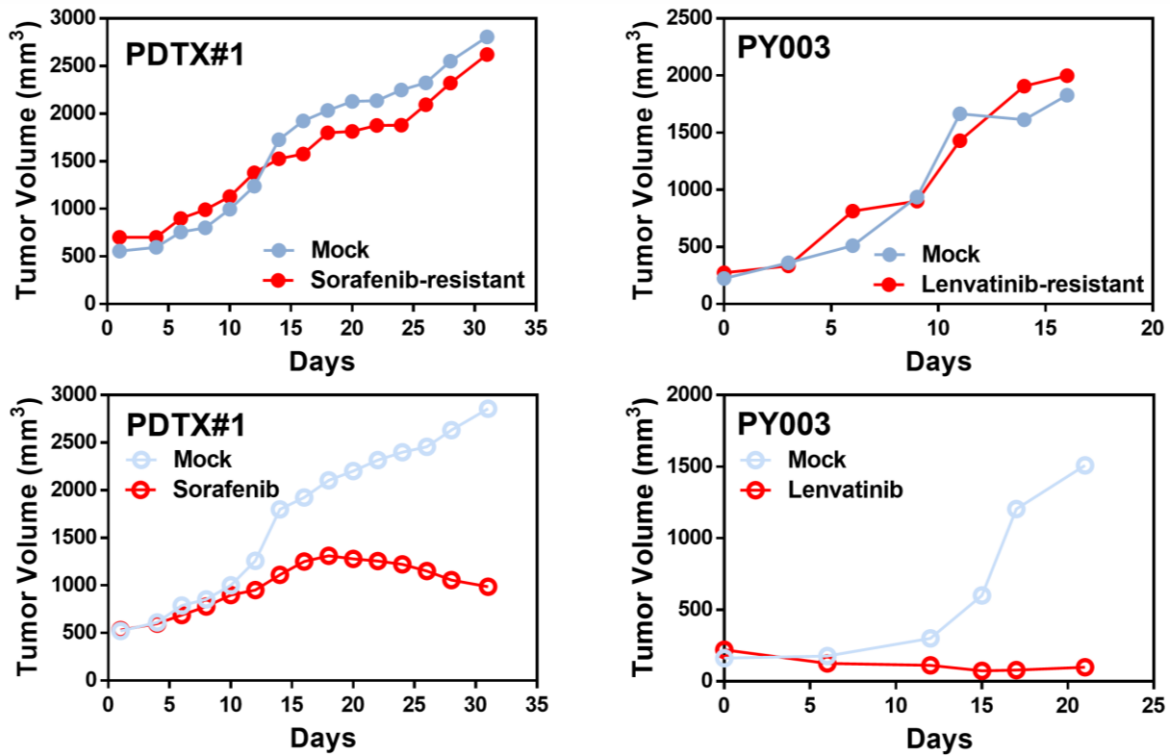


Figure 3.3. Tumor growth curves of both drug-resistant and drug-responsive PDXs.

(Upper, left) Sorafenib-resistant PDTX#1 was established by administering sorafenib orally at 100 mg/kg for three rounds. (Upper, right) Lenvatinib-resistant PY003 was established by administering lenvatinib orally at 30 mg/kg for four rounds. The dose response curves showed that there was no reduction in tumor volume in response to sorafenib/lenvatinib administration when compared to their corresponding mock controls. (Lower, left) Sorafenib-responsive PDTX#1 was harvested at day 31 and proceeded to next round of drug feeding. (Lower, right) Lenvatinib-responsive PY003 was harvested at day 21 and proceed to next round of drug feeding.

3.3.2 Cholesterol biosynthesis is the most upregulated pathway in both drug-resistant PDTXs

After successful establishment of drug-resistant PDTXs, total RNA was extracted using the protocol mentioned in the Methods. Samples were processed to perform RNA sequencing, and the expression profiles of the mock control and drug resistant PDTXs were then compared. Surprisingly, the superpathway of cholesterol biosynthesis was the most upregulated pathway in both resistant PDTXs, according to IPA (Figure 3.4A). Genes associated with cholesterol biosynthesis were commonly deregulated, as shown by a heat map illustration (Figure 3.4B). Moreover, filipin staining revealed that free cholesterol or cholesterol deposition was consistent with the sequencing results. Both drug-resistant PDTXs exhibited consistently higher cholesterol deposition than their mock counterparts (Figure 3.5).

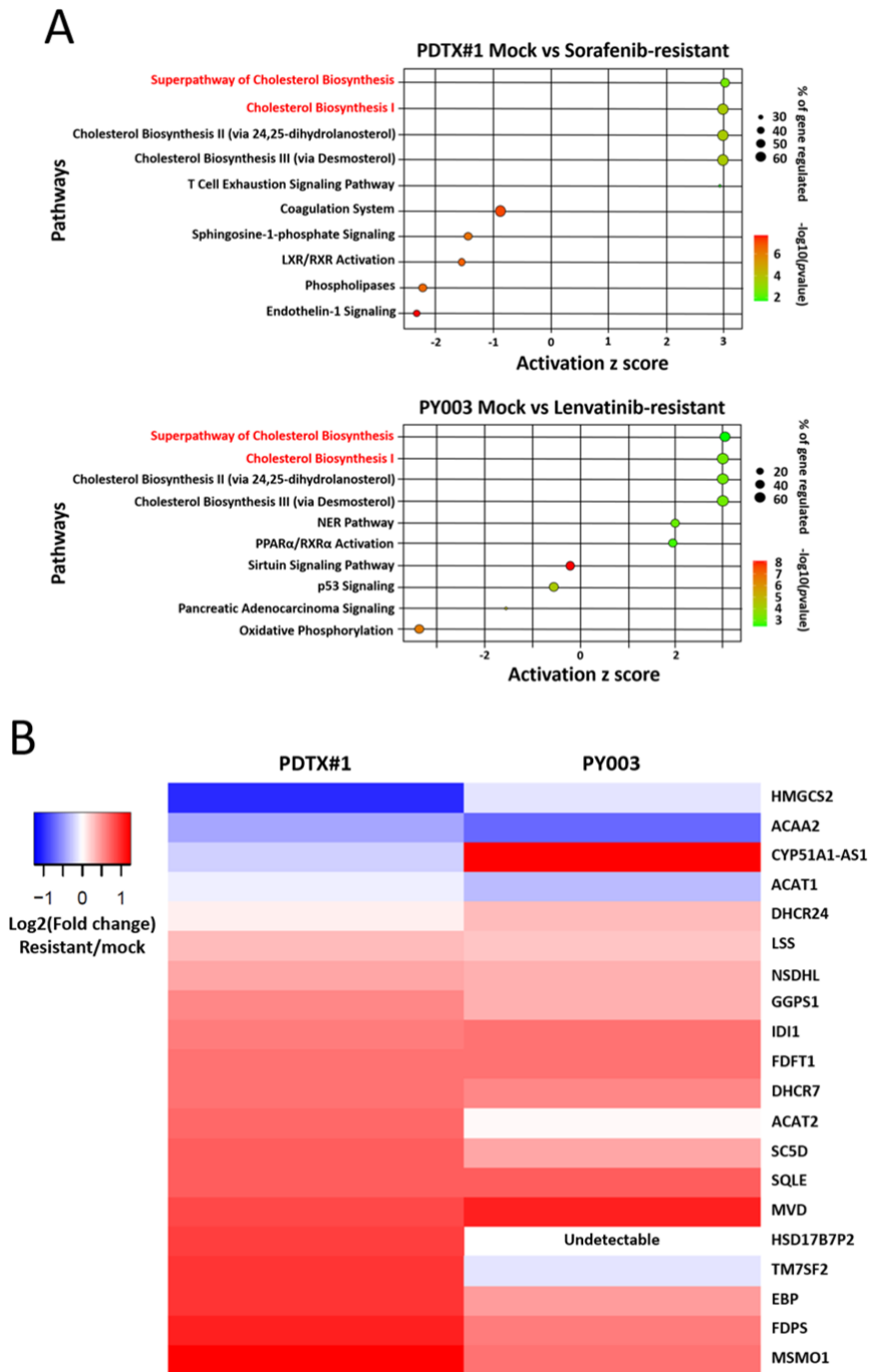


Figure 3.4. Cholesterol biosynthesis is commonly enriched in both drug-resistant PDTXs.

(A) IPA showing the top ten most dysregulated canonical pathways in sorafenib- and lenvatinib-resistant PDTXs, among which the superpathway of cholesterol biosynthesis and cholesterol biosynthesis I were most commonly upregulated compared to their corresponding mock controls. (B) A heatmap analysis was performed based on the quantity of different genes in cholesterol biosynthesis. The level of gene expression is indicated by the color index. Colors from blue to red indicate low to high expression, respectively, for the log₂-fold change of resistant compared to mock.

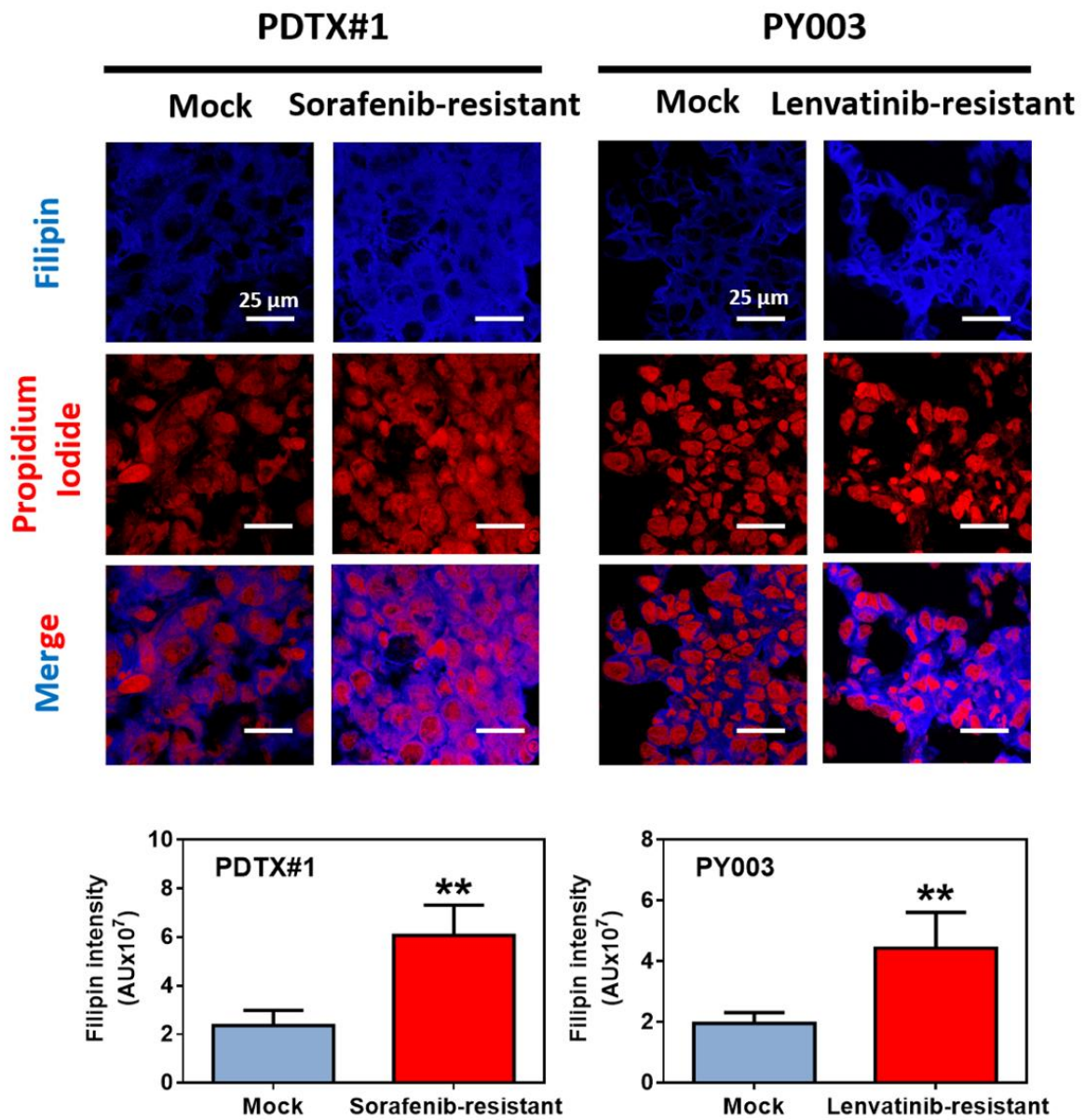


Figure 3.5. Filipin staining of cholesterol deposition in drug-resistant PDTXs.

Representative filipin staining of tumors from sorafenib- and lenvatinib-resistant PDTXs and their mock controls. Filipin intensity was quantified using Nikon NIS-Elements Software. Blue: filipin staining; Red: propidium iodide. Scale bar: 25 μm. Error bars indicate mean±SD (n = 3-5). ** $p < 0.05$ from Student's t-test.

3.3.3 SREBP2 is the upstream regulator of drug-resistant-mediated cholesterol biosynthesis

Cholesterol is the product of a series of complicated metabolic sequences that consist of different regulators and effectors. It is therefore important to identify the key signalling molecule involved in acquired drug resistance-mediated cholesterol biosynthesis. Upstream regulator analysis consistently found that SREBP2 was the upstream regulator in the abovementioned setting (Figure 3.6). In sorafenib-resistant PDTX#1, the activation z score reached 2.979, whereas in lenvatinib-resistant PY003, the activation z score was 3.002. Based on these findings, sorafenib- and lenvatinib-resistant HCC cells exhibited increased cholesterol biosynthesis due to SREBP regulation.

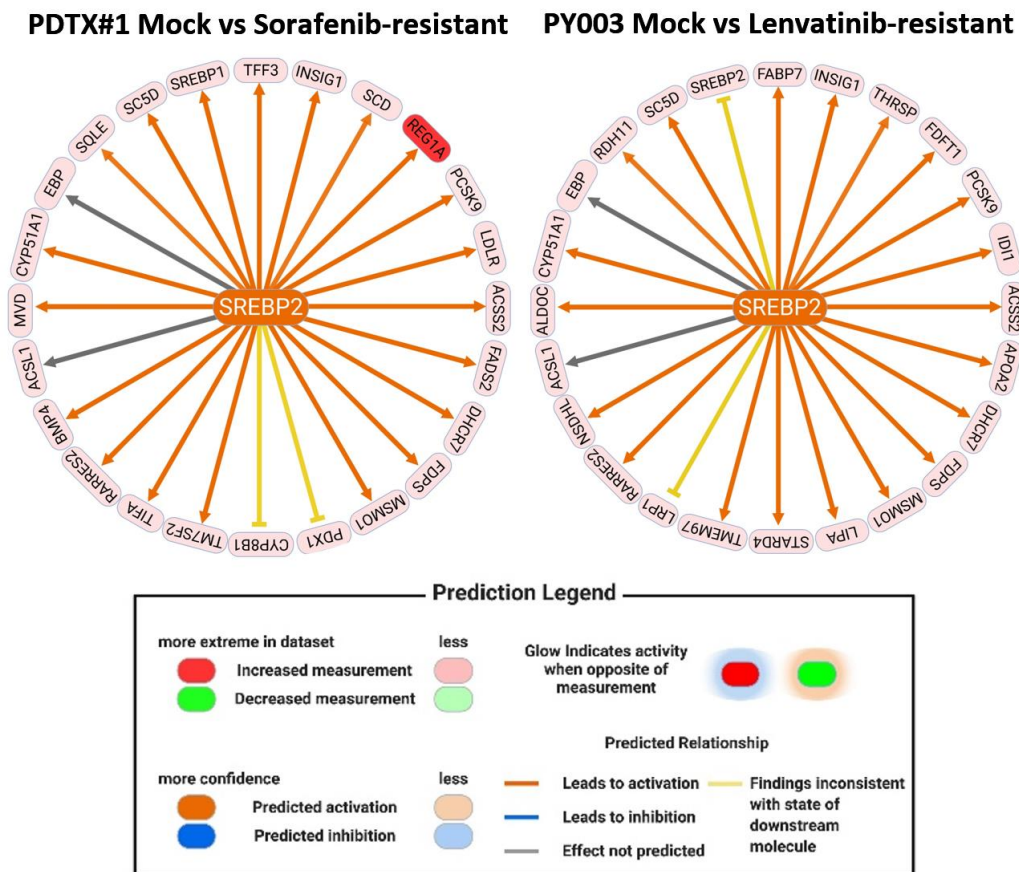


Figure 3.6. Upstream regulatory analysis of drug-resistant PDTXs.

SREBP2 was shown to be the upstream regulator of changes in cholesterol biosynthesis with activation z scores of 2.979- and 3.002-fold in the sorafenib-resistant PDTX#1 and lenvatinib-resistant PY003, respectively.

3.4 Discussion

The invention of sorafenib and lenvatinib and their approval for the treatment of advanced HCC has been a breakthrough for treating this disease though the overall survival benefit is rather unsatisfactory. One potential hurdle, as discussed in this Chapter, is the development of the acquired drug resistance to the TKIs. The establishment of both sorafenib- and lenvatinib-resistant models provides a first step that approximates the clinical setting to study the characteristics, mechanisms, and expression profiles of acquired drug resistance against these two first-line treatments for HCC.

Through continuous drug administration, the establishment of *in vitro* sorafenib-resistant HCC cell lines has been reported to be a practical method of investigating drug resistance (173). The cell line used for the development of resistant cells was experiencing a gradual increase of sorafenib dosage, from low to high slowly every few weeks. This process continues until the maximum tolerated dose has been reached. A mock control counterpart is produced by giving equal amount of DMSO over the same amount of time. The entire experimental setup is hence moved to the development of drug-resistant clones *in vivo* using a patient-derived tumor xenograft (PDTX) mouse model. Two PDTX models, PY003 and PDTX#1, were used for the development of the sorafenib-resistant and lenvatinib-resistant clones, respectively. The cells were derived from two clinical HCC tissue samples. These preclinical models may more accurately reflect what is occurring in patients, and these results may have a greater potential for clinical applications. The cells were subcutaneously injected into NOD-SCID mice, and these animals were treated with 100 mg/kg sorafenib for one month or 30 mg/kg lenvatinib for 21 days. After the end point of the first round of treatment, the tumors were harvested and reinoculated into a secondary mouse recipient to continue the process. For the successful development of sorafenib-resistant PDTX#1, it took three such rounds in total, while it took four rounds to fully develop lenvatinib-resistant PY003. The resistant tumors were not different from the size or volume of the mock control, even in response to the drug treatments.

The role of cholesterol dysregulation in cancer remains controversial. Certain cholesterol metabolites, such as dendrogenin A, were found to suppress the growth of melanoma and acute myeloid leukaemia (174). In contrast, cholesterol metabolism alterations have been shown to lead to the formation of oncometabolites that support tumor growth in breast and prostate cancers (175, 176). A similar situation is observed in HCC. Cholesterol and cholesterol esters

were found to play a role in NAFLD-induced HCC (177), while cholesterol was also reported to suppress HCC (178), as it is a critical component for the proper development of immune cells (179). Although current understanding of cholesterol is still context-specific, our findings showed that cholesterol biosynthesis was indeed critical for the regulation of drug resistance. Using both sorafenib- and lenvatinib-resistant PDTX models, the upregulation of cholesterol biosynthesis was not specific to individual drugs.

Both the increased endogenous synthesis of cholesterol and exposure to high circulating levels of cholesterol favor cancer progression. On the one hand, cholesterol is a critical structural component of lipid rafts, dynamic plasma membrane domains rich in RTKs and multiple-drug resistant efflux transporters (180). On the other hand, like other lipids, cholesterol acts as a second messenger that can activate oncogenic and stemness-related pathways, such as mTORC-1- and hedgehog-dependent pathways (114). The upregulation of cholesterol biosynthesis is also observed in drug-resistant colon cancer cells, non-small cell lung cancer, and breast cancer (114). Gene Ontology analysis revealed that the key enzymes involved in synthesizing cholesterol, or the mevalonate pathway, were enhanced in *in vitro* models (181). Such findings are consistent with our result of the enhanced expression of cholesterol synthesizing proteins in drug-resistant clones, for example, 7-dehydrocholesterol reductase (DHCR7), squalene epoxidase (SQLE) and farnesyl-diphosphate farnesyltransferase 1 (FDFT1).

Among the transcription factors that control the expression of the mevalonate pathway and cholesterol metabolism genes, the most active are SREBPs and LXRs. Both families play a role in drug resistance using either cholesterol metabolism-dependent or -independent mechanisms. Specifically, in the liver, SREBP2 is the predominant protein in the SREBP family (182). This is also consistent with the current findings, as SREBP2 was shown to be the upstream regulator of drug resistance-induced cholesterol biosynthesis. SREBP2 was previously reported to regulate cisplatin resistance in ovarian cancer cells by increasing the expression of LDLR, HMGCR, and FDFT1 genes (183). This again reinforces our current findings that SREBP2-induced cholesterol biosynthesis is not drug-specific or tissue-specific and that several cancers and drug mechanisms can activate this identical pathway to develop drug resistance.

In summary, cholesterol biosynthesis was shown to be upregulated in sorafenib- and lenvatinib-resistant clones along with prediction of SREBP2 as the upstream regulator of this process. Further investigation will elucidate the direct regulatory role of SREBP2 on cholesterol biosynthesis in CSCs, which are currently regarded as the primary driving force contributing to the plasticity of HCC.

Chapter 4
CHOLESTEROL BIOSYNTHESIS IS
PREFERENTIALLY ACTIVATED IN LIVER
CSCS

4 Cholesterol biosynthesis is preferentially activated in liver CSCs

4.1 Introduction

In Chapter 3, cholesterol biosynthesis was highly activated in drug-resistant HCC PDTX models. Recently, our team and others have demonstrated that drug-resistant HCC cells are endowed with enriched CSC populations (76, 77). Based on this solid evidence, we hypothesize that HCC cells acquire cancer stemness and drug resistance via regulation of cholesterol biosynthesis. To test this hypothesis, we utilized *in vitro* and *in vivo* models to enrich liver CSC populations and confirm the potential correlation between cholesterol biosynthesis and cancer stemness.

The first model we adopted was the culture of hepatospheres over 16 serial passages *in vitro* under continuous challenge with chemotherapeutic drugs, namely, doxorubicin and cisplatin, as a strategy to enrich the CSC populations. When comparing the drug-resistant hepatospheres to their differentiated counterparts, CSC properties, including tumorigenicity, self-renewal, expression of stemness-associated genes, and CSC surface marker expression, were all highly elevated (76). Using cDNA microarray analysis, the expression profiles between enriched liver CSC populations and their normal counterparts were analyzed. Identification of critical altered pathways preferentially deregulated in enriched liver CSC populations was further analyzed by IPA. Next, we further confirmed the potential targets by protein expression analysis.

Given that normal liver stem cells share similar properties to liver CSCs, it is crucial to examine whether cholesterol biosynthesis is preferentially activated in liver CSCs but not in normal liver stem cells. Therefore, we utilized mouse models to compare the expression profiles between liver regeneration and two HCC models using immunocompetent mice. First, we injected 0.1% 3,5-diethoxycarbonyl-1,4-dihydrocollidine (DDC) to induce liver regeneration in mice (184). Next, for the HCC models, we (1) injected plasmids of activated NRAS/AKT hydrodynamically into the tail vein of mice to induce HCC (169) and (2) administered diethylnitrosamine (DEN)/carbon tetrachloride (CCl₄) to the mice to induce fibrosis-related HCC (185). Upon harvesting, the livers were excised, and cell sorting was performed to sort CD133⁺ and CD133⁻ populations using a CD133-specific antibody (186). Similar to the first model, the expression profiles between CD133⁺ and CD133⁻ populations in liver regeneration and HCC models were analyzed by RNA sequencing analysis, and the altered pathways were analyzed by GSEA. With these two models, we could determine whether cholesterol

biosynthesis was preferentially activated in liver CSCs for specific therapeutic targeting against liver CSCs.

4.2 Experimental Outline

(1) *In vitro* and (2) *in vivo* liver CSC enrichment models were utilized to examine the potential activation of cholesterol biosynthesis in CSC-enriched liver populations. In *in vivo* HCC models, a mouse liver regeneration model was also included to examine the specificity of cholesterol biosynthesis in liver CSCs. A summary of the experimental design is shown below (Figure 4.1).

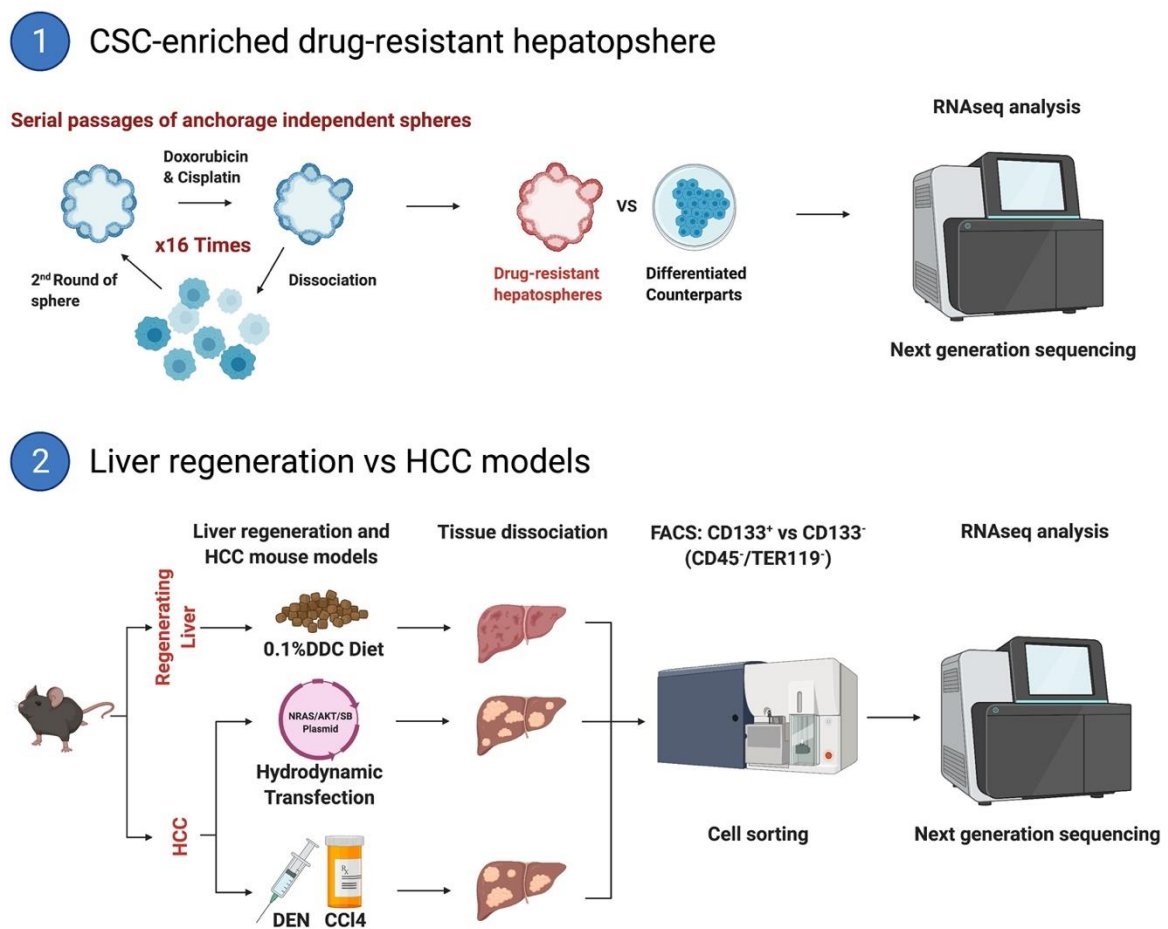


Figure 4.1. Experimental outline in Chapter 4.

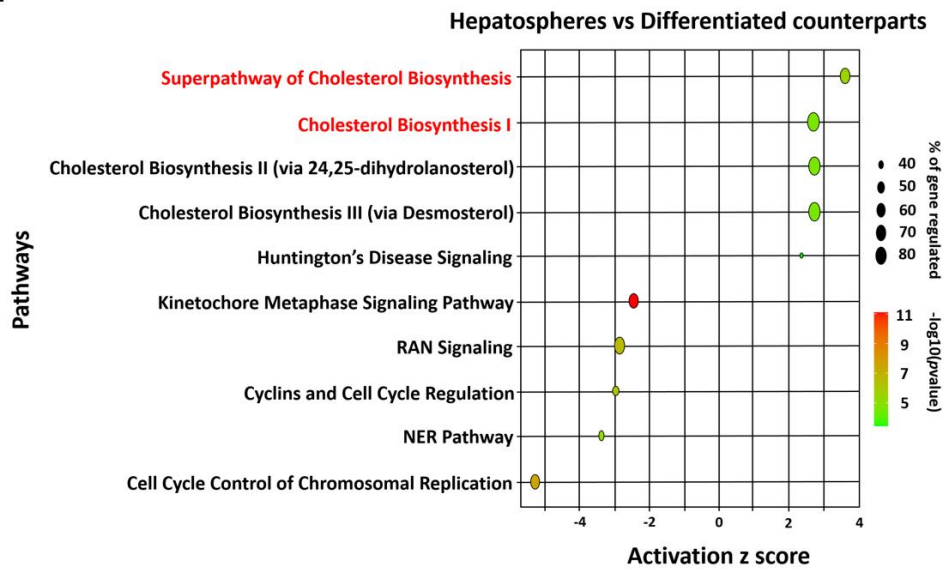
The diagram summarizes the methods used to identify the altered pathways in enriched liver CSC populations.

4.3 Results

4.3.1 SREBP2-mediated cholesterol biosynthesis is the most upregulated pathway in CSC-enriched hepatospheres

First, drug-resistant hepatospheres and their differentiated counterparts derived from PLC/PRF/5 cells, which phenotypically differed from their self-renewal and tumorigenicity (76), were compared. In brief, we established drug-resistant hepatospheres derived from PLC/PRF/5 cells via the administration of chemotherapeutic drugs, including cisplatin and doxorubicin, over 16 serial passages. Equal volumes of DMSO were administered to the PLC/PRF/5 counterparts. Persistently, the superpathway of cholesterol biosynthesis was the pathway most dysregulated with the highest activation z score via IPA analysis in the drug-resistant clones (Figure 4.2A). Using upstream regulator analysis, SREBP2 was repeatedly shown to be the master regulator of the cholesterol biosynthesis pathway, with an activation z score of 4.318 (Figure 4.2B). This result was confirmed by filipin staining of cholesterol deposition and IF staining of SREBP2 translocation in the PLC/PRF/5 hepatospheres (Figure 4.3A). Cholesterol and its upstream regulator SREBP2 were both enhanced in hepatospheres compared to the differentiated controls. Upon quantification, filipin was enhanced by 6-fold, while cytoplasmic and nuclear SREBP2 were enhanced by 7-fold and 3-fold, respectively, in the hepatospheres. The findings were further confirmed by western blot analysis probing for the expression of SREBP2 (Figure 4.3B). Both premature and mature forms of SREBP2 exhibited enrichment of approximately 1.6-fold.

A



B

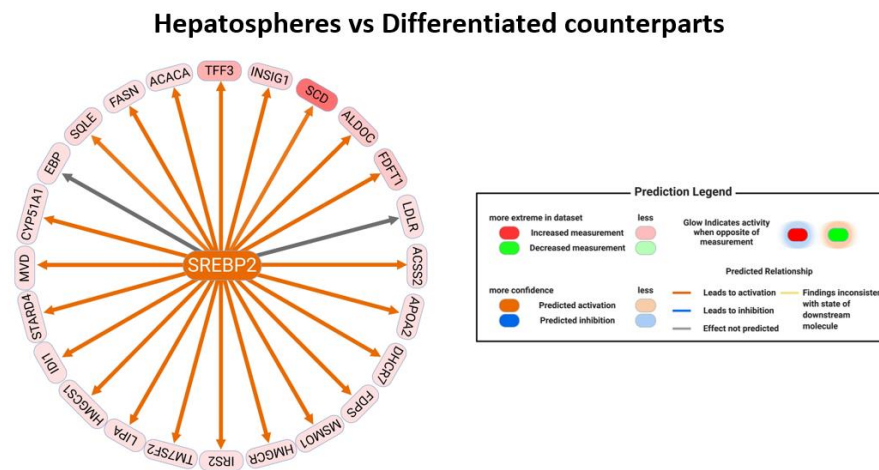


Figure 4.2. SREBP2-mediated cholesterol biosynthesis was upregulated in CSC-enriched HCC populations.

(A) IPA revealed that the superpathway of cholesterol biosynthesis was the mostly highly activated pathway with the greatest activation z score in drug-resistant hepatospheres compared to their differentiated counterparts. (B) Upstream regulator analysis revealed that SREBP2 was the upstream regulator of the overexpressed cholesterol biosynthesis in the drug-resistant hepatospheres.

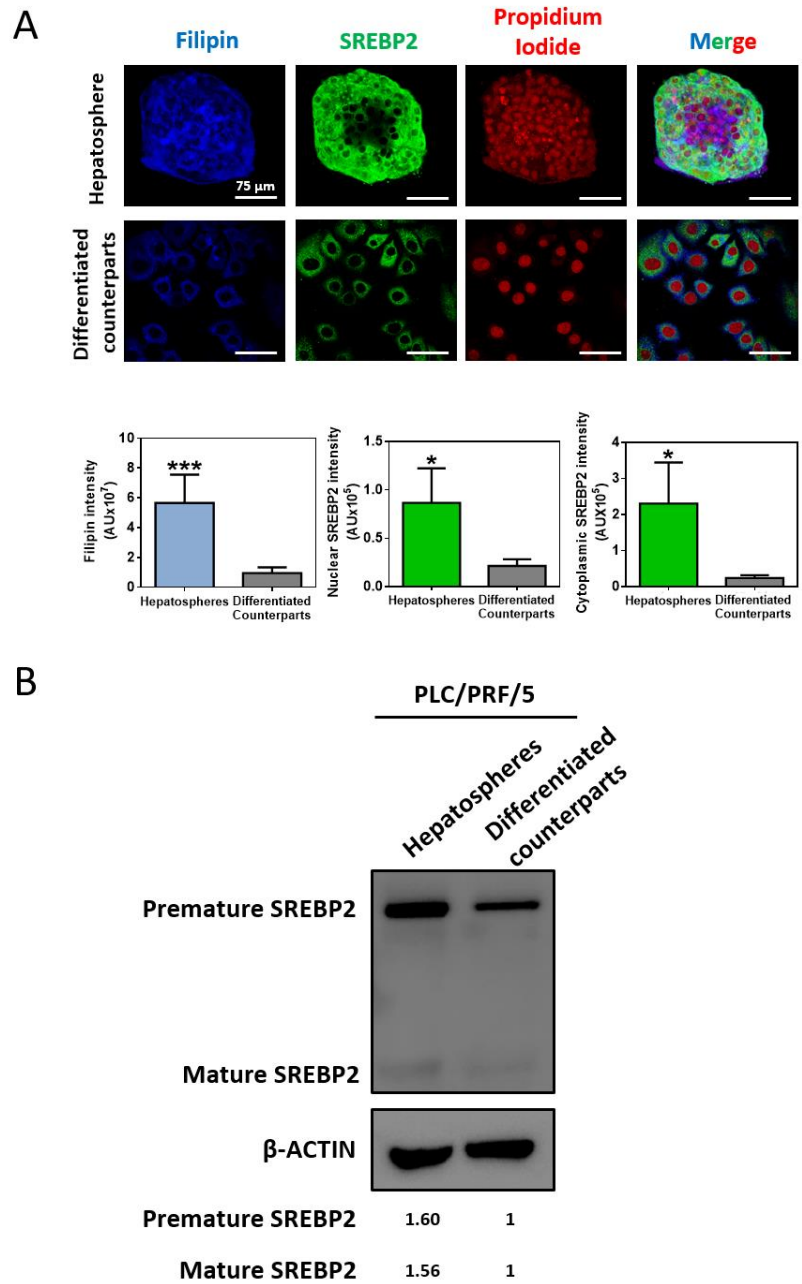


Figure 4.3. SREBP2-mediated cholesterol biosynthesis was enhanced in CSC-enriched hepatosphere population.

(A) Filipin and SREBP2 immunofluorescence staining in hepatospheres and differentiated counterparts were analyzed. Filipin and SREBP2 intensities were quantified using Nikon NIS-Elements Software. Blue: filipin staining; Green: SREBP2 staining; Red: propidium iodide. Scale bar: 75 μ m. Error bars indicate mean \pm SD (n = 3-5). * p <0.01, and *** p <0.001 from Student's t-test. (B) Western blot analysis of SREBP2 expression levels in hepatospheres and their differentiated counterparts. Expression levels were quantified using ImageJ.

4.3.2 Cholesterol homeostasis is increased in CD133⁺ liver CSCs, but not in regenerating liver cells

It is critical to evaluate whether cholesterol homeostasis is preferentially activated in CSCs but not in normal liver stem cells, although both stem cells and CSCs share molecular similarities. First, regeneration and HCC livers were induced in C57BL/6 mice. The regeneration model was achieved by feeding mice a 0.1% DDC diet. Meanwhile, two different methods for inducing HCC livers were employed, either by hydrodynamic plasmid transfection of activated forms of NRAS/AKT (169) or via DEN/CCl₄-induced fibrosis-related HCC (185). Livers were harvested upon completion of the treatments and subsequently subjected to cell sorting based on CD133 marker expression. Through negative selection of CD45 and TER119, pure hepatocytes were selected and compared for their CD133 expression levels. RNA sequencing analysis was performed to evaluate the expression profiles between CD133⁺ and CD133⁻ sorted cells among these three models. Upon Gene Set Enrichment Analysis (GSEA), cholesterol homeostasis was found to be the most highly upregulated pathway in CD133⁺ HCC cells compared to CD133⁺ liver stem cells (Figure 4.4). This finding highlights the significance and uniqueness of cholesterol activation in driving CSCs and acquired drug resistance.

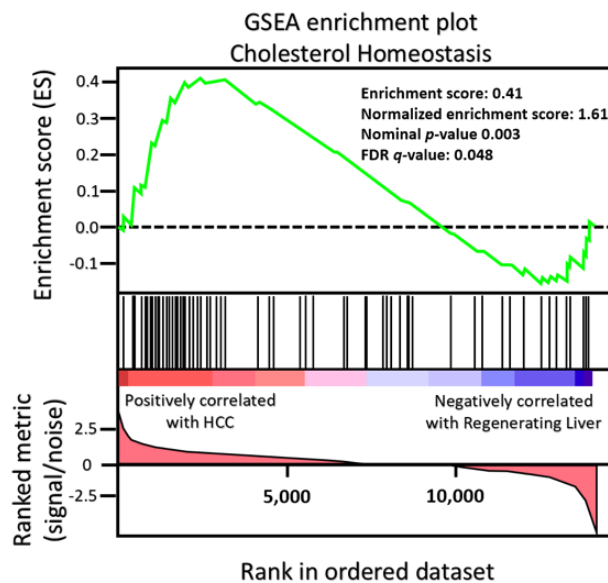


Figure 4.4. GSEA enrichment plot of CD133⁺ HCC models and regenerating liver cells.

Cholesterol homeostasis was positively correlated with CD133⁺ CSCs in HCC models but negatively correlated with CD133⁺ stem cells in regenerating liver. Normalized enrichment score: 1.61; nominal *p*-value: 0.003 & FDR *q*-value: 0.048.

4.4 Discussion

In this chapter, we found that cholesterol biosynthesis was crucial for the regulation of liver CSCs originating from mice and humans. Strikingly, this biosynthesis was preferentially activated in liver CSCs but not in normal stem cells.

This phenomenon was also found in several previous studies. Tontonoz and colleagues (157) demonstrated that *Lpcat3*, a phospholipid remodeling enzyme, stimulates cholesterol biosynthesis when it is inhibited and hence regulates intestinal stem cells and progenitor cells. The study also found that enhanced availability of cholesterol also stimulated crypt organoid growth, either by providing excessive cholesterol or by activating the SREBP2-mediated cholesterol biosynthesis pathway. These findings underline the importance of the SREBP2-mediated cholesterol cascade in tumorigenesis.

A similar effect has been observed in breast cancer stem cells (187). Using PDX-derived spheres to enrich CSC populations, Ehmsen and colleagues found that proteins associated with *de novo* cholesterol synthesis were highly increased compared to their control counterparts (187). They also found that the relationship had clinical relevance, as increased cholesterol biosynthesis predicted shorter recurrence-free survival in a breast cancer patient cohort (187). Moreover, the use of cholesterol-lowering drugs, statins, was effective in eradicating the formation of breast tumors, which indicates a therapeutic benefit of targeting cholesterol in cancer therapy (187).

On the other hand, intact cholesterol homeostasis was found to regulate the dormancy of hematopoietic stem and multipotential progenitor cells (HSPCs) (188). The study demonstrated that hematopoiesis and corresponding hematopoietic lineage decisions were controlled by the internal level of cholesterol. The deficiency of cholesterol transporters could dramatically increase HSPC mobilization. This connection was also reported in another setting of leukocytosis and augmented atherosclerosis when cholesterol homeostasis inhibited the proliferation of HSPCs (189).

Nevertheless, our findings and others have critically outlined the importance of cholesterol biosynthesis in tumorigenicity and acquired drug resistance mediated by CSCs. In addition, we reported in this chapter that the relationship was connected through SREBP2, and we will

further investigate the functional role of SREBP2-mediated cholesterol biosynthesis in CSCs and the mechanistic role of driving acquired drug resistance.

Chapter 5

SREBP2-MEDIATED CHOLESTEROL BIOSYNTHESIS REGULATES LIVER CSCS AND HAS CLINICAL SIGNIFICANCE

5 SREBP2-mediated cholesterol biosynthesis regulates liver CSCs and has clinical significance

5.1 Introduction

In Chapters 3 and 4, we demonstrated that cholesterol biosynthesis was preferentially activated in liver CSCs, which play a critical role in regulating resistance to cancer therapies. This was echoed the PDTX models in which this pathway was highly upregulated in both drug-resistant PDTXs. Moreover, the above models concomitantly indicated that SREBP2, the master regulator of cholesterol biosynthesis, was predicted to be an upstream regulator. Therefore, we investigated the functional role of SREBP2-mediated cholesterol biosynthesis in CSCs and drug resistance in the following chapters.

The SREBP family, which is a basic-helix-loop-helix leucine zipper (bHLH-Zip) transcription factor, contains three isoforms to date, including SREBP1a, SREBP1c and SREBP2 (190). From a distinct chromosomal location (22q13) than its subfamily members, SREBP2 is encoded by the separate SREBP2 gene (*SREBF2*) (128). Currently, only one transcript from this gene has been observed. Surprisingly, SREBP2 regulates sterol metabolism in every tissue (191). The protein structure of SREBP2 resembles a tripartite structure comprising (1) an N-terminal transcription factor domain; (2) a central hydrophobic region containing two transmembrane segments; and (3) a C-terminal guiding domain (128). SREBP2 is bound to the endoplasmic reticulum and nuclear envelope membranes in a hairpin manner, stretching the long N-terminal and C-terminal domains toward the cytoplasm and residing in the middle region inwards the lumen of the organelle (192). In the N-terminal domain, it simulates many of the transcription activators beginning with an acidic domain. When this segment is deleted, the protein loses the ability to activate transcription, as it fails to bind to the corresponding DNA sequence (193). Similar to many other bHLH-Zip family proteins, SREBP2 can recognize E boxes *in vitro*, but in the nucleus, it specifically binds to a conserved sequence of 5'-ATCACCCAC-3', which is distinguished as a SRE (128). This DNA element is categorically found in the promoter regions of genes involved in cholesterol synthesis and uptake pathways, such as HMGCR, LDLR and insulin-induced gene 1 (INSIG1).

Cancer cells are rapidly dividing cells that exhibit amplified demands for macromolecules and energy. Increasing evidence suggests that the primary functions of activated oncogenes and inactivated tumor suppressors are to rewire cellular metabolic pathways to drive tumorigenesis.

SREBP2 was found to be overexpressed in colon cancer, prostate cancer and breast cancer (181, 194, 195), and its overexpression is related to cell proliferation, migration and invasion and drug resistance (183, 196, 197). The mevalonate pathway, which is an alternative name of the cholesterol synthesis pathway, is increased in many cancers, conceivably through mutations in p53 and SREBP2, suggesting that statins (an FDA-approved drug inhibiting HMGCR, which makes mevalonate) could be potential cancer treatment agents (198). In a breast cancer study, using spheroid assays and genome-wide expression analysis, breast tumors were found to harbor mutated p53 and SREBP2 on SREBP2-controlled genes, leading to disruption of the mevalonate pathway in the breast tissue architecture (181).

SREBP2 has also been reported to be correlated with CSCs. In prostate cancer cells, SREBP2 promotes and regulates the stem cell population, prostate formation ability, tumorigenicity, cell growth and metastasis via transcriptional activation of c-Myc (199). Moreover, in colon cancer, knockdown of SREBP2 attenuates the expression of stemness markers such as CD44 and CD133 and inhibits tumor growth *in vivo* in xenograft models (197). However, a mechanistic relationship for how SREBP2 regulates stemness is lacking. Interestingly, as the final product of the mevalonate pathway, cholesterol was also reported to be the primary driver of stem cell proliferation in intestinal cancer (157). The availability of cholesterol, either through activation of SREBP2 or by exogenous administration, enhances intestinal cancer cell proliferation *in vivo* (157).

Taken together, both SREBP2 and cholesterol biosynthesis are critically involved in regulating cancer development through alteration of metabolism via a series of oncogenic pathways. However, the clinical relevance and functional role of SREBP2-mediated cholesterol biosynthesis in HCC remain poorly characterized. Whether this process regulates liver CSCs has not been explored. In this chapter, we examine the role of SREBP2-mediated cholesterol biosynthesis in cancer stemness by manipulating the expression levels of SREBP2 in HCC cells through lentiviral-based knockdown and CRISPR activation approaches and functionally characterizing them using a variety of CSC functional assays.

5.2 Experimental outline

(1) Upon successful genetic knockdown and overexpression of SREBP2 in selected HCC cells, (2) *in vitro* and (3) *in vivo* liver CSC functional assays were utilized to examine the potential relationship of SREBP2-mediated cholesterol biosynthesis in liver CSCs. (4) Rescue

experiments were attempted via administration of exogenous cholesterol. (5) A bioavailable cholesterol probe was further used to track the utilization of cholesterol in HCC cells if they possessed stem cell-like properties. (6) Finally, clinical relevance and significance were analyzed in patient cohorts. A summary of the experimental setting is shown below (Figure 5.1).

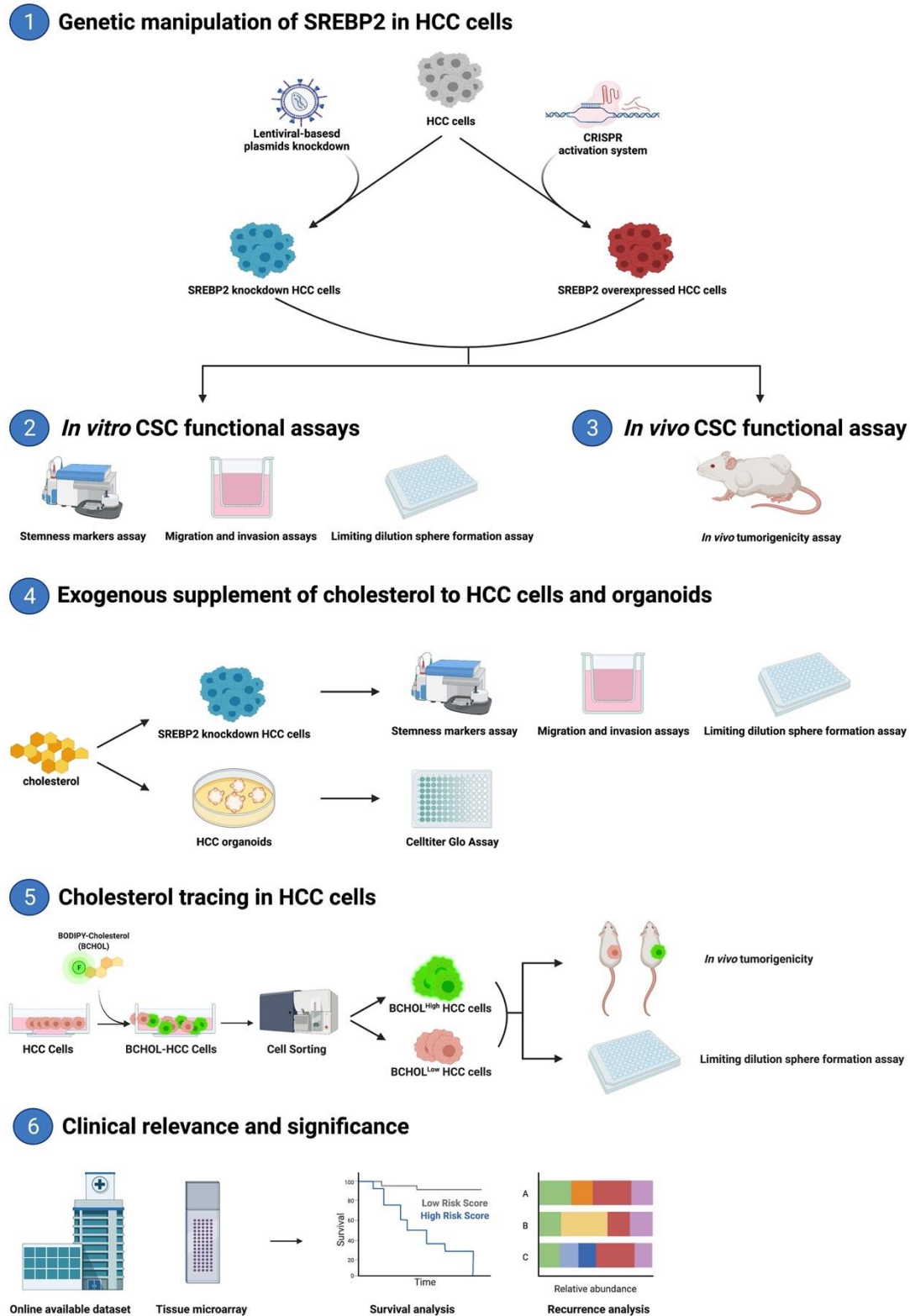


Figure 5.1. Experimental outline in Chapter 5.

The diagram summarizes the methods used to examine the role of SREBP2-mediated cholesterol biosynthesis in regulating CSC properties in HCC cells and the potential clinical relevance.

5.3 Results

5.3.1 SREBP2 expression and cholesterol levels in a panel of HCC cells

In a panel of HCC cell lines, using MIHA cells, a nontumorigenic normal liver cell line, as a control, the expression of premature and mature forms of SREBP2 in a variety of HCC cells was compared (Figure 5.2A). Four out of the five HCC cell lines tested exhibited dramatic increases in both forms of SREBP2, including PLC/PRF/5 and MHCC-97L cells. However, the remaining cell line, Hep3B, showed only mild expression of SREBP2 compared to MIHA cells. Correspondingly, the cholesterol level of these cells was aligned to the SREBP2 expression level. MHCC-97L cells contained the highest level of intracellular cholesterol, while Hep3B cells displayed the lowest cholesterol levels (Figure 5.2B). Therefore, for subsequent experiments, PLC/PRF/5 and MHCC-97L cells were selected to knockdown SREBP2 levels, while Hep3B cells were selected to overexpress SREBP2.

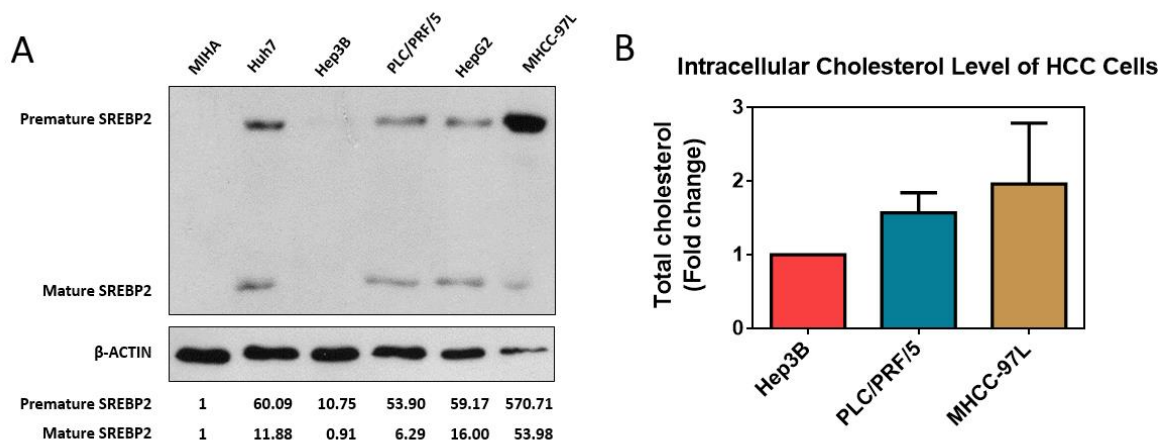


Figure 5.2. Expression of SREBP2 and level of cholesterol in a panel of HCC cells.

(A) Using western blot analysis, MIHA, a nontumorigenic normal liver cell, exhibited the lowest expression of premature and mature SREBP2 compared to other HCC cell lines. Quantification was performed using ImageJ. (B) Among the three chosen HCC cell lines, low SREBP2-expressing Hep3B cells showed the lowest cholesterol levels compared to high SREBP2-expressing PLC/PRF/5 and MHCC-97L cells.

5.3.2 SREBP2 regulates cholesterol biosynthesis genes and cholesterol levels in HCC cells

SREBP2 knockdown and overexpressing cells were successfully genetically engineered using lentiviral-based knockdown and CRISPR activation approaches, respectively. The SREBP2 protein levels of both forms, verified by western blot analysis, were decreased in the knockdown clones derived from PLC/PRF/5 and MHCC-97L cells and were enhanced in the overexpressing clones derived from Hep3B cells (Figure 5.3A). The alteration in SREBP2 levels correspondingly affected the total cholesterol levels (Figure 5.3B). The mRNA levels of genes responsible for *de novo* cholesterol biosynthesis, namely, *SREBP2*, *HMGCR*, *LDLR*, *INSIG1*, *MVD*, and *FDPS*, were also altered, corresponding to the SREBP2 levels in the cells (Figure 5.3C).

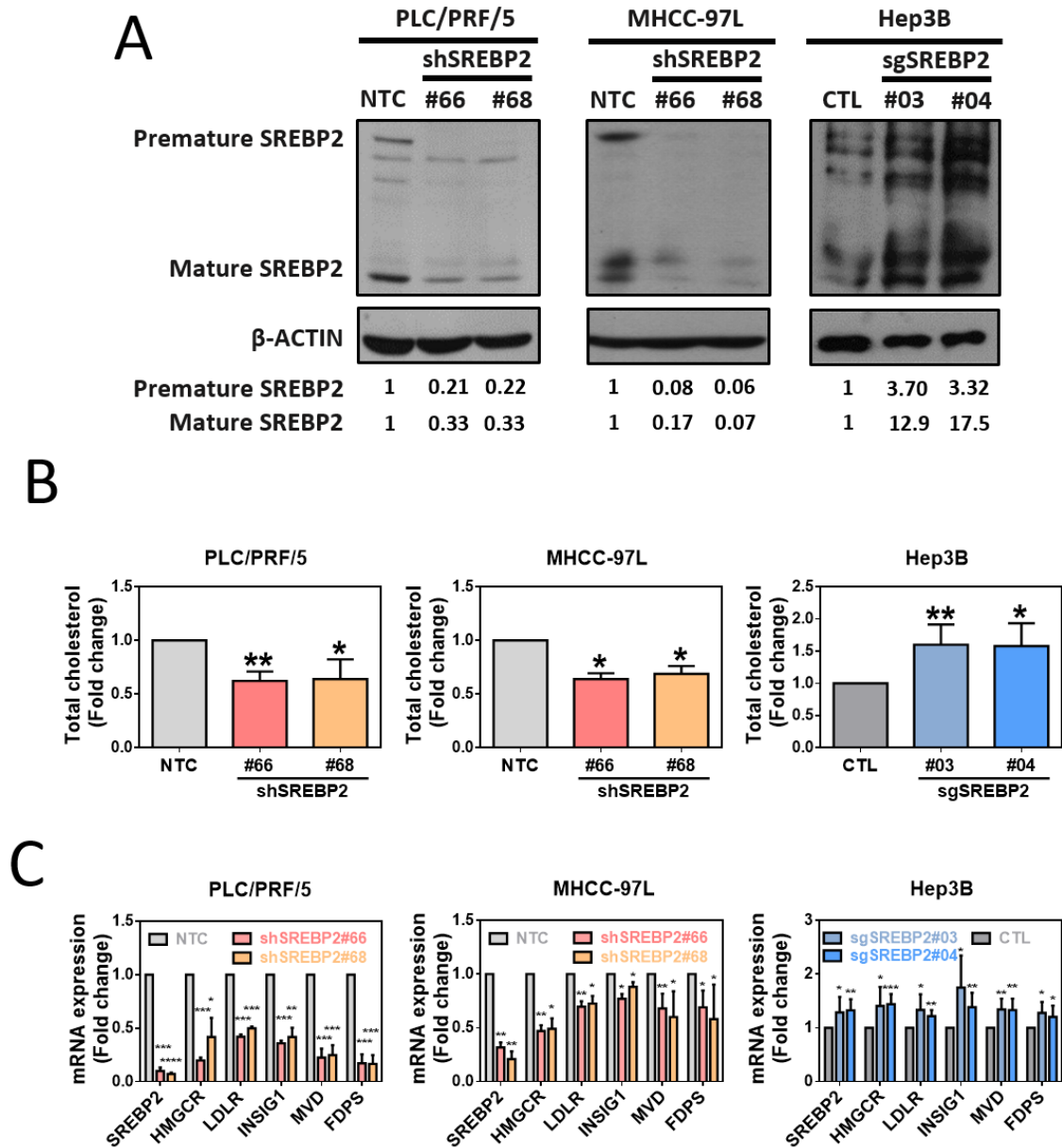


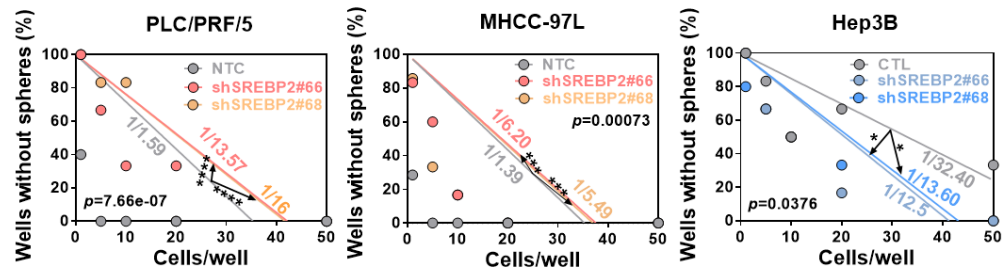
Figure 5.3. SREBP2 regulates cholesterol gene expression levels and total cholesterol levels.

(A) SREBP2 protein levels in non target control (NTC), shSREBP2 (#66 & #68) derived from PLC/PRF/5 and MHCC-97L cells, and control (CTL), sgSREBP2 (#03 & #04) derived from Hep3B cells were determined by western blot analysis. Quantification was performed using ImageJ. (B) Total cholesterol levels were decreased in shSREBP2 cells but increased in sgSREBP2 cells. (C) Similar effects were observed in genes responsible for cholesterol biosynthesis corresponding to SREBP2 genetic alterations. Error bars indicate mean \pm SD (n = 3-7). * p <0.05, ** p <0.01, and *** p <0.001 from Student's t-test.

5.3.3 SREBP2 regulates the self-renewal and tumorigenic ability of HCC cells

The role of SREBP2 in regulating CSC properties in HCC was further examined with respect to its ability to promote self-renewal and initiate tumor formation. The *in vitro* self-renewal ability of SREBP2 knockdown and overexpressing clones was determined by limiting dilution sphere formation assay. Knockdown of SREBP2 significantly reduced the incidence of cancer stem cell frequency (Figure 5.4A). In PLC/PRF/5 cells, shSREBP2#66 and shSREBP2#68 led to a decrease in the frequency of spheres formed by more than 8-fold. In MHCC-97L cells, the fold change was over 5 times higher in these two SREBP2 knockdown clones than in the NTC clone. Similarly, overexpression of SREBP2 promoted increased cancer stem cell frequency in Hep3B cells (Figure 5.4A). sgSREBP2#03 and sgSREBP2#04 cells displayed at least a 2-fold increase in the number of spheres observed in the assay. Next, an *in vivo* tumorigenic assay was performed to study the effect of SREBP2 manipulations on tumorigenicity in HCC cells. SREBP2 knockdown and overexpressing cells were subcutaneously inoculated into the flanks of NOD/SCID mice at several dilutions of cells to determine the tumor frequency. In both PLC/PRF/5 and MHCC-97L cells, SREBP2 knockdown resulted in a decrease in the size and number of tumors developed (Figure 5.4B). By calculating the tumor incidence rate, there was at least a 2-fold decrease in PLC/PRF/5 SREBP2 knockdown clones, whereas a dramatic 5243-fold decrease in MHCC-97L SREBP2 knockdown clones was observed (Table 5.1& Table 5.2). In contrast, the tumorigenicity of Hep3B cells was elevated in response to SREBP2 overexpression (Figure 5.4B). Overexpression of SREBP2 enhanced the tumor frequency by 8-fold (Table 5.3). In addition, tumor size was markedly increased compared to the CTL clone.

A



B

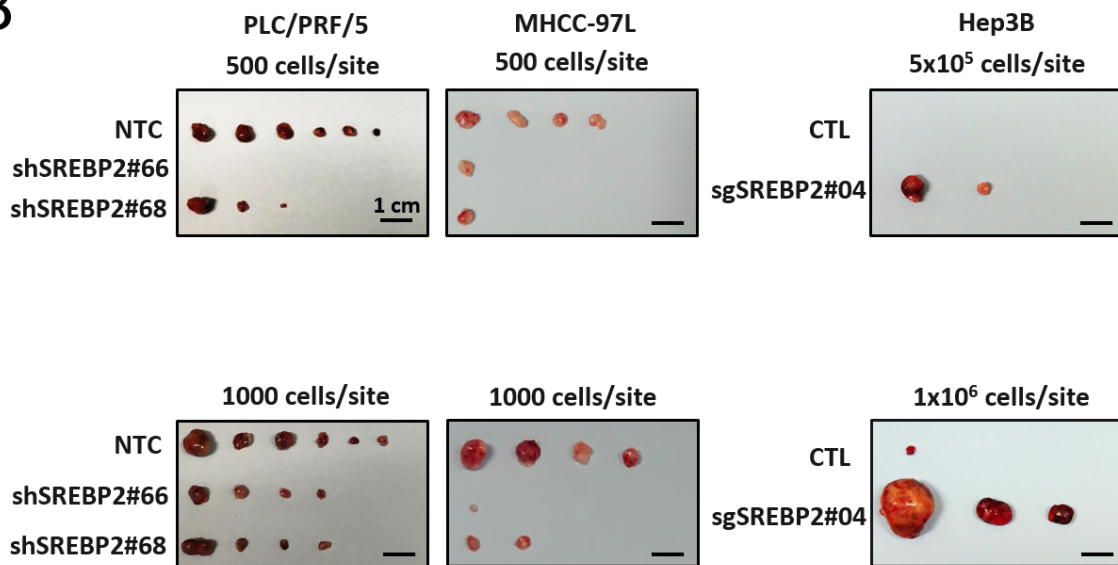


Figure 5.4. SREBP2 regulates self-renewal and tumorigenicity in HCC cells.

(A) *In vitro* limiting dilution sphere formation analysis showing the role of SREBP2 in regulating CSC self-renewal ability. (B) Left: knockdown of SREBP2 in PLC/PRF/5 and MHCC-97L cells showed suppressed tumorigenicity compared to that of NTC clones. Representative pictures have been shown at cell density of 500 and 1000 cells per injection site. Right: overexpression of SREBP2 enhanced tumorigenicity in Hep3B cells compared to that of CTL. Representative images are shown at a cell density of 5×10^5 and 1×10^6 cells per injection site. Scale bar: 1 cm. * $p < 0.05$, *** $p < 0.001$ and **** $p < 0.0001$ from Student's t-test.

Table 5.1. Primary engraftment of PLC/PRF/5 cells.

PLC/PRF/5	Tumor incidence rate			Extreme limiting dilution		
	500 cells	1000 cells	5000 cells	Estimated CSC frequency	95% CI	<i>p</i> -value
NTC	6/7	6/7	5/5	1/373	1/740-1/188	
shSREBP2#66	0/6	4/6	2/5	1/4331	1/10447-1/1795	<0.0001
shSREBP2#68	3/6	4/6	5/5	1/818	1/1732-1/386	0.121

Table 5.2. Primary engraftment of MHCC-97L cells.

MHCC-97L	Tumor incidence rate					Extreme limiting dilution		
	100 cells	500 cells	1000 cells	10000 cells	50000 cells	Estimated CSC frequency	95% CI	<i>p</i> -value
NTC	0/5	4/4	4/4	4/4	4/4	1/1	1/123-1/1	
shSREBP2#66	0/5	1/4	1/4	3/4	4/4	1/5243	1/14495-1/1896	<0.0001
shSREBP2#68	0/5	1/4	2/4	2/4	3/4	1/15574	1/41642-1/5825	<0.0001

Table 5.3. Primary engraftment of Hep3B cells.

Hep3B	Tumor incidence rate			Extreme limiting dilution		
	1x10 ⁵ cells	5x10 ⁵ cells	1x10 ⁶ cells	Estimated CSC frequency	95% CI	<i>p</i> -value
CTL	0/5	0/5	1/5	1/7511347	1/52790550-1/1068759	
sgSREBP2#04	1/5	2/5	3/5	1/940728	1/2170005-1/407819	0.0199

5.3.4 SREBP2 regulates the expression of liver CSC markers in HCC cells

The link between SREBP2 and cancer stemness was investigated by examining the expression of liver CSC markers in response to SREBP2 alterations. Expression of CD47 and CD133 was selected and analyzed using flow cytometry analysis (Figure 5.5). Repression of SREBP2 resulted in a significant decrease in the expression of CD47 and CD133 in both cell lines. In PLC/PRF/5 cells, SREBP2 knockdown led to at least 1.3-fold and 1.1-fold decreases in CD47 and CD133, respectively. In MHCC-97L cells, CD47 expression decreased by at least 1.8-fold, while CD133 expression decreased by at least 1.4-fold in SREBP2 knockdown clones. In contrast, overexpression of SREBP2 increased the expression of CD47 and CD133 in Hep3B cells, with an approximately 1.3-fold enhancement.

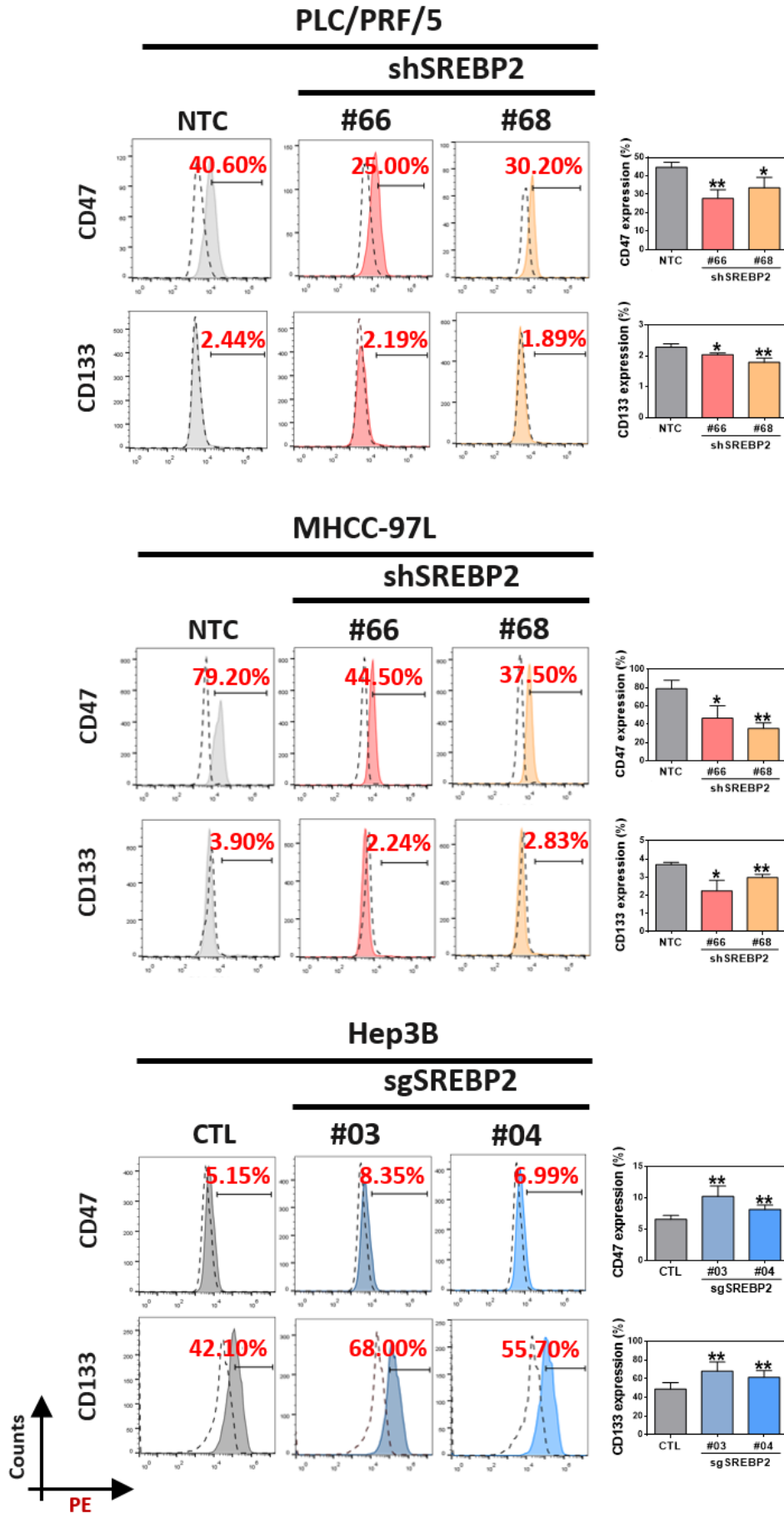


Figure 5.5. SREBP2 regulates expression of CSC markers in HCC cells.

Top and Middle: knockdown of SREBP2 suppressed expression of liver CSC markers, including CD47 and CD133 expression, in PLC/PRF/5 and MHCC-97L cells. Bottom: overexpression of SREBP2 increased CD47 and CD33 expression in Hep3B cells. Data were analyzed by a flow cytometer and analyzed using FlowJo. Error bars indicate mean \pm SD (n = 3-5). * p <0.05, and ** p <0.01 from Student's t-test.

5.3.5 SREBP2 regulates the migration and invasion abilities of HCC cells

CSCs are considered to be the primary driving force of metastatic precursors due to their EMT promotion properties (200, 201). Since SREBP2 was found to regulate liver CSCs, we hypothesized that SREBP2 would exert a similar regulatory effect on the migration and invasion abilities of cancer cells. This relationship of SREBP2 to the invasiveness of HCC cells was evaluated using cell migration (transwell) and invasion (Matrigel™ matrix-coated transwell) assays (Figure 5.6). Cell migration and invasion abilities were dramatically repressed in response to SREBP2 knockdown in PLC/PRF/5 and MHCC-97L cells. A 2.5-fold and 1.7-fold decrease was recorded in the number of migrated cells in shSREBP2 clones compared to the NTC clone in PLC/PRF/5 and MHCC-97L cells, respectively. Meanwhile, a moderately similar fold difference, 1.8- and 1.6-fold decreases, was observed in the number of invaded cells of shSREBP2 clones correspondingly in PLC/PRF/5 and MHCC-97L cells. In contrast, SREBP2 overexpression promoted the migration and invasiveness of Hep3B cells, leading to an approximately 1.5-fold increase in the number of migrated and invaded cells.

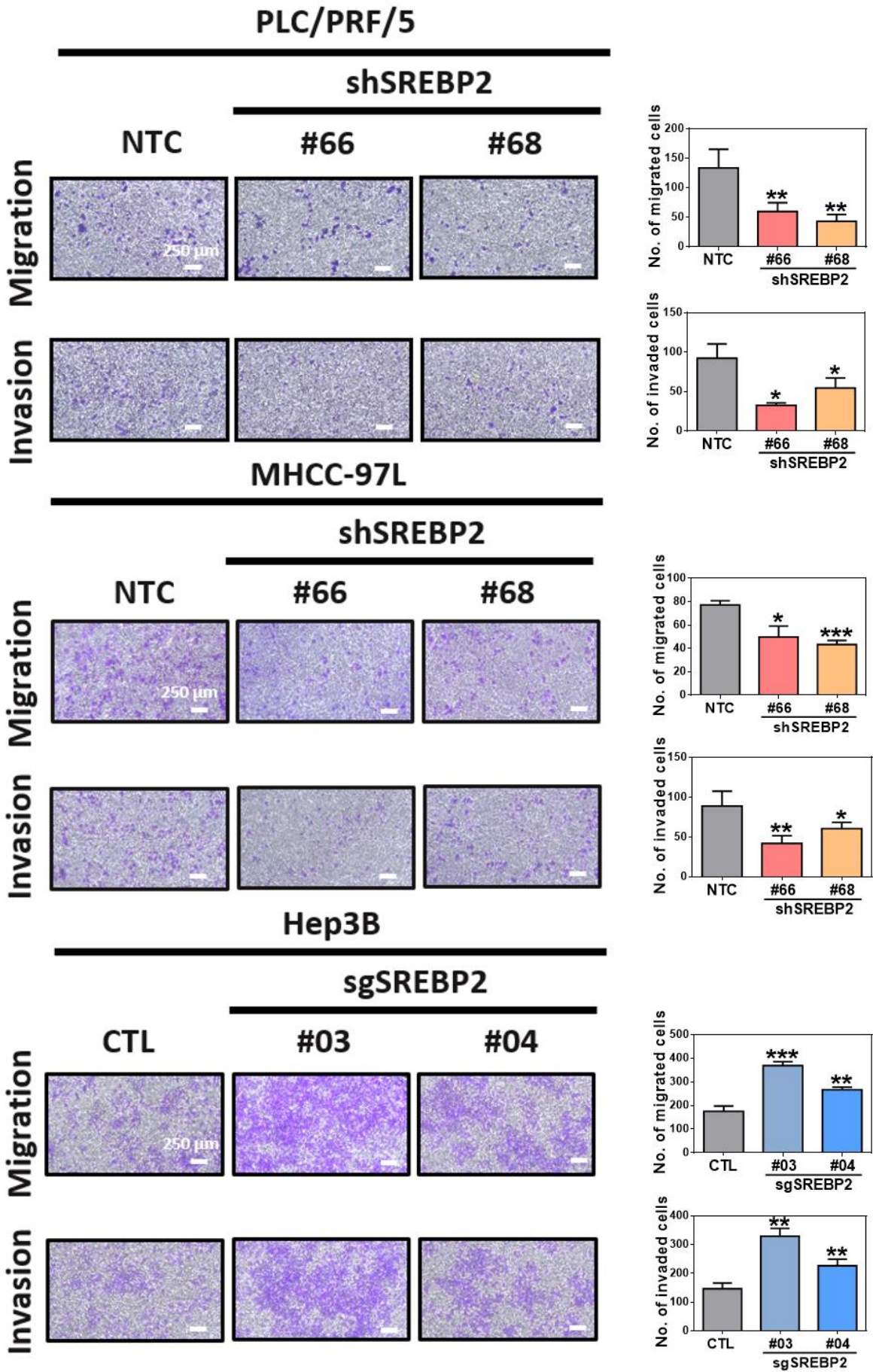


Figure 5.6. SREBP2 regulates the migration and invasion abilities of HCC cells.

Migration was examined using uncoated transwells, while invasion was assayed using Matrigel™ matrix-coated transwells. Top & Middle: suppression of SREBP2 in PLC/PRF/5 and MHCC-97L cells decreased the number of cells migrated or invaded cells. Bottom: overexpression of SREBP2 in Hep3B cells increased the number of migrated and invaded cells. Scale bar: 250 μm. Error bars indicate mean±SD (n = 3-5). * $p < 0.05$, ** $p < 0.01$ and *** $p < 0.001$ from Student's t-test.

5.3.6 Cholesterol biosynthesis is the major effector of SREBP2-mediated CSC signalling

To further confirm the role of cholesterol biosynthesis as the downstream effector of SREBP2 in mediating CSC function, exogenous cholesterol was added to SREBP2 knockdown HCC cells, followed by CSC functional assays. Since cholesterol was dissolved in methyl-β-cyclodextrin (MβCD) to aid in attaining the maximal availability of insoluble cholesterol to cells, the same amount of MβCD was added as a control for the following experiments. With consistent findings of shSREBP2 in regulating CSC properties, including self-renewal ability, liver CSC stemness marker expression, and migration and invasion aggressiveness, these properties were downregulated in response to SREBP2 levels compared to the NTC clone (Figure 5.7A-C). Strikingly, after administration of 5 μM cholesterol, these CSC properties were not only enhanced in NTC clones but also rescued the inhibitory effects of SREBP2 knockdown clones in MHCC-97L cells (Figure 5.7A-C).

In addition, exogenous cholesterol administration also enhanced HCC organoid expansion (Figure 5.8). Using a CellTiter-Glo® assay, exogenous administration of cholesterol at various doses (15 and 30 μM) increased the size of both HCC organoids and their proliferation rate in a dose-dependent manner. There was a 4- and 5-fold increase in proliferation when cholesterol was administered to the HCC organoids. Representative images are shown.

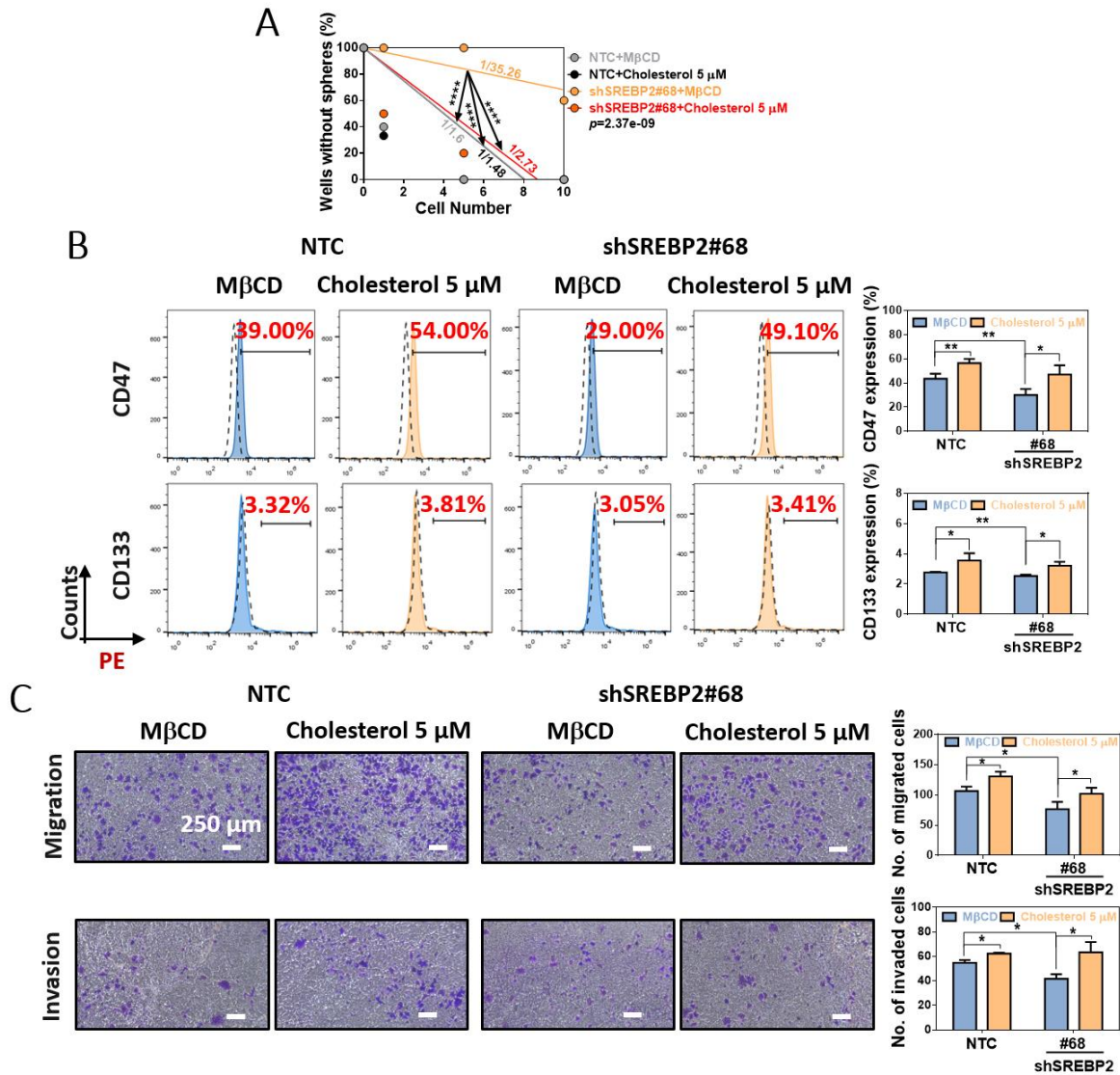


Figure 5.7. Cholesterol biosynthesis is the major effector of SREBP2-mediated CSC functions in HCC cells.

(A) *In vitro* limiting dilution sphere formation assay showed the role of cholesterol at 5 μM rescues the suppressed self-renewal ability in shSREBP2 MHCC-97L cells. (B) The addition of cholesterol not only enhanced expression levels of CD47 and CD133 in NTC clones, but also recovered the abolished expression of shSREBP2 MHCC-97L cells. (C) Addition of cholesterol enhanced both migration and invasion abilities in NTC and shSREBP2 MHCC-97L cells. Error bars indicate mean±SD (n = 3-6). * $p < 0.05$, ** $p < 0.01$, and *** $p < 0.001$ from Student's t-test.

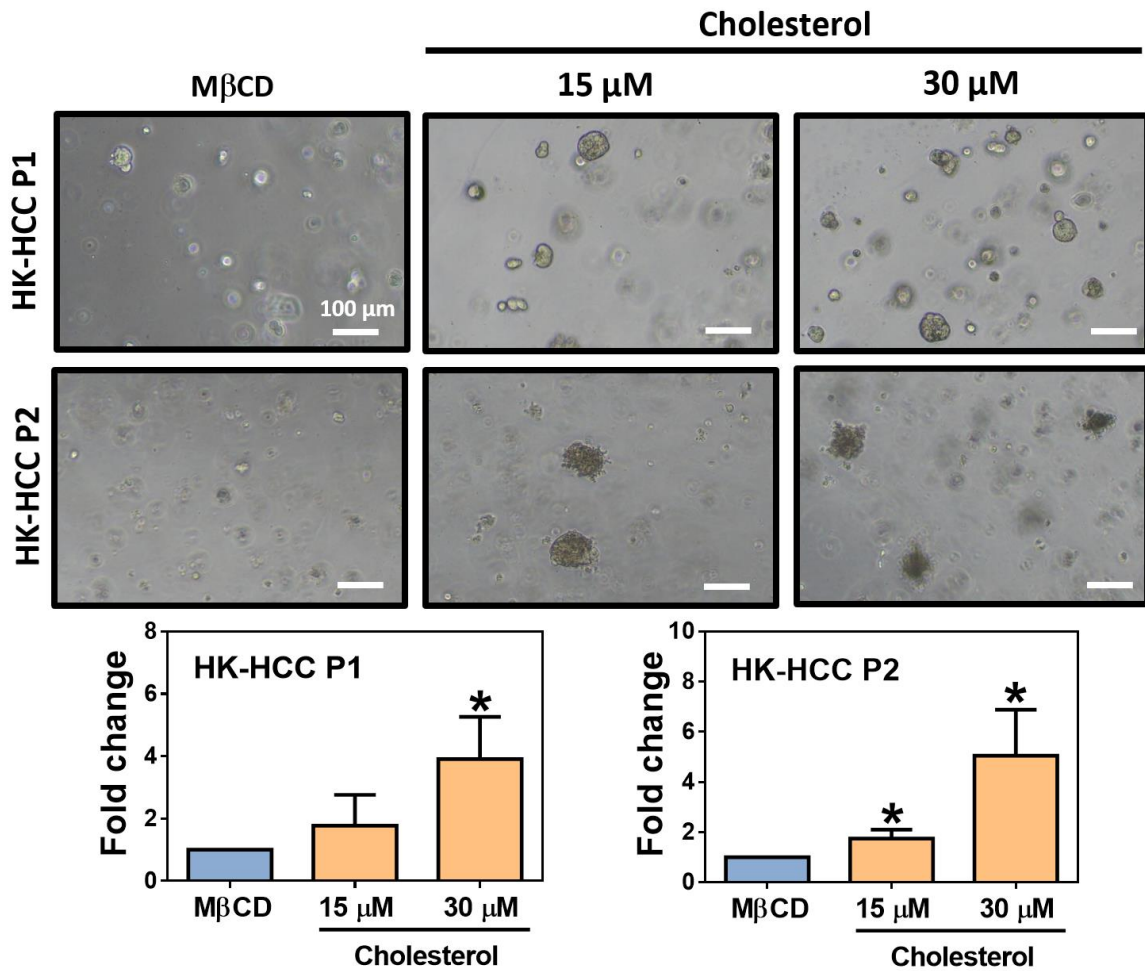


Figure 5.8. Cholesterol increases the size and proliferation rate of HCC cells *ex vivo*.

The growth of two HCC patient-derived organoids (HK-HCC P1 and HK-HCC P2) was significantly enhanced upon administration of cholesterol at 15 and 30 μM for 6 days using CellTiter-Glo® assay. Representative images of organoids treated with M β CD and cholesterol at 15 and 30 μM on day 6 are shown. Scale bar: 100 μm . Error bars indicate mean \pm SD (n = 3-5). * p <0.05 from Student's t-test.

5.3.7 High cholesterol-utilizing HCC cells exhibit enhanced liver CSC properties

In addition to investigating the role of exogenous cholesterol, we were interested in examining the role of endogenous cholesterol utilization in the regulation of liver CSCs. For this purpose, we utilized a special live cell dye, BODIPY-conjugated cholesterol (BCHOL), which is a fluorescent reporter, BODIPY, bound to cholesterol that can be taken up by cells and allows for signal detection. We first labelled PLC/PRF/5 cells with BCHOL and subjected them to FACS to separate them into two populations. PLC/PRF/5 cells with high uptake of BCHOL (BCHOL^{High}) were indicated to have high utilization of cholesterol. In contrast, cells with low uptake of BCHOL (BCHOL^{Low}) were indicated to have low utilization of cholesterol. Before cell sorting, the staining efficiency was approximately 72% (Figure 5.9A). Successful isolation of BCHOL^{High} and BCHOL^{Low} was confirmed by the percentage of BCHOL in the corresponding population. The BCHOL^{Low} population had only 1.42% staining, but the BCHOL^{High} population had an unprecedented 92% positive staining. Using an *in vitro* limiting dilution sphere formation assay, BCHOL^{High} PLC/PRF/5 cells exhibited enhanced cancer stem cell frequencies compared to BCHOL^{Low} PLC/PRF/5 cells (Figure 5.9B). The frequency was increased by 4.6-fold. Moreover, the *in vivo* tumorigenicity assay presented a trend of higher tumorigenicity in BCHOL^{High} PLC/PRF/5 cells than in BCHOL^{Low} PLC/PRF/5 cells, which was increased by 3-fold, from 1 stem cell in 3862 cells to 1 stem cell in 1192 cells (Figure 5.9C & Table 5.4).

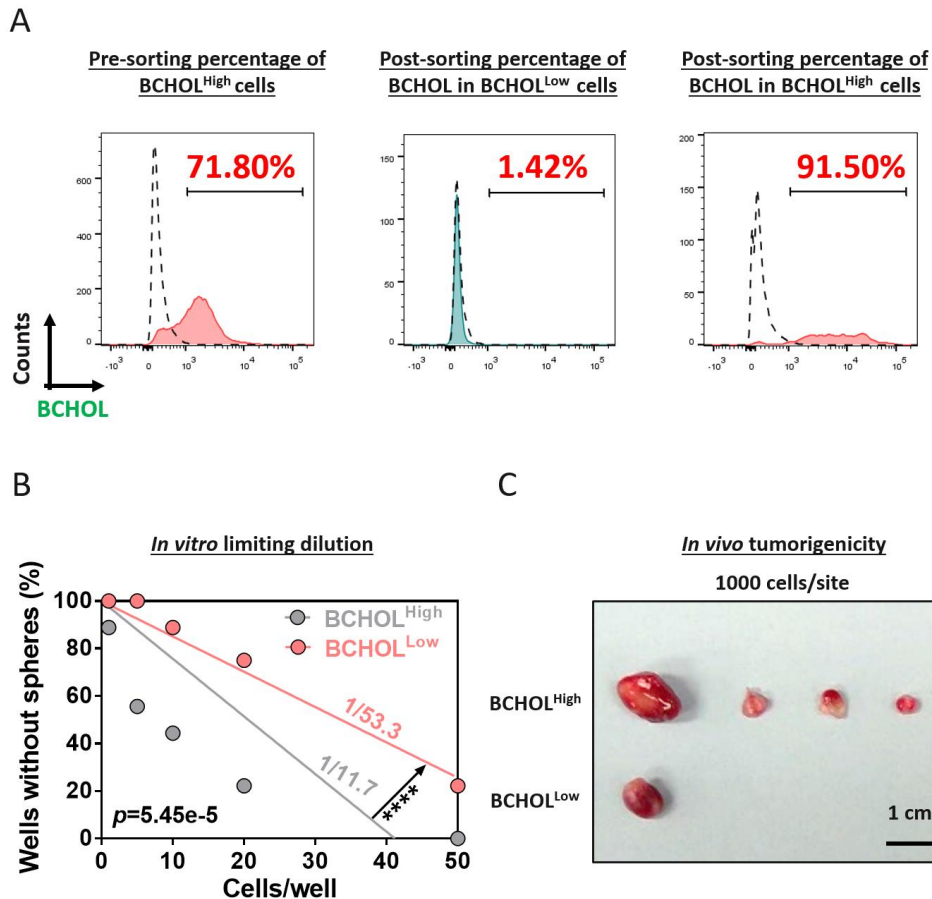


Figure 5.9. HCC cells with high cholesterol utilization exhibit enhanced liver CSC properties.

(A) Postsorting analysis showing that the BCHOL^{High} cells were 91.5% positive, while the BCHOL^{Low} cells were 1.42% positive. (B) *In vitro* limiting dilution sphere formation assay showing that BCHOL^{High} cells were endowed with enhanced self-renewal ability compared to their BCHOL^{Low} counterparts. (C) *In vivo* tumorigenicity assay showing that BCHOL^{High} cells were endowed with increased tumorigenic ability compared to their BCHOL^{Low} counterparts. 1000 cells per injection site are shown. Scale bar: 1 cm. **** $p < 0.0001$ from Student's t-test.

Table 5.4. Primary engraftment of PLC/PRF/5 cells.

PLC/PRF/5	Tumor incidence rate		Extreme limiting dilution		
	500 cells	1000 cells	Estimated CSC frequency	95% CI	<i>p</i> -value
BCHOL ^{High}	1/5	4/6	1/1192	1/2887-1/492	
BCHOL ^{Low}	1/5	1/6	1/3862	1/15617-1/955	0.14

5.3.8 SREBP2-mediated cholesterol biosynthesis promotes poor prognosis in HCC patients

Previous data have shown that SREBP2 mediates cholesterol biosynthesis in HCC and its relationship to liver CSCs. The clinical relevance of SREBP2 was then examined in two online available databases and one in-house clinical cohort consisting of 50 HCC patients. Expression of *SREBP2* mRNA was significantly upregulated in HCC tumor tissues compared to nontumor liver tissues in both the publicly available GSE14520 dataset and The Cancer Genome Atlas (TCGA) dataset (Figure 5.10A). In the in-house cohort, a tissue microarray consisting of 50 HCC samples and their corresponding paired nontumor liver tissue samples demonstrated that patients with high SREBP2 expression had shorter disease-free survival ($p=0.0002$) (Figure 5.10B). Although it did not reach a significant value, patients with high SREBP2 expression tended to experience poorer overall survival as well ($p=0.3467$). In addition, it was further shown that patients with high SREBP2 expression had a higher chance of experiencing HCC recurrence; 19 patients with high SREBP2 expression experienced recurrence of the disease, while 18 patients with low SREBP2 expression showed no relapse ($p=0.0006$, χ^2 test). Representative images of IHC staining are shown as a reference (Figure 5.10C). In the paired samples, case 49 exhibited low SREBP2 expression in both nontumor and tumor samples, while case 13 presented minimal SREBP2 expression in the nontumor sample but strong cytoplasmic and nuclear (mature form of SREBP2) staining in the corresponding tumor slide.

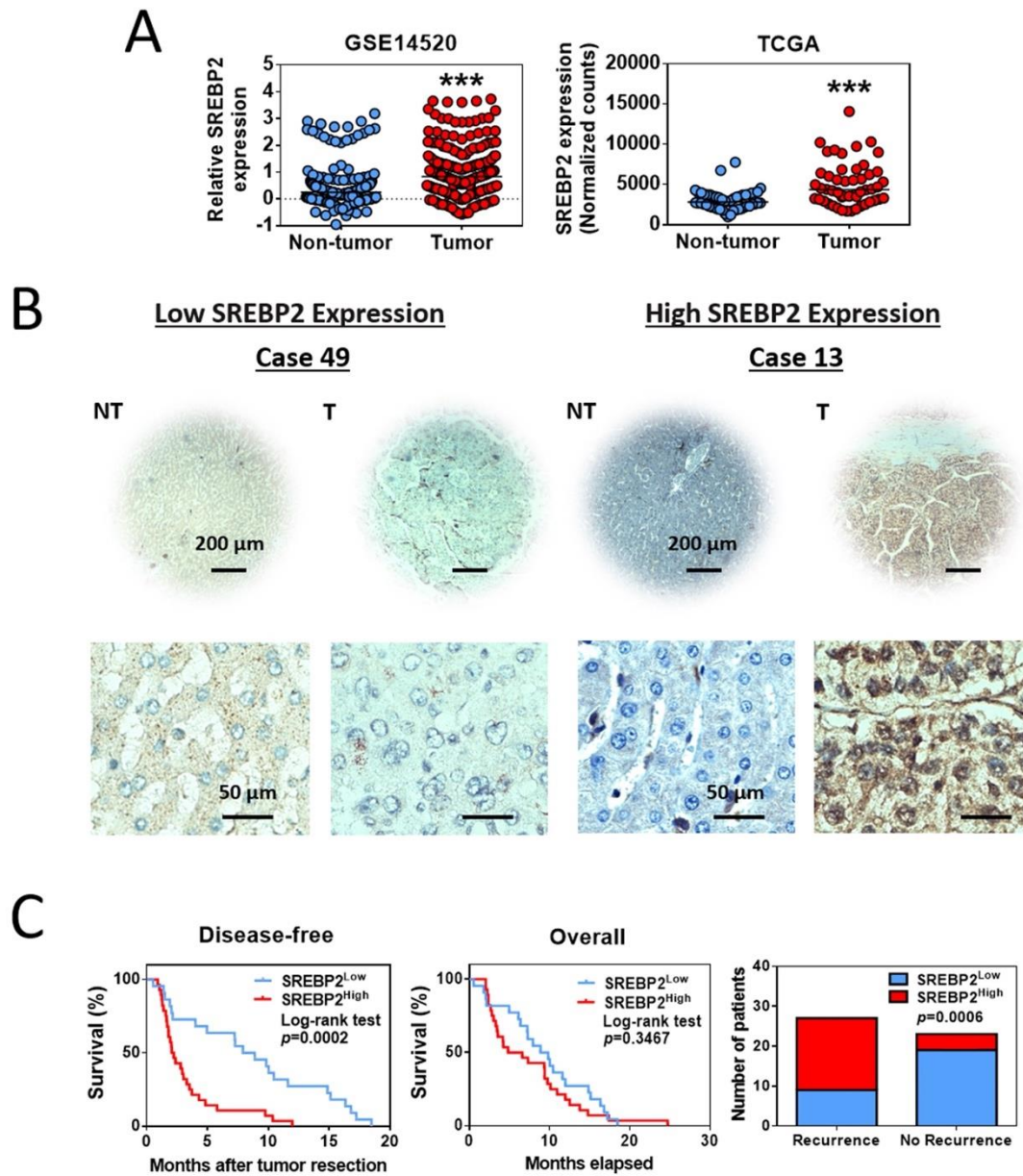


Figure 5.10. SREBP2 overexpression is correlated with poor prognosis.

(A) In publicly available datasets, including GSE14520 and TCGA, *SREBP2* mRNA was significantly upregulated in HCC tumor tissues compared to nontumor liver tissues ($***p<0.001$ from Student's t-test, GSE14520 dataset: nontumor sample number = 239 & tumor sample number = 247; TCGA dataset: paired cases = 50). (B) A tissue microarray consisting of 50 tumor tissues and corresponding nontumor liver tissues was subjected to IHC analysis. Patients with high SREBP2 expression ($n = 28$) displayed shorter disease-free survival ($p=0.0002$) than those with low SREBP2 expression with a higher recurrence rate ($p=0.006$). (C) Representative paired images are shown. Case 49 presents low SREBP2 expression, while case 13 shows a high amount of SREBP2. Scale bars: 50 and 200 μ m.

5.4 Discussion

CSCs are regarded as the origin of tumor formation. In addition, CSCs have also been linked to metastasis induction via EMT regulation (202). Overexpression of SREBP2 has been observed in many cancers and is related to poor clinical outcome. However, limited studies have investigated the mechanism of SREBP2-mediated cholesterol biosynthesis in tumorigenesis. Whether SREBP2 regulates CSCs remains largely unknown. In this chapter, the functional role of SREBP2-mediated cholesterol biosynthesis in regulating liver CSCs was analyzed using a variety of CSC functional assays.

The effect of SREBP2 on cholesterol biosynthesis in HCC cells was first examined by qPCR and cholesterol quantification analyses. The important genes involved in cholesterol biosynthesis are regulated by the master regulator SREBP2. The final product cholesterol is also altered in response to SREBP2 genetic manipulations. This observation is consistent with previous reports showing the role of SREBP2 in cholesterol metabolism (191) by binding to the promoter region of genes that consist of the conserved SRE sequence (203). Abolishing the N-terminal domain, which is the mature form of SREBP2, was also reported to result in loss of the ability to activate transcription, as it fails to bind to the corresponding DNA sequence (193). This further highlights the efficacy of SREBP2 knockdown and overexpression on its mature form (Figure 5.3A).

After successful establishment of SREBP2 knockdown and overexpression in HCC cells, the effects of SREBP2 on self-renewal ability and tumorigenicity were investigated by limiting dilution sphere formation assay and *in vivo* tumorigenicity assay. In the sphere formation assay, only cells that harbor self-renewal properties can grow in serum-deficient anchorage-independent culture conditions (77). CSCs are therefore enriched in this floating culture and form spheroids that exhibit enhanced CSC marker expression (203, 204). In addition, the contribution of SREBP2 to tumorigenicity was reported in different cancers, such as colon, prostate, and breast cancers (181, 194, 195). Both assays were based on limiting dilutions, which is widely used for the determination of CSC frequency (204, 205). Data from both assays were then subjected to extreme limiting dilution analysis, which is used to calculate the CSC frequency (170). Taken together, our results also revealed that the expression level of SREBP2 was associated with the viability of CSCs in HCC, affecting the sphere formation ability of malignant cells. SREBP2 alteration also impaired tumorigenicity when SREBP2 was

suppressed but promoted tumor formation when SREBP2 was enhanced. Therefore, our findings consolidate the role of SREBP2 in regulating self-renewal and tumorigenesis.

Next, we assessed the expression of CSC surface markers, including CD47 and CD133, in response to manipulation of SREBP2 levels. CD47 has been reported to be a CSC marker in various cancer types, such as lung and liver cancers, and it is associated with drug resistance and poor prognosis in cancer patients (76, 206-208). In a previous study, our team reported that CD47 overexpression in HCC cells conveyed CSC properties (76). There are two ongoing clinical trials, NCT02216409 and NCT02367196, focusing on neutralizing CD47 as an immunotherapeutic strategy. CD133 is considered a marker of CSCs in liver, colon, ovaries, and prostate cancers (209-212). CD133⁺ HCC cells exhibited increased proliferation, tumorigenicity, and *in vivo* clonogenicity and reduced levels of mature hepatocyte markers than CD133⁻ HCC cells (212, 213). Moreover, in the CSC-enriched sphere culture system, CD133 was significantly enriched (202). Knockdown of SREBP2 significantly reduced expression of these two important tumorigenic stem cell markers. Therefore, this indicates a direct role of SEBP2 in regulating liver CSC populations.

CSCs are reported to promote EMT to induce tumor migration and invasion (202). This is also linked to a key anabolic pathway related to SREBP, the PI3K-AKT-mTORC1-SREBP pathway (214). This activated pathway has implicated in many different classes of cancer and is involved in abnormal proliferation, malignant transformation, anti-apoptosis, resistance to cancer-treatment drugs and induction of metastasis (214). SREBP2 controls the synthesis of cholesterol, as we also demonstrated here. Many oncogenic proteins, such as p53, PTEN, and PI3K, converge on the PI3K-AKT-mTOR pathway, highly expressing both protein and cholesterol biosynthesis to respond to nutrient demands for cell growth (181). Based on our observations, SREBP2 plays an important role in regulating the aggressiveness of CSCs in HCC cells in terms of the migration and invasive abilities of CSCs in HCC cells.

In mammals, cholesterol is either synthesized *de novo* or absorbed from the daily diet. Nevertheless, *de novo* cholesterol biosynthesis remains the primary powerhouse for intracellular cholesterol synthesis. Nearly 70-80% of cholesterol inside the human body is synthesized by the liver, 10% by the small intestines, and the remaining cholesterol is derived from daily absorption (215). Cholesterol homeostasis has been previously linked to hematopoietic stem cell proliferation through regulation of IL-23/GCSF (188, 189). More recent studies have demonstrated that excess cholesterol through the inactivation of LpCat3

induces the proliferation of intestinal stem cells and promotes tumorigenicity in *Apc*^{min/+} mice (157). In our study, we also demonstrated that cholesterol was a crucial downstream effector of the SREBP2-mediated signalling cascade in regulating liver CSC properties. By supplementing bioavailable cholesterol to cultured cells, cholesterol directly and efficiently rescues the suppressive effects of SREBP2 knockdown on CSC properties. More importantly, exogenous cholesterol supports the exponential growth of HCC organoids, further consolidating the role of cholesterol as a downstream effector in tumorigenesis.

Meanwhile, with the advancement of chemical labelling and fluorescent techniques, BODIPY-cholesterol has been developed to tackle the lack of a vivid photostable fluorescent cholesterol probe (190). This probe behaves similarly to natural existing cholesterol in both normal and cholesterol-retaining diseased cells. Originally, this probe was developed to monitor the movement, membrane partitioning and trafficking of cholesterol in cells. Our team first utilized this probe to investigate the role of endogenous cholesterol in mediating CSC properties. With high utilization of cholesterol as represented by the uptake of BODIPY cholesterol, these cells exhibited stem cell-like properties, as evidenced by the increase in self-renewal and tumorigenicity.

Taken together, the results in this Chapter provide solid evidence demonstrating the clinical significance of cholesterol biosynthesis in the regulation of cancer stemness in HCC cells. In the next chapter, we functionally characterized and elucidated the role of cholesterol biosynthesis in the regulation of drug resistance, which is believed to be one of the distinct properties of CSCs.

Chapter 6
SREBP2-MEDIATED CHOLESTEROL
BIOSYNTHESIS IS A CRITICAL
DETERMINANT OF DRUG RESISTANCE IN
HCC CELLS

6 SREBP2-mediated cholesterol biosynthesis is a critical determinant of drug resistance in HCC cells

6.1 Introduction

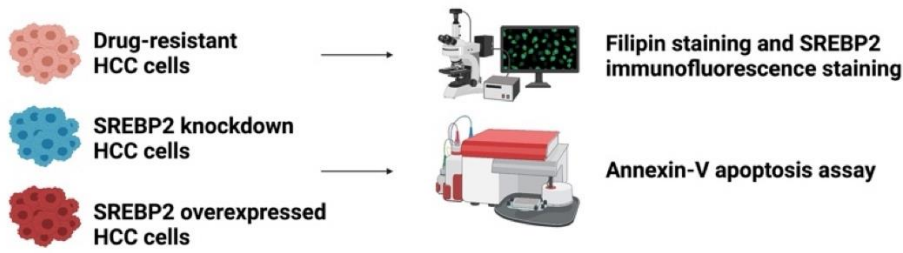
In Chapter 5, we investigated the functional role of SREBP2-mediated cholesterol biosynthesis in regulating cancer stem cell properties, including self-renewal, tumorigenicity, cell invasiveness and expression of liver CSC markers, by altering SREBP2 expression in HCC cells. In addition, we found that SREBP2 expression has clinical relevance in publicly available datasets as well as our in-house HCC tissue microarray. Based on the observation that SREBP2-mediated cholesterol biosynthesis was upregulated in sorafenib- and lenvatinib-resistant PDTXs in Chapter 3, it is reasonable to hypothesize that this process might be crucial for the development of acquired drug resistance to sorafenib and lenvatinib treatments.

SREBP2 and *de novo* cholesterol biosynthesis have been reported to regulate chemotherapy drug resistance in different cancers. In cisplatin-resistant ovarian cancer cells, SREBP2 was highly upregulated among 12 transcription factors when comparing the transcription regulatory network analysis of the cisplatin-resistant arm to the cisplatin-sensitive counterpart (183). More importantly, suppression of SREBP2 by RNA interference resulted in sensitization of ovarian cancer cells to cisplatin treatment (183). Using another chemotherapy drug, paclitaxel, SREBP2 was significantly upregulated in surviving ovarian cancer cells, highlighting the importance of SREBP2 signalling to survive throughout drug treatment. Furthermore, suppression of SREBP2 led to increased cell death upon paclitaxel treatment. However, the role of SREBP2-mediated biosynthesis in the development of drug resistance in HCC is unclear. In this chapter, we first functionally characterize the role of SREBP2-mediated cholesterol biosynthesis in drug resistance using lentiviral-based knockdown and CRISPR activation approaches. In addition, the corresponding mechanism in SREBP2 activation was elucidated using inhibitor and genetic knockdown approaches. Finally, the clinical relevance of SREBP2-mediated cholesterol biosynthesis was studied in a cohort of HCC samples in response to treatment with sorafenib.

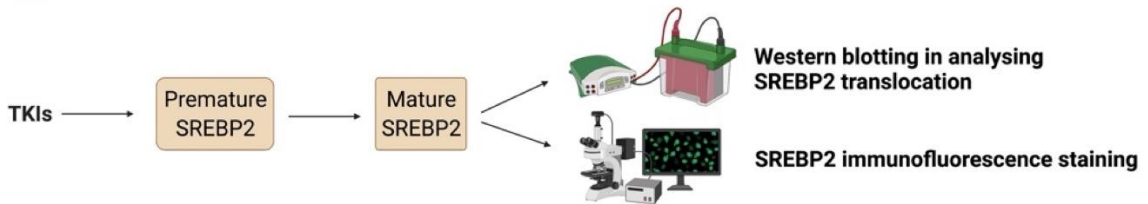
6.2 Experimental outline

(1) SREBP2-mediated cholesterol biosynthesis was first examined in drug-resistant, SREBP2-knockdown, and SREBP2-overexpressing HCC cells. (2) A mechanistic study of SREBP2 activation in response to sorafenib/lenvatinib treatment was performed. (3) Investigating the role of CASP3 activity in the regulation of SREBP2-mediated cholesterol biosynthesis was confirmed using inhibitor and genetic knockdown approaches. (4) Finally, verification of CASP3 and SREBP2 in online available clinical cohorts and an in-house HCC tissue microarray was executed. A summary of the experimental design is shown below (Figure 6.1).

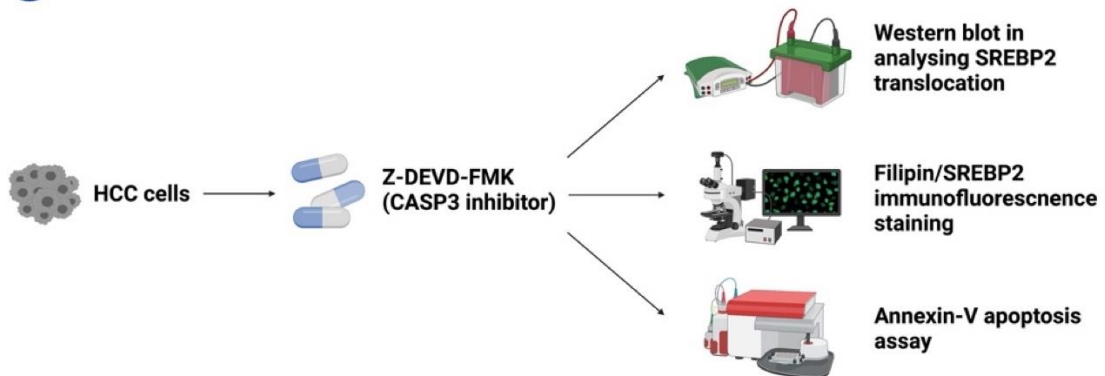
1 SREBP2-mediated cholesterol biosynthesis regulates drug resistance in HCC cells



2 Mechanistic study of SREBP2 translocation under TKI treatments



3 Role of CASP3 in regulation of SREBP2-mediated cholesterol biosynthesis in HCC cells



4 Clinical relevance and significance of CASP3/SREBP2

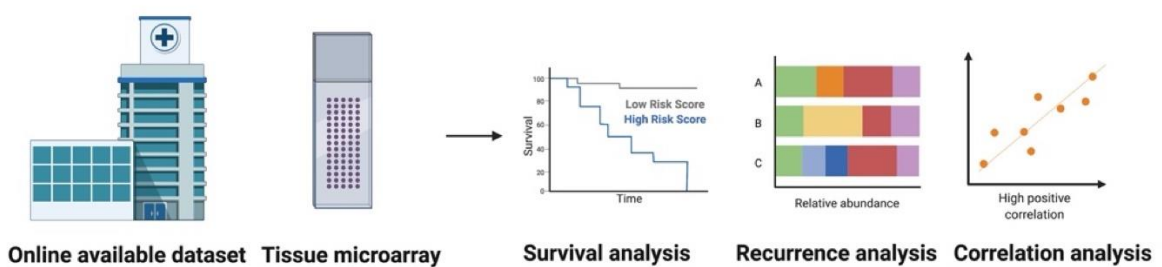


Figure 6.1. Experimental outline in Chapter 6.

The diagram summarizes the methods used to examine the role of SREBP2-mediated cholesterol biosynthesis in drug resistance in HCC cells and its potential upstream regulator.

6.3 Results

6.3.1 SREBP2-mediated cholesterol biosynthesis is activated in drug-resistant HCC cells

Consistent with the observation in drug-resistant HCC xenografts, sorafenib- and lenvatinib-resistant HCC cells derived from PLC/PRF/5 and MHCC-97L cells exhibited enriched SREBP2-mediated cholesterol biosynthesis, as demonstrated by filipin and SREBP2 fluorescent staining (Figure 6.2). An increase in SREBP2 has been demonstrated in both cytoplasmic (premature form) and nuclear (mature form) regions in drug-resistant HCC cells. The intensity of filipin was further quantified using Nikon NIS-Element Software. In PLC/PRF/5 cells, the sorafenib-resistant clone increased filipin staining by approximately 3-fold, while filipin staining was increased by approximately 2-fold in the lenvatinib-resistant clone. In addition, in MHCC-97L cells, filipin intensity was enhanced by approximately 2-fold in both sorafenib- and lenvatinib-resistant clones.

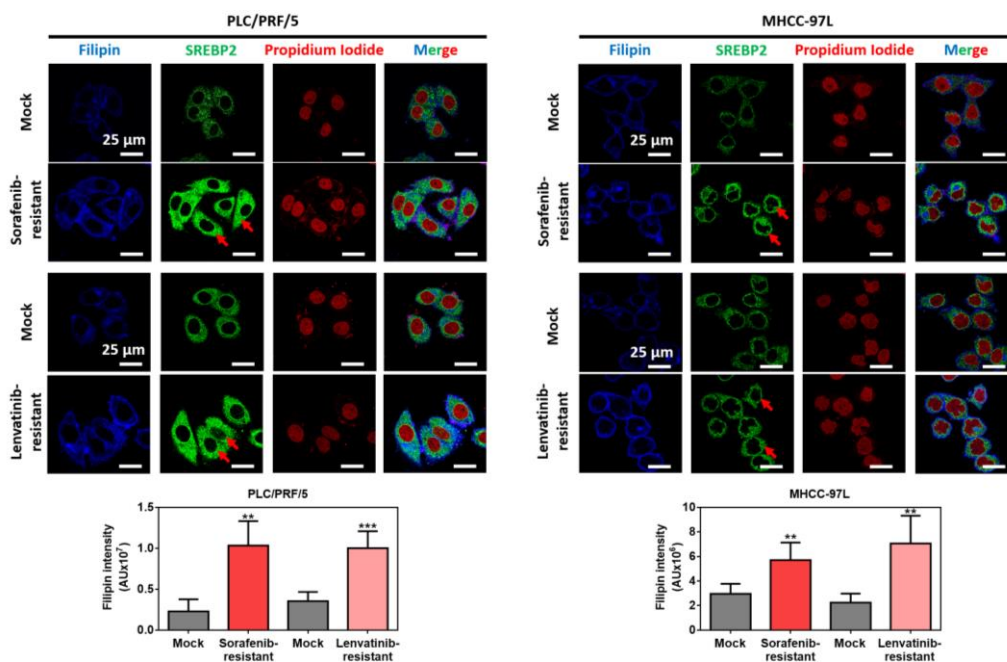


Figure 6.2. Cholesterol and SREBP2 are activated in drug-resistant HCC cells.

Filipin and SREBP2 immunofluorescence staining in (left) drug-resistant PLC/PRF/5 cells and (right) MHCC-97L cells. Increased cholesterol deposition was consistently observed in both cell lines and was quantified using Nikon NIS-Elements Software. Cytoplasmic and nuclear SREBP2 (indicated by arrows) were concomitantly enhanced. Blue: filipin staining; green: SREBP2 staining; red: propidium iodide. Scale bar: 25 μm. Error bars indicate mean ± SD (n = 3-5). ** $p < 0.01$, and *** $p < 0.001$ from Student's t-test.

6.3.2 SREBP2-mediated cholesterol biosynthesis regulates the sensitivity of HCC cells to sorafenib/lenvatinib treatments

Successful knockdown and overexpression of SREBP2 was established and demonstrated CSC regulatory properties in Chapter 5. Therefore, we next examined another important characteristic of CSCs in monitoring drug resistance in HCC cells. Utilizing SREBP2 knockdown and overexpressing clones, the cells were subjected to sorafenib/lenvatinib treatments for 48 hours and assayed using an Annexin-V apoptosis assay (Figure 6.3). In PLC/PRF/5 cells, shSREBP2 clones exhibited a 1.2-fold increase in apoptotic cells in response to treatment with sorafenib and a 2-fold increase in response to lenvatinib treatment. In MHCC-97L cells, SREBP2-suppressed clones demonstrated a 1.5- to 2-fold increase in apoptotic cells after sorafenib treatment and a 1.3- to 1.6-fold increase after lenvatinib treatment. The protective effect of SREBP2-mediated cholesterol biosynthesis was exemplified in SREBP2-overexpressing Hep3B cells, which displayed maximal 2.5-fold and 4.3-fold reductions in apoptotic cells when treated with sorafenib and lenvatinib, respectively.

To further examine whether cholesterol biosynthesis is the major downstream effector of SREBP2-mediated drug resistance, an apoptosis assay was performed in SREBP2 knockdown HCC cells treated with exogenous cholesterol (Figure 6.4). In SREBP2 knockdown MHCC-97L cells, administration of 5 μ M exogenous cholesterol offset the effects of SREBP2-mediated drug resistance in response to both sorafenib and lenvatinib treatments. The decrease was 2.7- and 4.3-fold when comparing the shSREBP2 clone to the cholesterol-supplemented shSREBP2 clone in the apoptosis assay.

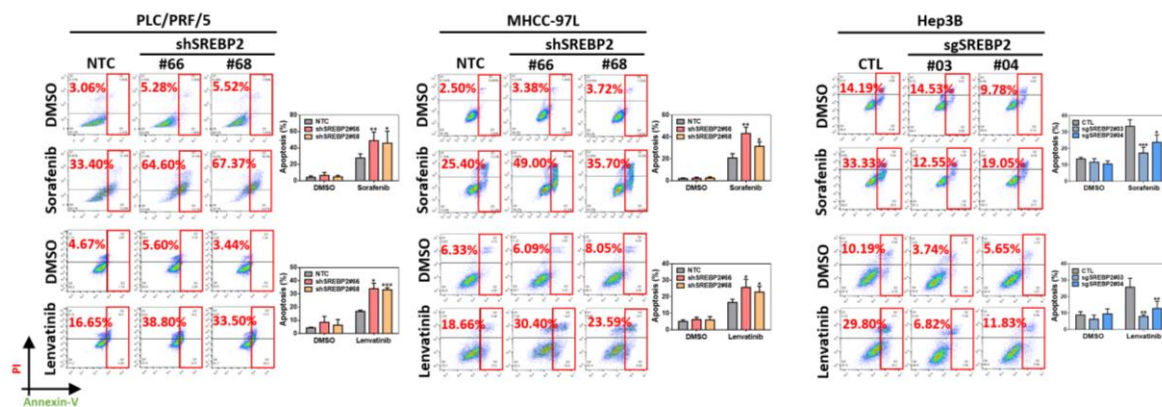


Figure 6.3. SREBP2 regulates the sensitivity of HCC cells to sorafenib and lenvatinib.

Apoptosis of shSREBP2 clones derived from PLC/PRF/5 and MHCC-97L cells and sgSREBP2 clones derived from Hep3B cells induced by either sorafenib (10 μ M or 15 μ M) or lenvatinib (40 μ M) were evaluated using an Annexin-V apoptosis assay. Error bars indicate mean \pm SD (n = 3-5). * p < 0.05, ** p < 0.01, and *** p < 0.001 from Student's t-test.

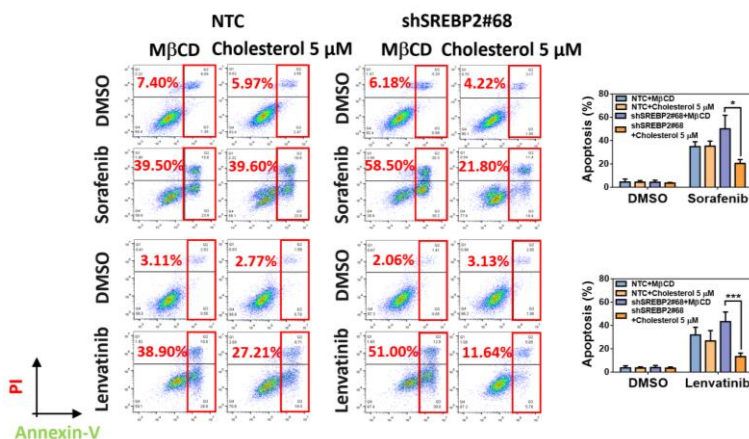


Figure 6.4. Cholesterol attenuates the efficacy of sorafenib and lenvatinib in shSREBP2 HCC cells.

Apoptosis of shSREBP2 clones derived from MHCC-97L cells induced by either sorafenib (15 μ M) or lenvatinib (40 μ M) were evaluated using an Annexin-V apoptosis assay. Error bars indicate mean \pm SD (n = 3-5). * p < 0.05, and *** p < 0.001 from Student's t-test.

6.3.3 Cleavage of SREBP2 occurs in response to drug treatment

To further elucidate the mechanism of acquired drug resistance mediated by SREBP2, we first aimed to detect whether there were any changes in SREBP2 expression in response to short-term drug treatment. Starting at 2 hr, HCC cells were administered sorafenib/lenvatinib, and the levels of SREBP2 were analyzed using western blot analysis. Interestingly, translocation of SREBP2, as demonstrated by a decrease in the immature (125 kDa) form and an increase in the mature (60 kDa) form of SREBP2, was observed when compared to the DMSO control in response to both sorafenib and lenvatinib in PLC/PRF/5 and MHCC-97L cells (Figure 6.5A). Quantification using ImageJ showed that the activation of SREBP2 was increased by at least 1.57-fold and up to 4.61-fold. Concomitantly, immunofluorescence staining of SREBP2 demonstrated similar results (Figure 6.5B). The translocation of SREBP2 was indicated by the elevated intensity of SREBP staining inside the nuclear region. The magnitude of SREBP2 activation was also consistently higher in MHCC-97L cells than in PLC/PRF/5 cells, as shown by both western blot analysis and immunofluorescence staining.

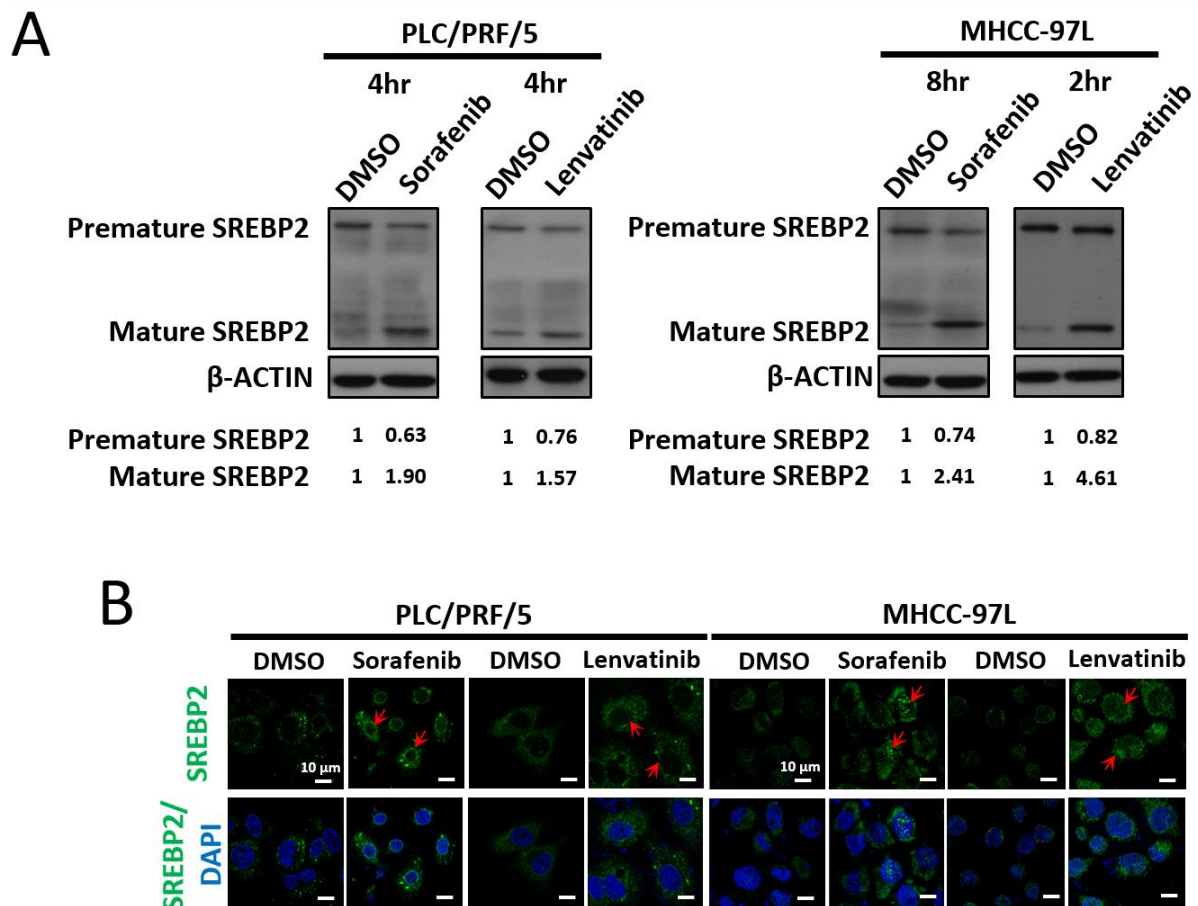


Figure 6.5. Short stress induced by drugs activates SREBP2 translocation.

(A) Expression of immature (125 kDa) and mature (60 kDa) SREBP2 in response to 2 hr, 4 hr, and 8 hr of sorafenib/lenvatinib treatment was evaluated by western blot analysis. Quantification was performed using ImageJ. (B) Increased nuclear SREBP2 (indicated by arrows) was demonstrated corresponding to the designated time points in PLC/PRF/5 and MHCC-97L cells. Green: SREBP2 staining; blue: DAPI staining. Scale bar: 10 μ m.

6.3.4 CASP3-mediated SREBP2 activation occurs in response to drug treatment

CASP3 has been shown to cleave SREBP2 in response to stress stimuli (216, 217). Based on this study, we hypothesized that CASP3-mediated SREBP2 activation is crucial for the development of acquired drug resistance to sorafenib/lenvatinib treatment. To test this hypothesis, we first utilized the CASP3 activity assay kit to examine its activity levels in drug-resistant PDTX samples. Consistently, sorafenib-resistant PDTX#1 and lenvatinib-resistant PY003 exhibited elevated CASP3 activity (Figure 6.6A) by 2-fold. This phenomenon was consistently observed in sorafenib- and lenvatinib-resistant PLC/PRF/5 and MHCC-97L cells (Figure 6.6A). Next, CASP3 activity was also examined in HCC cells in response to sorafenib/lenvatinib treatment. Under short-term treatment with sorafenib/lenvatinib, CASP3 activity levels were markedly induced in both PLC/PRF/5 and MHCC-97L cells (Figure 6.5B). The fold change showed a general trend that sorafenib induced higher CASP3 activity levels than lenvatinib, with over 100-fold versus 2-fold changes. The upregulation of CASP3 in drug-resistant cells and short-stress cells was confirmed by the increased expression of SREBP2, as demonstrated in previous chapters.

To further consolidate the relationship of CASP3 in activating SREBP2 in response to sorafenib/lenvatinib treatments, we employed both inhibitory and genetic knockdown of CASP3 approaches in MHCC-97L cells. First, using a specific CASP3 inhibitor, Z-DEVD-FMK, it was shown that the activation of SREBP2 was abolished, even in response to sorafenib/lenvatinib-induced stress (Figure 6.7A). By first focusing on DMSO and Z-DEVD-FMK treatment alone, the inhibition of CASP3 retained SREBP2 translocation, as observed by an increase in the premature form (125 kDa) and a decrease in the mature form (60 kDa) of SREBP2. Next, comparing drug alone to combination treatment, the induction of SREBP2 was decreased overall as the premature form of SREBP2 exhibited higher expression levels than that of the drug alone, whereas the mature form of SREBP2 presented lower expression in the combination treatment. The retention of SREBP2 leading to inhibited production of cholesterol due to CASP3 inhibition was demonstrated by filipin staining (Figure 6.7B). The protective effect of SREBP2-mediated cholesterol biosynthesis against drug treatment was also resensitized after the inhibition of CASP3 by Z-DEVD-FMK, as shown by the Annexin-V apoptotic assay (Figure 6.7C). Addition of a CASP3 inhibitor further enhanced the apoptotic cell rate induced by sorafenib and lenvatinib by 1.5-fold and 2.2-fold, respectively.

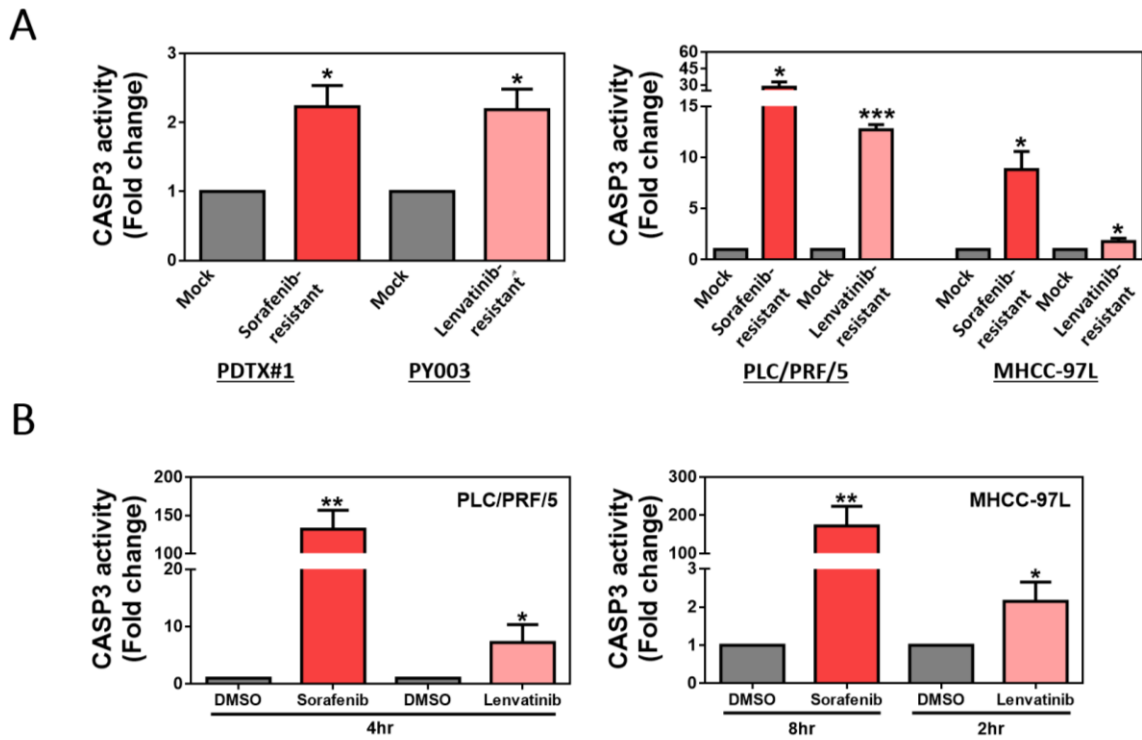


Figure 6.6. The activity of CASP3 is upregulated in response to drug challenges in HCC.

(A) CASP3 activity was increased in sorafenib- and lenvatinib-resistant HCC cells derived from PDTX#1, PY003, PLC/PRF/5 and MHCC-97L cells. (B) Increased CASP3 activity was observed in PLC/PRF/5 and MHCC-97L cells after treatment with sorafenib and lenvatinib. Error bars indicate mean \pm SD (n = 3-5). * p < 0.05, ** p < 0.01, and *** p < 0.001 from Student's t-test.

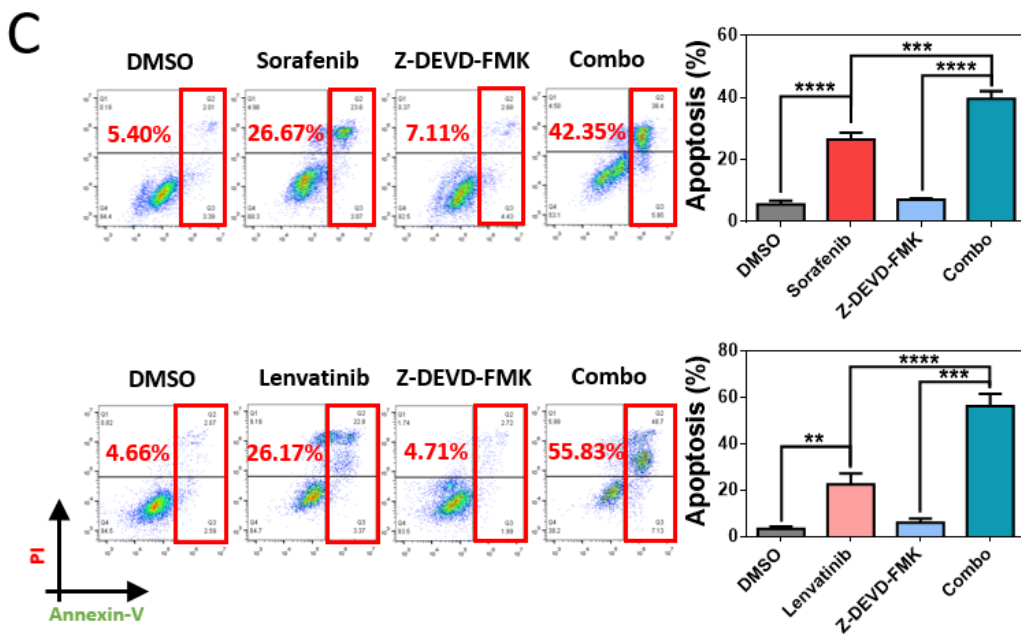
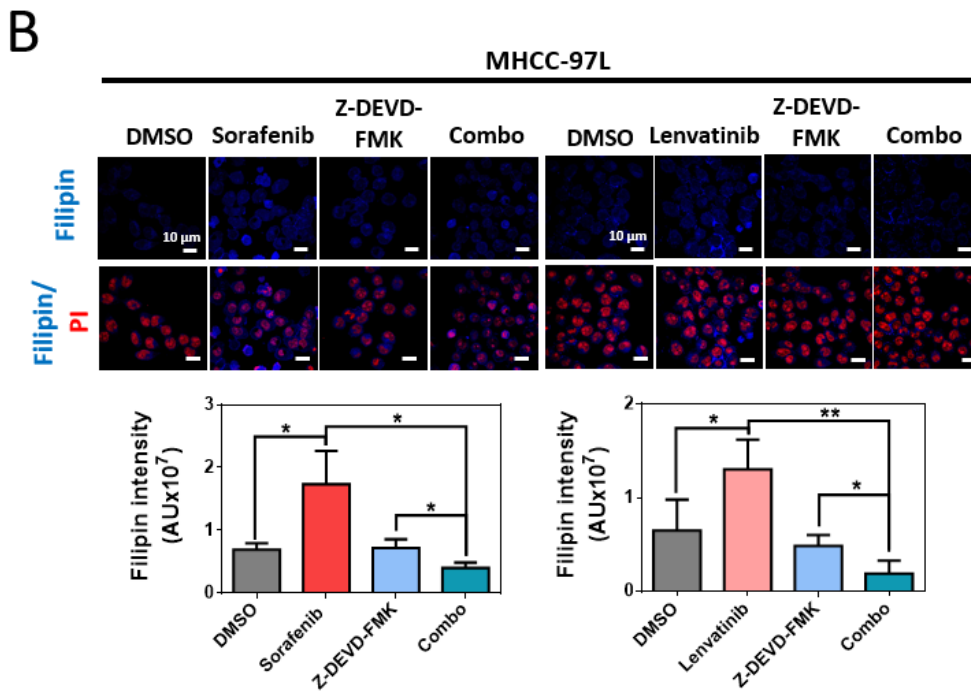
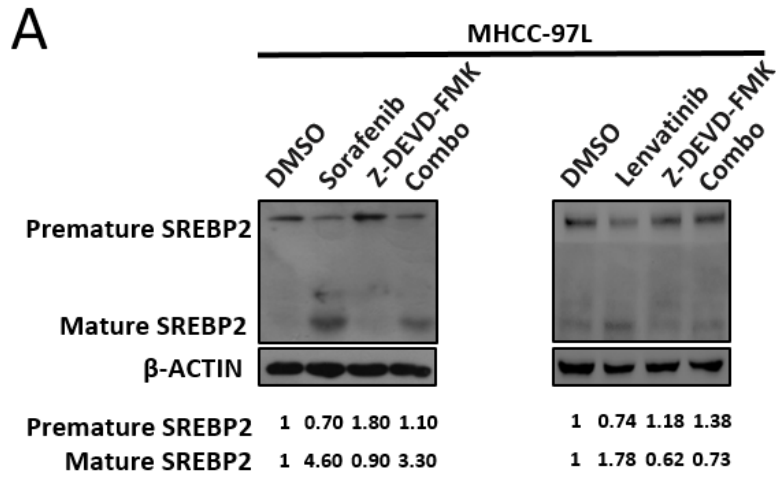


Figure 6.7. CASP3 induces SREBP2 activation in response to drug treatment in HCC cells.

(A) Expression of premature (125 kDa) and mature (60 kDa) SREBP2 in MHCC-97L cells treated with either sorafenib/lenvatinib, Z-DEVD-FMK or their combination was evaluated by western blot analysis. Quantification was performed using ImageJ. (B) Decreased filipin staining was observed in response to sorafenib/lenvatinib treatment in combination with Z-DEVD-FMK. The intensity of filipin staining was quantified using Nikon NIS-Element Software. Blue: filipin staining; red: propidium iodide. Scale bar: 10 μ m. (C) Inhibition of CASP3-induced SREBP2 activation sensitized MHCC-97L cells to sorafenib/lenvatinib treatments. Analysis was performed using an Annexin-V apoptosis assay. Error bars indicate mean \pm SD (n = 3-5). * p <0.05, ** p <0.01, *** p <0.001, and **** p <0.0001 from Student's t-test.

6.3.5 The clinical relevance of SREBP2 overexpression in drug resistance and its correlation with CASP3 expression

Using publicly available HCC datasets, we identified a crucial role for the CASP3/SREBP2 signalling axis in HCC clinical samples, with evidence of an increase in *CASP3* mRNA expression in paired tumor and nontumor samples in the TCGA cohort and a positive correlation between *CASP3* mRNA and *SREBP2* mRNA expression in the TCGA cohort (Figure 6.8A&B). Finally, we examined the clinical relevance of SREBP2 expression in HCC patients treated with sorafenib. In a tissue microarray consisting of 91 HCC samples from patients who received sorafenib in their treatment regimen, patients with high SREBP2 expression demonstrated reduced disease-free survival (p <0.0001) along with a higher chance of tumor recurrence (p =0.00002) (Figure 6.8C&D).

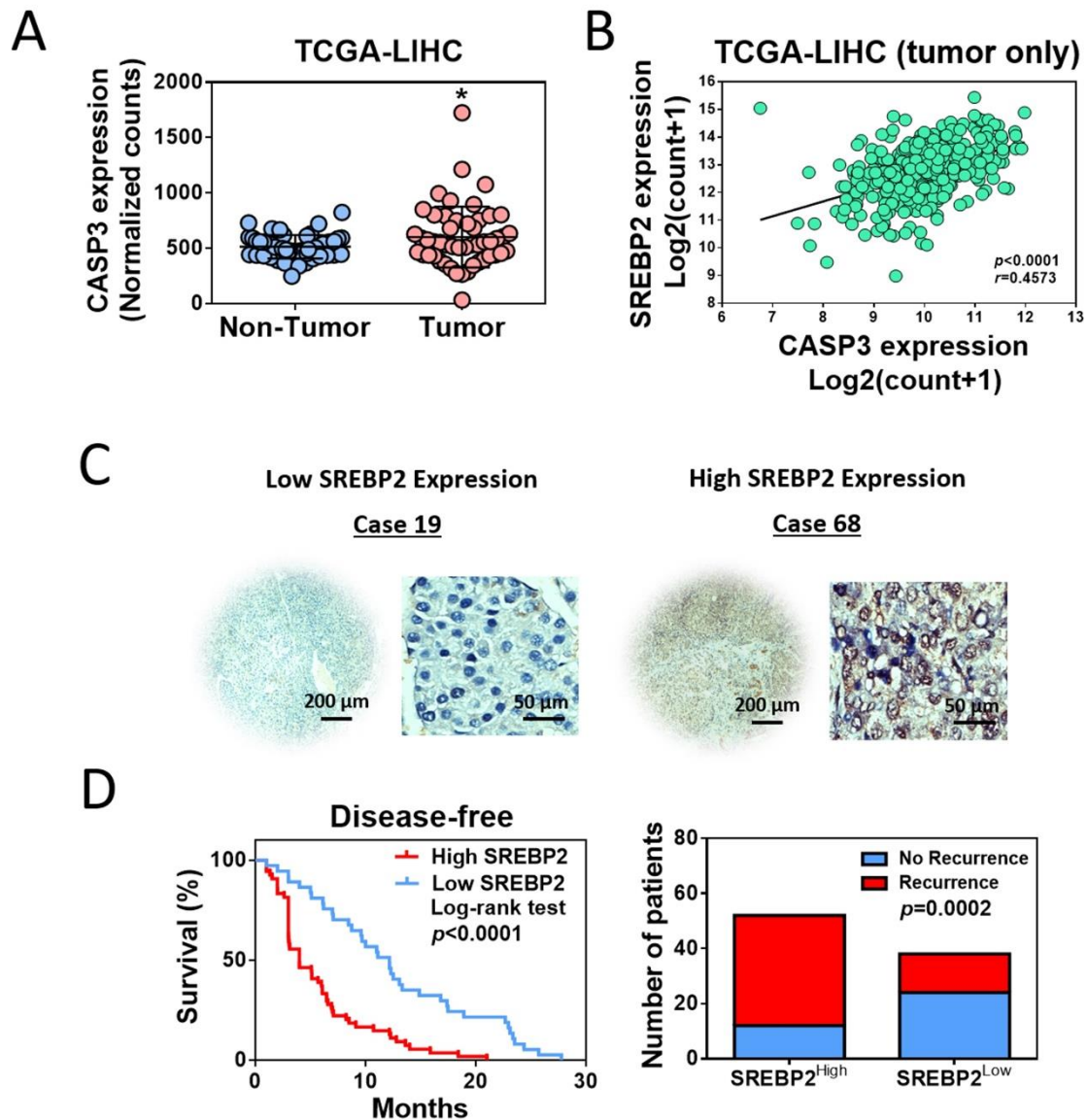


Figure 6.8. Expression of CASP3 and SREBP2 exhibit clinical significance and are correlated.

(A) mRNA levels of *CASP3* were elevated in HCC tumor tissues compared to nontumor liver tissues in TCGA datasets (paired samples, $n = 50$). $*p < 0.05$ from Student's t-test. (B) *CASP3* is positively correlated with *SREBP2* mRNA expression levels in TCGA HCC clinical samples ($r = 0.4573$, $****p < 0.0001$, $n = 371$). (C) A tissue microarray consisting of 91 tumor tissues after sorafenib treatment was subjected to IHC analysis. Representative cases are shown: case 19 exhibited low expression of SREBP2 while case 68 displayed high SREBP2 expression. Scale bars: 50 and 200 μ m. (D) Patients with high SREBP2 expression ($n = 54$) had shorter disease-free survival than those with low SREBP2 expression ($n = 37$). $****p < 0.0001$ from Log-rank t-test. The same pattern was consistent in the recurrence analysis: patients with high SREBP2 expression had a higher chance for tumor relapse. $***p = 0.0002$ from χ^2 test.

6.4 Discussion

The underlying mechanisms of the regulatory role of CASP3 in activating SREBP2 translocation to combat cellular stresses induced by TKIs in HCC cells has been poorly characterized. Therefore, CASP3 inhibitory methods, including small chemical inhibitors and genetic knockdown, were employed to examine these phenomena. Both approaches successfully abolished the activation of SREBP2, which was induced by sorafenib/lenvatinib treatment. Consequently, cholesterol production, as demonstrated by filipin staining, was also inhibited. The protective effect of SREBP2-mediated cholesterol biosynthesis was correspondingly suppressed after CASP3 retention. CASP3 activity, followed by the upregulation of SREBP2-mediated cholesterol biosynthesis, also demonstrated elevated activity levels in both drug-resistant PDTXs and HCC cells. More importantly, CASP3 was elevated in tumor samples in the clinical cohort, indicating the underlying potential role of CASP3 in tumorigenesis. Nonetheless, this CASP3-SREBP2 signalling cascade not only exhibited connections in *in vitro* experiments but also demonstrated clinical relevance in publicly available datasets. Finally, by studying the tissue microarray, SREBP2 was shown to have clinical significance in patients who received sorafenib, who displayed poorer survival and a higher chance of tumor relapse.

Reprogramming of lipid and sterol metabolism has been closely connected to a variety of cancers and supports fast tumor growth, which is coordinately regulated by the SREBP family (218). SREBP2, as discussed before, has been heavily implicated in various cancers, such as prostate cancer, breast cancer, and HCC (199, 219). In consideration of the oncogenic pathways, SREBP2 can be transcriptionally activated by c-Myc, PI3K/K-Ras-induced mTORC1 activation and TP53 mutation in different cancers (181, 199, 214). Moreover, the key enzymes involved in the mevalonate cholesterol producing pathway, which is regulated by SREBP2, also participate in driving oncogenic pathways. For example, farnesyl pyrophosphate synthase, an obligate intermediate in the pathway, is associated with poor survival in prostate cancer via activation of the small GTPase-AKT axis (220, 221). Additionally, squalene synthase has been shown to be a risk factor for non-small cell lung cancer and is associated with metastasis via the NF- κ B signalling cascade (222-224). In prostate cancer, the limiting factor for the mevalonate pathway that synthesizes cholesterol, HMGCR, was shown to be elevated in enzalutamide-resistant cancer cells (225). When simvastatin was administered as an HMGCR inhibitor, enzalutamide-resistant prostate cancer cells were more prone to respond to

enzalutamide treatment *in vitro* and *in vivo*, demonstrating the potential role of cholesterol as a downstream effector in acquired drug resistance (225). In lapatinib- and trastuzumab-resistant HER2⁺ breast cancer cells, targeting the mevalonate pathway has been proposed to overcome acquired drug resistance, which could be mediated by the oncogenic pathway mTORC1-YAP/TAZ signalling cascade (226). Therefore, these findings identify a novel target for cancer treatment in the cholesterol pathway. However, although the significance involves SREBP2 and its downstream effectors involved in *de novo* cholesterol biosynthesis pathway, it is still unclear how SREBP2 is activated, given that the SREBP family is tightly regulated by a protease cleavage cascade (128).

Some potential cleavage mechanisms have been introduced, such as ER stress and caspase family induction. In cells treated with thapsigargin, which was used to induce ER stress, proteolytic cleavage of SREBP2 was also demonstrated via conservative site-1 and site-2 protease cleavage (227). Activation of SREBP2 via an ER stress inducer was also verified by the increase in filipin staining (227). Moreover, ER stress calcium depletion was shown to be another independent effect of PCSK9 induction via SREBP2 cleavage (228). Upon peroxisome deficiency, hepatic ER stress was activated and subsequently induced an SREBP2-mediated sterol response mechanism (229). Although thapsigargin-induced ER stress demonstrated caspase-independent activation of SREBP2 (227), caspase-2 colocalized with S1P, activating SREBP2 under elevated ER stress in NAFLD progression to NASH (230). This has therefore introduced a potential role for the caspase family in sensing cellular stress to induce SREBP2 translocation. In an early structural study, CASP3, a cysteine protease, was shown to cleave the SREBP family at an aspartic acid between the basic leucine zipper domain and the first transmembrane domain, releasing the mature form of SREBPs (216). The apoptotic role of CASP3 in inducing SREBP2 activation was further explored in the field of hepatocytes, showing that CASP2 interacts with pro-CASP3 and that MAPK reduces this interaction, leading to activation of CASP3 and SREBP2 (231). This finding has potentially provided understanding of cellular stress being detected by CASP3, a specific enzyme that cleaves SREBP2, leading to the activation of cholesterol biosynthesis that helps to withstand stress and aid cells in recovering. This protective observation was confirmed in our experimental setting, in which we provided a further novel explanation of the CASP3-SREBP2 signalling cascade in combating drug stresses. However, it is acknowledged that the inhibitor (Z-DEVD-FMK) being used in this study to inhibit the activity of CASP3 has also the potency towards CASP6, 7, 8 and 10. This could show that the classic apoptosis pathway was attenuated and the drug-

induced cell death was activated via other compensatory pathways. This has therefore provided another future perspective to investigate which apoptotic pathway has been activated so to kill the cancer cells.

Taken together, a novel SREBP2-mediated cholesterol biosynthesis induced by CASP3 activity was shown to exert a strong protective effect on HCC cells in resisting TKI challenges. Although SREBP2 and cholesterol have previously been shown to activate several oncogenic pathways, it is still unclear which particular pathway could be activated under the abovementioned signalling cascade via which downstream effectors. It is therefore rational to investigate the potential pathways that could be directly activated by cholesterol or its metabolites. This will provide further therapeutic implications for targeting SREBP2-mediated cholesterol biosynthesis for the treatment of HCC.

Chapter 7

SHH SIGNALLING CASCADE IS THE DOWNSTREAM EFFECTOR OF SREBP2- MEDIATED CSC FUNCTIONS AND DRUG RESISTANCE

7 SHH signalling cascade is the downstream effector of SREBP2-mediated CSC functions and drug resistance

7.1 Introduction

In Chapter 6, SREBP2-mediated cholesterol biosynthesis in regulating drug resistance was extensively studied. The mechanism of initiating SREBP2-mediated cholesterol biosynthesis in response to drug treatment was elucidated, with CASP3 as the upstream effector showing a specific cleavage site on SREBP2. The suppression of CASP3 activity successfully abolished CSC functions and drug resistance mitigated by SREBP2-mediated cholesterol biosynthesis. However, a specific CSC-related pathway has yet to be identified under this signalling axis. Therefore, in this chapter, we aimed to elucidate the downstream effector of CASP3-SREBP2-mediated cholesterol biosynthesis.

Several well-established CSC-related signalling pathways are activated to drive liver cancer development. For example, Notch signalling is crucial for the stem cell renewal process (232, 233), and overexpression of NOTCH ligand and NOTCH3 is detected in HCC (234, 235). In CD24⁺CD133⁺ liver cancer cells, marked expression of the notch1 gene is observed, supporting stemness promotion *in vitro* and *in vivo* (73). Additionally, Wnt/ β -catenin plays a role in self-renewal or stem cell differentiation (236). Our team and others have previously identified that Wnt/ β -catenin activation is crucial in liver cancer stem cells via different mechanisms, including the interplay of UBE2T and Mule, Octamer4/microR-1246 signalling axis, and SOX9 and Frizzled-7 interaction (237-239). Additionally, the SHH pathway is found in approximately 60% of HCC, and suppression of the SHH pathway abolishes GLI-mediated gene expression (240). Oncogenic c-Myc expression can also be activated by SMO, an upstream regulator of the SHH pathway, during neoplastic transformation in liver cancers (241). Interestingly, the SHH pathway is activated by cholesterol or its oxygenated derivatives (242). Hence, we sought to determine whether SREBP2-mediated cholesterol biosynthesis drives the activation of the SHH pathway via cholesterol. The investigation of oxysterols will also be implemented.

Therefore, identifying which CSC-related signalling pathway is activated under the CASP3/SREBP2 axis is critical to provide a better therapeutic direction. We first employed RNA sequencing to analyze the differential expression profiles between SREBP2 knockdown cells and their mock control counterparts. Identification of downregulated pathways via GSEA

was further verified by western blot analysis in both SREBP2 knockdown and overexpression HCC cells. Further confirmation was performed using an inhibitor approach to examine whether the CSC-enhancing effect in SREBP2-overexpressing cells was compensated.

7.2 Experimental outline

(1) Identification of the CSC-related pathway and SHH pathway using RNA sequencing and further confirmation by western blot analysis of key signalling proteins in the pathway. (2) Administration of a GLI-1 inhibitor further proved that the SHH pathway is the downstream effector of SREBP2-mediated cholesterol biosynthesis. (3) Investigating the role of one of the oxysterols, 25-OHC, in driving the SREBP2-mediated SHH pathway. (4) Finally, verification of the correlation of cleaved CASP3, SREBP2 and GLI-1 in an in-house HCC tissue microarray was executed. A summary of the experimental setting is shown below (Figure 7.1).

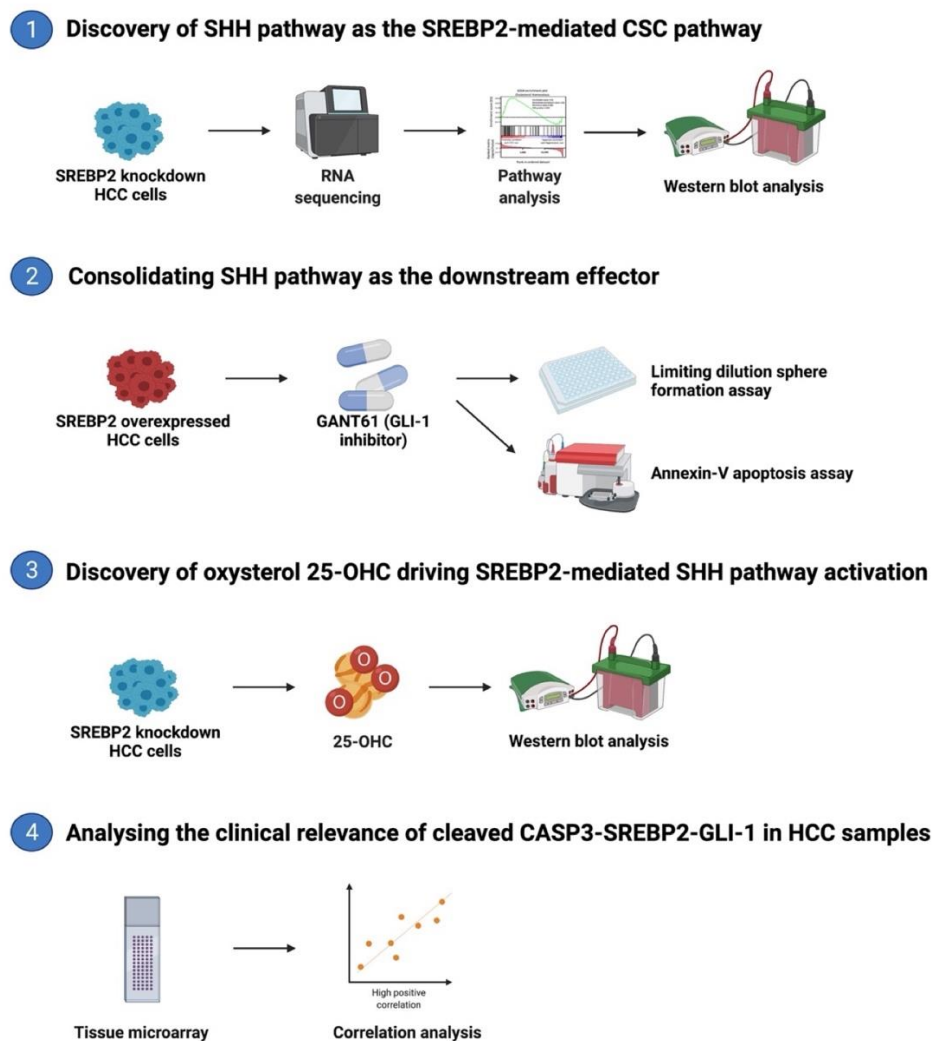


Figure 7.1. Experimental outline in Chapter 7.

The diagram summarizes the methods used to examine the downstream CSC-related pathway regulated by SREBP2-mediated cholesterol biosynthesis in HCC cells and their clinical correlation.

7.3 Results

7.3.1 The sonic hedgehog signalling pathway is regulated by SREBP2-mediated cholesterol biosynthesis

SREBP2 knockdown and NTC clones derived from MHCC-97L cells were subjected to RNA sequencing analysis. The data retrieved were analyzed using GSEA, which showed that sonic hedgehog signalling (SHH) is one of the downregulated pathways in shSREBP2 MHCC-97L cells (Figure 7.2A). The normalized enrichment score was -1.603 with a nominal p -value < 0.004 and FDR q -value 0.014. Western blot analysis further confirmed that key proteins in the SHH signalling pathway were regulated by SREBP2 levels in HCC cells (Figure 7.2B). In SREBP2 knockdown cells derived from PLC/PRF/5 and MHCC-97L cells, GLI-1, SUFU, SHH, PTCH1 and PTCH2 were downregulated, corresponding to the suppressed SREBP2 level. By contrast, SREBP2 overexpression in Hep3B cells enhanced the expression of these proteins.

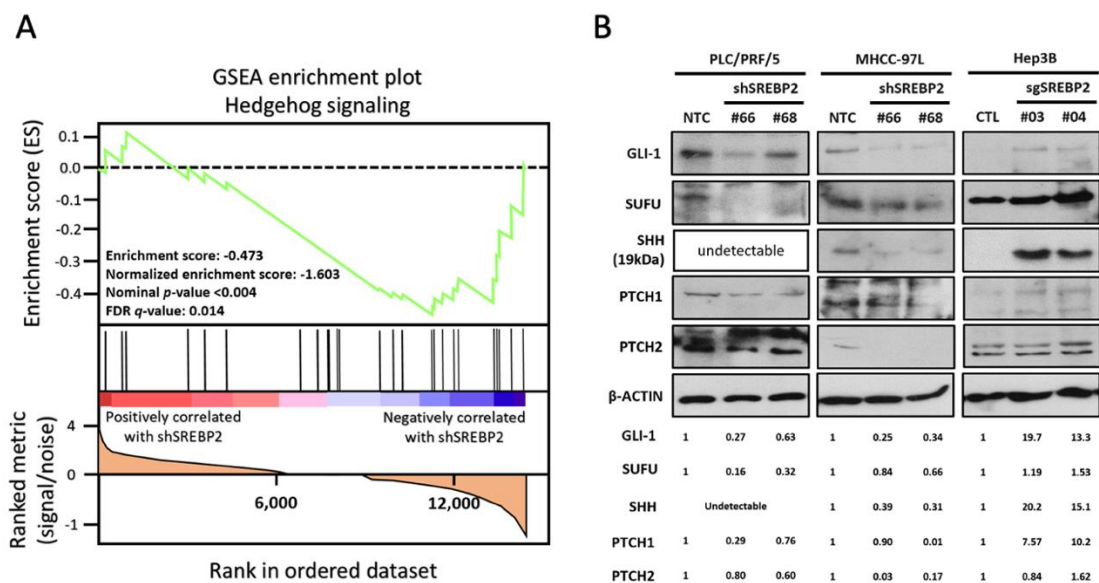


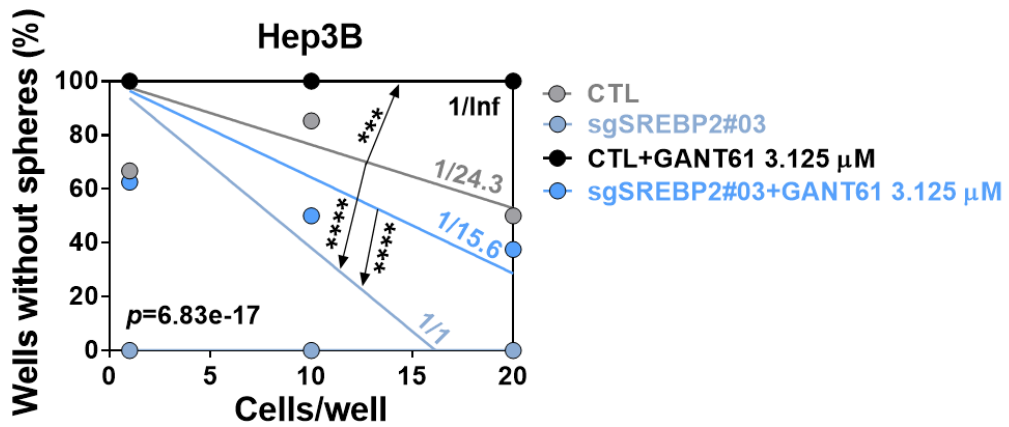
Figure 7.2. SREBP2-mediated cholesterol biosynthesis drives activation of the SHH signalling pathway.

(A) RNA sequencing was employed to compare the genetic profiles between shSREBP2#66 and NTC cells derived from MHCC-97L cells. GSEA showed that SHH signalling is downregulated in shSREBP2 cells with a normalized enrichment score of -1.603, nominal p -value < 0.004 and FDR q -value of 0.014. (B) Western blot analysis validated the key proteins involved in SHH signalling pathways, such as GLI-1, SUFU, SHH, PTCH1, and PTCH2. Quantification was performed using ImageJ.

7.3.2 Abolishment of SHH signalling offsets the SREBP2-mediated CSC properties

To further confirm the role of SHH as the downstream effector of SREBP2-mediated CSC stemness and drug resistance, we treated SREBP2-overexpressing Hep3B cells with GANT61, an inhibitor of GLI-1, to investigate whether the effects of SREBP2 overexpression can be eliminated by GLI-1 suppression. Following GLI-1 suppression, the *in vitro* self-renewal ability was suppressed by 15.6-fold in sgSREBP2#03 Hep3B cells (Figure 7.3A). Additionally, the administration of a GLI-1 inhibitor abolished the protective effect of SREBP2-mediated cholesterol biosynthesis against sorafenib/lenvatinib treatment (Figure 7.3B). In sorafenib treatment, GANT61 successfully enhanced the apoptotic cells induced by sorafenib by 2.32-fold in sgSREBP2#03 Hep3B cells. Additionally, lenvatinib treatment increased the number of apoptotic sgSREBP2#03 Hep3B cells by 2.68-fold when lenvatinib was administered.

A



B

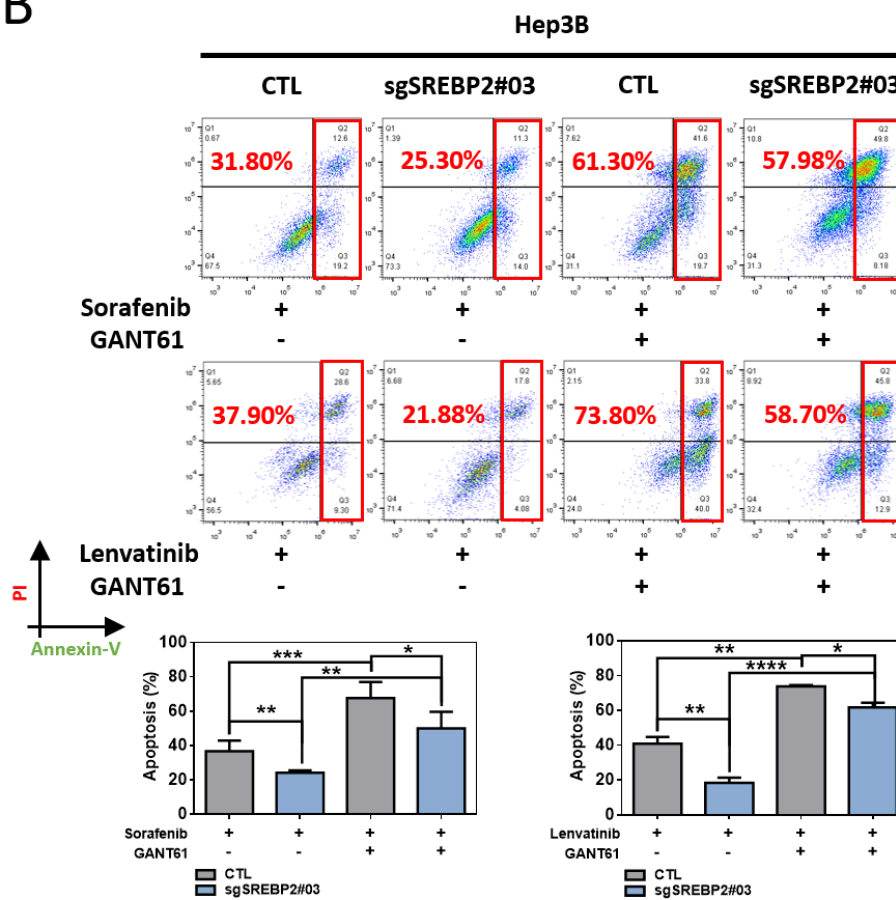


Figure 7.3. Inhibition of the SHH signalling pathway offsets elevated CSC properties via SREBP2-mediated cholesterol biosynthesis.

(A) The addition of GANT61 at 3.125 μ M offset the enhancing effect of SREBP2 overexpression on the self-renewal ability of sgSREBP2#03 Hep3B cells. (B) the addition of GANT61 at 5 μ M recovered the percentage of apoptotic cells in sgSREBP2#03 Hep3B cells in response to sorafenib/lenvatinib treatment. Error bars indicate means \pm SD (n = 3–6). * p <0.05, ** p <0.01, *** p <0.001, and **** p <0.0001 from Student's t-test.

7.3.3 Oxysterol 25-OHC is critical for SREBP2-mediated SHH signalling activation

Because intracellular cholesterol was previously reported to indirectly activate the sonic hedgehog (SHH) pathway via its metabolite oxysterols (243-245), we examined whether SREBP2-mediated cholesterol biosynthesis leads to activation of the SHH pathway by cholesterol metabolites. Using ELISA against CH25H, which is the enzyme responsible for 25-OHC, its activity level corresponded to SREBP2-mediated cholesterol biosynthesis (Figure 7.4A). In SREBP2 knockdown cells derived from PLC/PRF/5 and MHCC-97L cells, the activity level of CH25H was attenuated with respect to the SREBP2 level. Conversely, exogenous cholesterol administration in Hep3B cells at 5 μ M enhanced the CH25H activity level at different time points. Finally, the decisive effect of 25-OHC in activating the SHH pathway was demonstrated by western blot analysis (Figure 7.4B). Administration of 25-OHC at 15 μ M rescued the suppression of SHH signalling proteins, including GLI-1, SUFU, SHH, PTCH1 and PTCH2, in SREBP2 knockdown clones derived from MHCC-97L cells at a physiological concentration of approximately 5 μ M.

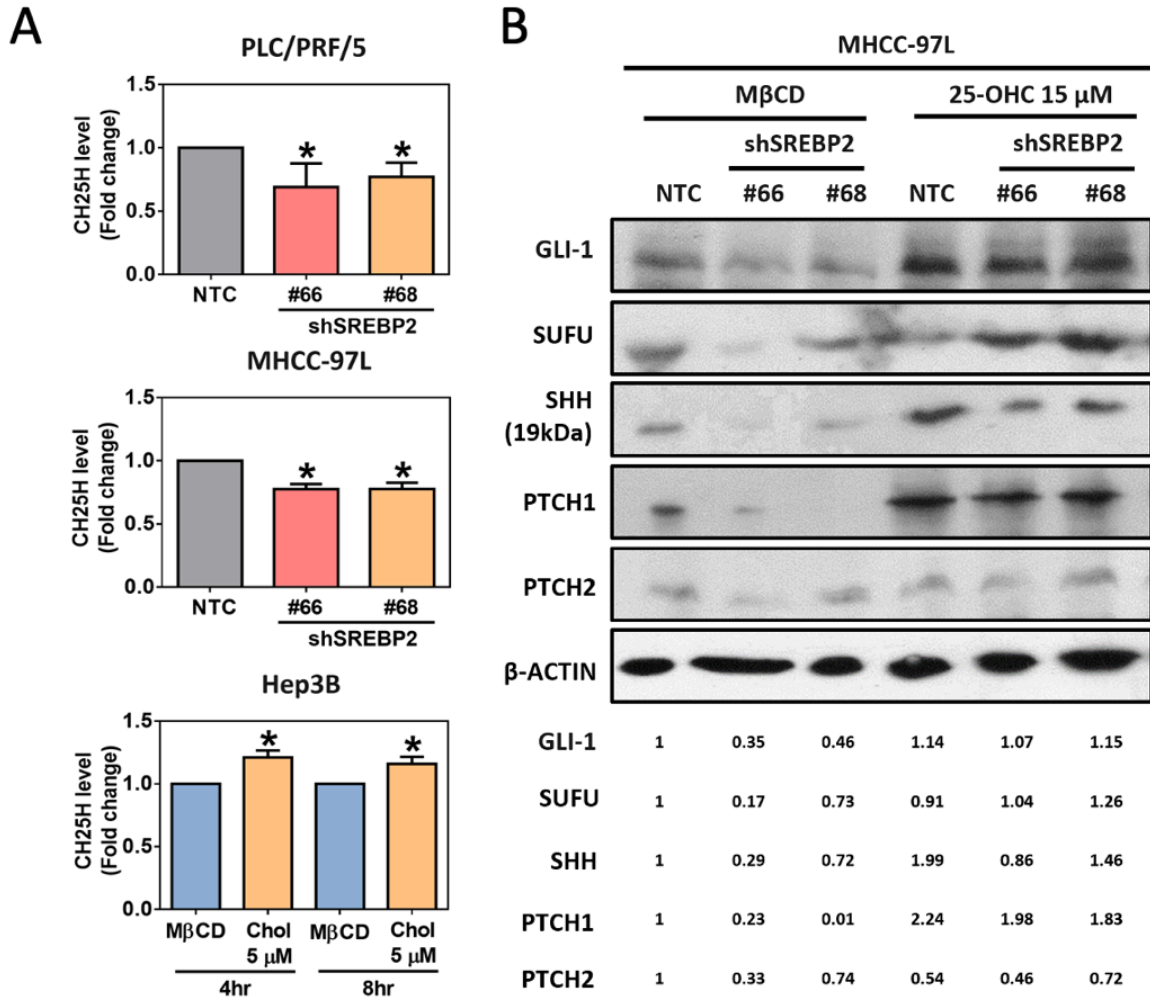


Figure 7.4. Oxysterol 25-OHC drives SREBP2-mediated SHH signalling activation.

(A) CH25H levels of shSREBP2#66 and shSREBP2#68 relative to NTC derived from PLC/PRF/5 and MHCC-97L cells, and cholesterol-treated (Chol) at 5 μM relative to MβCD at 4 hr and 8 hr of treatments were evaluated by ELISA. (B) 25-OHC at 15 μM mitigated the suppressive effects of shSREBP2 cells on the expression of GLI-1, SUFU, SHH, PTCH1 and PTCH2. Quantification was performed using ImageJ. Error bars indicate means±SD (n = 3–6). * $p < 0.05$ from Student's t-test.

7.3.4 Correlation among cleaved CASP3, SREBP2 and GLI-1 in HCC clinical samples

The clinical relevance of the CASP3-SREBP2-SHH signalling axis was investigated. Consistent with previous results of activated CASP3 activity and SREBP2-mediated cholesterol biosynthesis in drug-resistant HCC cells, GLI-1 expression was also highly upregulated in sorafenib- and lenvatinib-resistant HCC PDTXs and PLC/PRF/5 and MHCC-97L cells (Figure 7.5C). The clinicopathological correlation was further analyzed in 50 in-house HCC patient samples (Figure 7.5A). Through IHC staining of cleaved CASP3, SREBP2, and GLI-1 on the tissue microarray, the expression was quantified as high or low. Following comparison, these three proteins were clinically and significantly correlated with each other (Figure 7.5B).

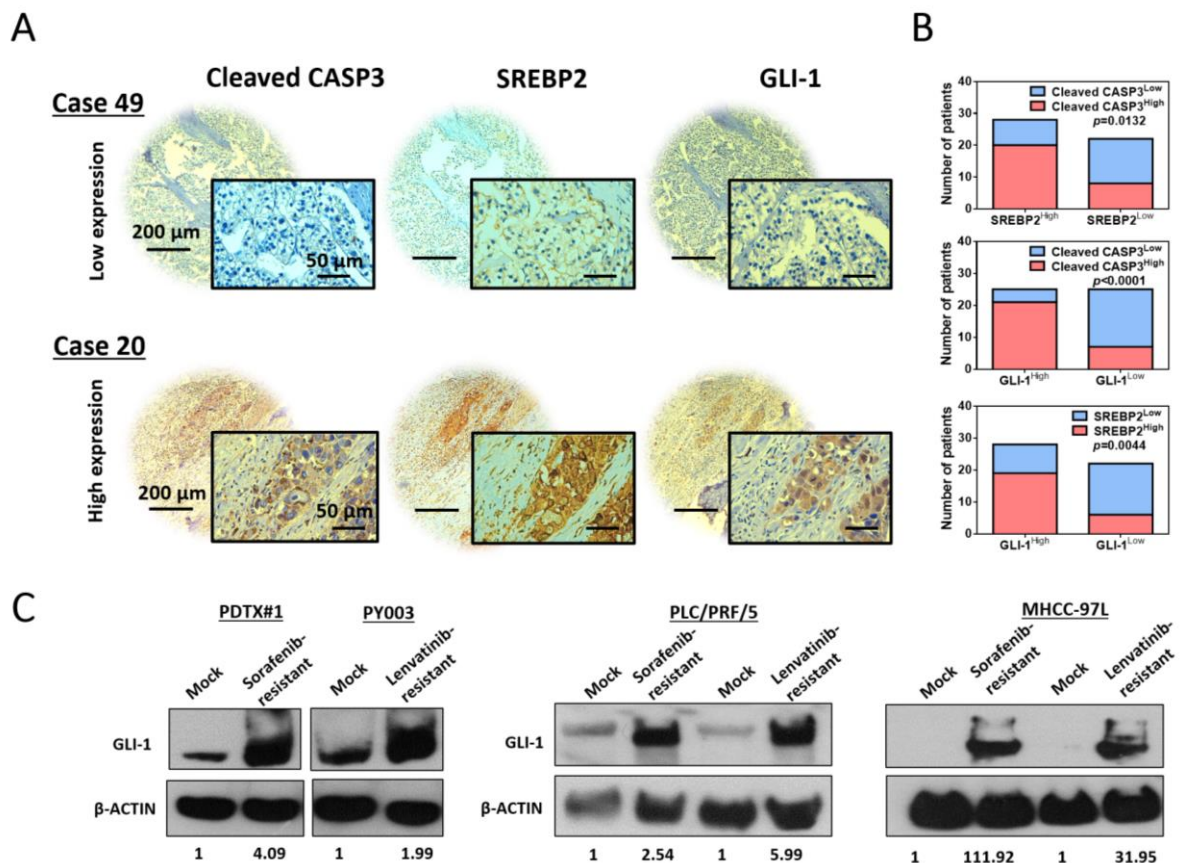


Figure 7.5. Cleaved CASP3, SREBP2 and GLI-1 are clinically related to each other.

(A) A tissue microarray comprising 50 tumor tissues and corresponding nontumor liver tissues was subjected to IHC analysis. Case 20 showed high expression of cleaved CASP3, SREBP2 and GLI-1, and case 49 showed low expression of these proteins. Scale bars: 50 and 200 μm . (B) Correlation analysis revealed that cleaved CASP3 to SREBP2 was $p=0.0132$, SREBP2 to GLI-1 was $p=0.0044$, and cleaved CASP3 to GLI-1 was $p<0.0001$. (C) GLI-1 expression was upregulated in sorafenib- and lenvatinib-resistant HCC cells derived from PDTX#1, PY003, PLC/PRF/5 and MHCC-97L cells. Quantification was performed in ImageJ.

7.4 Discussion

In this chapter, the SHH pathway was elucidated as the downstream effector of SREBP2-mediated cholesterol biosynthesis in regulating CSC properties and drug resistance. By RNA sequencing, the SHH pathway was downregulated in SREBP2 knockdown HCC cells. The key signalling proteins in the SHH pathway, including GLI-1, SUFU, SHH, PTCH1 and PTCH2, were regulated according to SREBP2 levels in HCC cells. Suppression of the SHH pathway using the GLI-1 inhibitor GANT61 effectively rescued the enhanced CSC properties, including *in vitro* self-renewal ability and drug resistance, in SREBP2-overexpressing Hep3B cells. More importantly, the study found that one of the cholesterol-derived oxysterols, 25-OHC, possessed oncogenic properties in HCC because it regulates the activation of the SREBP2-mediated SHH pathway. Finally, the clinical correlation among cleaved CASP3, SREBP2, and GLI-1 was evaluated in the HCC patient cohort, and they were significantly correlated with each other. Therefore, this chapter identified a novel pathway in driving acquired drug resistance in HCC by mediating the CASP3-SREBP2-SHH signalling axis.

The SHH pathway is a well-established signalling pathway that drives CSCs. SHH signalling is activated during mammalian embryonic development and remains quiescent in adult tissues (246). However, the abnormal activation of SHH signalling results in the tumorigenesis of brain, skin, pancreas, stomach, colon, lung, liver, gallbladder, lung, and prostate cancers (247). The SHH pathway is categorized based on canonical and noncanonical activation. The canonical transduction pathway comprises key components, including GLI-1, GLI-2, GLI-3, SUFU, SHH, PTCH1, PTCH2 and SMO (248). The noncanonical pathway is a GLI-independent action of SMO and PTCH, and activation of the SHH signalling pathway may be due to other signalling proteins, such as protein kinase A, Rho, or GTPase, to drive gene expression (249). Additionally, cholesterol and its oxysterols also activate the SHH pathway (242). The inhibition of the sterol synthetic pathway at different checkpoints using either simvastatin, zaragozic acid, triparanol or ketoconazole attenuates SHH signalling and proliferation in medulloblastoma cells (244, 245, 250). However, regardless of the induction method, activation of SHH signalling promotes *in vitro* self-renewal ability in anaplastic thyroid cancer cells by GLI-1-induced SNAIL expression (251). Furthermore, the SHH pathway enhances the invasiveness of HCC cells by promoting the epithelial-mesenchymal transition (252). Our team previously reported that the canonical SHH pathway is activated by NRF2 overexpression in HCC cells, thus promoting CSC phenotypes and driving drug

resistance (95). Therefore, our data further consolidates the tumorigenesis of the SHH pathway in driving CSC properties in HCC. We further revealed that 25-OHC is an important oxysterol in mediating SREBP2-mediated SHH activation.

Oxysterols are oxygenated derivatives from cholesterol formed in the human body or ingested from the diet. They affect many cellular functions and physiological processes by modulating the activity of many other proteins or some ATP binding cassette transporters (253). Therefore, abnormalities in oxysterol activity have led to several pathological conditions, such as atherosclerosis, neurodegenerative disorders or diabetes mellitus type 2 (254, 255). Currently, accumulating evidence has suggested that oxysterols also play a role in the formation of tumors, including colon, prostate, breast and bile duct cancers (253, 256-258). In particular, in breast cancer, 27-hydroxycholesterol (27-OHC) is a well-established oncometabolite inducing breast malignancy. 27-OHC not only promotes the migration of breast cancer cells but also acts as a navigator for metastasis to the bone (259, 260). Additionally, 27-OHC supports CSC properties, such as the EMT, in breast cancers (259). 27-OHC may also influence prostate cancer by enhancing prostate-specific antigen (PSA), thus stimulating cancer cell proliferation (261). 25-OHC is another oxysterol that shows a relationship in driving resistance to therapy. It was shown to induce estrogen receptor target genes in breast cancer, suggesting that 25-OHC substitutes estrogen in activating ER-mediated gene transcription and plays a role in regulating drug resistance (163). Furthermore, in HCC, although oxysterols are elevated, such as 4 β -hydroxycholesterol, 7 α -hydroxycholesterol and 25-OHC, in HCV-induced HCC patients, the detailed contribution is unknown (262). Therefore, considering the current findings in this chapter, we not only consolidated the carcinogenic role of oxysterols in SREBP2-mediated cholesterol biosynthesis but also filled the gap that elevated 25-OHC mediates the SHH pathway to promote CSC properties and drug resistance.

Taken together, the elucidation of SREBP2-mediated cholesterol biosynthesis and its oxysterol 25-OHC in activating the SHH signalling pathway has demonstrated a novel signalling axis in HCC tumorigenesis. Considering the importance of cholesterol biosynthesis as the central intermediate, the therapeutic implication of targeting cholesterol biosynthesis in treating HCC as a novel treatment option should be investigated.

Chapter 8

SIMVASTATIN ENHANCES THE EFFECT OF DRUG TREATMENT IN *ORGANOTYPIC EX VIVO* HUMAN HCC CLINICAL SAMPLES AND HCC PDTX MODELS

8 Simvastatin enhances the effect of drug treatment in *organotypic ex vivo* human HCC clinical samples and HCC PDTX models

8.1 Introduction

In Chapter 7, the SHH signalling pathway was elucidated as the downstream effector of the CASP3-SREBP2-mediated cholesterol biosynthesis cascade in regulating CSC functions and drug resistance. One of the oxysterols derived from cholesterol, 25-OHC, also has oncogenic properties because it drives SREBP2-mediated SHH signalling activation. The signalling axis was further confirmed clinically in an in-house HCC patient cohort, and cleaved CASP3, SREBP2, and GLI-1 were significantly correlated with each other in tumor samples. Thus, targeting the abovementioned signalling axis in overriding drug resistance in HCC is clinically valuable. Cholesterol biosynthesis is preferentially activated in CSCs (Figure 4.4) and most commonly upregulated in sorafenib- and lenvatinib-resistant PDTXs (Figure 3.4). Thus, we aimed to test the therapeutic efficacy of targeting cholesterol biosynthesis using statin, an FDA-approved cholesterol-lowering drug, to treat HCC.

The process of producing cholesterol involves more than 20 enzymes that are potential candidates for drug intervention (263). Among those proteins, HMGCR is the first rate-limiting catalytic enzyme elucidated in the pathway in which it converts HMG-CoA to mevalonic acid (264). Regarding its important involvement in producing cholesterol, statins have been marketed since the 1990s and used to specifically inhibit HMGCR activity by acting as HMG-CoA analogs (265). To date, seven statins have been synthesized based on their distinctive lipophilicity, pharmacokinetic profiles, side effects and mostly their ability to decrease cholesterol production (266). They are simvastatin, fluvastatin, atorvastatin, rosuvastatin, lovastatin, pravastatin and pitavastatin. In a clinical article reviewing the effect of different statins on lowering low-density lipoprotein cholesterol, atorvastatin and simvastatin ranked the highest. Although pravastatin induces fewer side effects because of its weakest pharmacokinetic drug interactions (267), its effect on lowering total cholesterol is also the weakest among those seven statins (268). Additionally, rosuvastatin is regarded as the most potent statin in regulating dyslipidaemia because of its polar interaction between the methane sulfonamide group and HMGCR (268, 269).

Statin were first used in treating cardiovascular diseases, atherosclerosis, and liver diseases arising from excessive cholesterol deposition (270, 271). However, because of the

accumulation of evidence in dysregulated cholesterol metabolic profiles in cancers, statins have been introduced as anticancer drugs (272). In prostate cancers, statins effectively reduced mortality and recurrence by suppressing PSA levels in a dose-dependent manner in patients who received radical prostatectomy (273). In renal cell carcinoma, patients benefit from using statins to extend their overall survival rate, from 18.9 months to 25.6 months (274). Additionally, in several epidemiologic studies, the risk of cancers, including gastric, colorectal, liver, prostate, and pancreatic cancers, was reduced after administering statins (275-279). These clinical studies were further supported by laboratory experiments showing that statins effectively suppressed the proliferation of human cancer cell lines, including lymphocytic leukaemia, pancreatic, and breast cancer cell lines (280-282).

Taken together, the evidence presented supports the rationale to test the therapeutic efficacy of targeting cholesterol biosynthesis using statins combined with sorafenib/lenvatinib in treating HCC. Among the statins, we chose simvastatin because of its popularity in cancer therapy and its efficacy in reducing cancer-specific mortality compared with other hydrophilic statins (283). In the experimental setting, we tested the drug sensitization effect of simvastatin at three different levels, *in vitro*, *ex vivo* and *in vivo*, in HCC cells.

8.2 Experimental outline

(1) Simvastatin was administered to HCC cells to consolidate SREBP2-mediated cholesterol biosynthesis in regulating CSC functions and drug resistance. (2) Simvastatin was administered to HCC organoids to validate the therapeutic efficacy of targeting cholesterol biosynthesis. (3) Simvastatin was fed to PDTX mice, and the tumor size, volume and growth were measured to demonstrate the therapeutic implications of targeting cholesterol *in vivo* models. A summary of the experimental setting is shown below (Figure 8.1).

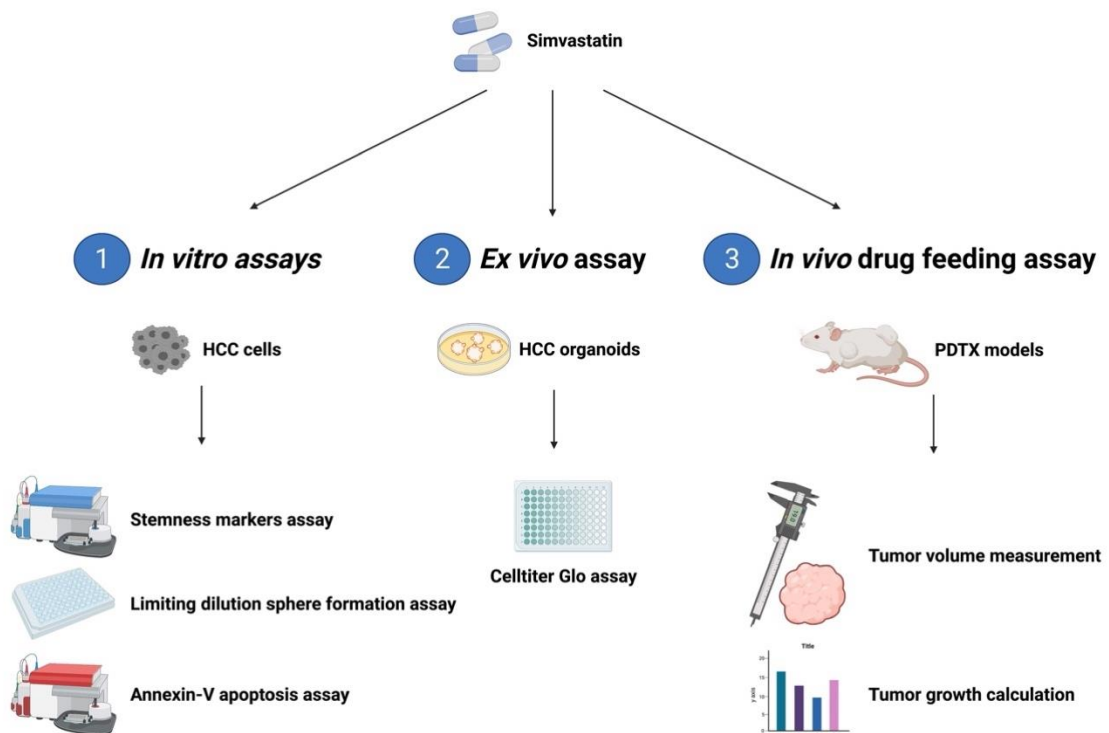


Figure 8.1. Experimental outline in Chapter 8.

The diagram summarizes the methods used to examine the effect of simvastatin on targeting cholesterol biosynthesis to treat HCC.

8.3 Results

8.3.1 Simvastatin regulates CSC properties and drug resistance

The efficacy of targeting cholesterol biosynthesis by simvastatin was first tested in HCC cells *in vitro*. The cell viability MTT assay was used to determine the IC₅₀ of simvastatin in PLC/PRF/5 cells, which was 34.30 μ M (Figure 8.2A). Next, treatment with 20 μ M simvastatin suppressed the expression of CSC stemness markers, including CD47 and CD133 (Figure 8.2B). Additionally, 2.11- and 1.68-fold decreases were observed in CD47 and CD133 surface marker detection, respectively. After that, the *in vitro* self-renewal ability was attenuated after simvastatin administration (Figure 8.2C). Using a limiting dilution sphere formation assay, PLC/PRF/5 cells were seeded in a serially diluted manner and grown for 8 days with simvastatin supplementation at 0.625 and 1.25 μ M. The cancer stem cell frequencies were recorded based on the incidence of spheres found in each well and analyzed using extreme limiting dilution analysis. Continuous suppression of cholesterol production via simvastatin successfully decreased the formation of CSCs by 3.35- and 6.76-fold, respectively, compared with the mock control. Finally, simvastatin effectively sensitized the drug efficacy of sorafenib and lenvatinib (Figure 8.2D). Following the coadministration of sorafenib/lenvatinib and simvastatin to PLC/PRF/5 cells, the apoptotic cell rate increased 1.58- and 2.06-fold with sorafenib and lenvatinib treatment, respectively.

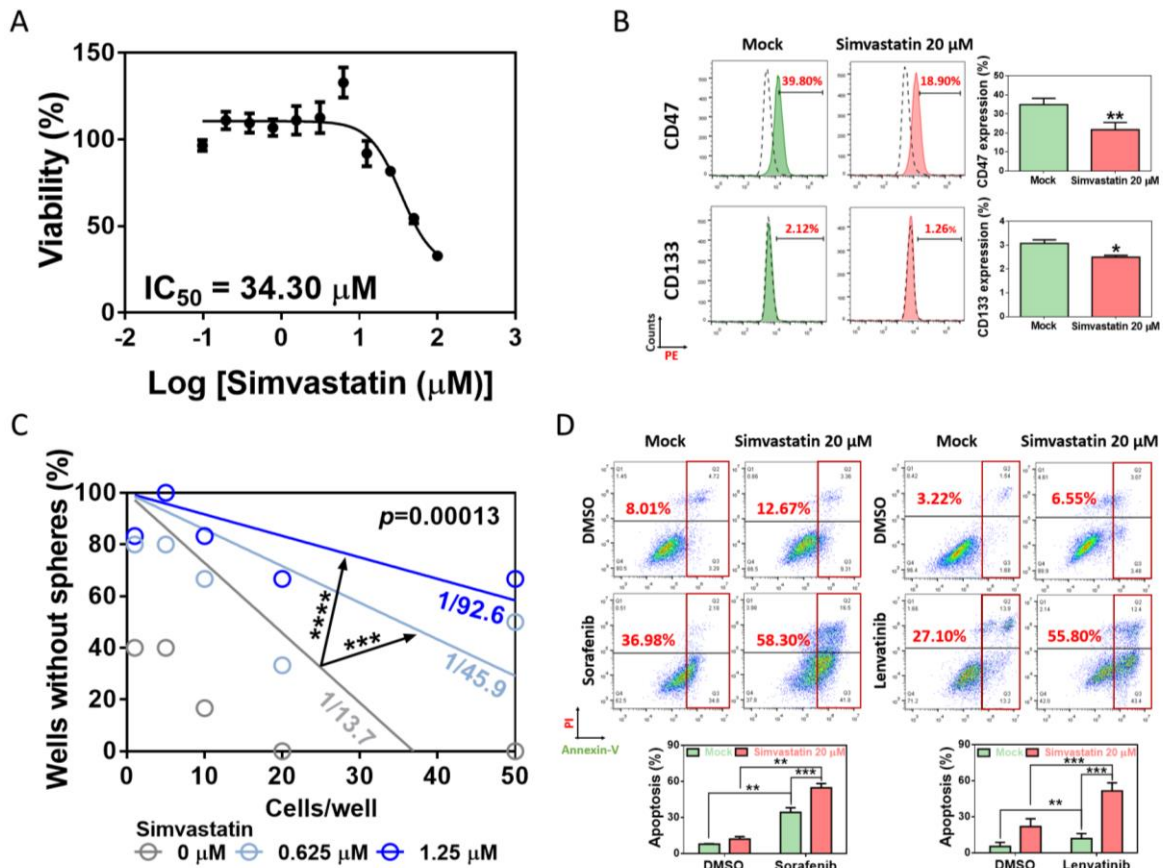


Figure 8.2. Simvastatin regulates liver CSC properties and drug resistance.

(A) The IC_{50} of simvastatin in PLC/PRF/5 cells was determined by the MTT assay. (B) CD47 and CD133 expression levels were analyzed in PLC/PRF/5 cells following treatment with simvastatin at 20 μM for 48 hr. (C) PLC/PRF/5 cells were seeded in a limiting dilution manner with mock (0 μM) and simvastatin (0.625 and 1.25 μM). The number of wells containing spheres was counted after 8 days. (D) Simvastatin sensitized sorafenib (10 μM) or lenvatinib (40 μM) treatment in PLC/PRF/5 cells. Error bars indicate means \pm SD (n = 3–5). * p <0.05. ** p <0.01, *** p <0.001 and **** p <0.0001 from Student's t-test.

8.3.2 Simvastatin enhances the effect of drug treatment in *organotypic ex vivo* human HCC clinical samples

The data of simvastatin in reversing liver CSC properties and drug resistance prompted us to examine the combined effect of simvastatin with sorafenib/lenvatinib in HCC treatment. Using a CellTiter-Glo® assay, we found that combination treatment resulted in the most significant reduction in the growth of HCC patient-derived organoids (HKU-HCC P1), in which simvastatin treatment sensitized HCC cells to sorafenib/lenvatinib (Figure 8.3).

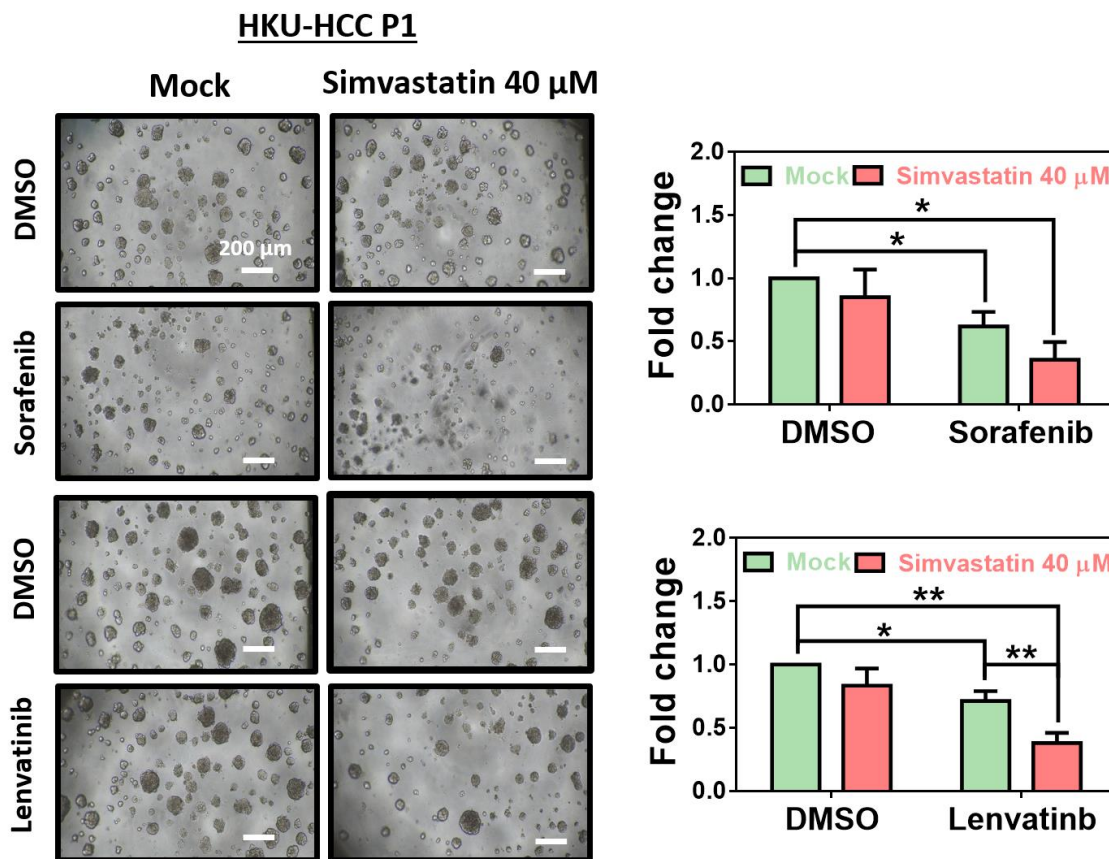


Figure 8.3. Simvastatin enhances drug efficacy in HCC organoids.

(Left) representative photos of HCC patient-derived organoid culture (HKU-HCC P1), which was treated with DMSO, sorafenib (8 μ M)/lenvatinib (40 μ M), simvastatin (40 μ M), or combo for 6 days. Scale bar: 200 μ m. (Right) The relative growth rate to mock was determined using the CellTiter-Glo® assay. Error bars indicate means \pm SD (n = 3–4). * p <0.05 and ** p <0.01 from Student's t-test.

8.3.3 Simvastatin enhances the effect of drug treatment in HCC PDTX models

To further confirm the therapeutic effect of simvastatin in treating HCC, we administered a single dose of 4 mg/kg (equivalent to a dose of 40 mg to treat patients with high cholesterol) of simvastatin alone, a single dose of 30 mg/kg of sorafenib alone or a combined dose of simvastatin plus sorafenib *in vivo* using HCC xenografts derived from PY003. The tumors after treatment for 21 days are shown (Figure 8.4A). The responding tumor volumes were recorded every 3 days and plotted against the treatment period (Figure 8.4B). Remarkably, the combination treatment reduced the tumor volumes of PY003 by 37% relative to the original tumor volume on Day 0 (Figure 8.4C). We also evaluated the effects of these drug combinations in sorafenib-resistant PDTX#1 cells. Consistently, simvastatin/sorafenib exerted the greatest tumor suppressive effects compared with single-agent treatment and mock controls (Figure 8.4A-C). The ability of simvastatin to lower cholesterol was verified by filipin staining, confirming its therapeutic efficacy in targeting cholesterol biosynthesis (Figure 8.5). During the *in vivo* drug feeding experiment, no significant weight loss was observed in the animals throughout the period (Figure 8.6).

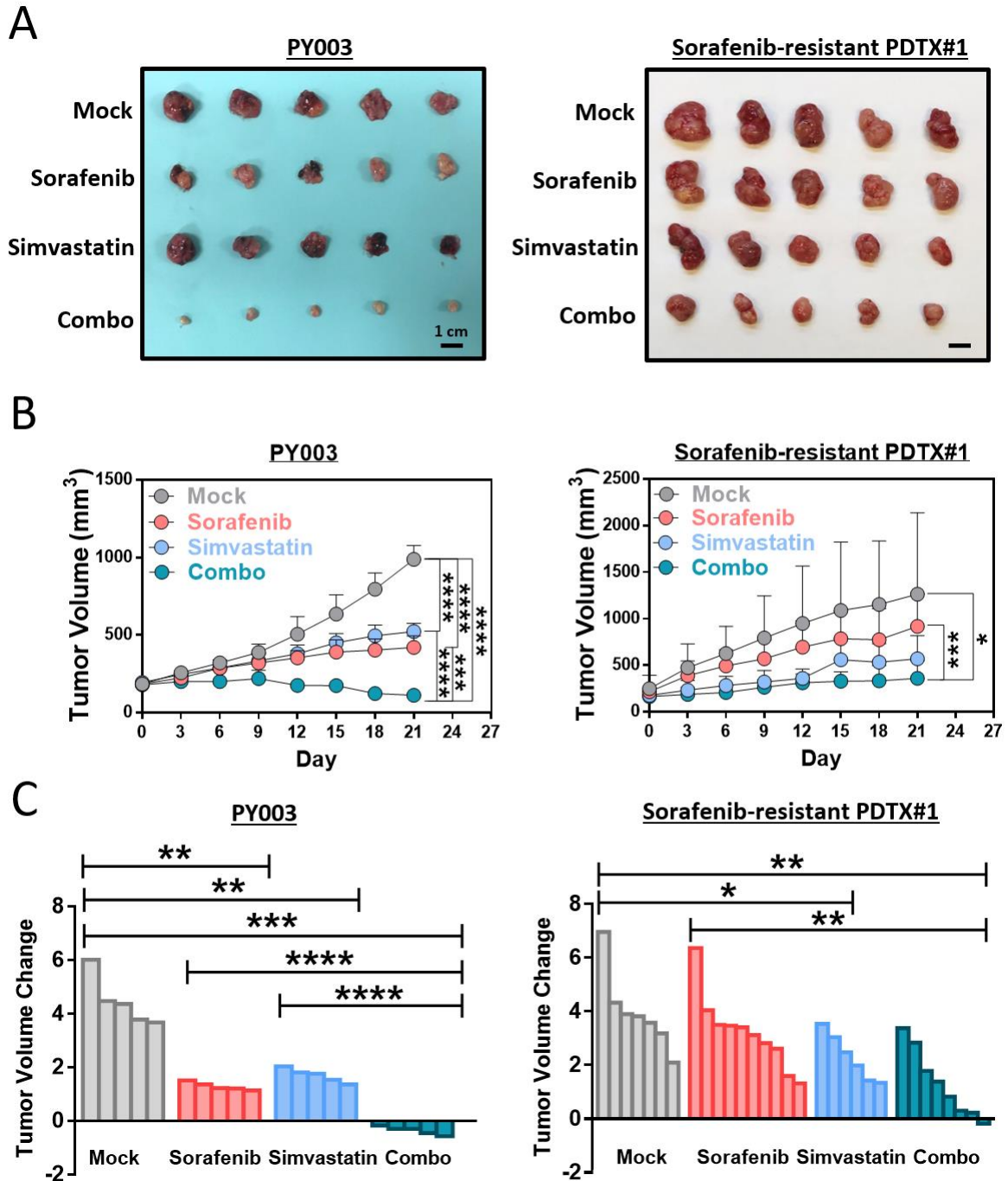


Figure 8.4. Simvastatin enhances the drug effect in two HCC PDTX models.

(A) Response of PY003 and sorafenib-resistant PDTX#1 xenografts to treatment for 21 days with simvastatin (4 mg/kg), sorafenib (30 mg/kg) or both drugs. The tumor images at the end of treatment are shown. Scale bar: 1 cm. (B) The tumor volume was recorded every 3 days throughout the 21-day treatment. (C) Waterfall plot of the response of each tumor after 21-day treatment. Error bars indicate means \pm SD (n = 3–10). * p <0.05, ** p <0.01, *** p <0.001 and **** p <0.0001 from Student's t-test.

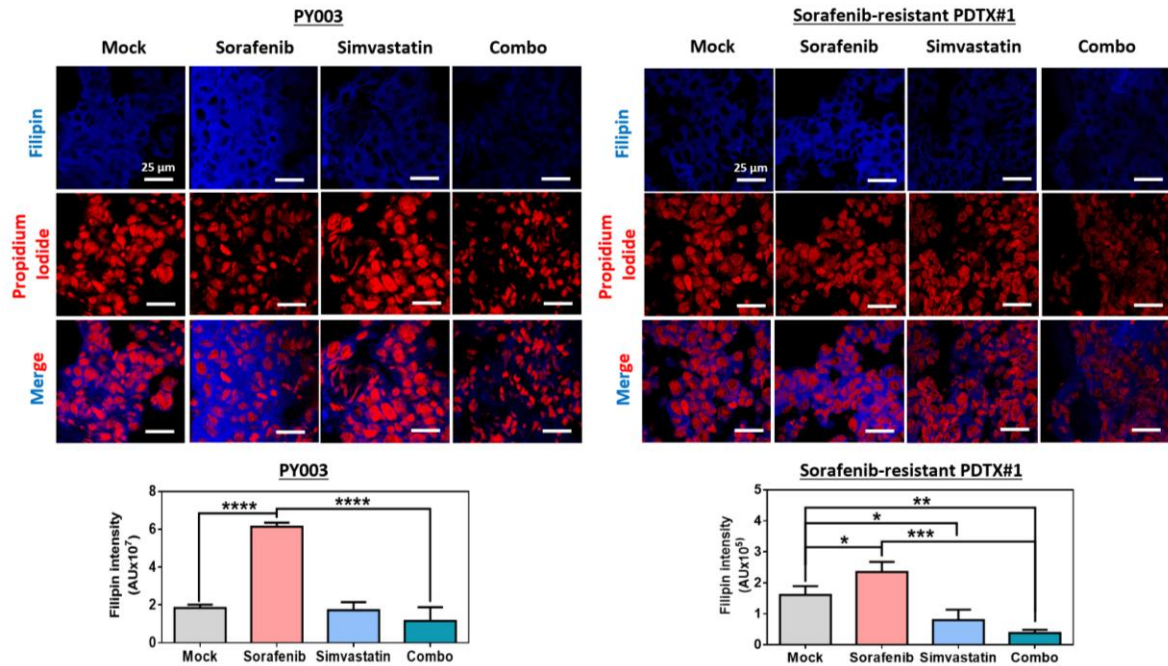


Figure 8.5. Simvastatin suppresses cholesterol deposition in two HCC PDTX models.

Representative images of filipin staining of tumors from mock, sorafenib, simvastatin and combo treatment are shown. Blue: filipin staining; Red: propidium iodide. Filipin quantification was performed using Nikon EIS-Element Software. Error bars indicate means \pm SD (n = 3–6). * p <0.05, ** p <0.01, *** p <0.001, and **** p <0.0001 from Student's t-test.

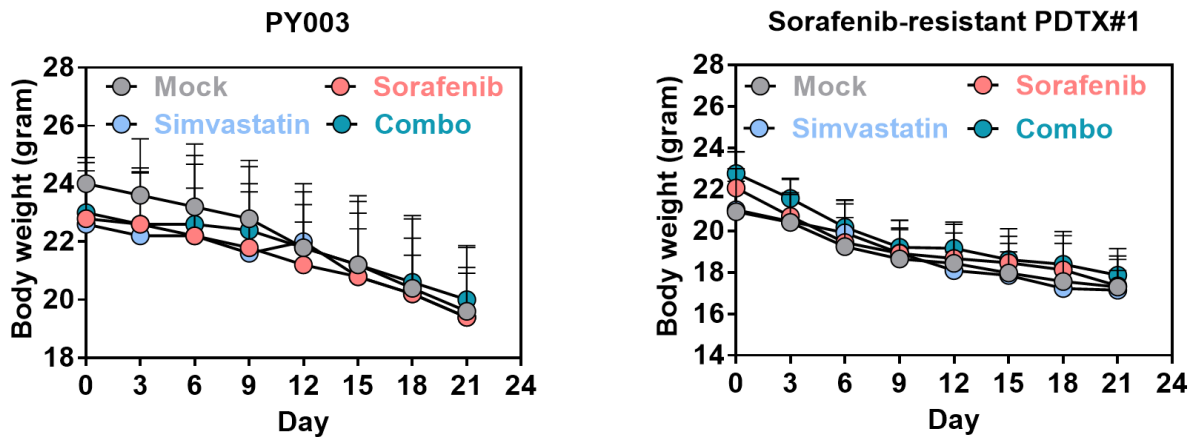


Figure 8.6. Combo treatment of simvastatin and sorafenib shows no viable side-effect in PDTX mice.

The body weights of two PDTX models were recorded every 3 days during the 21-day treatment period. No notable change in the body weight was observed after combined treatment for PY003 and sorafenib-resistant PDTX#1 xenografts of nude mice. Error bars indicate means \pm SD (n = 3–10).

8.4 Discussion

In this chapter, the therapeutic efficacy of targeting cholesterol biosynthesis to treat HCC by simvastatin was evaluated at three different levels. First, the therapeutic efficacy was validated *in vitro* in HCC cells such that, following the suppression of cholesterol production, the CSC properties, including stemness marker expression and self-renewal ability, were decreased. After that, combined with sorafenib/lenvatinib, simvastatin showed the greatest sensitization of drug efficacy in HCC cells. Second, the significance of targeting cholesterol biosynthesis was consolidated *ex vivo* in HCC patient-derived organoids that, following inhibition of cholesterol production, the proliferation and growth of organoids were attenuated under treatment with sorafenib/lenvatinib combined with simvastatin. Finally, this novel treatment strategy was tested *in vivo* in HCC PDX mice. The combined treatment of sorafenib and simvastatin generated the greatest tumor suppressive effect in both PDX models, PY003 and sorafenib-resistant PDX#1.

The importance of statins has been evaluated extensively recently as an anticancer regimen. In breast cancer, lovastatin was used to activate the LKB1-AMPK-P38MAPK-p53-survivin cascade, causing breast cancer cell apoptosis (284). The coadministration of fluvastatin and vorinostat effectively reduced renal cancer growth *in vitro* and *in vivo* by activating AMPK-ER stress-histone acetylation (285). In cyclooxygenase-2 (COX-2)-overexpressing HCC cells, the combined use of NS398, a COX-2 inhibitor, and simvastatin exerted synergistic effects in suppressing HCC cells by downregulating the NF- κ B-AKT signalling axis (286). A similar treatment regimen in our study model of combining sorafenib and simvastatin was also recently tested in HCC. By establishing sorafenib-resistant HCC cells, the combined treatment augmented the sensitivity to sorafenib by suppressing HIF-1 α /PPAR- γ /PKM2 (287). The SHH pathway, as discussed in the previous chapter, was demonstrated to be the downstream effector of SREBP2-mediated cholesterol biosynthesis. By suppressing cholesterol production by simvastatin, others have shown that simvastatin enhances the efficiency of gemcitabine, a chemotherapeutic agent, in treating pancreatic ductal adenocarcinoma by reducing CSC features through SHH signalling (288). Therefore, the preclinical data published have corroborated our current research findings.

Compared with other statins, such as atorvastatin, lovastatin, pravastatin, fluvastatin and rosuvastatin, simvastatin shows the best prolongation of lung cancer patient survival (289).

Another study supported this rationale, reporting that p53-mutated patients who received simvastatin had a reduced 5-year mortality via lipid raft modulation (290). In multiple myeloma (MM) cancers, simvastatin, the most widely used statin in the studied cohort, reduced the mortality risk in both sexes (291). A potential explanation may be the positive effect of statins in regulating the host immune response by inducing B lymphocyte survival and alleviating mesenchymal stromal cell-induced T cell suppression (292). However, two recent clinical studies (NCT01075555, NCT01357486) comparing pravastatin with sorafenib and sorafenib alone provided a rather disappointing result in treating both Child–Pugh A and Child-Pugh B HCC patients (293, 294). Adding pravastatin to sorafenib showed no difference in overall survival (10.7 months vs. 10.5 months, in Child-Pugh A HCC 4.0 months vs. 3.8 months in Child-Pugh B HCC) or in any secondary survival endpoints in advanced HCC patients. However, the researchers did not discourage the application of cholesterol-lowering strategies in treating HCC. They argued that pravastatin is the optimal statin for advanced HCC. As discussed here, other more potent statin candidates can be considered, such as simvastatin. Another ongoing clinical study in Taiwan is examining sorafenib combined with atorvastatin for advanced HCC (NCT03275376). The interest in targeting cholesterol biosynthesis has also been extended to other clinical trials (Table 8.1).

Although promising data from epidemiologic, preclinical, and some clinical studies have shown the therapeutic efficacy of statins as anticancer agents, the statin type, dose, and treatment duration should be considered carefully and thoroughly. Despite the overall cholesterol suppressing ability of each statin, lipophilic statins (simvastatin, atorvastatin, lovastatin, fluvastatin, and pitavastatin) are more likely to reach extrahepatic cells, whereas hydrophilic statins (rosuvastatin and pravastatin) are more hepatoselective (295). Lipophilic statin use is correlated with reduced cancer risk and recurrence, but not hydrophilic statin use, in breast cancer patients (296, 297). Additionally, atorvastatin and fluvastatin reduces prostate tumor cell growth and induces apoptosis in a time-dependent manner (298, 299). However, interestingly, only atorvastatin is identified in prostatic tissue after acute treatment relative to the serum (298, 300). This finding implies that, for any long treatment period, the pharmacokinetic profile of certain statins may grant higher drug concentrations within certain malignant tissues over time.

In conclusion, this chapter has demonstrated the therapeutic efficacy of statin use, particularly simvastatin, in overriding drug resistance in HCC. As a proof of concept, targeting cholesterol

biosynthesis as a novel treatment regimen has corroborated published preclinical and clinical studies. However, careful consideration of the types of statins should be implemented, as well as the dose and duration of the treatment period.

Table 8.1. Summary of the main clinical trials using statins in cancer therapy.

Disease	Trial number	Start date	Study	Drugs
Prostate cancer	NCT02497638	06/2020	Biguanide and Lipitor in delaying androgen trial	Atorvastatin and metformin
	NCT04026230	08/2019	Impact of atorvastatin on androgen deprived-prostate cancer progression	Atorvastatin
	NCT03819101	03/2019	Acetylsalicylic acid and atorvastatin in castrate-resistant prostate cancer trial	Atorvastatin and acetylsalicylic acid
Breast cancer	NCT03324425	06/2019	Simvastatin and dual AntiHER2 treatment for metastatic breast cancer	Simvastatin
	NCT03872388	01/2019	Atorvastatin treatment for patients in triple negative breast cancer who failed neoadjuvant chemotherapy	Atorvastatin and capecitabine
	NCT03971019	03/2018	Survival benefits of statin use in breast cancer patients	Statins
	NCT03454529	03/2018	Simvastatin treatment on breast cancer cell proliferation in women with early stage breast cancers	Simvastatin
Hepatocellular carcinoma	NCT03275376	12/2017	Atorvastatin and sorafenib treatment in advanced HCC	Atorvastatin and sorafenib
	NCT03024684	01/2017	Atorvastatin in preventing HCC relapse after curative treatments	Atorvastatin
Stomach cancer	NCT03086291	01/2018	Simvastatin of high dose for patients of GI tract cancer who failed chemotherapy	Simvastatin

CHAPTER 9
CONCLUSION AND FUTURE PERSEPCTIVE

9 Conclusion and future perspective

9.1 Conclusion

In spite of the abundance of therapeutic options available, HCC remains one of the most fatal and common cancers in the world. The emergence of acquired drug resistance is an obstacle to effective HCC treatment. Resistance to molecularly targeted drugs, such as TKIs, develops in most cancer patients and limits their long-term survival. But with the discovery of liver CSCs, it changed the perceptives regarding tumorigenesis and subsequently the strategy in developing novel cancer treatments.

In the CSC model, it suggests that the tumor initiation, self-renewal and differentiation are maintained by a small subset of cancer cells within the tumor bulk with stem cell-like features, which contribute to the tumor heterogeneity. Therefore, CSCs are believed to be responsible for the development of acquired drug resistance, leading to a poor prognosis of HCC patients. Therefore, targeting CSC pathways may be a promising strategy to overcome drug resistance in HCC patients.

For advanced-stage HCC patients, sorafenib and lenvatinib are the only two FDA-approved drugs. However, the clinical results are discouraging. Sorafenib, the first approved tyrosine kinase inhibitor in treating HCC, can only extend patients' overall survival by 3 months. Whereas the second approved drug, lenvatinib, is non-inferior to sorafenib in terms of survival benefit. Therefore, understanding the mechanism of acquired drug resistance is therefore highly warranted.

In order to mimic the clinical situation of the acquired drug resistance, we administrated sorafenib/lenvatinib to the PDTXs for three to four rounds of drug administration. Subsequently, sorafenib- and lenvatinib-resistant PDTXs were successfully established by the observation that there was no tumor suppression effect of the sorafenib/lenvatinib treatments. Using RNA sequencing coupled with IPA analysis, cholesterol biosynthesis was mostly and commonly enriched in both sorafenib- and lenvatinib-resistant PDTXs. The corresponding genes responsible for cholesterol biosynthesis were also highly upregulated in the resistant clones when compared to their mock controls, including *MVD*, *FDPS*, *SC5D*, or *SQLE*, etc. The result of the pathway analysis was further verified by the filipin staining, which stained for free cholesterol deposition.

Since drug resistant cells are endowed with enhanced CSC populations, we hypothesized that cholesterol biosynthesis was also activated in liver CSCs. To investigate this hypothesis, we enriched CSC population by serial passage of hepatospheres under chemotherapeutic drugs administration, and the pathway analysis also showed upregulation of cholesterol biosynthesis in enriched liver CSC populations when compared with the mock counterparts. Likewise, filipin staining confirmed that enhanced cholesterol deposition was observed in hepatospheres when compared to the differentiated HCC cells. Given the high similar expression profiles between CSCs and normal stem cells, it is important to determine if cholesterol biosynthesis was preferentially activated in the liver CSC populations. We first sorted CD133⁺ cells and CD133⁻ cells from a liver regeneration mouse model and two HCC mouse models. Next, we analysed the enriched signalling pathways in CD133⁺ cells, using CD133⁻ cells as corresponding baselines, in these three mouse models by RNA sequencing analysis. When compared to that of regenerating liver, cholesterol homeostasis was found to be the most commonly upregulated pathway in CD133⁺ HCC cells from two HCC mouse models. Lastly, using upstream regulatory analysis, the activated cholesterol biosynthesis in sorafenib-, lenvatinib- and chemo-resistant PDTXs and hepatospheres was commonly regulated by SREBP2. IF staining and western blot analysis confirmed the upregulation and activation of SREBP2 in CSC-enriched hepatospheres.

In view of the potential regulatory role of SREBP2-mediated cholesterol biosynthesis in driving drug resistance via augmentation of CSCs in HCC, we genetically manipulated the expression of SREBP2 in HCC cells by lentiviral-based CRISPR activation and knockdown approaches. The alteration of SREBP2 changed the expression of genes involved in cholesterol biosynthesis, such as *MVD*, *FDPS*, or *HMGCR*, which was accompanied with changes in intracellular cholesterol level. Moreover, SREBP2-mediated cholesterol biosynthesis was found to regulate liver CSC properties including abilities in tumor initiation, self-renewal, cell invasiveness and expression of liver CSC markers. The SREBP2-mediated cholesterol biosynthesis was clinically relevant in publicly available datasets and in-house HCC patient cohort, and related to poorer disease-free survival and higher recurrence rate. Most importantly, SREBP2-mediated cholesterol biosynthesis conferred drug resistance. In sorafenib- and lenvatinib-resistant HCC cells, both SREBP2 and cholesterol deposition were highly activated. Consistently, suppression of SREBP2 sensitized the effect of sorafenib/lenvatinib in HCC cells while SREBP2 overexpression exerted the opposite effect. We have examined the clinical

relevance of SREBP2 in HCC patients treated with sorafenib. In a tissue microarray consisting of 91 HCC samples from patients who had been treated with sorafenib, patients with high SREBP2 expression had shorter disease-free survival.

The mechanism behind the upregulation of SREBP2-mediated cholesterol biosynthesis in the acquired drug resistance was further investigated. CASP3 has a specific cleavage site on SREBP2, and hence is able to activate the transcriptional activities of SREBP2. We first confirmed that CASP3 activity level was upregulated in sorafenib- and lenvatinib-resistant cells derived from HCC PDTXs and cell lines. The mRNA level of *CASP3* was also overexpressed in tumor samples in publicly available HCC dataset. Interestingly, suppression of CASP3 activity by inhibitor approach suppressed nuclear translocation of SREBP2 and cholesterol deposition, resulting in increased cell apoptosis after sorafenib/lenvatinib treatments.

By comparing the gene expression profiles between SREBP2-repressing HCC cells with their NTC cells, SHH pathway was involved in the CASP3-SREBP2-mediated cholesterol biosynthesis axis, mediating cancer stemness and drug resistance. The expression of signalling proteins involved in the canonical SHH pathway activation were altered correspondingly upon changes in SREBP2 expression. Meanwhile, GLI-1, the major effector of SHH pathway, was found to be overexpressed in drug-resistant PDTXs and HCC cell lines. Hence, suppression of SHH pathway by targeting GLI-1 via its specific inhibitor showed rescue effects in self-renewal and drug resistance in SREBP2 overexpressing HCC cells. We further examined an oxygenated derivative from cholesterol, 25-OHC, in regulating the SREBP2-activated SHH pathway. In HCC clinical samples, cleaved CASP3, SREBP2, and GLI-1 were significantly correlated to each other, consolidating the importance of this signalling axis in combating therapeutic treatments via mediating CSCs population.

Prior in examining the therapeutic implication of targeting cholesterol biosynthesis in treating HCC, we confirmed the role of cholesterol in mediating CSC properties and drug resistance. By supplementing exogenous cholesterol to SREBP2 knockdown HCC cells, CSC suppressive effects were liberated. The administration of exogenous cholesterol also promoted growth and proliferation in *ex vivo* patient-derived HCC organoids. Furthermore, the suppression of cholesterol biosynthesis by simvastatin, an FDA-approved drug in lowering cholesterol, suppressed CSC properties and sensitized drug efficacy in HCC cells. Meanwhile, simvastatin

also induced significant growth suppression in HCC organoids when combining with sorafenib and lenvatinib. The therapeutic implication of targeting cholesterol biosynthesis was further extended to *in vivo* PDTX models. The combined treatment of simvastatin and sorafenib generated the greatest suppression of tumor size and volume.

In summary, the study has elucidated a novel signalling axis in developing the acquired drug resistance by expanding CSC populations via CASP3-dependent, SREBP2-mediated cholesterol biosynthesis (Figure 9.1). Targeting cholesterol biosynthesis is effectively overcome the drug resistance in HCC cancer cells.

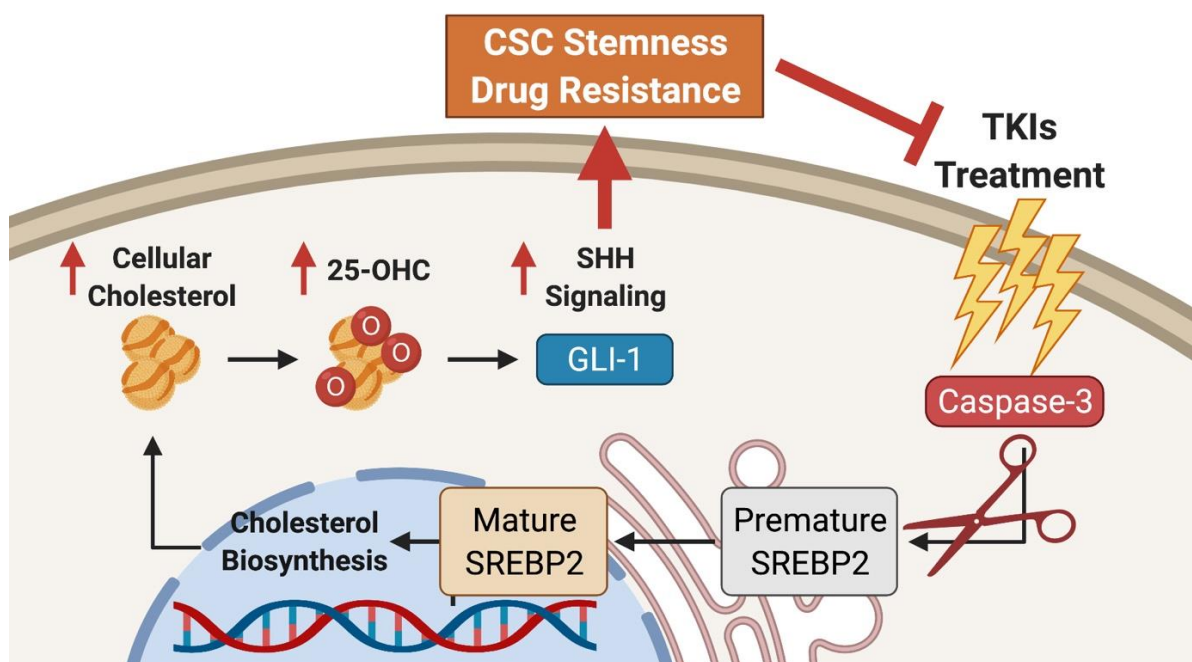


Figure 9.1 Summary of the study.

The mechanism of acquired drug resistance to TKIs treatment is driven by CASP3-induced SREBP2-mediated cholesterol biosynthesis-driven SHH signalling pathway.

9.2 Future perspective

In this study, CASP3 driven and SREBP2-mediated cholesterol biosynthesis was induced by sorafenib/lenvatinib treatment, which has been shown to propagate CSC populations via activation of SHH pathway. Giving the crucial role of cholesterol biosynthesis in augmenting the acquired drug resistance, acetyl-CoA, the early precursor for producing cholesterol, is also a precursor in synthesizing fatty acids. The *de novo* fatty acid synthesis and cholesterol

biosynthesis contributed to tumorigenesis in many cancers, including HCC. Also, in Figure 3.4, the mRNA expression of *HMGCS2*, *ACAA2*, *ACAT1* were decreased in drug-resistant clones that these are mitochondrial enzymes involved in fatty acid beta-oxidation, which indicated that fatty acid catabolism was inhibited when cholesterol biosynthesis was enhanced. However, different reports in the literature point to fatty acid synthesis as a metabolic process contributing to drug resistance in HCC (301-304). Although SREBP2-mediated cholesterol biosynthesis has been shown to support the growth of HCC lesions independently and mainly under conditions where fatty acid biosynthesis is inhibited (305), it is still worth to analyse how metabolism of other non-steroid lipids is altered in the drug-resistant xenografts. Also, the filipin staining alone is not enough to stain other forms of cholesterol as it can only stain free cholesterol, but not cholesteryl esters which are also important carcinogens for tumor development (306-309). The ratio of cholesteryl esters over free cholesterol was also suggested to be a diagnostic marker for HCC (306). Therefore, the current study was limited in analysing the solely role of cholesterol in mediating drug resistance, other molecules arising from acetyl-CoA should be further analysed in a parallel using cholesterol, triglycerides, and fatty acid lipidomic analysis.

Secondly, only CASP3 was investigated in this study. Though CASP3 is the central signalling protein in the apoptosis pathway, it is relevant to analyse if other caspase family members, such as CASP2, CASP7, CASP8, or CASP9, have also been involved in above-mentioned signalling axis. Particularly CASP2 was previously reported to activate S1P and hence SREBP2 under ER stress (230). A pan-inhibitor of caspase activity should be used to analyse whether the death is enhanced. Also, the mechanism between the balance between apoptotic and nonapoptotic role of CASP3 is remained unsolved in this study. Is the nonapoptotic role of CASP3 intrinsically determined arising from the heterogeneity of tumors? If not, what triggers CASP3 to switch from apoptotic initiator to a cell protector by activating the SREBP2-mediated cholesterol biosynthesis? Though in our study, the mechanism is largely irrelevant to the duration of cancer cells experiencing drug stresses, as no matter a short timepoint or a long-established resistant period, the CASP3 activity level was enhanced leading the cleavage of SREBP2.

Lastly, simvastatin was the only statin being investigated in this study. As mentioned previously, the distinct pharmacokinetics of each statin could yield distinctive combined effects, though they all can lower cholesterol production (269, 283, 310-312). For example, atorvastatin

was shown to be superior to simvastatin in lowering LDL cholesterol levels (313, 314). Though the researchers continued to search for the best regimen of statins treatment for advanced HCC, pravastatin showed no combined effect with sorafenib (293, 294). Also, simvastatin has an intrinsic limitation that it shares the same liver metabolic enzyme, CYP3A4, which could potentially attenuate the efficacy of sorafenib/simvastatin in treating HCC (315, 316). Apart from that, other cholesterol lowering strategies could perhaps be investigated. In the *de novo* cholesterol biosynthesis, there are more than 20 enzymes involved. SQLE has recently been considered as another rate-limiting enzyme in this complex metabolic pathway (124). SQLE has also been regarded as the key tumor driver in HCC via mediating cholesterol biosynthesis (177). A novel small protein, CASIMO1, was shown to interact with SQLE and hence influencing the lipid droplet formation (317). Apart from attenuating cholesterol biosynthesis, the blocking of cholesterol intake by ezetimibe (318) and suppression of cholesterol esterification by avasimibe (319) could further contribute to the understanding of cholesterol homeostasis in tumorigenesis.

References

1. Bishayee A. The role of inflammation and liver cancer. *Adv Exp Med Biol.* 2014;816:401-35.
2. Yang JD, Hainaut P, Gores GJ, Amadou A, Plymoth A, Roberts LR. A global view of hepatocellular carcinoma: trends, risk, prevention and management. *Nat Rev Gastroenterol Hepatol.* 2019;16(10):589-604.
3. Sung H, Ferlay J, Siegel RL, Laversanne M, Soerjomataram I, Jemal A, et al. Global Cancer Statistics 2020: GLOBOCAN Estimates of Incidence and Mortality Worldwide for 36 Cancers in 185 Countries. *CA Cancer J Clin.* 2021;71(3):209-49.
4. Schuppan D, Afdhal NH. Liver cirrhosis. *Lancet.* 2008;371(9615):838-51.
5. Smith MS, Edwards MJ, Upfold JB. The effects of hyperthermia on the fetus. *Dev Med Child Neurol.* 1986;28(6):806-9.
6. Zheng R, Qu C, Zhang S, Zeng H, Sun K, Gu X, et al. Liver cancer incidence and mortality in China: Temporal trends and projections to 2030. *Chin J Cancer Res.* 2018;30(6):571-9.
7. Hong Kong Cancer Registry HA. Leading Cancer Sites in Hong Kong in 2018. 2020.
8. Marengo A, Rosso C, Bugianesi E. Liver Cancer: Connections with Obesity, Fatty Liver, and Cirrhosis. *Annu Rev Med.* 2016;67:103-17.
9. Arnold M, Abnet CC, Neale RE, Vignat J, Giovannucci EL, McGlynn KA, et al. Global Burden of 5 Major Types of Gastrointestinal Cancer. *Gastroenterology.* 2020;159(1):335-49 e15.
10. Petrick JL, Florio AA, Znaor A, Ruggieri D, Laversanne M, Alvarez CS, et al. International trends in hepatocellular carcinoma incidence, 1978-2012. *Int J Cancer.* 2020;147(2):317-30.
11. Chang MH, Chen CJ, Lai MS, Hsu HM, Wu TC, Kong MS, et al. Universal hepatitis B vaccination in Taiwan and the incidence of hepatocellular carcinoma in children. Taiwan Childhood Hepatoma Study Group. *N Engl J Med.* 1997;336(26):1855-9.
12. Plummer M, de Martel C, Vignat J, Ferlay J, Bray F, Franceschi S. Global burden of cancers attributable to infections in 2012: a synthetic analysis. *Lancet Glob Health.* 2016;4(9):e609-16.
13. Florio AA, Ferlay J, Znaor A, Ruggieri D, Alvarez CS, Laversanne M, et al. Global trends in intrahepatic and extrahepatic cholangiocarcinoma incidence from 1993 to 2012. *Cancer.* 2020;126(11):2666-78.
14. Younossi ZM, Koenig AB, Abdelatif D, Fazel Y, Henry L, Wymer M. Global epidemiology of nonalcoholic fatty liver disease-Meta-analytic assessment of prevalence, incidence, and outcomes. *Hepatology.* 2016;64(1):73-84.
15. Adams LA, Lymp JF, St Sauver J, Sanderson SO, Lindor KD, Feldstein A, et al. The natural history of nonalcoholic fatty liver disease: a population-based cohort study. *Gastroenterology.* 2005;129(1):113-21.
16. White DL, Kanwal F, El-Serag HB. Association between nonalcoholic fatty liver disease and risk for hepatocellular cancer, based on systematic review. *Clin Gastroenterol Hepatol.* 2012;10(12):1342-59 e2.
17. Estes C, Anstee QM, Arias-Loste MT, Bantel H, Bellentani S, Caballeria J, et al. Modeling NAFLD disease burden in China, France, Germany, Italy, Japan, Spain, United Kingdom, and United States for the period 2016-2030. *J Hepatol.* 2018;69(4):896-904.
18. Forner A, Reig M, Bruix J. Hepatocellular carcinoma. *Lancet.* 2018;391(10127):1301-14.
19. Kim E, Viatour P. Hepatocellular carcinoma: old friends and new tricks. *Exp Mol Med.* 2020;52(12):1898-907.

20. Bruix J, Sherman M, Llovet JM, Beaugrand M, Lencioni R, Burroughs AK, et al. Clinical management of hepatocellular carcinoma. Conclusions of the Barcelona-2000 EASL conference. European Association for the Study of the Liver. *J Hepatol.* 2001;35(3):421-30.
21. Llovet JM, Ricci S, Mazzaferro V, Hilgard P, Gane E, Blanc JF, et al. Sorafenib in advanced hepatocellular carcinoma. *N Engl J Med.* 2008;359(4):378-90.
22. Kudo M, Finn RS, Qin S, Han KH, Ikeda K, Piscaglia F, et al. Lenvatinib versus sorafenib in first-line treatment of patients with unresectable hepatocellular carcinoma: a randomised phase 3 non-inferiority trial. *Lancet.* 2018;391(10126):1163-73.
23. Imamura H, Matsuyama Y, Tanaka E, Ohkubo T, Hasegawa K, Miyagawa S, et al. Risk factors contributing to early and late phase intrahepatic recurrence of hepatocellular carcinoma after hepatectomy. *J Hepatol.* 2003;38(2):200-7.
24. Llovet JM, Bru C, Bruix J. Prognosis of hepatocellular carcinoma: the BCLC staging classification. *Semin Liver Dis.* 1999;19(3):329-38.
25. Teh SH, Christein J, Donohue J, Que F, Kendrick M, Farnell M, et al. Hepatic resection of hepatocellular carcinoma in patients with cirrhosis: Model of End-Stage Liver Disease (MELD) score predicts perioperative mortality. *J Gastrointest Surg.* 2005;9(9):1207-15; discussion 15.
26. Yang JD, Roberts LR. Hepatocellular carcinoma: A global view. *Nat Rev Gastroenterol Hepatol.* 2010;7(8):448-58.
27. Mazzaferro V, Regalia E, Doci R, Andreola S, Pulvirenti A, Bozzetti F, et al. Liver transplantation for the treatment of small hepatocellular carcinomas in patients with cirrhosis. *N Engl J Med.* 1996;334(11):693-9.
28. Yao FY, Ferrell L, Bass NM, Watson JJ, Bacchetti P, Venook A, et al. Liver transplantation for hepatocellular carcinoma: expansion of the tumor size limits does not adversely impact survival. *Hepatology.* 2001;33(6):1394-403.
29. Yao FY, Kerlan RK, Jr., Hirose R, Davern TJ, 3rd, Bass NM, Feng S, et al. Excellent outcome following down-staging of hepatocellular carcinoma prior to liver transplantation: an intention-to-treat analysis. *Hepatology.* 2008;48(3):819-27.
30. Trotter JF, Wachs M, Everson GT, Kam I. Adult-to-adult transplantation of the right hepatic lobe from a living donor. *N Engl J Med.* 2002;346(14):1074-82.
31. Vakili K, Pomposelli JJ, Cheah YL, Akoad M, Lewis WD, Khettry U, et al. Living donor liver transplantation for hepatocellular carcinoma: Increased recurrence but improved survival. *Liver Transpl.* 2009;15(12):1861-6.
32. Lin SM, Lin CJ, Lin CC, Hsu CW, Chen YC. Radiofrequency ablation improves prognosis compared with ethanol injection for hepatocellular carcinoma \leq 4 cm. *Gastroenterology.* 2004;127(6):1714-23.
33. Vilana R, Bruix J, Bru C, Ayuso C, Sole M, Rodes J. Tumor size determines the efficacy of percutaneous ethanol injection for the treatment of small hepatocellular carcinoma. *Hepatology.* 1992;16(2):353-7.
34. Lo CM, Ngan H, Tso WK, Liu CL, Lam CM, Poon RT, et al. Randomized controlled trial of transarterial lipiodol chemoembolization for unresectable hepatocellular carcinoma. *Hepatology.* 2002;35(5):1164-71.
35. Alba E, Valls C, Dominguez J, Martinez L, Escalante E, Llado L, et al. Transcatheter arterial chemoembolization in patients with hepatocellular carcinoma on the waiting list for orthotopic liver transplantation. *AJR Am J Roentgenol.* 2008;190(5):1341-8.
36. Wilhelm S, Carter C, Lynch M, Lowinger T, Dumas J, Smith RA, et al. Discovery and development of sorafenib: a multikinase inhibitor for treating cancer. *Nat Rev Drug Discov.* 2006;5(10):835-44.

37. Mossenta M, Busato D, Baboci L, Cintio FD, Toffoli G, Bo MD. New Insight into Therapies Targeting Angiogenesis in Hepatocellular Carcinoma. *Cancers (Basel)*. 2019;11(8).
38. Onuma AE, Zhang H, Huang H, Williams TM, Noonan A, Tsung A. Immune Checkpoint Inhibitors in Hepatocellular Cancer: Current Understanding on Mechanisms of Resistance and Biomarkers of Response to Treatment. *Gene Expr*. 2020;20(1):53-65.
39. Voutsadakis IA. PD-1 inhibitors monotherapy in hepatocellular carcinoma: Meta-analysis and systematic review. *Hepatobiliary Pancreat Dis Int*. 2019;18(6):505-10.
40. Cheng H, Sun G, Chen H, Li Y, Han Z, Li Y, et al. Trends in the treatment of advanced hepatocellular carcinoma: immune checkpoint blockade immunotherapy and related combination therapies. *Am J Cancer Res*. 2019;9(8):1536-45.
41. El-Khoueiry AB, Sangro B, Yau T, Crocenzi TS, Kudo M, Hsu C, et al. Nivolumab in patients with advanced hepatocellular carcinoma (CheckMate 040): an open-label, non-comparative, phase 1/2 dose escalation and expansion trial. *Lancet*. 2017;389(10088):2492-502.
42. Finn RS, Qin S, Ikeda M, Galle PR, Ducreux M, Kim TY, et al. Atezolizumab plus Bevacizumab in Unresectable Hepatocellular Carcinoma. *N Engl J Med*. 2020;382(20):1894-905.
43. Yang X, Wang D, Lin J, Yang X, Zhao H. Atezolizumab plus bevacizumab for unresectable hepatocellular carcinoma. *Lancet Oncol*. 2020;21(9):e412.
44. Kreso A, Dick JE. Evolution of the cancer stem cell model. *Cell Stem Cell*. 2014;14(3):275-91.
45. Valent P, Bonnet D, De Maria R, Lapidot T, Copland M, Melo JV, et al. Cancer stem cell definitions and terminology: the devil is in the details. *Nat Rev Cancer*. 2012;12(11):767-75.
46. Chiba T, Iwama A, Yokosuka O. Cancer stem cells in hepatocellular carcinoma: Therapeutic implications based on stem cell biology. *Hepatol Res*. 2016;46(1):50-7.
47. Afify SM, Seno M. Conversion of Stem Cells to Cancer Stem Cells: Undercurrent of Cancer Initiation. *Cancers (Basel)*. 2019;11(3).
48. Maurizi G, Verma N, Gadi A, Mansukhani A, Basilico C. Sox2 is required for tumor development and cancer cell proliferation in osteosarcoma. *Oncogene*. 2018;37(33):4626-32.
49. Jeter CR, Yang T, Wang J, Chao HP, Tang DG. Concise Review: NANOG in Cancer Stem Cells and Tumor Development: An Update and Outstanding Questions. *Stem Cells*. 2015;33(8):2381-90.
50. Xiao Y, Yang X, Miao Y, He X, Wang M, Sha W. Inhibition of cell proliferation and tumor growth of colorectal cancer by inhibitors of Wnt and Notch signaling pathways. *Oncol Lett*. 2016;12(5):3695-700.
51. Zhan T, Rindtorff N, Boutros M. Wnt signaling in cancer. *Oncogene*. 2017;36(11):1461-73.
52. Yamashita T, Budhu A, Forgues M, Wang XW. Activation of hepatic stem cell marker EpCAM by Wnt-beta-catenin signaling in hepatocellular carcinoma. *Cancer Res*. 2007;67(22):10831-9.
53. Guo H, Lu Y, Wang J, Liu X, Keller ET, Liu Q, et al. Targeting the Notch signaling pathway in cancer therapeutics. *Thorac Cancer*. 2014;5(6):473-86.
54. Yang T, Rycak K, Liu ZM, Tang DG. Cancer stem cells: constantly evolving and functionally heterogeneous therapeutic targets. *Cancer Res*. 2014;74(11):2922-7.
55. Schepers AG, Snippert HJ, Stange DE, van den Born M, van Es JH, van de Wetering M, et al. Lineage tracing reveals Lgr5+ stem cell activity in mouse intestinal adenomas. *Science*. 2012;337(6095):730-5.

56. Shimokawa M, Ohta Y, Nishikori S, Matano M, Takano A, Fujii M, et al. Visualization and targeting of LGR5(+) human colon cancer stem cells. *Nature*. 2017;545(7653):187-92.
57. Mourao L, Jacquemin G, Huyghe M, Nawrocki WJ, Menssouri N, Servant N, et al. Lineage tracing of Notch1-expressing cells in intestinal tumours reveals a distinct population of cancer stem cells. *Sci Rep*. 2019;9(1):888.
58. Ribatti D, Tamma R, Annese T. Epithelial-Mesenchymal Transition in Cancer: A Historical Overview. *Transl Oncol*. 2020;13(6):100773.
59. Kim DH, Xing T, Yang Z, Dudek R, Lu Q, Chen YH. Epithelial Mesenchymal Transition in Embryonic Development, Tissue Repair and Cancer: A Comprehensive Overview. *J Clin Med*. 2017;7(1).
60. Mani SA, Guo W, Liao MJ, Eaton EN, Ayyanan A, Zhou AY, et al. The epithelial-mesenchymal transition generates cells with properties of stem cells. *Cell*. 2008;133(4):704-15.
61. Zhou P, Li B, Liu F, Zhang M, Wang Q, Liu Y, et al. The epithelial to mesenchymal transition (EMT) and cancer stem cells: implication for treatment resistance in pancreatic cancer. *Mol Cancer*. 2017;16(1):52.
62. Migita T, Ueda A, Ohishi T, Hatano M, Seimiya H, Horiguchi SI, et al. Epithelial-mesenchymal transition promotes SOX2 and NANOG expression in bladder cancer. *Lab Invest*. 2017.
63. Gao H, Teng C, Huang W, Peng J, Wang C. SOX2 Promotes the Epithelial to Mesenchymal Transition of Esophageal Squamous Cells by Modulating Slug Expression through the Activation of STAT3/HIF-alpha Signaling. *Int J Mol Sci*. 2015;16(9):21643-57.
64. Ghuwalewala S, Ghatak D, Das P, Dey S, Sarkar S, Alam N, et al. CD44(high)CD24(low) molecular signature determines the Cancer Stem Cell and EMT phenotype in Oral Squamous Cell Carcinoma. *Stem Cell Res*. 2016;16(2):405-17.
65. Liu S, Cong Y, Wang D, Sun Y, Deng L, Liu Y, et al. Breast cancer stem cells transition between epithelial and mesenchymal states reflective of their normal counterparts. *Stem Cell Reports*. 2014;2(1):78-91.
66. Jing Y, Han Z, Zhang S, Liu Y, Wei L. Epithelial-Mesenchymal Transition in tumor microenvironment. *Cell Biosci*. 2011;1:29.
67. Hirschmann-Jax C, Foster AE, Wulf GG, Nuchtern JG, Jax TW, Gobel U, et al. A distinct "side population" of cells with high drug efflux capacity in human tumor cells. *Proc Natl Acad Sci U S A*. 2004;101(39):14228-33.
68. Ginestier C, Hur MH, Charafe-Jauffret E, Monville F, Dutcher J, Brown M, et al. ALDH1 is a marker of normal and malignant human mammary stem cells and a predictor of poor clinical outcome. *Cell Stem Cell*. 2007;1(5):555-67.
69. Ma S, Chan KW, Lee TK, Tang KH, Wo JY, Zheng BJ, et al. Aldehyde dehydrogenase discriminates the CD133 liver cancer stem cell populations. *Mol Cancer Res*. 2008;6(7):1146-53.
70. Muramatsu S, Tanaka S, Mogushi K, Adikrisna R, Aihara A, Ban D, et al. Visualization of stem cell features in human hepatocellular carcinoma reveals in vivo significance of tumor-host interaction and clinical course. *Hepatology*. 2013;58(1):218-28.
71. Haraguchi N, Ishii H, Mimori K, Tanaka F, Ohkuma M, Kim HM, et al. CD13 is a therapeutic target in human liver cancer stem cells. *J Clin Invest*. 2010;120(9):3326-39.
72. Yamada T, Abei M, Danjoh I, Shiota R, Yamashita T, Hyodo I, et al. Identification of a unique hepatocellular carcinoma line, Li-7, with CD13(+) cancer stem cells hierarchy and population change upon its differentiation during culture and effects of sorafenib. *BMC Cancer*. 2015;15:260.

73. Wang R, Li Y, Tsung A, Huang H, Du Q, Yang M, et al. iNOS promotes CD24(+)CD133(+) liver cancer stem cell phenotype through a TACE/ADAM17-dependent Notch signaling pathway. *Proc Natl Acad Sci U S A*. 2018;115(43):E10127-E36.
74. Lee TK, Castilho A, Cheung VC, Tang KH, Ma S, Ng IO. CD24(+) liver tumor-initiating cells drive self-renewal and tumor initiation through STAT3-mediated NANOG regulation. *Cell Stem Cell*. 2011;9(1):50-63.
75. Dang H, Steinway SN, Ding W, Rountree CB. Induction of tumor initiation is dependent on CD44s in c-Met(+) hepatocellular carcinoma. *BMC Cancer*. 2015;15:161.
76. Lee TK, Cheung VC, Lu P, Lau EY, Ma S, Tang KH, et al. Blockade of CD47-mediated cathepsin S/protease-activated receptor 2 signaling provides a therapeutic target for hepatocellular carcinoma. *Hepatology*. 2014;60(1):179-91.
77. Lo J, Lau EY, Ching RH, Cheng BY, Ma MK, Ng IO, et al. Nuclear factor kappa B-mediated CD47 up-regulation promotes sorafenib resistance and its blockade synergizes the effect of sorafenib in hepatocellular carcinoma in mice. *Hepatology*. 2015;62(2):534-45.
78. Zeng SS, Yamashita T, Kondo M, Nio K, Hayashi T, Hara Y, et al. The transcription factor SALL4 regulates stemness of EpCAM-positive hepatocellular carcinoma. *J Hepatol*. 2014;60(1):127-34.
79. Yamashita T, Ji J, Budhu A, Forgues M, Yang W, Wang HY, et al. EpCAM-positive hepatocellular carcinoma cells are tumor-initiating cells with stem/progenitor cell features. *Gastroenterology*. 2009;136(3):1012-24.
80. Liu S, Li N, Yu X, Xiao X, Cheng K, Hu J, et al. Expression of intercellular adhesion molecule 1 by hepatocellular carcinoma stem cells and circulating tumor cells. *Gastroenterology*. 2013;144(5):1031-41 e10.
81. Cheng BY, Lau EY, Leung HW, Leung CO, Ho NP, Gurung S, et al. IRAK1 Augments Cancer Stemness and Drug Resistance via the AP-1/AKR1B10 Signaling Cascade in Hepatocellular Carcinoma. *Cancer Res*. 2018;78(9):2332-42.
82. Huch M, Dorrell C, Boj SF, van Es JH, Li VS, van de Wetering M, et al. In vitro expansion of single Lgr5+ liver stem cells induced by Wnt-driven regeneration. *Nature*. 2013;494(7436):247-50.
83. Lei ZJ, Wang J, Xiao HL, Guo Y, Wang T, Li Q, et al. Lysine-specific demethylase 1 promotes the stemness and chemoresistance of Lgr5(+) liver cancer initiating cells by suppressing negative regulators of beta-catenin signaling. *Oncogene*. 2015;34(24):3188-98.
84. Tsui YM, Sze KM, Tung EK, Ho DW, Lee TK, Ng IO. Dishevelled-3 phosphorylation is governed by HIPK2/PP1/alpha/ITCH axis and the non-phosphorylated form promotes cancer stemness via LGR5 in hepatocellular carcinoma. *Oncotarget*. 2017;8(24):39430-42.
85. Cai C, Zhu X. The Wnt/beta-catenin pathway regulates self-renewal of cancer stem-like cells in human gastric cancer. *Mol Med Rep*. 2012;5(5):1191-6.
86. Kim SY, Kang JW, Song X, Kim BK, Yoo YD, Kwon YT, et al. Role of the IL-6-JAK1-STAT3-Oct-4 pathway in the conversion of non-stem cancer cells into cancer stem-like cells. *Cell Signal*. 2013;25(4):961-9.
87. Park JH, Shin JE, Park HW. The Role of Hippo Pathway in Cancer Stem Cell Biology. *Mol Cells*. 2018;41(2):83-92.
88. Guo Y, Pan Q, Zhang J, Xu X, Liu X, Wang Q, et al. Functional and clinical evidence that TAZ is a candidate oncogene in hepatocellular carcinoma. *J Cell Biochem*. 2015;116(11):2465-75.
89. Hayashi H, Higashi T, Yokoyama N, Kaida T, Sakamoto K, Fukushima Y, et al. An Imbalance in TAZ and YAP Expression in Hepatocellular Carcinoma Confers Cancer Stem Cell-like Behaviors Contributing to Disease Progression. *Cancer Res*. 2015;75(22):4985-97.

90. Xu L, Tong X, Zhang S, Yin F, Li X, Wei H, et al. ASPP2 suppresses stem cell-like characteristics and chemoresistance by inhibiting the Src/FAK/Snail axis in hepatocellular carcinoma. *Tumour Biol.* 2016;37(10):13669-77.
91. Lau EY, Lo J, Cheng BY, Ma MK, Lee JM, Ng JK, et al. Cancer-Associated Fibroblasts Regulate Tumor-Initiating Cell Plasticity in Hepatocellular Carcinoma through c-Met/FRA1/HEY1 Signaling. *Cell Rep.* 2016;15(6):1175-89.
92. Della Corte CM, Viscardi G, Papaccio F, Esposito G, Martini G, Ciardiello D, et al. Implication of the Hedgehog pathway in hepatocellular carcinoma. *World J Gastroenterol.* 2017;23(24):4330-40.
93. Che L, Yuan YH, Jia J, Ren J. Activation of sonic hedgehog signaling pathway is an independent potential prognosis predictor in human hepatocellular carcinoma patients. *Chin J Cancer Res.* 2012;24(4):323-31.
94. Jeng KS, Sheen IS, Jeng WJ, Yu MC, Hsiao HI, Chang FY, et al. Activation of the sonic hedgehog signaling pathway occurs in the CD133 positive cells of mouse liver cancer Hepa 1-6 cells. *Onco Targets Ther.* 2013;6:1047-55.
95. Leung HW, Lau EYT, Leung CON, Lei MML, Mok EHK, Ma VWS, et al. NRF2/SHH signaling cascade promotes tumor-initiating cell lineage and drug resistance in hepatocellular carcinoma. *Cancer Lett.* 2020;476:48-56.
96. Tsui YM, Chan LK, Ng IO. Cancer stemness in hepatocellular carcinoma: mechanisms and translational potential. *Br J Cancer.* 2020;122(10):1428-40.
97. Chen W, Dong J, Haiech J, Kilhoffer MC, Zeniou M. Cancer Stem Cell Quiescence and Plasticity as Major Challenges in Cancer Therapy. *Stem Cells Int.* 2016;2016:1740936.
98. Moore N, Lyle S. Quiescent, slow-cycling stem cell populations in cancer: a review of the evidence and discussion of significance. *J Oncol.* 2011;2011.
99. Chen J, Li Y, Yu TS, McKay RM, Burns DK, Kernie SG, et al. A restricted cell population propagates glioblastoma growth after chemotherapy. *Nature.* 2012;488(7412):522-6.
100. Kurtova AV, Xiao J, Mo Q, Pazhanisamy S, Krasnow R, Lerner SP, et al. Blocking PGE2-induced tumour repopulation abrogates bladder cancer chemoresistance. *Nature.* 2015;517(7533):209-13.
101. Qi XS, Pajonk F, McCloskey S, Low DA, Kupelian P, Steinberg M, et al. Radioresistance of the breast tumor is highly correlated to its level of cancer stem cell and its clinical implication for breast irradiation. *Radiother Oncol.* 2017;124(3):455-61.
102. Izumiya M, Kabashima A, Higuchi H, Igarashi T, Sakai G, Iizuka H, et al. Chemoresistance is associated with cancer stem cell-like properties and epithelial-to-mesenchymal transition in pancreatic cancer cells. *Anticancer Res.* 2012;32(9):3847-53.
103. Nagano O, Okazaki S, Saya H. Redox regulation in stem-like cancer cells by CD44 variant isoforms. *Oncogene.* 2013;32(44):5191-8.
104. Diehn M, Cho RW, Lobo NA, Kalisky T, Dorie MJ, Kulp AN, et al. Association of reactive oxygen species levels and radioresistance in cancer stem cells. *Nature.* 2009;458(7239):780-3.
105. Bao S, Wu Q, McLendon RE, Hao Y, Shi Q, Hjelmeland AB, et al. Glioma stem cells promote radioresistance by preferential activation of the DNA damage response. *Nature.* 2006;444(7120):756-60.
106. Wang J, Wakeman TP, Lathia JD, Hjelmeland AB, Wang XF, White RR, et al. Notch promotes radioresistance of glioma stem cells. *Stem Cells.* 2010;28(1):17-28.
107. Wu Y, Zhang J, Zhang X, Zhou H, Liu G, Li Q. Cancer Stem Cells: A Potential Breakthrough in HCC-Targeted Therapy. *Front Pharmacol.* 2020;11:198.

108. Chen CL, Uthaya Kumar DB, Punj V, Xu J, Sher L, Tahara SM, et al. NANOG Metabolically Reprograms Tumor-Initiating Stem-like Cells through Tumorigenic Changes in Oxidative Phosphorylation and Fatty Acid Metabolism. *Cell Metab.* 2016;23(1):206-19.
109. Cheng Z, Lei Z, Yang P, Si A, Xiang D, Zhou J, et al. Long non-coding RNA THOR promotes liver cancer stem cells expansion via beta-catenin pathway. *Gene.* 2019;684:95-103.
110. Zheng H, Pomyen Y, Hernandez MO, Li C, Livak F, Tang W, et al. Single-cell analysis reveals cancer stem cell heterogeneity in hepatocellular carcinoma. *Hepatology.* 2018;68(1):127-40.
111. Sakabe T, Azumi J, Umekita Y, Toriguchi K, Hatano E, Hirooka Y, et al. Expression of Cancer Stem Cell-associated DKK1 mRNA Serves as Prognostic Marker for Hepatocellular Carcinoma. *Anticancer Res.* 2017;37(9):4881-8.
112. Gorin A, Gabitova L, Astsaturov I. Regulation of cholesterol biosynthesis and cancer signaling. *Curr Opin Pharmacol.* 2012;12(6):710-6.
113. DuBroff R, de Lorgeril M. Cholesterol confusion and statin controversy. *World J Cardiol.* 2015;7(7):404-9.
114. Ding X, Zhang W, Li S, Yang H. The role of cholesterol metabolism in cancer. *Am J Cancer Res.* 2019;9(2):219-27.
115. Pelton K, Freeman MR, Solomon KR. Cholesterol and prostate cancer. *Curr Opin Pharmacol.* 2012;12(6):751-9.
116. Llaverias G, Danilo C, Mercier I, Daumer K, Capozza F, Williams TM, et al. Role of cholesterol in the development and progression of breast cancer. *Am J Pathol.* 2011;178(1):402-12.
117. Heir T, Falk RS, Robsahm TE, Sandvik L, Erikssen J, Tretli S. Cholesterol and prostate cancer risk: a long-term prospective cohort study. *BMC Cancer.* 2016;16:643.
118. Asano K, Kubo M, Yonemoto K, Doi Y, Ninomiya T, Tanizaki Y, et al. Impact of serum total cholesterol on the incidence of gastric cancer in a population-based prospective study: the Hisayama study. *Int J Cancer.* 2008;122(4):909-14.
119. Cerqueira NM, Oliveira EF, Gesto DS, Santos-Martins D, Moreira C, Moorthy HN, et al. Cholesterol Biosynthesis: A Mechanistic Overview. *Biochemistry.* 2016;55(39):5483-506.
120. Mok EHK, Lee TKW. The Pivotal Role of the Dysregulation of Cholesterol Homeostasis in Cancer: Implications for Therapeutic Targets. *Cancers (Basel).* 2020;12(6).
121. Berndt N, Hamilton AD, Sebt SM. Targeting protein prenylation for cancer therapy. *Nat Rev Cancer.* 2011;11(11):775-91.
122. Sorrentino G, Ruggeri N, Specchia V, Cordenonsi M, Mano M, Dupont S, et al. Metabolic control of YAP and TAZ by the mevalonate pathway. *Nat Cell Biol.* 2014;16(4):357-66.
123. Al-Haidari AA, Syk I, Thorlacius H. HMG-CoA reductase regulates CCL17-induced colon cancer cell migration via geranylgeranylation and RhoA activation. *Biochem Biophys Res Commun.* 2014;446(1):68-72.
124. Tan JME, Cook ECL, van den Berg M, Scheij S, Zelcer N, Loregger A. Differential use of E2 ubiquitin conjugating enzymes for regulated degradation of the rate-limiting enzymes HMGCR and SQLE in cholesterol biosynthesis. *Atherosclerosis.* 2019;281:137-42.
125. Hu J, Zhang Z, Shen WJ, Azhar S. Cellular cholesterol delivery, intracellular processing and utilization for biosynthesis of steroid hormones. *Nutr Metab (Lond).* 2010;7:47.
126. Madison BB. Srebp2: A master regulator of sterol and fatty acid synthesis. *J Lipid Res.* 2016;57(3):333-5.
127. Horton JD, Goldstein JL, Brown MS. SREBPs: activators of the complete program of cholesterol and fatty acid synthesis in the liver. *J Clin Invest.* 2002;109(9):1125-31.

128. Brown MS, Goldstein JL. The SREBP pathway: regulation of cholesterol metabolism by proteolysis of a membrane-bound transcription factor. *Cell*. 1997;89(3):331-40.
129. Eberle D, Hegarty B, Bossard P, Ferre P, Foufelle F. SREBP transcription factors: master regulators of lipid homeostasis. *Biochimie*. 2004;86(11):839-48.
130. Peterson TR, Sengupta SS, Harris TE, Carmack AE, Kang SA, Balderas E, et al. mTOR complex 1 regulates lipin 1 localization to control the SREBP pathway. *Cell*. 2011;146(3):408-20.
131. Chen Y, Hughes-Fulford M. Human prostate cancer cells lack feedback regulation of low-density lipoprotein receptor and its regulator, SREBP2. *Int J Cancer*. 2001;91(1):41-5.
132. Siperstein MD, Fagan VM. Deletion of the Cholesterol-Negative Feedback System in Liver Tumors. *Cancer Res*. 1964;24:1108-15.
133. Antalis CJ, Arnold T, Rasool T, Lee B, Buhman KK, Siddiqui RA. High ACAT1 expression in estrogen receptor negative basal-like breast cancer cells is associated with LDL-induced proliferation. *Breast Cancer Res Treat*. 2010;122(3):661-70.
134. Jiang Y, Sun A, Zhao Y, Ying W, Sun H, Yang X, et al. Proteomics identifies new therapeutic targets of early-stage hepatocellular carcinoma. *Nature*. 2019;567(7747):257-61.
135. Geng F, Cheng X, Wu X, Yoo JY, Cheng C, Guo JY, et al. Inhibition of SOAT1 Suppresses Glioblastoma Growth via Blocking SREBP-1-Mediated Lipogenesis. *Clin Cancer Res*. 2016;22(21):5337-48.
136. Saraon P, Trudel D, Kron K, Dmitromanolakis A, Trachtenberg J, Bapat B, et al. Evaluation and prognostic significance of ACAT1 as a marker of prostate cancer progression. *Prostate*. 2014;74(4):372-80.
137. Bell AW. Lipid metabolism in liver and selected tissues and in the whole body of ruminant animals. *Prog Lipid Res*. 1979;18(3):117-64.
138. Venturini I, Amedei R, Modonesi G, Cosenza R, Miglioli L, Cioni G, et al. May plasma cholesterol level be considered a neoplastic marker in liver disease from cirrhosis to hepatocellular carcinoma? *Ital J Gastroenterol Hepatol*. 1999;31(1):61-5.
139. Mayengbam SS, Singh A, Pillai AD, Bhat MK. Influence of cholesterol on cancer progression and therapy. *Transl Oncol*. 2021;14(6):101043.
140. Venturini I, Zeneroli ML, Corsi L, Baraldi C, Ferrarese C, Pecora N, et al. Diazepam binding inhibitor and total cholesterol plasma levels in cirrhosis and hepatocellular carcinoma. *Regul Pept*. 1998;74(1):31-4.
141. Ahaneku JE, Taylor GO, Olubuyide IO, Agbedana EO. Abnormal lipid and lipoprotein patterns in liver cirrhosis with and without hepatocellular carcinoma. *J Pak Med Assoc*. 1992;42(11):260-3.
142. Muraji T, Woolley MM, Sinatra F, Siegel SM, Isaacs H. The prognostic implication of hypercholesterolemia in infants and children with hepatoblastoma. *J Pediatr Surg*. 1985;20(3):228-30.
143. Bricker LA, Morris HP, Siperstein MD. Loss of the cholesterol feedback system in the intact hepatoma-bearing rat. *J Clin Invest*. 1972;51(2):206-15.
144. Kitahara CM, Berrington de Gonzalez A, Freedman ND, Huxley R, Mok Y, Jee SH, et al. Total cholesterol and cancer risk in a large prospective study in Korea. *J Clin Oncol*. 2011;29(12):1592-8.
145. Zhao J, Zhao Y, Wang H, Gu X, Ji J, Gao C. Association between metabolic abnormalities and HBV related hepatocellular carcinoma in Chinese: a cross-sectional study. *Nutr J*. 2011;10:49.
146. Khatatb MA, Eslam M, Mousa YI, Ela-adawy N, Fathy S, Shatat M, et al. Association between metabolic abnormalities and hepatitis C-related hepatocellular carcinoma. *Ann Hepatol*. 2012;11(4):487-94.

147. Saito N, Sairenchi T, Irie F, Iso H, Iimura K, Watanabe H, et al. Low serum LDL cholesterol levels are associated with elevated mortality from liver cancer in Japan: the Ibaraki Prefectural health study. *Tohoku J Exp Med.* 2013;229(3):203-11.
148. Colhoun EDt, Forsberg CG, Chavin KD, Baliga PK, Taber DJ. Incidence and risk factors of hepatocellular carcinoma after orthotopic liver transplantation. *Surgery.* 2017;161(3):830-6.
149. Lee YL, Li WC, Tsai TH, Chiang HY, Ting CT. Body mass index and cholesterol level predict surgical outcome in patients with hepatocellular carcinoma in Taiwan - a cohort study. *Oncotarget.* 2016;7(16):22948-59.
150. Lau EY, Ho NP, Lee TK. Cancer Stem Cells and Their Microenvironment: Biology and Therapeutic Implications. *Stem Cells Int.* 2017;2017:3714190.
151. Mitra A, Mishra L, Li S. EMT, CTCs and CSCs in tumor relapse and drug-resistance. *Oncotarget.* 2015;6(13):10697-711.
152. Bono B, Ostano P, Peritore M, Gregnanin I, Belgiovine C, Liguori M, et al. Cells with stemness features are generated from in vitro transformed human fibroblasts. *Sci Rep.* 2018;8(1):13838.
153. Wang C, Li P, Xuan J, Zhu C, Liu J, Shan L, et al. Cholesterol Enhances Colorectal Cancer Progression via ROS Elevation and MAPK Signaling Pathway Activation. *Cell Physiol Biochem.* 2017;42(2):729-42.
154. Kim HY, Kim DK, Bae SH, Gwak H, Jeon JH, Kim JK, et al. Farnesyl diphosphate synthase is important for the maintenance of glioblastoma stemness. *Exp Mol Med.* 2018;50(10):1-12.
155. Sharma A, Bandyopadhyaya S, Chowdhury K, Sharma T, Maheshwari R, Das A, et al. Metformin exhibited anticancer activity by lowering cellular cholesterol content in breast cancer cells. *PLoS One.* 2019;14(1):e0209435.
156. Saito T, Chiba T, Yuki K, Zen Y, Oshima M, Koide S, et al. Metformin, a diabetes drug, eliminates tumor-initiating hepatocellular carcinoma cells. *PLoS One.* 2013;8(7):e70010.
157. Wang B, Rong X, Palladino END, Wang J, Fogelman AM, Martin MG, et al. Phospholipid Remodeling and Cholesterol Availability Regulate Intestinal Stemness and Tumorigenesis. *Cell Stem Cell.* 2018;22(2):206-20 e4.
158. Montero J, Morales A, Llacuna L, Lluís JM, Terrones O, Basanez G, et al. Mitochondrial cholesterol contributes to chemotherapy resistance in hepatocellular carcinoma. *Cancer Res.* 2008;68(13):5246-56.
159. Wang SF, Chou YC, Mazumder N, Kao FJ, Nagy LD, Guengerich FP, et al. 7-Ketocholesterol induces P-glycoprotein through PI3K/mTOR signaling in hepatoma cells. *Biochem Pharmacol.* 2013;86(4):548-60.
160. Wang S, Yao Y, Rao C, Zheng G, Chen W. 25-HC decreases the sensitivity of human gastric cancer cells to 5-fluorouracil and promotes cells invasion via the TLR2/NF-kappaB signaling pathway. *Int J Oncol.* 2019;54(3):966-80.
161. Criscuolo D, Avolio R, Calice G, Laezza C, Paladino S, Navarra G, et al. Cholesterol Homeostasis Modulates Platinum Sensitivity in Human Ovarian Cancer. *Cells.* 2020;9(4).
162. Kim S, Lee M, Dhanasekaran DN, Song YS. Activation of LXRA/beta by cholesterol in malignant ascites promotes chemoresistance in ovarian cancer. *BMC Cancer.* 2018;18(1):1232.
163. Simigdala N, Gao Q, Pancholi S, Roberg-Larsen H, Zvelebil M, Ribas R, et al. Cholesterol biosynthesis pathway as a novel mechanism of resistance to estrogen deprivation in estrogen receptor-positive breast cancer. *Breast Cancer Res.* 2016;18(1):58.

164. Kimbung S, Lettiero B, Feldt M, Bosch A, Borgquist S. High expression of cholesterol biosynthesis genes is associated with resistance to statin treatment and inferior survival in breast cancer. *Oncotarget*. 2016;7(37):59640-51.
165. Bandyopadhyay S, Li J, Traer E, Tyner JW, Zhou A, Oh ST, et al. Cholesterol esterification inhibition and imatinib treatment synergistically inhibit growth of BCR-ABL mutation-independent resistant chronic myelogenous leukemia. *PLoS One*. 2017;12(7):e0179558.
166. Wu Y, Si R, Tang H, He Z, Zhu H, Wang L, et al. Cholesterol reduces the sensitivity to platinum-based chemotherapy via upregulating ABCG2 in lung adenocarcinoma. *Biochem Biophys Res Commun*. 2015;457(4):614-20.
167. Athavale D, Chouhan S, Pandey V, Mayengbam SS, Singh S, Bhat MK. Hepatocellular carcinoma-associated hypercholesterolemia: involvement of proprotein-convertase-subtilisin-kexin type-9 (PCSK9). *Cancer Metab*. 2018;6:16.
168. Xiang D, Cheng Z, Liu H, Wang X, Han T, Sun W, et al. Shp2 promotes liver cancer stem cell expansion by augmenting beta-catenin signaling and predicts chemotherapeutic response of patients. *Hepatology*. 2017;65(5):1566-80.
169. Leung CON, Tong M, Chung KPS, Zhou L, Che N, Tang KH, et al. Overriding Adaptive Resistance to Sorafenib Through Combination Therapy With Src Homology 2 Domain-Containing Phosphatase 2 Blockade in Hepatocellular Carcinoma. *Hepatology*. 2020;72(1):155-68.
170. Hu Y, Smyth GK. ELDA: extreme limiting dilution analysis for comparing depleted and enriched populations in stem cell and other assays. *J Immunol Methods*. 2009;347(1-2):70-8.
171. Li WC, Ralphs KL, Tosh D. Isolation and culture of adult mouse hepatocytes. *Methods Mol Biol*. 2010;633:185-96.
172. Subramanian A, Tamayo P, Mootha VK, Mukherjee S, Ebert BL, Gillette MA, et al. Gene set enrichment analysis: a knowledge-based approach for interpreting genome-wide expression profiles. *Proc Natl Acad Sci U S A*. 2005;102(43):15545-50.
173. Tang W, Chen Z, Zhang W, Cheng Y, Zhang B, Wu F, et al. The mechanisms of sorafenib resistance in hepatocellular carcinoma: theoretical basis and therapeutic aspects. *Signal Transduct Target Ther*. 2020;5(1):87.
174. Segala G, David M, de Medina P, Poirot MC, Serhan N, Vergez F, et al. Dendrogenin A drives LXR to trigger lethal autophagy in cancers. *Nat Commun*. 2017;8(1):1903.
175. Silvente-Poirot S, Dalenc F, Poirot M. The Effects of Cholesterol-Derived Oncometabolites on Nuclear Receptor Function in Cancer. *Cancer Res*. 2018;78(17):4803-8.
176. McDonnell DP, Park S, Goulet MT, Jasper J, Wardell SE, Chang CY, et al. Obesity, cholesterol metabolism, and breast cancer pathogenesis. *Cancer Res*. 2014;74(18):4976-82.
177. Liu D, Wong CC, Fu L, Chen H, Zhao L, Li C, et al. Squalene epoxidase drives NAFLD-induced hepatocellular carcinoma and is a pharmaceutical target. *Sci Transl Med*. 2018;10(437).
178. Yang Z, Qin W, Chen Y, Yuan B, Song X, Wang B, et al. Cholesterol inhibits hepatocellular carcinoma invasion and metastasis by promoting CD44 localization in lipid rafts. *Cancer Lett*. 2018;429:66-77.
179. Aguilar-Ballester M, Herrero-Cervera A, Vinue A, Martinez-Hervas S, Gonzalez-Navarro H. Impact of Cholesterol Metabolism in Immune Cell Function and Atherosclerosis. *Nutrients*. 2020;12(7).
180. Szilagy JT, Vetrano AM, Laskin JD, Aleksunes LM. Localization of the placental BCRP/ABCG2 transporter to lipid rafts: Role for cholesterol in mediating efflux activity. *Placenta*. 2017;55:29-36.

181. Freed-Pastor WA, Mizuno H, Zhao X, Langerod A, Moon SH, Rodriguez-Barrueco R, et al. Mutant p53 disrupts mammary tissue architecture via the mevalonate pathway. *Cell*. 2012;148(1-2):244-58.
182. Xue L, Qi H, Zhang H, Ding L, Huang Q, Zhao D, et al. Targeting SREBP-2-Regulated Mevalonate Metabolism for Cancer Therapy. *Front Oncol*. 2020;10:1510.
183. Zheng L, Li L, Lu Y, Jiang F, Yang XA. SREBP2 contributes to cisplatin resistance in ovarian cancer cells. *Exp Biol Med (Maywood)*. 2018;243(7):655-62.
184. Yamazaki Y, Moore R, Negishi M. Nuclear receptor CAR (NR1I3) is essential for DDC-induced liver injury and oval cell proliferation in mouse liver. *Lab Invest*. 2011;91(11):1624-33.
185. Tang J, Meng Q, Shi R, Xu Y. PRMT6 serves an oncogenic role in lung adenocarcinoma via regulating p18. *Mol Med Rep*. 2020;22(4):3161-72.
186. Ma S. Biology and clinical implications of CD133(+) liver cancer stem cells. *Exp Cell Res*. 2013;319(2):126-32.
187. Ehmsen S, Pedersen MH, Wang G, Terp MG, Arslanagic A, Hood BL, et al. Increased Cholesterol Biosynthesis Is a Key Characteristic of Breast Cancer Stem Cells Influencing Patient Outcome. *Cell Rep*. 2019;27(13):3927-38 e6.
188. Westerterp M, Gourion-Arsiquaud S, Murphy AJ, Shih A, Cremers S, Levine RL, et al. Regulation of hematopoietic stem and progenitor cell mobilization by cholesterol efflux pathways. *Cell Stem Cell*. 2012;11(2):195-206.
189. Yvan-Charvet L, Pagler T, Gautier EL, Avagyan S, Siry RL, Han S, et al. ATP-binding cassette transporters and HDL suppress hematopoietic stem cell proliferation. *Science*. 2010;328(5986):1689-93.
190. Yokoyama C, Wang X, Briggs MR, Admon A, Wu J, Hua X, et al. SREBP-1, a basic-helix-loop-helix-leucine zipper protein that controls transcription of the low density lipoprotein receptor gene. *Cell*. 1993;75(1):187-97.
191. Shao W, Espenshade PJ. Expanding roles for SREBP in metabolism. *Cell Metab*. 2012;16(4):414-9.
192. Goldstein JL, DeBose-Boyd RA, Brown MS. Protein sensors for membrane sterols. *Cell*. 2006;124(1):35-46.
193. Tontonoz P, Kim JB, Graves RA, Spiegelman BM. ADD1: a novel helix-loop-helix transcription factor associated with adipocyte determination and differentiation. *Mol Cell Biol*. 1993;13(8):4753-9.
194. Broitman SA, Cerda S, Wilkinson Jt. Cholesterol metabolism and colon cancer. *Prog Food Nutr Sci*. 1993;17(1):1-40.
195. Alfaqih MA, Nelson ER, Liu W, Safi R, Jasper JS, Macias E, et al. CYP27A1 Loss Dysregulates Cholesterol Homeostasis in Prostate Cancer. *Cancer Res*. 2017;77(7):1662-73.
196. Kondo A, Yamamoto S, Nakaki R, Shimamura T, Hamakubo T, Sakai J, et al. Extracellular Acidic pH Activates the Sterol Regulatory Element-Binding Protein 2 to Promote Tumor Progression. *Cell Rep*. 2017;18(9):2228-42.
197. Wen YA, Xiong X, Zaytseva YY, Napier DL, Vallee E, Li AT, et al. Downregulation of SREBP inhibits tumor growth and initiation by altering cellular metabolism in colon cancer. *Cell Death Dis*. 2018;9(3):265.
198. Teresi RE, Planchon SM, Waite KA, Eng C. Regulation of the PTEN promoter by statins and SREBP. *Hum Mol Genet*. 2008;17(7):919-28.
199. Li X, Wu JB, Li Q, Shigemura K, Chung LW, Huang WC. SREBP-2 promotes stem cell-like properties and metastasis by transcriptional activation of c-Myc in prostate cancer. *Oncotarget*. 2016;7(11):12869-84.
200. Shiozawa Y, Nie B, Pienta KJ, Morgan TM, Taichman RS. Cancer stem cells and their role in metastasis. *Pharmacol Ther*. 2013;138(2):285-93.

201. Ayob AZ, Ramasamy TS. Cancer stem cells as key drivers of tumour progression. *J Biomed Sci.* 2018;25(1):20.
202. Tanabe S, Quader S, Cabral H, Ono R. Interplay of EMT and CSC in Cancer and the Potential Therapeutic Strategies. *Front Pharmacol.* 2020;11:904.
203. Ishiguro T, Ohata H, Sato A, Yamawaki K, Enomoto T, Okamoto K. Tumor-derived spheroids: Relevance to cancer stem cells and clinical applications. *Cancer Sci.* 2017;108(3):283-9.
204. Shaheen S, Ahmed M, Lorenzi F, Nateri AS. Spheroid-Formation (Colonosphere) Assay for in Vitro Assessment and Expansion of Stem Cells in Colon Cancer. *Stem Cell Rev Rep.* 2016;12(4):492-9.
205. Sieburg HB, Cho RH, Muller-Sieburg CE. Limiting dilution analysis for estimating the frequency of hematopoietic stem cells: uncertainty and significance. *Exp Hematol.* 2002;30(12):1436-43.
206. Jaiswal S, Jamieson CH, Pang WW, Park CY, Chao MP, Majeti R, et al. CD47 is upregulated on circulating hematopoietic stem cells and leukemia cells to avoid phagocytosis. *Cell.* 2009;138(2):271-85.
207. Wang JH, Huang ST, Zhang L, Liu ZG, Liang RX, Jiang SW, et al. Combined prognostic value of the cancer stem cell markers CD47 and CD133 in esophageal squamous cell carcinoma. *Cancer Med.* 2019;8(3):1315-25.
208. Liu L, Zhang L, Yang L, Li H, Li R, Yu J, et al. Anti-CD47 Antibody As a Targeted Therapeutic Agent for Human Lung Cancer and Cancer Stem Cells. *Front Immunol.* 2017;8:404.
209. Vander Griend DJ, Karthaus WL, Dalrymple S, Meeker A, DeMarzo AM, Isaacs JT. The role of CD133 in normal human prostate stem cells and malignant cancer-initiating cells. *Cancer Res.* 2008;68(23):9703-11.
210. Shmelkov SV, Butler JM, Hooper AT, Hormigo A, Kushner J, Milde T, et al. CD133 expression is not restricted to stem cells, and both CD133+ and CD133- metastatic colon cancer cells initiate tumors. *J Clin Invest.* 2008;118(6):2111-20.
211. Qin Q, Sun Y, Fei M, Zhang J, Jia Y, Gu M, et al. Expression of putative stem marker nestin and CD133 in advanced serous ovarian cancer. *Neoplasma.* 2012;59(3):310-5.
212. Suetsugu A, Nagaki M, Aoki H, Motohashi T, Kunisada T, Moriwaki H. Characterization of CD133+ hepatocellular carcinoma cells as cancer stem/progenitor cells. *Biochem Biophys Res Commun.* 2006;351(4):820-4.
213. Yin S, Li J, Hu C, Chen X, Yao M, Yan M, et al. CD133 positive hepatocellular carcinoma cells possess high capacity for tumorigenicity. *Int J Cancer.* 2007;120(7):1444-50.
214. Ricoult SJ, Yecies JL, Ben-Sahra I, Manning BD. Oncogenic PI3K and K-Ras stimulate de novo lipid synthesis through mTORC1 and SREBP. *Oncogene.* 2016;35(10):1250-60.
215. Holtta-Vuori M, Uronen RL, Repakova J, Salonen E, Vattulainen I, Panula P, et al. BODIPY-cholesterol: a new tool to visualize sterol trafficking in living cells and organisms. *Traffic.* 2008;9(11):1839-49.
216. Wang X, Zelenski NG, Yang J, Sakai J, Brown MS, Goldstein JL. Cleavage of sterol regulatory element binding proteins (SREBPs) by CPP32 during apoptosis. *EMBO J.* 1996;15(5):1012-20.
217. Pai JT, Brown MS, Goldstein JL. Purification and cDNA cloning of a second apoptosis-related cysteine protease that cleaves and activates sterol regulatory element binding proteins. *Proc Natl Acad Sci U S A.* 1996;93(11):5437-42.
218. Cheng C, Geng F, Cheng X, Guo D. Lipid metabolism reprogramming and its potential targets in cancer. *Cancer Commun (Lond).* 2018;38(1):27.

219. Armengol S, Arretxe E, Enzunza L, Llorente I, Mendibil U, Navarro-Imaz H, et al. SREBP-2-driven transcriptional activation of human SND1 oncogene. *Oncotarget*. 2017;8(64):108181-94.
220. Todenhofer T, Hennenlotter J, Kuhs U, Gerber V, Gakis G, Vogel U, et al. Altered expression of farnesyl pyrophosphate synthase in prostate cancer: evidence for a role of the mevalonate pathway in disease progression? *World J Urol*. 2013;31(2):345-50.
221. Seshacharyulu P, Rachagani S, Muniyan S, Siddiqui JA, Cruz E, Sharma S, et al. FDPS cooperates with PTEN loss to promote prostate cancer progression through modulation of small GTPases/AKT axis. *Oncogene*. 2019;38(26):5265-80.
222. Dehghani M, Samani Z, Abidi H, Manzouri L, Mahmoudi R, Hosseini Teshnizi S, et al. Relationship of SNP rs2645429 in Farnesyl-Diphosphate Farnesyltransferase 1 Gene Promoter with Susceptibility to Lung Cancer. *Int J Genomics*. 2018;2018:4863757.
223. Yang YF, Jan YH, Liu YP, Yang CJ, Su CY, Chang YC, et al. Squalene synthase induces tumor necrosis factor receptor 1 enrichment in lipid rafts to promote lung cancer metastasis. *Am J Respir Crit Care Med*. 2014;190(6):675-87.
224. Ge H, Zhao Y, Shi X, Tan Z, Chi X, He M, et al. Squalene epoxidase promotes the proliferation and metastasis of lung squamous cell carcinoma cells through extracellular signal-regulated kinase signaling. *Thorac Cancer*. 2019;10(3):428-36.
225. Kong Y, Cheng L, Mao F, Zhang Z, Zhang Y, Farah E, et al. Inhibition of cholesterol biosynthesis overcomes enzalutamide resistance in castration-resistant prostate cancer (CRPC). *J Biol Chem*. 2018;293(37):14328-41.
226. Sethunath V, Hu H, De Angelis C, Veeraraghavan J, Qin L, Wang N, et al. Targeting the Mevalonate Pathway to Overcome Acquired Anti-HER2 Treatment Resistance in Breast Cancer. *Mol Cancer Res*. 2019;17(11):2318-30.
227. Colgan SM, Tang D, Werstuck GH, Austin RC. Endoplasmic reticulum stress causes the activation of sterol regulatory element binding protein-2. *Int J Biochem Cell Biol*. 2007;39(10):1843-51.
228. Lebeau P, Al-Hashimi A, Sood S, Lhotak S, Yu P, Gyulay G, et al. Endoplasmic Reticulum Stress and Ca²⁺ Depletion Differentially Modulate the Sterol Regulatory Protein PCSK9 to Control Lipid Metabolism. *J Biol Chem*. 2017;292(4):1510-23.
229. Kovacs WJ, Charles KN, Walter KM, Shackelford JE, Wikander TM, Richards MJ, et al. Peroxisome deficiency-induced ER stress and SREBP-2 pathway activation in the liver of newborn PEX2 knock-out mice. *Biochim Biophys Acta*. 2012;1821(6):895-907.
230. Kim JY, Garcia-Carbonell R, Yamachika S, Zhao P, Dhar D, Loomba R, et al. ER Stress Drives Lipogenesis and Steatohepatitis via Caspase-2 Activation of S1P. *Cell*. 2018;175(1):133-45 e15.
231. Pham DD, Do HT, Bruelle C, Kukkonen JP, Eriksson O, Mogollon I, et al. p75 Neurotrophin Receptor Signaling Activates Sterol Regulatory Element-binding Protein-2 in Hepatocyte Cells via p38 Mitogen-activated Protein Kinase and Caspase-3. *J Biol Chem*. 2016;291(20):10747-58.
232. Androutsellis-Theotokis A, Leker RR, Soldner F, Hoepfner DJ, Ravin R, Poser SW, et al. Notch signalling regulates stem cell numbers in vitro and in vivo. *Nature*. 2006;442(7104):823-6.
233. Artavanis-Tsakonas S, Rand MD, Lake RJ. Notch signaling: cell fate control and signal integration in development. *Science*. 1999;284(5415):770-6.
234. Gao J, Chen C, Hong L, Wang J, Du Y, Song J, et al. Expression of Jagged1 and its association with hepatitis B virus X protein in hepatocellular carcinoma. *Biochem Biophys Res Commun*. 2007;356(2):341-7.
235. Giovannini C, Lacchini M, Gramantieri L, Chieco P, Bolondi L. Notch3 intracellular domain accumulates in HepG2 cell line. *Anticancer Res*. 2006;26(3A):2123-7.

236. Merle P, de la Monte S, Kim M, Herrmann M, Tanaka S, Von Dem Bussche A, et al. Functional consequences of frizzled-7 receptor overexpression in human hepatocellular carcinoma. *Gastroenterology*. 2004;127(4):1110-22.
237. Ho NPY, Leung CON, Wong TL, Lau EYT, Lei MML, Mok EHK, et al. The interplay of UBE2T and Mule in regulating Wnt/beta-catenin activation to promote hepatocellular carcinoma progression. *Cell Death Dis*. 2021;12(2):148.
238. Chai S, Ng KY, Tong M, Lau EY, Lee TK, Chan KW, et al. Octamer 4/microRNA-1246 signaling axis drives Wnt/beta-catenin activation in liver cancer stem cells. *Hepatology*. 2016;64(6):2062-76.
239. Leung CO, Mak WN, Kai AK, Chan KS, Lee TK, Ng IO, et al. Sox9 confers stemness properties in hepatocellular carcinoma through Frizzled-7 mediated Wnt/beta-catenin signaling. *Oncotarget*. 2016;7(20):29371-86.
240. Sicklick JK, Li YX, Jayaraman A, Kannangai R, Qi Y, Vivekanandan P, et al. Dysregulation of the Hedgehog pathway in human hepatocarcinogenesis. *Carcinogenesis*. 2006;27(4):748-57.
241. Huang S, He J, Zhang X, Bian Y, Yang L, Xie G, et al. Activation of the hedgehog pathway in human hepatocellular carcinomas. *Carcinogenesis*. 2006;27(7):1334-40.
242. Huang P, Nedelcu D, Watanabe M, Jao C, Kim Y, Liu J, et al. Cellular Cholesterol Directly Activates Smoothed in Hedgehog Signaling. *Cell*. 2016;166(5):1176-87 e14.
243. Nedelcu D, Liu J, Xu Y, Jao C, Salic A. Oxysterol binding to the extracellular domain of Smoothed in Hedgehog signaling. *Nat Chem Biol*. 2013;9(9):557-64.
244. Corcoran RB, Scott MP. Oxysterols stimulate Sonic hedgehog signal transduction and proliferation of medulloblastoma cells. *Proc Natl Acad Sci U S A*. 2006;103(22):8408-13.
245. Dwyer JR, Sever N, Carlson M, Nelson SF, Beachy PA, Parhami F. Oxysterols are novel activators of the hedgehog signaling pathway in pluripotent mesenchymal cells. *J Biol Chem*. 2007;282(12):8959-68.
246. Park SM, Jang HJ, Lee JH. Roles of Primary Cilia in the Developing Brain. *Front Cell Neurosci*. 2019;13:218.
247. Montagnani V, Stecca B. Role of Protein Kinases in Hedgehog Pathway Control and Implications for Cancer Therapy. *Cancers (Basel)*. 2019;11(4).
248. Espinosa-Bustos C, Mella J, Soto-Delgado J, Salas CO. State of the art of Smo antagonists for cancer therapy: advances in the target receptor and new ligand structures. *Future Med Chem*. 2019;11(6):617-38.
249. Riobo NA. Cholesterol and its derivatives in Sonic Hedgehog signaling and cancer. *Curr Opin Pharmacol*. 2012;12(6):736-41.
250. Nachtergaele S, Mydock LK, Krishnan K, Rammohan J, Schlesinger PH, Covey DF, et al. Oxysterols are allosteric activators of the oncoprotein Smoothed. *Nat Chem Biol*. 2012;8(2):211-20.
251. Heiden KB, Williamson AJ, Doscas ME, Ye J, Wang Y, Liu D, et al. The sonic hedgehog signaling pathway maintains the cancer stem cell self-renewal of anaplastic thyroid cancer by inducing snail expression. *J Clin Endocrinol Metab*. 2014;99(11):E2178-87.
252. Liu Z, Tu K, Wang Y, Yao B, Li Q, Wang L, et al. Hypoxia Accelerates Aggressiveness of Hepatocellular Carcinoma Cells Involving Oxidative Stress, Epithelial-Mesenchymal Transition and Non-Canonical Hedgehog Signaling. *Cell Physiol Biochem*. 2017;44(5):1856-68.
253. Kloudova A, Guengerich FP, Soucek P. The Role of Oxysterols in Human Cancer. *Trends Endocrinol Metab*. 2017;28(7):485-96.
254. Brown AJ, Jessup W. Oxysterols and atherosclerosis. *Atherosclerosis*. 1999;142(1):1-28.

255. Bjorkhem I, Cedazo-Minguez A, Leoni V, Meaney S. Oxysterols and neurodegenerative diseases. *Mol Aspects Med.* 2009;30(3):171-9.
256. Biasi F, Chiarotto E, Sottero B, Maina M, Mascia C, Guina T, et al. Evidence of cell damage induced by major components of a diet-compatible mixture of oxysterols in human colon cancer CaCo-2 cell line. *Biochimie.* 2013;95(3):632-40.
257. Dufour J, Viennois E, De Boussac H, Baron S, Lobaccaro JM. Oxysterol receptors, AKT and prostate cancer. *Curr Opin Pharmacol.* 2012;12(6):724-8.
258. Yoon JH, Canbay AE, Werneburg NW, Lee SP, Gores GJ. Oxysterols induce cyclooxygenase-2 expression in cholangiocytes: implications for biliary tract carcinogenesis. *Hepatology.* 2004;39(3):732-8.
259. Torres CG, Ramirez ME, Cruz P, Epanan MJ, Valladares LE, Sierralta WD. 27-hydroxycholesterol induces the transition of MCF7 cells into a mesenchymal phenotype. *Oncol Rep.* 2011;26(2):389-97.
260. Silva J, Dasgupta S, Wang G, Krishnamurthy K, Ritter E, Bieberich E. Lipids isolated from bone induce the migration of human breast cancer cells. *J Lipid Res.* 2006;47(4):724-33.
261. Raza S, Meyer M, Schommer J, Hammer KD, Guo B, Ghribi O. 27-Hydroxycholesterol stimulates cell proliferation and resistance to docetaxel-induced apoptosis in prostate epithelial cells. *Med Oncol.* 2016;33(2):12.
262. Ikegami T, Honda A, Miyazaki T, Kohjima M, Nakamuta M, Matsuzaki Y. Increased serum oxysterol concentrations in patients with chronic hepatitis C virus infection. *Biochem Biophys Res Commun.* 2014;446(3):736-40.
263. Yang J, Wang L, Jia R. Role of de novo cholesterol synthesis enzymes in cancer. *J Cancer.* 2020;11(7):1761-7.
264. Sharpe LJ, Brown AJ. Controlling cholesterol synthesis beyond 3-hydroxy-3-methylglutaryl-CoA reductase (HMGCR). *J Biol Chem.* 2013;288(26):18707-15.
265. Endo A. A historical perspective on the discovery of statins. *Proc Jpn Acad Ser B Phys Biol Sci.* 2010;86(5):484-93.
266. Igel M, Sudhop T, von Bergmann K. Metabolism and drug interactions of 3-hydroxy-3-methylglutaryl coenzyme A-reductase inhibitors (statins). *Eur J Clin Pharmacol.* 2001;57(5):357-64.
267. Chong PH, Seeger JD, Franklin C. Clinically relevant differences between the statins: implications for therapeutic selection. *Am J Med.* 2001;111(5):390-400.
268. Zhang X, Xing L, Jia X, Pang X, Xiang Q, Zhao X, et al. Comparative Lipid-Lowering/Increasing Efficacy of 7 Statins in Patients with Dyslipidemia, Cardiovascular Diseases, or Diabetes Mellitus: Systematic Review and Network Meta-Analyses of 50 Randomized Controlled Trials. *Cardiovasc Ther.* 2020;2020:3987065.
269. Meor Anuar Shuhaili MFR, Samsudin IN, Stanslas J, Hasan S, Thambiah SC. Effects of Different Types of Statins on Lipid Profile: A Perspective on Asians. *Int J Endocrinol Metab.* 2017;15(2):e43319.
270. Simon TG, Butt AA. Lipid dysregulation in hepatitis C virus, and impact of statin therapy upon clinical outcomes. *World J Gastroenterol.* 2015;21(27):8293-303.
271. Antoniou GA, Fisher RK, Georgiadis GS, Antoniou SA, Torella F. Statin therapy in lower limb peripheral arterial disease: Systematic review and meta-analysis. *Vascul Pharmacol.* 2014;63(2):79-87.
272. Fatehi Hassanabad A. Current perspectives on statins as potential anti-cancer therapeutics: clinical outcomes and underlying molecular mechanisms. *Transl Lung Cancer Res.* 2019;8(5):692-9.

273. Song C, Park S, Park J, Shim M, Kim A, Jeong IG, et al. Statin use after radical prostatectomy reduces biochemical recurrence in men with prostate cancer. *Prostate*. 2015;75(2):211-7.
274. McKay RR, Lin X, Albiges L, Fay AP, Kaymakcalan MD, Mickey SS, et al. Statins and survival outcomes in patients with metastatic renal cell carcinoma. *Eur J Cancer*. 2016;52:155-62.
275. Singh PP, Singh S. Statins are associated with reduced risk of gastric cancer: a systematic review and meta-analysis. *Ann Oncol*. 2013;24(7):1721-30.
276. Mamtani R, Lewis JD, Scott FI, Ahmad T, Goldberg DS, Datta J, et al. Disentangling the Association between Statins, Cholesterol, and Colorectal Cancer: A Nested Case-Control Study. *PLoS Med*. 2016;13(4):e1002007.
277. Shi M, Zheng H, Nie B, Gong W, Cui X. Statin use and risk of liver cancer: an update meta-analysis. *BMJ Open*. 2014;4(9):e005399.
278. Bansal D, Undela K, D'Cruz S, Schifano F. Statin use and risk of prostate cancer: a meta-analysis of observational studies. *PLoS One*. 2012;7(10):e46691.
279. Khurana V, Sheth A, Caldito G, Barkin JS. Statins reduce the risk of pancreatic cancer in humans: a case-control study of half a million veterans. *Pancreas*. 2007;34(2):260-5.
280. Bjarnadottir O, Romero Q, Bendahl PO, Jirstrom K, Ryden L, Loman N, et al. Targeting HMG-CoA reductase with statins in a window-of-opportunity breast cancer trial. *Breast Cancer Res Treat*. 2013;138(2):499-508.
281. Benakanakere I, Johnson T, Sleightholm R, Villeda V, Arya M, Bobba R, et al. Targeting cholesterol synthesis increases chemoimmuno-sensitivity in chronic lymphocytic leukemia cells. *Exp Hematol Oncol*. 2014;3:24.
282. Gbelcova H, Lenicek M, Zelenka J, Knejzlik Z, Dvorakova G, Zadinova M, et al. Differences in antitumor effects of various statins on human pancreatic cancer. *Int J Cancer*. 2008;122(6):1214-21.
283. Di Bello E, Zwergel C, Mai A, Valente S. The Innovative Potential of Statins in Cancer: New Targets for New Therapies. *Front Chem*. 2020;8:516.
284. Huang SW, Chyuan IT, Shiue C, Yu MC, Hsu YF, Hsu MJ. Lovastatin-mediated MCF-7 cancer cell death involves LKB1-AMPK-p38MAPK-p53-survivin signalling cascade. *J Cell Mol Med*. 2020;24(2):1822-36.
285. Okubo K, Isono M, Miyai K, Asano T, Sato A. Fluvastatin potentiates anticancer activity of vorinostat in renal cancer cells. *Cancer Sci*. 2020;111(1):112-26.
286. Lee SJ, Hwang JW, Yim H, Yim HJ, Woo SU, Suh SJ, et al. Synergistic effect of simvastatin plus NS398 on inhibition of proliferation and survival in hepatocellular carcinoma cell line. *J Gastroenterol Hepatol*. 2014;29(6):1299-307.
287. Feng J, Dai W, Mao Y, Wu L, Li J, Chen K, et al. Simvastatin re-sensitizes hepatocellular carcinoma cells to sorafenib by inhibiting HIF-1alpha/PPAR-gamma/PKM2-mediated glycolysis. *J Exp Clin Cancer Res*. 2020;39(1):24.
288. Yin Y, Liu L, Zhao Z, Yin L, Bauer N, Nwaeburu CC, et al. Simvastatin inhibits sonic hedgehog signaling and stemness features of pancreatic cancer. *Cancer Lett*. 2018;426:14-24.
289. Cardwell CR, Mc Menamin U, Hughes CM, Murray LJ. Statin use and survival from lung cancer: a population-based cohort study. *Cancer Epidemiol Biomarkers Prev*. 2015;24(5):833-41.
290. Chou CW, Lin CH, Hsiao TH, Lo CC, Hsieh CY, Huang CC, et al. Therapeutic effects of statins against lung adenocarcinoma via p53 mutant-mediated apoptosis. *Sci Rep*. 2019;9(1):20403.
291. Branvall E, Ekberg S, Eloranta S, Wasterlid T, Birmann BM, Smedby KE. Statin use is associated with improved survival in multiple myeloma: A Swedish population-based study of 4315 patients. *Am J Hematol*. 2020;95(6):652-61.

292. Musso A, Zocchi MR, Poggi A. Relevance of the mevalonate biosynthetic pathway in the regulation of bone marrow mesenchymal stromal cell-mediated effects on T-cell proliferation and B-cell survival. *Haematologica*. 2011;96(1):16-23.
293. Jouve JL, Lecomte T, Bouche O, Barbier E, Khemissa Akouz F, Riachi G, et al. Pravastatin combination with sorafenib does not improve survival in advanced hepatocellular carcinoma. *J Hepatol*. 2019;71(3):516-22.
294. Blanc JF, Khemissa F, Bronowicki JP, Montereyard C, Perarnau JM, Bourgeois V, et al. Phase 2 trial comparing sorafenib, pravastatin, their combination or supportive care in HCC with Child-Pugh B cirrhosis. *Hepatol Int*. 2021;15(1):93-104.
295. Dale KM, Coleman CI, Henyan NN, Kluger J, White CM. Statins and cancer risk: a meta-analysis. *JAMA*. 2006;295(1):74-80.
296. Cauley JA, McTiernan A, Rodabough RJ, LaCroix A, Bauer DC, Margolis KL, et al. Statin use and breast cancer: prospective results from the Women's Health Initiative. *J Natl Cancer Inst*. 2006;98(10):700-7.
297. Ahern TP, Pedersen L, Tarp M, Cronin-Fenton DP, Garne JP, Silliman RA, et al. Statin prescriptions and breast cancer recurrence risk: a Danish nationwide prospective cohort study. *J Natl Cancer Inst*. 2011;103(19):1461-8.
298. Murtola TJ, Syvala H, Tolonen T, Helminen M, Riikonen J, Koskimaki J, et al. Atorvastatin Versus Placebo for Prostate Cancer Before Radical Prostatectomy-A Randomized, Double-blind, Placebo-controlled Clinical Trial. *Eur Urol*. 2018;74(6):697-701.
299. Longo J, Hamilton RJ, Masoomian M, Khurram N, Branchard E, Mullen PJ, et al. A pilot window-of-opportunity study of preoperative fluvastatin in localized prostate cancer. *Prostate Cancer Prostatic Dis*. 2020;23(4):630-7.
300. Knuutila E, Riikonen J, Syvala H, Auriola S, Murtola TJ. Access and concentrations of atorvastatin in the prostate in men with prostate cancer. *Prostate*. 2019;79(12):1412-9.
301. Hayes CN, Zhang P, Chayama K. The Role of Lipids in Hepatocellular Carcinoma. In: Tirnitz-Parker JEE, editor. *Hepatocellular Carcinoma*. Brisbane (AU)2019.
302. Hung YH, Chan YS, Chang YS, Lee KT, Hsu HP, Yen MC, et al. Fatty acid metabolic enzyme acyl-CoA thioesterase 8 promotes the development of hepatocellular carcinoma. *Oncol Rep*. 2014;31(6):2797-803.
303. Che L, Paliogiannis P, Cigliano A, Pilo MG, Chen X, Calvisi DF. Pathogenetic, Prognostic, and Therapeutic Role of Fatty Acid Synthase in Human Hepatocellular Carcinoma. *Front Oncol*. 2019;9:1412.
304. Wang M, Han J, Xing H, Zhang H, Li Z, Liang L, et al. Dysregulated fatty acid metabolism in hepatocellular carcinoma. *Hepat Oncol*. 2016;3(4):241-51.
305. Che L, Chi W, Qiao Y, Zhang J, Song X, Liu Y, et al. Cholesterol biosynthesis supports the growth of hepatocarcinoma lesions depleted of fatty acid synthase in mice and humans. *Gut*. 2020;69(1):177-86.
306. Krautbauer S, Weiss TS, Wiest R, Schacherer D, Liebisch G, Buechler C. Diagnostic Value of Systemic Cholesteryl Ester/Free Cholesterol Ratio in Hepatocellular Carcinoma. *Anticancer Res*. 2017;37(7):3527-35.
307. de Gonzalo-Calvo D, Lopez-Vilaro L, Nasarre L, Perez-Olabarria M, Vazquez T, Escuin D, et al. Intratumor cholesteryl ester accumulation is associated with human breast cancer proliferation and aggressive potential: a molecular and clinicopathological study. *BMC Cancer*. 2015;15:460.
308. Tosi MR, Tugnoli V. Cholesteryl esters in malignancy. *Clin Chim Acta*. 2005;359(1-2):27-45.
309. Peck B, Schulze A. Cholesteryl esters: fueling the fury of prostate cancer. *Cell Metab*. 2014;19(3):350-2.

310. Islam MM, Poly TN, Walther BA, Yang HC, Jack Li YC. Statin Use and the Risk of Hepatocellular Carcinoma: A Meta-Analysis of Observational Studies. *Cancers (Basel)*. 2020;12(3).
311. Vallianou NG, Kostantinou A, Kougias M, Kazazis C. Statins and cancer. *Anticancer Agents Med Chem*. 2014;14(5):706-12.
312. Sopkova J, Vidomanova E, Strnadel J, Skovierova H, Halasova E. The role of statins as therapeutic agents in cancer. *Gen Physiol Biophys*. 2017;36(5):501-11.
313. Farnier M, Portal JJ, Maigret P. Efficacy of atorvastatin compared with simvastatin in patients with hypercholesterolemia. *J Cardiovasc Pharmacol Ther*. 2000;5(1):27-32.
314. Wu CC, Sy R, Tanphaichitr V, Hin AT, Suyono S, Lee YT. Comparing the efficacy and safety of atorvastatin and simvastatin in Asians with elevated low-density lipoprotein-cholesterol--a multinational, multicenter, double-blind study. *J Formos Med Assoc*. 2002;101(7):478-87.
315. Ghassabian S, Gillani TB, Rawling T, Crettol S, Nair PC, Murray M. Sorafenib N-Oxide Is an Inhibitor of Human Hepatic CYP3A4. *AAPS J*. 2019;21(2):15.
316. Neuvonen PJ. Drug interactions with HMG-CoA reductase inhibitors (statins): the importance of CYP enzymes, transporters and pharmacogenetics. *Curr Opin Investig Drugs*. 2010;11(3):323-32.
317. Polycarpou-Schwarz M, Gross M, Mestdagh P, Schott J, Grund SE, Hildenbrand C, et al. The cancer-associated microprotein CASIMO1 controls cell proliferation and interacts with squalene epoxidase modulating lipid droplet formation. *Oncogene*. 2018;37(34):4750-68.
318. Hammersley D, Signy M. Ezetimibe: an update on its clinical usefulness in specific patient groups. *Ther Adv Chronic Dis*. 2017;8(1):4-11.
319. Raal FJ, Marais AD, Klepack E, Lovalvo J, McLain R, Heinonen T. Avasimibe, an ACAT inhibitor, enhances the lipid lowering effect of atorvastatin in subjects with homozygous familial hypercholesterolemia. *Atherosclerosis*. 2003;171(2):273-9.

Appendices

Copyright approval letter for use of Figure 1.1.

THE LANCET

"In patients with first-time myocardial infarction, all combinations of aspirin, clopidogrel, and statins & antplatelets are associated with increased risk of nonfatal and fatal bleeding, compared with aspirin alone."

Aspirin, Clopidogrel, and Statins

Thank you for your order!

Dear Mr. Ho Kit Mok,

Thank you for placing your order through Copyright Clearance Center's RightsLink® service.

Order Summary

Licensee:	Mr. Ho Kit Mok
Order Date:	Aug 18, 2021
Order Number:	5131810048882
Publication:	The Lancet
Title:	Hepatocellular carcinoma
Type of Use:	reuse in a thesis/dissertation
Order Total:	0.00 USD

View or print complete [details](#) of your order and the publisher's terms and conditions.

Sincerely,

Copyright Clearance Center

Tel: +1-855-239-3415 / +1-978-646-2777
customercare@copyright.com
<https://myaccount.copyright.com>

Copyright approval letter for use of Figure 1.2.

SPRINGER NATURE

Thank you for your order!

Dear Mr. Ho Kit Mok,

Thank you for placing your order through Copyright Clearance Center's RightsLink® service.

Order Summary

Licensee: Mr. Ho Kit Mok
Order Date: Aug 20, 2021
Order Number: 5132980863001
Publication: Nature Reviews Drug Discovery
Title: Discovery and development of sorafenib: a multikinase inhibitor for treating cancer
Type of Use: Thesis/Dissertation
Order Total: 0.00 USD

View or print complete [details](#) of your order and the publisher's terms and conditions.

Sincerely,

Copyright Clearance Center

Tel: +1-855-239-3415 / +1-978-646-2777
customer care@copyright.com
<https://myaccount.copyright.com>



RightsLink®



Review

New Insight into Therapies Targeting Angiogenesis in Hepatocellular Carcinoma

Monica Mossenta ^{1,2,†}, Davide Busato ^{1,2,†}, Lorena Baboci ¹, Federica Di Cintio ^{1,2}, Giuseppe Toffoli ^{1,*}  and Michele Dal Bo ¹

¹ Experimental and Clinical Pharmacology Unit, Centro di Riferimento Oncologico di Aviano (CRO), Istituto di Ricovero e Cura a Carattere Scientifico (IRCCS), 33081 Aviano (PN), Italy

² Department of Life Sciences, University of Trieste, 34127 Trieste, Italy

* Correspondence: gtoffoli@ ; Tel.: +39-0434-659612 (659667); Fax: +39-0434-659799

† These authors contributed equally to this work.

Received: 1 July 2019; Accepted: 29 July 2019; Published: 31 July 2019



© 2019 by the authors. Licensee MDPI, Basel, Switzerland. This article is an open access article distributed under the terms and conditions of the Creative Commons Attribution (CC BY) license (<http://creativecommons.org/licenses/by/4.0/>).

MDPI Open Access Information and Policy

All articles published by MDPI are made immediately available worldwide under an open access license. This means:

- everyone has free and unlimited access to the full-text of *all* articles published in MDPI journals;
- everyone is free to re-use the published material if proper accreditation/citation of the original publication is given;
- open access publication is supported by the authors' institutes or research funding agencies by payment of a comparatively low **Article Processing Charge (APC)** for accepted articles.

Permissions

No special permission is required to reuse all or part of article published by MDPI, including figures and tables. For articles published under an open access Creative Common CC BY license, any part of the article may be reused without permission provided that the original article is clearly cited. Reuse of an article does not imply endorsement by the authors or MDPI.



Review

Conversion of Stem Cells to Cancer Stem Cells: Undercurrent of Cancer Initiation

Said M. Afify ^{1,2} and Masaharu Seno ^{1,3,*}

¹ Department of Medical Bioengineering, Graduate School of Natural Science and Technology, Okayama University, Okayama 700-8530, Japan; saidafify@

² Division of Biochemistry, Faculty of Science, Menoufia University, Shebin El Koum-Menoufia 32511, Egypt

³ Laboratory of Nano-Biotechnology, Graduate School of Interdisciplinary Science and Engineering in Health Systems, Okayama University, Okayama 700-8530, Japan

* Correspondence: mseno@ ; Tel.: +81-86-251-8216

Received: 31 January 2019; Accepted: 6 March 2019; Published: 11 March 2019



© 2019 by the authors. Licensee MDPI, Basel, Switzerland. This article is an open access article distributed under the terms and conditions of the Creative Commons Attribution (CC BY) license (<http://creativecommons.org/licenses/by/4.0/>).

MDPI Open Access Information and Policy

All articles published by MDPI are made immediately available worldwide under an open access license. This means:

- everyone has free and unlimited access to the full-text of *all* articles published in MDPI journals;
- everyone is free to re-use the published material if proper accreditation/citation of the original publication is given;
- open access publication is supported by the authors' institutes or research funding agencies by payment of a comparatively low **Article Processing Charge (APC)** for accepted articles.

Permissions

No special permission is required to reuse all or part of article published by MDPI, including figures and tables. For articles published under an open access Creative Common CC BY license, any part of the article may be reused without permission provided that the original article is clearly cited. Reuse of an article does not imply endorsement by the authors or MDPI.



REVIEW ARTICLE

Cancer stemness in hepatocellular carcinoma: mechanisms and translational potential

Yu-Man Tsui^{1,2}, Lo-Kong Chan^{1,2} and Irene Oi-Lin Ng^{1,2}

Note This work is published under the standard license to publish agreement. After 12 months the work will become freely available and the license terms will switch to a Creative Commons Attribution 4.0 International (CC BY 4.0).

SPRINGER NATURE

Cancer stemness in hepatocellular carcinoma: mechanisms and translational potential

Author: Yu-Man Tsui et al

Publication: British Journal of Cancer

Publisher: Springer Nature

Date: Mar 31, 2020

Copyright © 2020, The Author(s), under exclusive licence to Cancer Research UK

Creative Commons

This is an open access article distributed under the terms of the [Creative Commons CC BY](#) license, which permits unrestricted use, distribution, and reproduction in any medium, provided the original work is properly cited.

You are not required to obtain permission to reuse this article.

To request permission for a type of use not listed, please contact [Springer Nature](#)

Creative Commons licence for Figure 1.6.



Review

The Pivotal Role of the Dysregulation of Cholesterol Homeostasis in Cancer: Implications for Therapeutic Targets

Etienne Ho Kit Mok ¹ and Terence Kin Wah Lee ^{1,2,*}

¹ Department of Applied Biology and Chemical Technology, The Hong Kong Polytechnic University, Hong Kong 999077, China; ho-kit.mok@

² State Key Laboratory of Chemical Biology and Drug Discovery, The Hong Kong Polytechnic University, Hong Kong 999077, China

* Correspondence: terence.kw.lee@ ; Tel.: +852-3400-8799; Fax: +852-2364-9932

Received: 1 May 2020; Accepted: 28 May 2020; Published: 29 May 2020



© 2020 by the authors. Licensee MDPI, Basel, Switzerland. This article is an open access article distributed under the terms and conditions of the Creative Commons Attribution (CC BY) license (<http://creativecommons.org/licenses/by/4.0/>).

MDPI Open Access Information and Policy

All articles published by MDPI are made immediately available worldwide under an open access license. This means:

- everyone has free and unlimited access to the full-text of *all* articles published in MDPI journals;
- everyone is free to re-use the published material if proper accreditation/citation of the original publication is given;
- open access publication is supported by the authors' institutes or research funding agencies by payment of a comparatively low **Article Processing Charge (APC)** for accepted articles.

Permissions

No special permission is required to reuse all or part of article published by MDPI, including figures and tables. For articles published under an open access Creative Common CC BY license, any part of the article may be reused without permission provided that the original article is clearly cited. Reuse of an article does not imply endorsement by the authors or MDPI.

Copyright approval letter for use of Figure 3.1A.

THE LANCET

"In patients with first-time myocardial infarction, all combinations of aspirin, clopidogrel, and statins of any intensity are associated with increased risk of more-fatal and total bleeding, compared with aspirin alone."



Thank you for your order!

Dear Mr. Ho Kit Mok,

Thank you for placing your order through Copyright Clearance Center's RightsLink® service.

Order Summary

Licensee: Mr. Ho Kit Mok

Order Date: Aug 25, 2021

Order Number: 5135730729931

Publication: The Lancet

Title: Lenvatinib versus sorafenib in first-line treatment of patients with unresectable hepatocellular carcinoma: a randomised phase 3 non-inferiority trial

Type of Use: reuse in a thesis/dissertation

Order Total: 0.00 USD

View or print complete [details](#) of your order and the publisher's terms and conditions.

Sincerely,

Copyright Clearance Center

Tel: +1-855-239-3415 / +1-978-646-2777
customercare@copyright.com
<https://myaccount.copyright.com>



RightsLink®

Statement of use of content for Figure 3.1B.

The NEW ENGLAND JOURNAL of MEDICINE

ORIGINAL ARTICLE

Sorafenib in Advanced Hepatocellular Carcinoma

Josep M. Llovet, M.D., Sergio Ricci, M.D., Vincenzo Mazzaferro, M.D., Philip Hilgard, M.D., Edward Gane, M.D., Jean-Frédéric Blanc, M.D., Andre Cosme de Oliveira, M.D., Armando Santoro, M.D., Jean-Luc Raoul, M.D., Alejandro Forner, M.D., Myron Schwartz, M.D., Camillo Porta, M.D., Stefan Zeuzem, M.D., Luigi Bolondi, M.D., Tim F. Greten, M.D., Peter R. Galle, M.D., Jean-François Seitz, M.D., Ivan Borbath, M.D., Dieter Häussinger, M.D., Tom Giannaris, B.Sc., Minghua Shan, Ph.D., Marius Moscovici, M.D., Dimitris Voliotis, M.D., and Jordi Bruix, M.D.,
for the SHARP Investigators Study Group*

Sorafenib in Advanced Hepatocellular Carcinoma



Author: Josep M. Llovet, Sergio Ricci, Vincenzo Mazzaferro, et al

Publication: The New England Journal of Medicine

Publisher: Massachusetts Medical Society

Date: Jul 24, 2008

Copyright © 2008, Massachusetts Medical Society

Reuse of Content Within a Thesis or Dissertation

Content (full-text or portions thereof) may be used in print and electronic versions of a dissertation or thesis without formal permission from the Massachusetts Medical Society (MMS), Publisher of the *New England Journal of Medicine*.

The following credit line must be printed along with the copyrighted material:

Reproduced with permission from (scientific reference citation), Copyright Massachusetts Medical Society.